UNIVERSITY OF SOUTHAMPTON

FACULTY OF ENGINEERING, SCIENCE AND MATHEMATICS

School of Ocean and Earth Science

Tritium speciation in nuclear decommissioning materials

by

Dae Ji Kim,

BSc, MSc

Thesis for the degree of Doctoral of Philosophy

April 2009

UNIVERSITY OF SOUTHAMPTON

ABSTRACT

FACULTY OF ENGINEERING, SCIENCE AND MATHEMATICS
SCHOOL OF OCEAN AND EARTH SCIENCE

Doctor of Philosophy

Tritium speciation in nuclear decommissioning materials

By Dae Ji Kim

Tritium is a by-product of civil nuclear reactors, military nuclear applications, fusion programmes and radiopharmaceutical production. It commonly occurs, though not exclusively, as tritiated water (HTO) or organically-bound tritium (OBT) in the environment but may exist as other forms in nuclear-related construction and fabrication materials. During the lifetime of nuclear sites (especially those involving heavy water) tritium becomes variably incorporated into the fabric of the buildings. When nuclear decommissioning works and environmental assessments are undertaken it is necessary to accurately evaluate tritium activities in a wide range of materials prior to any waste sentencing. Of the various materials comprising UK radioactive wastes, concrete and metal account for approximately 20% of the total weight of low level waste (LLW) and 12% and 35% of the total weight of intermediate level waste (ILW).

Proper sampling and storage of samples are significant factors in achieving accurate tritium activities. The degree of loss of ^{3}H and cross-contamination can be significantly reduced by storing samples in an air/water tight container in a freezer (-18°C). The potential for tritium contamination is dependent on the ^{3}H form. Most ^{3}H loss originates from tritiated water which is easily exchanged with atmospheric hydrogen in the form of water vapour at room temperature. However, the loss of more strongly bound ^{3}H, produced in-situ in materials by neutron activation, is not significant even at room temperature. Such tritium is tightly retained in materials and does not readily exchange with water or diffuse.

In nuclear reactor environments tritium may be produced via several neutron-induced reactions, $^{2}H(n,\gamma)^{3}H$, $^{6}Li(n,\alpha)^{3}H$, $^{10}B(n,2\alpha)^{3}H$ and ternary fission (fission yield <0.01%). It may also exist as tritiated water (HTO) that is able to migrate readily and can adsorb onto various construction materials such as structural concrete. In such locations it exists as a weakly-bound form that can be lost at ambient temperatures. Bioshield concretes present a special case and systematic analysis of a sequence of sub-samples taken from a bioshield core (from UKAEA Winfrith) has identified a strongly-bound form of ^{3}H in addition to the weakly bound form. The strongly bound ^{3}H in concrete is held more strongly in mineral lattices and requires a temperature of >850°C to achieve quantitative recovery. This more strongly retained tritium originates from neutron capture of trace lithium (^{6}Li and potentially ^{10}B) distributed throughout minerals in the concrete. The highest proportion of strongly bound ^{3}H was observed in the core sections closest to the core. Weakly bound tritium is associated with water loss from hydrated mineral components.

Tritium is retained in metals by absorption by free water, hydrated surface oxidation layer, H ingress into bulk metal and also as lattice-bound tritium produced via *in-situ* neutron activation. Away from the possible influence of neutrons, the main ^{3}H contamination to metals arises from absorption and diffusion via atmospheric exposure to the HTO. Here contamination is mainly confined to the metal surface layer. The tritium penetration rate into metal surfaces is controlled by the metal type and its surface condition. Where metals are exposed to a significant neutron flux and contain ^{6}Li, ^{7}Li and ^{10}B then *in situ* ^{3}H production will occur which may propagate beyond the surface layer. In such cases tritium may exist in two forms namely a weakly bound HTO form and a non-HTO strongly bound form. The HTO form is readily lost at moderate temperatures (~120°C) whereas the non-HTO requires up to 850°C for complete extraction.

Contents

LIST OF FIGURES

LIST OF TABLES

Graduate School of the National Oceanography Centre, Southampton

This PhD. Dissertation by

Dae Ji Kim

has been produced under the supervision of the following people:

Supervisors

Dr Ian W Croudace

Dr Phillip E Warwick

Chair of Advisory Panel

Professor Eric P Achterberg

Declaration

The work presented in this thesis was predominantly carried out by myself and was done wholly whilst in candidature for a research degree at this University. Some data were produced by other researchers in the Geosciences Advisory Unit at the National Oceanography Centre, Southampton. In all such cases this is stated in the relevant section and in the list of authors on the papers.

Signed:

Date:

Acknowledgements

This study was funded by the Ministry of Education and Human Resources Development of the Korean government (No. 2003-6). School of Ocean and Earth Science, University of Southampton supported part of educational tuition fee.

I would like to thank my supervisors Dr Ian Croudace and Dr Phil Warwick for their valued supervision and support especially for their generous time and guidance in scientific writing during whole this study. I would also like to thank Prof. Eric Achterberg for acting as Chairman of my Advisory Panel.

I would like to thank to Dr Nicola Holland for assistance with many graphic works and tutoring, Dr Jung-Suk Oh and Dr Pawel Gaca for radioanalytical support and for sharing their experiences. Additionally, thank you to Richard Marsh for sharing many references. I would like to thank Dr John Langley in the School of Chemistry for GC-MS analysis and Bob Jones and John Ford (polished sample preparation) and Dr Richard Pearce (SEM Analysis).

On a personal level I thank a former NOCS colleague and friend David Wilkinson for many conversations and advice and for leading me on many sports challenges. Similar thanks go to Paul and Thanos for many conversations and discussions during the whole of my PhD time. Finally, and significantly I thank my friends, Hui-Sun and his wife Hee-Sook and Hang-peel, for their generous support, especially to my children.

부모님과 가족들에게

긴 터널을 이제야 통과 한 듯 합니다. 오랜 시간 이 한번의 끝을 기다려 주신 부모님께 죄송함과 감사의 마음을 짧은 글로 대신 하고자 합니다. 돌이켜 보면, 좀더 쉽게 부모님 걱정을 덜어드릴 여러번의 기회가 있었던 것 같습니다. 하지만, 매번 그 기회를 뿌리치고, 이렇게 멀리 돌아와버린 아들을 말없이 지켜봐 주신 부모님의 마음을 감히 짐작조차 하기 어려울 정도입니다.

“ 마음을 비우자”

저에겐 특별한 의미로 다가오는 문구입니다. 아울러 제가 살아갈 남은 인생에 좋은 지침의 문구가 될 것 같습니다. 오랜기간 저를 말없이 후원해 주신 아버지 그리고 가슴 저리도록 저를 격력해 주신 어머니께 감사드립니다. 생각보다 길어진 사위의 학위과정을 오랜기간 지켜봐 주신 장인, 장모님께 죄송함과 감사의 마음을 전합니다. 한결 같은 이해와 격려가 아니었다면 흔들림 없이 여기 까지 올 수 없었을 겁니다. 오늘의 결실이 남은 저의 모든 숙제를 풀어갈 좋은 밑거름이 되리라 생각합니다.

많이 부족한 사람이 맏아들, 맏사위 자리에서 가족들을 힘들게 한 것 같습니다. 저를 위해 희생해 준 모든 가족들에게 이 자리를 빌어 감사하단 말을 전합니다. 저의 빈자리를 누구보다 잘 채워준 동생 가족과, 모두 떠나보내고 많이 외로웠을 큰처남 가족들에게 특별히 고마움을 전합니다. 서로 가까운 곳에서 더 재미나게 지낼 그 날을 기약해 봅니다.

심약한 제 주변의 너무나도 강인한 가족들 덕분에 제가 꼿꼿히 서 있을 수 있었습니다. 지금까지 저를 있게 해준 모둔 분들께 감사드리며, 저를 통해 그분들이 존재감을 느낄 수 있었으면 좋겠습니다. 논문에 담긴 모든 결실을 가족들과 함께 하고 싶습니다.

To: Younglim, Jinho and Mingyung

사랑하는 나의 아내 영임에게, 지면에 다 쓸 수 없을 만큼 많은 일들을 함께 겪어 오면서 늘 긍정적인 당신의 내조가 없었다면, 이 논문의 한 지면을 빌려 고맙다는 말조차도 하지 못했을 것 같다. 학위가 마무리 되는 과정에서 겪었던 많은 고민의 시간들이 헛되지 않도록, 더 많은 희망을 보여주는 남편, 가장의 모습을 보여줄께. 잘 참고 기다려줘서 고맙고, 사랑한다.

아들 진호에게, 3 살 어린 나이에 먼 나라 영국에서 낯설고, 힘들었지만 잘 적응해서 밝고 건강하게 자라줘서 고맙고, 자랑스럽구나. 어리다고만 생각했던 진호가 해준 진심어린 조언을 지금도 잊을 수가 없구나. 진호에게 좋은 본보기가 되는 아버지의 모습을 보여줄 수 있도록 더욱 노력할께.

내 딸 민경, 민경이를 떠올리면 항상 입가엔 환한 웃음이 번진단다. 넘치는 에너지와 활력으로 온 가족에게 기쁨을 줘서 고맙고, 건강하게 자라줘서 고맙다. 활짝 웃는 민경이 덕분에 아빠는 더 힘을 낼 수 있었던 것 같다. 학위 끝무렵 특히 많은 재롱과 웃음을 선사해준 민경아 사랑한다.

가족이라서 함께 더 행복한 순간보다, 가족이기때문에 더 많이 힘들어했던 시간이 많았던 것은 아닌가 새삼 생각하게 됩니다. 하지만 그 가족의 힘으로 결국 이자리에 서게 되었습니다. 이 논문과 관련된 모든 결실을 영임, 진호, 민경과 함께 합니다.

휴식은 그동안 놓친 소중한 것들,
내 소중한 사람들과 함께할 수 있는 황금 같은 시간이다.
때로는 여유를 즐겨야 더 나아갈 수 있다.

-좋은 생각 중에서-

Abbreviations

$^{3}H_{total}$	Total tritium
Bq	Becquerel, the SI unit of radioactivity
BWR	Boiling Water Reactor
Ci	Curies, the pre-SI unit of radioactivity
DEFRA	Department for Environment, Food and Rural Affairs
EA	Environment Agency
FBR	Fast Breeder Reactor
FSA	Food Standard Agency
GBq	Gigabecquerel; 10^{9} Becquerel
GCR	Gas Cooled Reactor
HLW	High Level Wastes
HPA	Health Protection Agency
HT	Tritiated gas
HTGR	High Temperature Gas cooled Reactor
HTO	Tritiated water
IAEA	International Atomic Energy Authority
ICRP	International Commission on Radiological Protection
ILW	Intermediate Level Wastes
ITER	International Thermonuclear Experimental Reactor
KNEF	Korea Nuclear Energy Foundation
LLW	Low Level Wastes
LMFBR	Liquid Metal-cooled Fast Breeder Reactor
LSC	Liquid Scintillation Counting
LWR	Light Water Reactor
MAFF	Ministry of Agriculture, Fisheries and Food; former department of FSA
MTR	Material Test Reactor, Dounreay, UK
MWe	Megawatts electric
NCRP	National Council on Radiation Protection and Measurement
NDA	Nuclear Decommissioning Authority
NIF	National ignition Facility
OBT	Organically bound tritium
PWR	Pressurized Water Reactor
SAM	Surface Activity Monitor
SEPA	Scottish Environment Protection Agency
SGHWR	Steam Generating Heavy Water Reactor
SQP(E)	Spectral Quench Parameter of the Internal Standard
Sv	Sieverts, SI unit of dose
T	Tritium
TBq	Terabecquerel; 10^{12} Becquerel
THORP	Thermal Oxide Reprocessing Plant
TU	Tritium units; 1 ^{3}H atom per 10^{18} H atoms
UKAEA	The United Kingdom Atomic Energy Authority
UNSCEAR	United Nations Scientific Committee on the Effects of Atomic Radiation
WHO	World Health Organization

Chapter 1

Introduction

1 Introduction

Historically, nuclear technology has been beset by bad publicity (e.g. Windscale Fire in 1957, Three Mile Island 1979, and Chernobyl 1986) because of its association with nuclear weaponry (atmospheric and underground nuclear device tests), poorly controlled nuclear discharges and nuclear accidents at both military and civil nuclear sites. There is little doubt that the legacy of the Cold War produced dire environmental consequences in several countries including the USA, former USSR, UK, France, China, India and Pakistan. There are some critical concerns related with safety such as a radiation leak, nuclear accidents and variety types of waste from each nuclear facility. In spite of the above problems, the cessation of the Cold War has led to significant remediation of some formerly contaminated sites though Russia still has significant problems.

Nuclear reactors are producing a significant fraction of the electricity used in many countries of the world. France employed it to the largest extent, generating 80% of its electric energy (Eisenbud and Gesell, 1997; Guen, 2009). As the energy requirements of the world increase and as the reserves of fossil fuel become smaller, nuclear energy will play an increasingly important role in civilian economies. Its use may be encouraged because, unlike energy derived from fossil fuels, it does not add to the atmospheric burden of greenhouse gases resulting current global warming and could provide a partial solution to lowering the CO_2 linked to energy production.

A wide range of early generation nuclear facilities (military and civil) are undergoing decommissioning worldwide. These include research reactors, civil nuclear power plants, isotope production plants, particle accelerators, experimental fusion facilities, isotopic enrichment facilities etc. A significant number of first and second generation nuclear research sites and nuclear power plants in the UK are now being decommissioned and many others are due to begin decommissioning within the next decade (Table 1.1). The nature of decommissioning works will vary from site to site but, in most cases, will involve either the extensive clean out, demolition of buildings and other facilities, and remediation of the land. With this process, large volumes of waste materials will be generated. Some of these materials will be contaminated with radioactivity, therefore, they must be treated as radioactive waste and carefully disposed of in accordance with the requirements of national radioactivity regulations. A diversity of methods are being used for analyzing these waste products dependent on sample type and activity. During this process there is the opportunity for the development of more efficient and cost-effective procedures.

Table 1.1: Nuclear facilities under the NDA (Nuclear Decommissioning Authority) and British Energy, UK

Category	Facilities	Location	Age	Licensed to	Status (owner)	Features
Operational power stations	Dungeness B (2 AGR)	Romney Marsh, Kent	Since 1983		Operational (British Energy)	Net electrical output of Dungeness B is 1090 MWe and estimated decommissioning date is 2018.
	Hartlepool (2 AGR)	Cleveland	Since 1983		Operational (British Energy)	It provides electricity for over 3% of the UK using two 1575 MWe advanced gas reactors to heat two 660 MWe generators, giving a total generating capacity of 1,320 MWe. Estimated decommissioning date is 2014.
	Heysham (4 AGR)	Lancashire	Since 1983		Operational (British Energy)	The site is divided into two separately-managed stations, Heysham 1 and Heysham 2, both of the advanced gas-cooled reactor (AGR) type, with two reactors each. The total installed capacity is 2400 MWe. Estimated decommissioning date: 2014
	Hinkley Point B (2 AGR)	Somerset	Since 1976		Operational (British Energy)	Its net electrical output is 860 MWe. Operating at its currently reduced level of around 70% of full output, Hinkley Point B is capable of supplying over 1 million homes. Estimated decommissioning date is 2016
	Hunterstone B (2 AGR)	Ayrshire	Since 1976		Operational (British Energy)	Its net electrical output is 840 MWe. Operating at its current (May 2008) reduced level of around 70% of full output. Estimated decommissioning date is 2016
	Oldbury (2 Magnox)	Gloucestershire	Since 1967	Magnox Electric plc	Operational (NDA)	Oldbury Power Station will cease operations at the end of 2010. Fuel will be progressively removed from the reactors and sent to Sellafield for treatment.
	Torness (2 AGR)	Lothian	Since 1988		Operational (British Energy)	The station consists of two advanced gas-cooled reactor (AGR) capable of producing a peak rating of 1364 MWe. It is expected to operate until 2023.
	Sizewell B (1 PWR)	Suffolk	Since 1994		Operational (British Energy)	It generates 1188 MWe net electrical output and supplies 3% of the UK's entire electricity needs**.** Estimated decommissioning date is 2035
	Wylfa (2 Magnox)	Angelsey, North Wales	Since 1971	Magnox Electric plc	Operational (NDA)	The last and largest power station of Magnox type to be built in the UK. It will cease to do so in 2010. Fuel will be progressively removed from the reactors and sent to Sellafield for treatment.
Non-operational power stations	Berkeley (2 Magnox)	Berkeley, Gloucestershire	1962 - 1989	Magnox Electric plc	Decommissioning (NDA)	One of the UK's first nuclear power stations. It has largely been decommissioned and should be on the first Magnox power stations to enter care and maintenance. A large area of land adjacent to the power station was delicensed in December 2006.

Category	Facilities	Location	Age	Licensed to	Status (owner)	Features
	Bradwell (2 Magnox)	Bradwell, Essex	1962 - 2002	Magnox Electric plc	Decommissioning (NDA)	Bradwell power station has successfully moved to the decommissioning stage in its lifecycle.
	Calder Hall (4 Magnox)	Sellafield site, Cumbria	1956 - 2003	British Nuclear Group SLC	Preparation for defuelling and Care & Maintenance (NDA)	The world's first commercial nuclear power station. Calder Hall Power Station supplied strategic materials to the Ministry of Defence (MoD), steam and electricity to Sellafield and electricity to the grid.
	Chapelcross (4 Magnox)	Dumfries, Scotland	1959 - 2004	from BNFL to Magnox Electric plc	Entering defuelling stage (NDA)	The first nuclear power station in Scotland and electricity generation ceased in June 2004. The site supplied strategic materials to the Ministry of Defence and was used to test fuel assemblies for later nuclear power stations. It is now entering the defuelling phase. Fuel will be progressively removed from the reactors and sent to Sellafield for treatment.
	Dungeness A (2 Magnox)	Dungeness, Kent	1965 - 2006	Magnox Electric plc	Defuelling (NDA)	An Environmental Impact Assessment for Decommissioning (EIAD) was approved in 2006. Fuel will be removed from the reactors and sent to Sellafield for treatment.
	Hinkley Point A (2 Magnox)	Somerset	1965 - 2000	Magnox Electric plc	Decommissioning (NDA)	Following successful completion of reactor de-fuelling operations in November 2004, 4 months ahead of schedule, Hinkley Point A is now into its decommissioning phase and preparations for care and maintenance. The site has implemented the new organisational structure required for the future decommissioning work.
	Hunterston A (2 Magnox)	West Kilbride, Ayrshire	1964 - 1989	from BNFL to Magnox Electric plc	Decommissioning (NDA)	All fuel has been removed from the reactors and the station is well into decommissioning
	Sizewell A (2 Magnox)	Suffolk	1966 - 2006	Magnox Electric plc	Defuelling (NDA)	An Environmental Impact Assessment for Decommissioning (EIAD) was approved in 2006. Fuel will be removed from the reactors and sent to Sellafield for treatment.
	Trawsfynydd (2 Manox)	Gwynedd, North Wales	1965 - 1991	from BNFL to Magnox Electric plc	Decommissioning (NDA)	Unique power station built inland adjacent to a lake which provided cooling water. Trawsfynydd ceased to generate electricity in 1991. All fuel has been removed from the reactors and decommissioning is well underway.

Category	Facilities	Location	Age	Licensed to	Status (owner)	Features
Fuel Plants	Capenhurst	Ellesmere Port, Cheshire	1953 - 1982	BNFL	Decommissioning (NDA)	Capenhurst was home to a uranium enrichment plant and associated facilities that ceased operation in 1982. Most of the plant has now been removed from the site and decommissioning is expected to be completed mid 2009. Over the next decade or so, the site will store uranium materials. The Site will store part of the UK's stock of uranium materials up to the year 2120.
	Sellafield	Cumbria	Since 1947	BNFL	Defuelling & Partial Decommissioning (NDA)	Sellafield is a large, complex nuclear chemical facility, which has supported the civil nuclear power programme since the 1940s. Operations at Sellafield include treatment of fuels removed from nuclear power stations; Mixed Oxide (MOX) fuel fabrication; and storage of nuclear materials and radioactive wastes. Decommissioning has been underway since the 1980s and there is still much to do.
	Springfields	Lancashire	Since 1946	Springfields Fuels Ltd	Operational & Partial Decommissioning (NDA)	Springfields manufactures nuclear fuel products for the UK's nuclear power stations and for international customers. Fuel manufacture is scheduled to continue until 2023. Springfields is also undertaking decommissioning activities and to date 87 buildings have been fully demolished.
Storage sites	LLW Repository	Drigg, Cumbria	Since 1959	LLW Repository Ltd	Operating (NDA)	This Low Level Waste (LLW) Repository has operated as a national LLW disposal facility since 1959. Wastes are compacted and placed in containers before being transferred to the facility. Following a major upgrade of disposal operations in 1995, all LLW is now disposed of in engineered concrete vaults. Plutonium Contaminated Materials are being removed from the site for long-term storage at nearby Sellafield.
Fusion research	Culham Science Centre (JET)	Oxfordshire	Since 1983	Not applicable	Operational (NDA)	The Joint European Torus (JET), located at Culham in Oxfordshire, is the world's largest fusion research machine. JET is operated by UKAEA under a contract from EURATOM under the terms of the European Fusion Development Agreement (EFDA) which covers the costs of the operational programme. The NDA will take responsibility for the decommissioning programme that is expected to be completed by the end of 2020. .

Category	Facilities	Location	Age	Licensed to	Status (owner)	Features
Decommissioned research facilities	Dounreay (2 FBR)	Caithness, Scotland	1950s - 1994	UKAEA	Defuelling and Decommissioning (NDA)	Dounreay was a research reactor site with fuel treatment facilities. There were three reactors, the last of which ceased operation in 1994 and the site is now being decommissioned.
	Harwell (5 reactors)	Oxfordshire	1946 - 1990	UKAEA	Decommissioning (NDA)	Harwell was Britain's first Atomic Energy Research Establishment (GLEEP). The site accommodated five research reactors of various types. Harwell also had a number of other nuclear research facilities, together with plutonium handling facilities, radioactive laboratories, nuclear waste treatment and storage facilities. Decommissioning is well underway – two of the reactors have been completely removed, and the fuel has been removed from the remaining three which are now being decommissioning. More than 100 other facilities have been removed from the site and others are being decommissioned. It is expected that decommissioning will be completed by 2025.
	Windscale (1 AGR and 2 Piles)	Sellafield site, Cumbria	Opened in 1947	UKAEA	Decommissioning (NDA)	Windscale is a separate licensed site located on the Sellafield site in Cumbria. It comprises three reactors, two of which were shutdown in 1957 and the third in 1981. Decommissioning activities began in the mid 1980s and are expected to continue until 2015.
	Winfrith (8 of various type reactor e.g. HTGR, SGHWR)	Dorset	1958 - 1990	UKAEA	Decommissioning (NDA)	Winfrith was an experimental reactor research and development site. Eight research reactors of various types and sizes have operated on the site. Winfrith also had a number of other facilities including fuel manufacture and examination, plutonium laboratories, nuclear waste treatment and storage and radioactive laboratories. Six of the reactors have been removed from the site; the two remaining have had fuel removed and are in various stages of decommissioning. Parts of the Winfrith site have been delicensed and it is expected that the remaining decommissioning will be completed by 2018.

The data were quoted from the http://www.nda.gov.uk/sites/ and World nuclear industry Handbook (Tarlton, 2006)

1.1 Radioactive waste

Radioactive wastes are materials contaminated by, or incorporating radioactivity above certain levels defined in legislation. Solid radioactive waste is divided into four categories (Table 1.2) according to its radioactivity content and the heat it produces; as Very Low level Waste (VLLW), Low Level Waste (LLW), Intermediate Level Waste (ILW), and High Level Waste (HLW); (IAEA, 1994). The majority of radioactive waste is "low-level waste", meaning it has low levels of radioactivity per mass or volume. This type of waste is diverse in composition and may consist of building materials, wood, metal, concrete, laboratory arisings, used protective clothing etc. which although only slightly contaminated are still potentially hazardous. For the material to be classified as exempt under the Substances of Low Activity (SoLA) Exemption Order (HMSO, 1993) and therefore Below Regulatory Concern (BRC), the total specific activity of the sample must be <0.4 Bq/g, and surface contamination <4.0 Bq/cm^2 $\beta+\gamma$ and <0.4 Bq/cm^2 α.

In the total volume of radioactive waste from all sources in the UK, 90.4% is LLW, 9.5% is ILW and less than 0.1% is HLW (NIREX and DEFRA, 2005). However, HLW contains about 95% of the radioactivity in all waste arising from the nuclear power generation programme (Figure 1.1). The VLLW is disposed by incineration and landfill disposal. Most of the UK's solid LLW is disposed of to the near-surface disposal facility at Drigg. However there are currently no disposal facilities in the UK for HLW and ILW. These wastes are being accumulated in stores. The major components of LLW are soil, metals and building materials (e.g. concrete, cement and rubble) whist the major components of ILW is metals, largely in the form of fuel cladding and fuel element debris, as well as plant items and equipment. Other major contributors are graphite from reactor cores, building materials (cement and rubble), and miscellaneous inorganic materals such as sludge and floc wastes (Table 1.3).

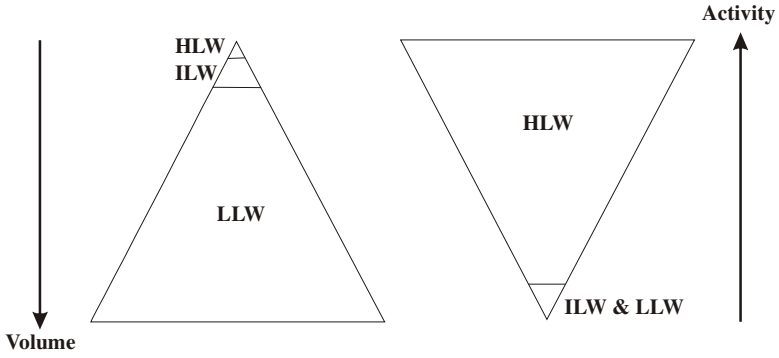

Figure 1.1: The ratio of total volume and activity of radioactive waste type (NIREX and DEFRA, 2005)

The issue of disposal methods for nuclear waste is a pressing current problem for the international nuclear industry and has significance for future nuclear programmes. The sources of radioactive waste are diverse and are not all derived from nuclear sources *sensu strictu* (Table 1.4). A current concern in nuclear facilities is the safe disposal and isolation of radioactive waste from these facilities. These materials must be isolated from the biosphere until the radioactivity contained in them has diminished to a safe level.

Table 1.2: Types of radioactive waste (NDA and DEFRA, 2008)

Category	Characteristics
High level waste (HLW)	▪ Highly radioactive wastes that arise by-product of nuclear power generation ▪ Heat generating waste ▪ With time, heat and radioactive content are decreased ▪ Although the relative amount of HLW is small with respect to the total volumes of radioactive waster produced in nuclear power programes, it contains 99% of the radioactivity ▪ After ~50 years, it is decayed sufficiently to be placed in a geological repository. ▪ Most of this waste has accumulated since the early 1950s at Sellafield and Dounreay, primarily from the reprocessing of spent nuclear fuel.
Intermediate level waste (ILW)	▪ Not heat generating. ▪ It arises mainly from the reprocessing of spent fuel, and from general operations, maintenance and decommissioning of nuclear facilities. • Claddings separated from spent nuclear fuel • Filters and other wastes from effluent treatments • Worn-out plant and equipment; isotopes used in medical treatments • Radioactive materials used in industry and defence. (e.g. resins, chemical sludge and contaminated materials from reactor decommissioning
Low level waste (LLW)	▪ Radioactivity waste exceeding 4GBq/tonne alpha or 12GBq/tonne of beta/gamma activity ▪ Radioactivity content below the lower limit for ILW. ▪ It arises mainly from contamination of equipment, clothing and cleaning materials during routine operations and maintenance of nuclear facilities, and during decommissioning. ▪ The waste is chemically and materially heterogeneous, and includes a wide range of materials such as metal, soils, building rubble and miscellaneous scrap. ▪ Low level waste is divided into four classes, class A, B, C and GTCC, which means “Greater than Class C”.
Very low level waste (VLLW)	▪ This waste is a subset of LLW and is uniquely defined in term of activity and volume because it is intended to cover small volumes of low-activity wastes that may be disposed of with ordinary refuse. ▪ It is defined as each $0.1m^3$ containing less than 400 kBq of total activity or single items containing less than 40 kBq of total activity.
Radiologically clean	▪ This waste is similar to LLW in terms of material and composition But it has either never been contaminated or by analysis has been shown to be not contaminated or is waste complying with Schedule 1 of RSA ’93.

These data are from NDA (Nuclear decommissioning Authority; http://www.nda.gov.uk) and (IAEA, 1994).

Table 1.3: Estimated composition of radioactive wastes in the UK (DEFRA, 2002)

Material	Low level waste (%)	Intermediate level waste (%)
Soil	46	2
Metals	22	35
Concrete	21	12
Organics	7	4
Inorganics	-	18
Graphite	2	28

Note: Most of the UKs solid LLW is disposed of to the near-surface disposal facility (Low Level Waste Repository) at Drigg. The Drigg, operated by NDA, has been the principal national disposal site for low level radioactive waste in the UK. Based on the safety assessment of the facility, the annual limit for tritium is 0.05 TBq.

Table 1.4: Sources of radioactive waste

Waste sources	Features
*NORM/ **TE NORM	▪ Processing of substances containing natural radioactivity. ▪ Mainly alpha particles emitting matter from the decay chains of uranium and thorium. ▪ The main source of radiation in the human body is potassium, K-40.
Coal	▪ Coal contains a small amount of radioactive nuclides (e.g., uranium and thorium) ▪ They become more concentrated in the fly ash. However, the radioactivity of this is very low. ▪ A small amount of the fly ash ends up in the atmosphere where it can be inhaled.
Oil and gas	▪ Residues from the oil and gas industry often contain radium and daughters. ▪ The sulphate scale from an oil well can be very radium rich, while the water, oil and gas from a well often contains radon. ▪ The radon decays to form solid radioisotopes which form coatings on the inside of pipework. ▪ In oil processing plant, the area where propane is processed is often one of the more contaminated areas of the plant as radon has a similar boiling point as propane.
Mineral processing	▪ Wastes from mineral processing can contain natural radioactivity ▪ The largest source of this is phosphate mining operations.
Medical/ radiopharmaceutical	▪ A range of radiolabelled organic molecules for pharmaceutical applications and life science research are produced. A range of liquid by-products and waste products of these processes are produced. ▪ Radioactive medical waste can be divided into two main classes. In diagnostic nuclear medicine a number of short-lived gamma emitters such as technetium-99m are used. Many of these can be disposed of after leaving it to decay for a short time before disposal as normal trash. Other isotopes used in medicine, with half-lives in parentheses: • Y-90 , used for treating lymphoma (2.7 days) • I-131 , used for thyroid function tests and for treating thyroid cancer (8.0 days) • Sr-89, used for treating bone cancer, intravenous injection (52 days) • Ir-192 , used for brachytherapy (74 days) • Co-60, used for brachytherapy and external radiotheraphy (5.3 years) • Cs-137, used for brachytherapy, external radiotheraphy (30 years)

Waste sources	Features
Industrial	▪ Industrial source waste can contain alpha, beta, neutron or gamma emitters. ▪ Gamma emitters are used in radiography while neutron emitting sources are used in a range of applications, such as oil well logging.
Nuclear fuel cycle	▪ Waste from the front end of the nuclear cycle is usually alpha emitting waste from the extraction of uranium. It often contains radium and its decay products ▪ The back end of the nuclear fuel cycle contains fission product that emit beta and gamma radiation, and may contain actinides that emit alpha particles, such as U-234, Np-237, Pu-238, and Am-241, and even sometimes some neutron emitters such as californium (Cf). These isotopes are formed in nuclear reactors.
Proliferation concerns	▪ When dealing with uranium and plutonium, the possibility that they may be used to build nuclear weapons is often a concern. ▪ High-level waste from nuclear reactors may contain plutonium. • A mixture of plutonium-239: Highly suitable for building nuclear weapons • Plutonium-240: An undesirable contaminant and highly radioactive • Plutonium-241& plutonium-238: The isotopes are difficult to separate. ▪ Deep storage areas have the potential to become "plutonium mines", from which material for nuclear weapons can be acquired with relatively little difficulty.
Nuclear weapons reprocessing	Waste from nuclear weapons reprocessing (as opposed to production, which requires primary processing from reactor fuel) is unlikely to contain much beta or gamma activity other than tritium and americium. It is more likely to contain alpha emitting actinides such as Pu-239 which is a fissile material used in bombs, plus some material with much higher specific activities, such as Pu-238 or polonium.

**NORM: Naturally occurring radioactive material.*
*** TE NORM: Technically enhanced NORM*

Aims and Objectives

In this study, tritium (^{3}H) is specifically of interest because it can constitute an important component of nuclear waste arising from nuclear sites (power producers, military and reprocessing plants). Particularly important and voluminous materials that contain tritium are concrete and metals which are used in bioshield construction and also as a structural material. The radioactivity in concrete and metals therefore requires consideration when deciding on waste sentencing.

Although large quantities of radioactivity of tritium, its energy per decay is very small. However the presence of tritium (mainly HTO form) is widespread in the environment and its incorporation and radiological impact into the human body with various forms are significant concern for the radiological protection purpose. Therefore, in order to improve the safety and reliability of tritium wastes treatment, investigation of radiation hazards of tritium resulting from the release of tritium and activation products during normal operations as well as decommissioning programmes are required. For this accurate tritium analysis and understanding of tritium speciation in various materials is essential.

This study mainly include following elements:

- Evaluate tritium measurement approach (accuracy and precision), catalyst function and thermal evolution profiles for a range of decommissioning materials: **Chapter 3**
- Study of ^{3}H speciation for different decommissioning materials including structural concrete, bioshield concrete and metals: **Chapter 4 and 6**
- Storage approaches for radioanalytical impact to accurate ^{3}H analysis: **Chapter 5**

1.2 Tritium (^{3}H)

The three isotopes of hydrogen are i) protium, ^{1}H, the most abundant hydrogen isotope (99.985%), ii) deuterium (0.015%), ^{2}H, and iii) tritium (trace), ^{3}H, a radioactive isotope of hydrogen. Unlike the isotopes of other elements, the relatively large mass differences of hydrogen, deuterium and tritium leads to appreciable differences in properties of the elements and their compounds.

The existence of tritium was theoretically predicted by Wigner in 1933. It was discovered by Rutherford, Oliphant and Harteck in 1934, when they bombarded deuterium with high-energy deuterons. The half-life of tritium was established by Alvarez and Cornog (Alvarez and Cornog, 1939). Tritium is widely distributed throughout in the environment due to its ubiquitous form as tritiated water and its persistence in the environment (NCRP, 1979).

Table 1.5: Some characteristics of tritium

	Tritium (^{3}H)
Characteristics	▪ Pure, low energy, beta emitter (E_{max}=18.6 keV) ▪ Half-life = 12.32 years
Sources	▪ Natural cosmogenic production ▪ Atmospheric weapon testing (50s-60s) ▪ Fuel reprocessing ▪ Nuclear reactor operation ▪ Nuclear fusion research (e.g. JET)

Tritium a pure beta emitter (i.e. with no associated gamma ray emission) with a half-life of 12.32 years (Lucas and Unterweger, 2000) which decays to ^{3}He and the emitted beta has a mean energy of 5.7 keV and a maximum energy of 18.6 keV (NCRP, 1985). The low-energy beta radiation from tritium has limitation to penetrate human skin, so tritium is more potentially hazardous if inhaled or ingested.

$$ {}^{3}_{1}H \rightarrow {}^{3}_{2}He^{+} + e^{-} + \overline{\nu_e} $$

Tritium has a sufficiently long half-life and residence times in the atmosphere and hydrosphere sufficient for transport processes to distribute it worldwide. Its radiological impact is therefore not limited to the region of release, and it may be distributed globally in a nearly uniform manner. Owing to its relatively long half-life, high isotopic exchange rates and ease of incorporation into living organisms, it is important to control its release from nuclear facilities and waste management sites to the environment by the use of appropriate waste management strategies and practices.

1.2.1 Sources of tritium

Tritium is produced both naturally, by spallation reactions in the stratosphere, and also through anthropogenically process including atmospheric nuclear weapons testing, as a ternary fission product from nuclear fuel cycle, nuclear fuel reprocessing facilities and radiopharmaceutical industry.

Natural source of tritium

Tritium is continually produced in the stratosphere through the interaction of high energy cosmic rays with the atmospheric gases. Tritium is mainly produced via the fast neutron interaction with atmospheric nitrogen and oxygen-16.

$$^{14}_{7}N + {}^{1}n \rightarrow {}^{12}_{6}C + {}^{3}_{1}H$$

$$^{16}_{8}O + {}^{1}n \rightarrow {}^{14}_{7}N + {}^{3}_{1}H$$

Cosmic ray-induced spallation reactions produce 7.2×10^{16} Bq of ^{3}H per year (Kaufman and Libby, 1954; UNSCEAR, 1977; Okada and Momoshima, 1993; UNSCEAR, 2000). It is estimated that the global ^{3}H inventory from this source is 1.3×10^{18} Bq with the majority being located in the oceans (UNSCEAR, 2000). Tritium then combines with itself to form tritium gas ($^{3}H_2$), or with oxygen to form tritiated water (HTO) which is predominantly transferred to the surface by precipitation (NCRP, 1979). For this reason tritium has been used as a tracer in a range of studies (e.g. meteorology, glaciology, oceanography and hydrology).

Table 1.6: Estimated activity from cosmogenic tritium (UNSCEAR, 2000)

Global atmospheric inventory	1275 PBq
Produced in the atmosphere at a rate	72 PBq/year
Concentration in troposphere	1.4 mBq/m^3
Average annual effective dose to humans	10 nSv

Source from UNSCEAR (2000)

Minute amounts of tritium are also produced in the Earth's crust, when ^{6}Li in rocks is bombarded by neutrons from the spontaneous fission of uranium (Kaufman and Libby, 1954; Craig and Lal, 1961).

$$^{6}_{3}Li + {}^{1}n \rightarrow {}^{4}_{2}He + {}^{3}_{1}H$$

Anthropogenic source of tritium

Significant anthropogenic tritium was produced in the atmosphere through nuclear weapon testing between 1945 and 1980. At present, however, anthropogenic tritium is mainly produced in nuclear fuel reprocessing facilities, nuclear power stations, radiolabelling facilities, research institutes, pharmaceutical and medical establishments. Tritium is also produced through ternary fission although the quantities of tritium produced are small.

i) Nuclear weapon testing

Significant quantities of radioactivity have been released to the environment as a result of the atmospheric nuclear weapon testing as a by-product of nuclear fission, neutron capture and via its use in nuclear fusion booster reactions (Table 1.7). It is estimated that a total of 1.67×10^{20} Bq ^{3}H was released via atmospheric weapon testing (UNSCEAR, 1977). Since 1963, the cessation of atmospheric nuclear weapon tests the released activity of ^{3}H has decayed, with a half-life of 12.32yr, in the atmosphere. Nowadays, the levels of tritium in the atmosphere have almost returned to the levels of the pre-testing era (Villa and Manjon, 2004).

Underground thermonuclear device tests have been conducted on a wide scale since the Partial Test Ban Treaty agreement in 1963. This has not significantly added to the inventory of tritium in the atmosphere and surface waters, but an inventory of uncertain magnitude exists underground at the test sites (NCRP, 1979).

Table 1.7: Estimated fission yields from atmospheric nuclear weapons tests

Year	Country	Number of tests	Fission yield (~MT)
1945	USA	3	0.05
1946	USA	2	0.04
1948	USA	3	0.1
1949	USSR	1	0.02
1951	USA/USSR	17	0.54
1952	UK/USA	11	6.62
1953	UK/USA	13	0.29
1954	USA/USSR	7	30.1
1955	USA/USSR	17	1.67
1956	UK/USA/USSR	27	12.3
1957	UK/USA/USSR	45	10.89
1958	UK/USA/USSR	83	28.94
1960	France	3	0.11
1961	France/USSR	51	25.42
1962	USA/USSR	77	76.55
1964	China	1	0.02
1965	China	1	0.04
1966	France/China	8	1.3
1967	France/China	5	1.92
1968	France/China	6	5.3
1969	China	11	2
1970	France/China	9	4.55
1971	France/China	6	1.97
1972	France/China	5	0.24
1973	France/China	6	1.65
1974	France/China	8	1.55
1976	China	3	2.37
1977	China	1	0.02
1978	China	2	0.04
1980	China	1	0.45
Total		**423**	**217**

Source: UNSCEAR (1982)

ii) Nuclear reactor origin (fission reactors)

Nuclear reactors are used for many purposes: for the generation of electrical power, radioisotope production, the production of weapons grade plutonium for nuclear weapons and submarine/ship propulsion. Over 500 nuclear power plants are being operated in the world (Table 1.8). Tritium is produced by a variety of processes in nuclear power plants; fission processes, neutron capture by lithium or deuterium and decay processes (Bonka, 1979). Approximately 1 in 10^4 fissions of a ^{235}U nucleus induced by a thermal neutron produces a triton so that tritium production is a by-product of nuclear fission. Normally, fission is a binary process, in which only two particles (the primary fission fragments) are formed when the fissioning nucleus splits. Much less frequently, more than two particles are formed and if precisely three particles appear, the fission event is classified as a ternary event (Wegemans, 1991). Ternary fission occur once every few hundred fission events. The ternary fission emission probability depends on Z and A of the fissioning system.

Tritium is produced in reactors by thermal and fast neutron activation of various light elements in reactors (e.g. ^2H, ^3He, ^6Li and ^{10}B) and the quantities depends on cross-section of the elements (NCRP, 1979). Tritium is a by-product of the operation of nuclear reactors resulting from neutron capture by boron (σ_{th} = 1.27 barns) in control rods of light water reactor such as boiling water reactor; BWR (NCRP, 1979).

$$^{10}_{5}B + {}^{1}n \rightarrow 2\,^{4}_{2}He + {}^{3}_{1}H$$

Tritium is also produced in the reactor by lithium-6 (σ_{th} = 940 barns) via neutron capture (NCRP, 1979; Hou, 2005) that is used in the large scale tritium production.

$$^{6}_{3}Li + {}^{1}n \rightarrow {}^{4}_{2}He + {}^{3}_{1}H$$

Tritium is also produced from deuterons (^2H, σ_{th} = 0.00052 barns) via neutron capture (NCRP, 1979; Hou, 2005) which is especially significant in heavy water moderated reactors such as CANDU or SGHWR.

$$^{2}_{1}H + {}^{1}n \rightarrow {}^{3}_{1}H$$

Tritium may also be produced in reactor and particle accelerators by ^3He (σ_{th} = 5330 barns) via neutron irradiation (Hou, 2005).

$$^{3}_{1}He + {}^{1}n \rightarrow {}^{3}_{1}H + p$$

Tritium produced from nuclear power plants has become more significant than that from nuclear weapons tests with the passage of time as a source of tritium in the environment (Sinclair, 1987). Therefore the global distribution of tritium is not uniform and local enrichments are observed in the vicinity of Nuclear Power Plants (Villa and Manjon, 2004).

Several kinds of reactors are used globally as Pressurized Water Reactor (PWR; this reactor called LWR because of light water used as moderator), Pressurized Heavy Water Reactor (PHWR or CANDU), Steam Generating Heavy water Reactor (SGHWR), Boiling Water Reactor (BWR), Gas Cooled Reactor (GCR) and Liquid Metal-Cooled Fast Breeder Reactor (LMFBR). LWR is the most common reactor type in the world and PHWR is the most important reactor type in terms of tritium production by nuclear reactor (Table 1.9). In LWR reactors, tritium is mainly generated by ternary fission in the nuclear fuel and by neutron reactions with light elements such as hydrogen, boron and lithium in control rods or burnable poison dissolved in the primary water coolant. On the other hand, the amount of tritium generated in PHWR (e.g. CANDU reactors and now decommissioned SGHWR UKAEA, Winfrith, UK) by neutron capture reactions of deuterium in heavy water exceeds that in LWR by almost a 100-fold (Harolf and Baker, 1985; Johnson et al., 1992); (Table 1.10).

Table 1.8: Nuclear power stations in the world (Unit: MWe gross capacity of electricity, May 2009)

Nation	In operation		In construction		The future plan		Total	
	Capacity (MWe)	No. of power plant	Capacity (MWe)	No. of power plant	Capacity (MWe)	No. of power plant	Capacity (MWe)	No. of power plant
USA	106302	104	1200	1	9400	8	116902	113
France	66020	59	1630	1			67650	60
Japan	47935	53	3948	4	16552	12	68435	69
Russia	23242	31	6210	8	5850	5	35302	44
German	21457	17					21457	17
R. Korea	17716	20	6800	6	2800	2	27316	28
Ukraine	13818	15	2000	2			15818	17
Canada	13288	18					13288	18
UK	11952	19					11952	19
Sweden	9384	10					9384	10
China	9118	11	13335	13	13609	13	36062	37
Spain	7727	8					7727	8
Belgium	6117	7					6117	7
Taiwan	5164	6	2700	2			7864	8
India	4120	17	3160	6	6800	8	14080	31
Czech	3880	6					3880	6
Swiss	3372	5					3372	5
Finland	2800	4	1700	1			4500	5
Brazil	2007	2			1350	1	3357	3
Bulgaria	2000	2			2000	2	4000	4
Hungary	1970	4					1970	4
S. Africa	1890	2			110	2	2000	4
Slovakia	1827	4	880	2			2707	6
Lithuania	1500	1					1500	1
Rumania	1410	2	2118	3			3528	5
Mexico	1364	2					1364	2
Argentina	1005	2	745	1			1750	3
Slovenia	727	1					727	1
Netherlands	510	1					510	1
Pakistan	462	2	325	1			787	3
Armenia	408	1					408	1
Iran			1000	1	360	1	1360	2
Indonesia					4000	4	4000	4
Egypt					1872	2	1872	2
Israel					664	1	664	1
Turkey					NA	3	NA	3
Kazakhstan					NA	1	NA	1
Vietnam					NA	1	NA	1
Total	390492	436	47751	52	65367	66	503610	554

These data quoted from JAIF (Japan Atomic Industrial Forum)
http://www.kaif.or.kr/pds/10.asp

Table 1.9: Comparison of LWR and PHWR

Categories	LWR	PHWR (CANDU/SGHWR)
Fuel	Enriched uranium	Natural uranium
Fuel replacement	At the end of the life of the reactor 1/3 of fuel replacement	In operation
Coolant (or moderator)	Light water (H_2O)	Heavy water (D_2O)
Developed in	USA	CANADA/UK
% of World reactors	60%	5%
Advantages	▪ Relatively cheap due to normal water (H_2O) is used as a coolant (moderator) ▪ Effective to obtain energy due to the thermal conductivity of H_2O is high	▪ Relatively cheap to purchase fuel since natural uranium is used as a fuel (can reduce the technology and expenses to enrich an uranium) ▪ No reactor suspension for fuel replacement ▪ Neutron reduction effect is high due to cross-section for D_2O is smaller than H_2O
Disadvantages	▪ Fuel supply is relatively difficult ▪ Uranium enrichment account for 40% of total expenses ▪ Country which have no uranium enrichment technology rely on entirely import of fuel. ▪ To replacement of fuel, reactor was suspended for 50~70 days a year.	▪ Difficult to obtain heavy water and expensive ▪ The scale of PHWR is larger than LWR due to raw uranium is used as a fuel ▪ PHWR construction costs is higher than LWR

Plutonium, as a nuclear fuel, produced in the HWR is more than 2 times as large as those in LWR
These data quoted from KNEF (Korea Nuclear Energy Foundation; http://www.knef.or.kr)

Table 1.10: Estimated ^3H production rates ($GBq \cdot GW(e)^{-1} \cdot a^{-1}$) from various types of reactors.

	Fuel	Coolant	Moderator	Total
LWR-PWR	5.18×10^5	3.70×10^4	NA	5.55×10^5
LWR-BWR	5.18×10^5	Low	NA	5.18×10^5
HWR	5.18×10^5	1.85×10^6	5.18×10^7	5.42×10^7
GCR	5.18×10^5	Low	$(0\text{-}1.85)\times10^5$	$(5.18\text{-}7.03)\times10^5$
GCR-HTGR	5.18×10^5	1.85×10^5	$(0.18\text{-}7.40)\times10^4$	$(5.2\text{-}5.9)\times10^5$
FBR	7.40×10^5	7.40×10^4	NA	8.14×10^5

Note: **LWR**, light water reactor; **PWR**, pressurized water reactor; **BWR**, boiling water reactor; **HWR**, heavy water reactor; **GCR**, gas cooled reactor; **HTGR**, high temperature gas cooled reactor; **FBR**, fast breeder reactor. **NA**: data not available. These data were compiled from McKay (McKay, 1980) and summarized by IAEA (IAEA, 2004).

iii) Authorised discharges from nuclear sites

Tritium has been released into the marine and terrestrial environments through routine releases from nuclear facilities (Figure 1.2, see also Table 1.12 at page 22) and accidental releases following nuclear incidents. Such tritium releases may be associated with a wide range of chemical species and accumulation of the tritium in the environment is of special concern.

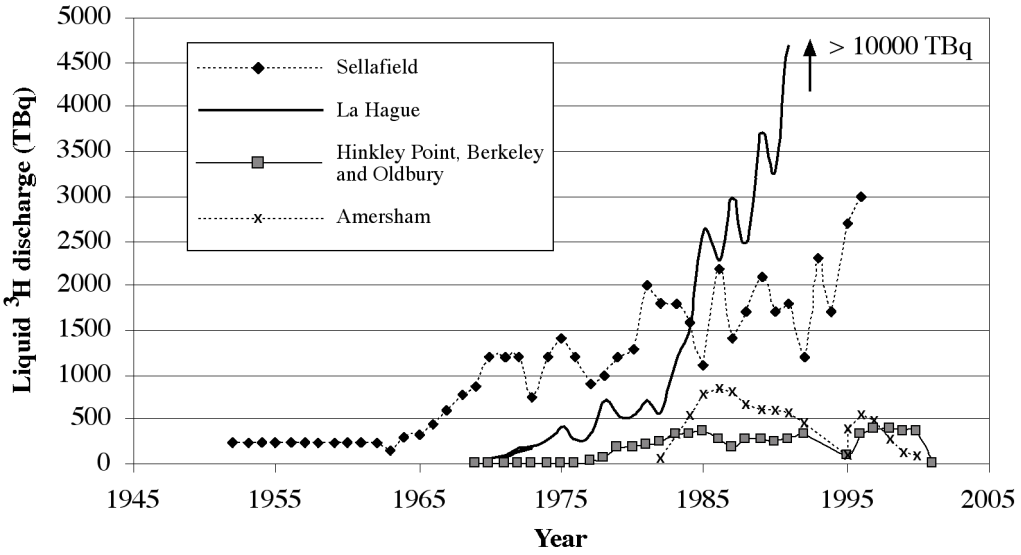

Figure 1.2: Anthropogenic sources of ^{3}H in European seas; nuclear and radio-pharmaceutical sources. (Mitchell, 1968-1978; Hunt, 1979-1989; Camplin, 1992-1995; FSA and SEPA, 1996; 1997; 1998; 1999; 2000; 2001; 2002; EA, 2003; EA et al., 2003; 2004).

Tritium is produced in reactors by neutron activation of ^{2}H, ^{3}He, ^{6}Li and ^{10}B and is formed in the reactor components (e.g. moderator and coolant). Most of the fission product tritium produced in fuel rods is usually retained within the fuel and is not released to the environment at the reactor site; it is released only during fuel reprocessing, if fuel reprocessing is carried out (IAEA, 2004). Tritium in reactor core materials may remain where it is formed and be accumulated until the reactor is decommissioned. However, the activity produced in the coolant is partly or entirely released in the effluent streams, depending on the waste management practices at the nuclear power stations (IAEA, 2004). Releases to the environment are mainly in the form of HTO in reactors that use water as the primary coolant. As a consequence of commercial nuclear power operations, 297 PBq of ^{3}H has been released worldwide to atmosphere by nuclear reactor and reprocessing plants, and 126 PBq of ^{3}H has been released worldwide to sea by reprocessing plants (UNSCEAR, 2000). The typical discharge rates of tritium from various types of reactor are summarized (IAEA, 2004); (Table 1.11). In these cases such discharges were found not to lead to

bioaccumulation in marine biota (Warwick et al., 2003) because HTO form should be rapidly excreted.

Table 1.11: Typical tritium discharge rates ($GBq \cdot GW(e)^{-1} \cdot a^{-1}$) from various types of reactor (IAEA, 2004).

	Gaseous effluent	Liquid effluent
PWR (zircaloy cladding)	3.70×10^{3}	2.59×10^{4}
BWR	1.85×10^{3}	3.70×10^{3}
HWR	7.40×10^{5}	1.85×10^{5}
GCR	7.40×103	1.11×10^{4}

Note: These data were compiled from IAEA report (IAEA, 2004)

Discharge limits for radioisotopes are established in most countries in accordance with the recommendations of the International Commission on Radiological Protection (ICRP). These limits differ from one site to another depending on assumptions made on the nature of the effluent and on the environment into which the discharges are made.

GE Healthcare (Amersham), Cardiff, UK

Radiolabelled organic compounds are widely used in life sciences and are synthesized by a small number of companies worldwide. Tritium is the commonest and most favoured radiolabel used and following the synthesis of specific compounds many by-products and intermediates would be collected for interim storage before finally being disposed under liquid waste authorization. Since 1982 Amersham has been permitted to discharge these liquid effluents containing the tritium-bearing compounds (often called organically bound tritium or OBT e.g. alcohols, sugars, peptides etc) into the Severn Estuary although recent revisions to the authorizations have occurred resulting in greatly reduced discharges.

Sellafield, Cumbria, UK

Sellafield, now about to be stopped operation and decommissioned, is a nuclear processing and former electricity generating site, close to Seascale on the coast of the Irish Sea in Cumbria, England. Facilities at the site include the THORP (Thermal Oxide Reprocessing Plant) nuclear fuel reprocessing plant and the Magnox nuclear fuel reprocessing plant. It is also the site of the remains of Calder Hall, the world's first commercial nuclear power stations, now being decommissioned, as well as some other older nuclear facilities. In the UK, the greatest discharge to the environment of tritium arises from the nuclear fuel reprocessing plant and associated facilities at Sellafield, which discharged about 1600 TBq

in liquid forms and 90 TBq in gaseous forms in 2005 (EA et al., 2006); (Table 1.12). Reprocessing will give the largest releases of tritium in the nuclear fuel cycle. During reprocessing of LWR spent fuel, ca 63% of tritium will be released to the atmosphere and 13.5% will be released in aqueous waste streams (Kullen et al., 1975).

La Hague, France

The COGEMA La Hague site is a nuclear fuel reprocessing plant of AREVA in La Hague on the French Cotentin Peninsula that currently has nearly half of the world's light water reactor spent nuclear fuel reprocessing capacity. It treats spent nuclear fuel from France, Japan, Germany, Belgium, Switzerland, Italy and the Netherlands. The fuel reprocessing plant at La Hague routinely discharges radioactive waste, including tritium to the English Channel.

Table 1.12: Authorised ^{3}H discharges from various sources (HPA, 2007)

Annual discharges of tritium in UK (2005)	
Sellafield	1600 TBq (liquid) 90 TBq (gaseous)
Nuclear Power stations	2300 TBq (99% of liquid)
Chapelcross ^{3}H production plant	300 TBq (gaseous)
GE Healthcare, Cardiff (now ceased operations)	330 TBq (90% of gaseous and some as organic compounds)
Devonport and Faslane dockyards	0.27 TBq
Non-UK discharges	
La Hague, France	12000 TBq (in 2003)
Savannah River, USA	8440 TBq (pa peak to atmosphere in early 1960s) 930 TBq (pa peak liquid in early 1970s)
Ontario Power generation, Canada	1200 TBq (tritiated water in 2005)

iv) Decommissioning

The main difference of nuclear decommissioning to the dismantling of a conventional facility is the possible presence of radioactive or fission product in a nuclear facility that requires special precautions. A wide range of nuclear facilities have been decommissioned so far including nuclear power plants, research reactors, isotope production plants. During decommissioning of nuclear power plants, a range of wastes containing tritium generated both as a fission product and as activation product will be produced.

Decommissioning works typically involve the extensive clean out, refurbishment or demolition of buildings and other facilities, and remediation of the land. As a result, large

volumes of potentially radioactive waste materials will be generated which require accurate characterization prior to waste sentencing. The International Atomic Energy Agency (IAEA) has defined three options for decommissioning, the definitions of which have been internationally adopted (www.world-nuclear.org):

Immediate Dismantling (or Early Site Release/Decon in the US): This option allows for the facility to be removed from regulatory control relatively soon after shutdown or termination of regulated activities. Usually, the final dismantling or decontamination activities begin within a few months or years, depending on the facility. Following removal from regulatory control, the site is then available for re-use.

Safe Enclosure (or Safestor(e)): This option postpones the final removal of controls for a longer period, usually in the order of 40 to 60 years. The facility is placed into a safe storage configuration until the eventual dismantling and decontamination activities occur.

Entombment: This option entails placing the facility into a condition that will allow the remaining on-site radioactive material to remain on-site without the requirement of ever removing it totally. This option usually involves reducing the size of the area where the radioactive material is located and then encasing the facility in a long-lived structure such as concrete, that will last for a period of time to ensure the remaining radioactivity is no longer of concern.

v) Potential future source (fusion reactor)

The experimental fusion research reactor, JET (Joint European Torus) or the new ITER (International Thermonuclear Experimental Reactor; under construction), is also a potential tritium source and is likely to become more significant in the future as the best fuel for fusion is currently considered to be a mixture of deuterium and tritium. Deuterium can be derived from water which is abundant and available everywhere and tritium can be produced from neutron irradiation of lithium, which is plentiful in the Earth's crust.

$$^{6}_{3}Li + {}^{1}n \rightarrow {}^{4}_{2}He + {}^{3}_{1}H$$

Fusion reactors generate energy by nuclear fusion reactions; energy is released when the nuclides of hydrogen combine. The natural product of the fusion reaction is a small amount of helium, which is harmless to life and does not contribute to global warming. However more concern is tritium due to some amount of tritium will be continually produced during normal operation but it is difficult to retain completely. There would be no acute danger, but

the cumulative effect on the world's population from a fusion economy could be a matter of concern.

$$^{2}_{1}H + {}^{3}_{1}H \rightarrow {}^{4}_{2}He + {}^{1}_{0}n + 17.6MeV$$

Several lithium ceramic materials such as Li_2O, $LiA1O_2$, Li_2ZrO_3 and Li_4SiO_4 are considered as breeding materials in the blanket of a D-T fusion reactor. For this reason, tritium is also produced via fast neutron irradiation by a blanket surrounding a fusion reactor in the nuclear fusion fuel cycle (Nishikawa et al., 1997).

Table 1.13: ^{3}H discharges from fusion reactors

Fusion inventories	
Tokamak Fusion Test Reactor (Princeton)	Site limit 1680 TBq (5g) 37000 TBq processed over 3 years (100g)
Joint European Torus, Culham	Maximum inventory 7200 TBq (20g)
ITER, Cadarache (planned)	?

These data were compiled from the Meeting of Radiological Protection of tritium (Goodhead, 2009)

1.3 Tritium forms

Tritium is ubiquitous in the environment and can occur as $T_{2\ (g)}$, $HTO_{\ (l)}$, and OBT (organically bound tritium) which are classified as exchangeable or non-exchangeable bound organic tritium. In the marine environment, it most commonly occurs as $HTO_{(l)}$ (NCRP, 1985). The radiological significance of tritium is dependent on the chemical form of the tritium molecule.

HT (Tritiated hydrogen gas, T_2 or possibly DT)

Tritium exists a gas (T_2 or $^{3}H_2$) at standard temperature (273.15 K) and pressure (1 bar) and rapidly combines with oxygen to form a liquid, tritiated water T_2O or partially tritiated HTO. Though tritium is discharged as HT or HTO form in the environment, most of tritium in the environment exists in the HTO form. Tritium gas would be easily converted to tritiated water in the atmosphere in the presence of a suitable catalyst (Roesch, 1950). Altitude has a pronounced influence on the occurrence of tritium in the atmosphere where HT is the dominant form in the region from 10 to 40 km (NCRP, 1979).

HTO (Tritiated water vapour)

Tritiated water (HTO) is a form of water where the usual hydrogen atoms are replaced with tritium and is the most common form of tritium in the environment (NCRP, 1979). It is also

called tritium oxide, or T_2O or ^3H_2O. Tritiated water is diluted and dispersed on its release into the marine environment and has been used as a radiotracer for large-scale ocean circulation (Jenkins and Rhines, 1980). HTO is potentially more radiotoxic than HT because it may be retained for a greater period of time in the human body in this form (Ware and Allott, 1999). A previous study determined that in the range 25 to 80°C, the vapour pressure of HTO is less than H_2O and HTO has a higher boiling point (100.76°C) than H_2O (Price, 1958).

OBT (Organically bound tritium)

Organically bound tritium (OBT) is defined as a tritium atom that is bound to a carbon, sulfur, oxygen and nitrogen atom in an organic molecule by an exchange or enzymatically catalyzed reaction (Diabate and Strack, 1993). It is commonly considered that organic tritium can be divided into two fractions such as an exchangeable fraction and a non-exchangeable fraction (Lang and Manson, 1960; Mann, 1971; Epstein et al., 1979; Grinsted and Wilson, 1979; Guenot and Belot, 1984; Sweet and Murphy C.E, 1984).

Exchangeable form: Exchangeable organic tritium is essentially bound to oxygen, nitrogen, phosphorus or sulphur atoms in an organic molecule, and is in isotopic equilibrium with free water and local atmospheric moisture.

Non-exchangeable form: By contrast, non-exchangeable organic tritium is mainly bound to carbon atoms (C-^{3}H) in the material, thus it is tightly held to the organic structure because C-^{3}H bounds are stable (Diabate and Strack, 1993). It can only be released on decomposition of the organic compounds.

Depending on the researcher, OBT is either only the non-exchangeable fraction of the organic tritium or the totality of the organic tritium. Today, it seems that OBT is only the non-exchangeable fraction (Pointurier et al., 2004). OBT is also classified as hydrophilic OBT and hydrophobic OBT depending on the association with water. Hydrophilic OBT may remain in solution, whilst hydrophobic OBT is more likely to be absorbed onto colloids or suspended particle and consumed by biota, where it can be incorporated into biomass or excreted (Blaylock *et al*, 1986). OBT has a longer average residence time in biota than HTO and leads to a higher dose coefficient.

1.4 Applications for tritium

Firearms optics: Tritium is used in combat and hunting grade firearm optics, including the ACOG (Advanced Combat Optical Gunsight), to provide an illuminated graticule for low-light condition aiming (Waller et al., 2007).

Self-powered lighting: The emitted electrons from small amounts of tritium cause phosphors to glow so as to make self-powered lighting devices called tracers which are now used in watches and exit signs (Guthrie, 1972). It is also used in certain countries to make glowing keychains, and compasses. These take the place of radium, which can cause bone cancer, and so has been banned in most countries for decades.

Nuclear weapons: Tritium is used in thermonuclear weapons to obtain higher yields, either through boosting of fission, or through thermonuclear fusion. Increasing yield from tritium injection is due to increased fission efficiency from the high flux of neutrons produced by the fusion of tritium (IAEA, 2004). However, as tritium quickly decays and is difficult to contain, many thermonuclear weapons contain lithium instead, because the high neutron fluxes will produce tritium from the lithium when the bomb detonates. Lithium and tritium are used in many thermonuclear weapons.

Controlled nuclear fusion: Tritium is an important fuel for controlled nuclear fusion in both magnetic confinement and inertial confinement fusion reactor designs (Alizadeh, 2006). The experimental fusion reactor ITER and the National Ignition Facility (NIF) will use Deuterium-Tritium (D-T) fuel. The D-T reaction is favored since it has the largest fusion cross-section (~ 5 barns peak) and reaches this maximum cross-section at the lowest energy (~ 65 keV center-of-masses) of any potential fusion fuel.

Labeled radiopharmaceutical: Tritium is widely used as a radiolabel in radiopharmaceutical studies (Lockley, 2007). It has the advantage that hydrogen appears in almost all organic chemicals making it easy to find a place to put tritium on the molecule under investigation. It has the disadvantage of producing a comparatively weak signal. However, tritium is used as a transient tracer and has the ability to “outline” the biological, chemical, and physical paths (along with climate change) throughout the world oceans because of its evolving distribution. Tritium can thus be used as a tool to examine ocean circulation and ventilation and, for oceanographic and atmospheric science interests, is usually measured in Tritium Units where 1 TU is defined as the ratio of 1 tritium atom to 10^{18} hydrogen atoms (Okada and Momoshima, 1993).

1.5 Tritium in the environment

The importance of tritium distribution in the ecosystem in general and in food chains particularly has received attention with the increased use of atomic energy for peaceful purpose. Hydrogen is the most abundant element present in most materials, most is chemically bound as hydrocarbons, carbohydrates or water. If tritium is present in a material containing hydrogen, the tritium atoms will exchange with hydrogen atoms to form a tritiated molecule of the material. The tritium is oxidised to tritiated water (HTO) or isotopic exchange occurred with atmospheric water vapour at the temperature range *ca* 16~25°C (NCRP, 1979). Previous study demonstrated that tritium gas would be easily converted to tritiated water in the atmosphere (Roesch, 1950; Hemmer, 1954). When tritium atoms are formed by cosmic radiation, they have a high kinetic energy. The most probable reaction for tritium atoms is a collision with oxygen and subsequent reaction would be expected to yield HTO in the atmosphere (Harteck, 1954). HTO is easily evaporated and migrated in the atmosphere and reached to the land and into ocean by precipitation and vapour exchange (Figure 1.3); (NCRP, 1979). The mean residence time of tritiated water vapour in the troposphere ranges from 21 to 40 days (Alizadeh, 2006).

Tritiated water reached to the earth crust by precipitation will be diffused into soil and eventually reaches the groundwater. This tritiated water will behave in a similar manner as typical water (NCRP, 1979). HTO can be absorbed into non-flowering plants (e.g. mosses, fungi and lichens) at a rapid rate because these plants freely exchange tissue-water with the atmosphere (Ichimasa et al., 1989; Daillant et al., 2004; Kim et al., 2008). Transfer of tritium into plants also occurs through stomata on the leaf surface and uptake of soil water via root (Murphy, 1993; Brudenell et al., 1997). Direct uptake of HTO vapour via stomata is more significant than HTO absorption from precipitation and soil water (Brudenell et al., 1999). HTO absorbed into a plant could be participated in photosynthetic reactions; photosynthesis is the main process that HTO is transferred to organically bound tritium (Rudran, 1988). Organically bound tritium (OBT) in plants occurs in either exchangeable or non-exchangeable form (Diabate and Strack, 1993; Hill and Johnson, 1993). Exchangeable OBT behaves in the same manner as HTO. Most of OBT, however, is in the non-exchangeable form and has considerably longer retention time compared to HTO (Guenot and Belot, 1984). OBT, created by plants, are migrated to biota include human via food chain which has longer residence time in human body than HT, inhaled mainly via human respiration systems or the skin.

Tritium also reaches to the ocean by a variety of pathways; directly by precipitation and discharge from nuclear facility and indirectly from runoff of groundwater. Tritium in the oceans becomes rapidly distributed in the thin surface layer of relatively warm, 50-100 m deep, known as the mixed layer (EPA, 1974). Residence time in the mixed layer is about 22 years at 75 m depth, but this varies with geographic location. In contrast to the oceans, most lakes are mixed vertically each year (Coyle, 1978). Tritium is absorbed by marine organism by respiration and consumption via food chain by which tritiated water will be changed to organic compounds combined to molecular structure of the organism. These organic compounds, especially those in planktonic unicellular algae, enter the food chain rapidly. Previous study showed that the significance of organically synthesized tritium to other organisms (Patzer et al., 1974). Tritium is also excreted by biota, with the overall residence time depending on the size of the organism and the composition of the tritiated molecule (Diabate and Strack, 1993). With this procedure, the possibility of tritium accumulation in the marine ecosystem will be arisen. Previous study demonstrated that in the sediment environment in salt marsh and mud flat sediments in the Severn estuary, ^{3}H accumulation by OBT discharges from Amersharm plc. is reported (Morris, 2006). Tritium is transported around estuary with suspended fine sediment by tidal currents. OBT is relatively immobile in the sediment; it has been retained for over 10 years. ^{3}H has an extended residence time in the estuary, with potential for re-release by erosion into the estuary in the future.

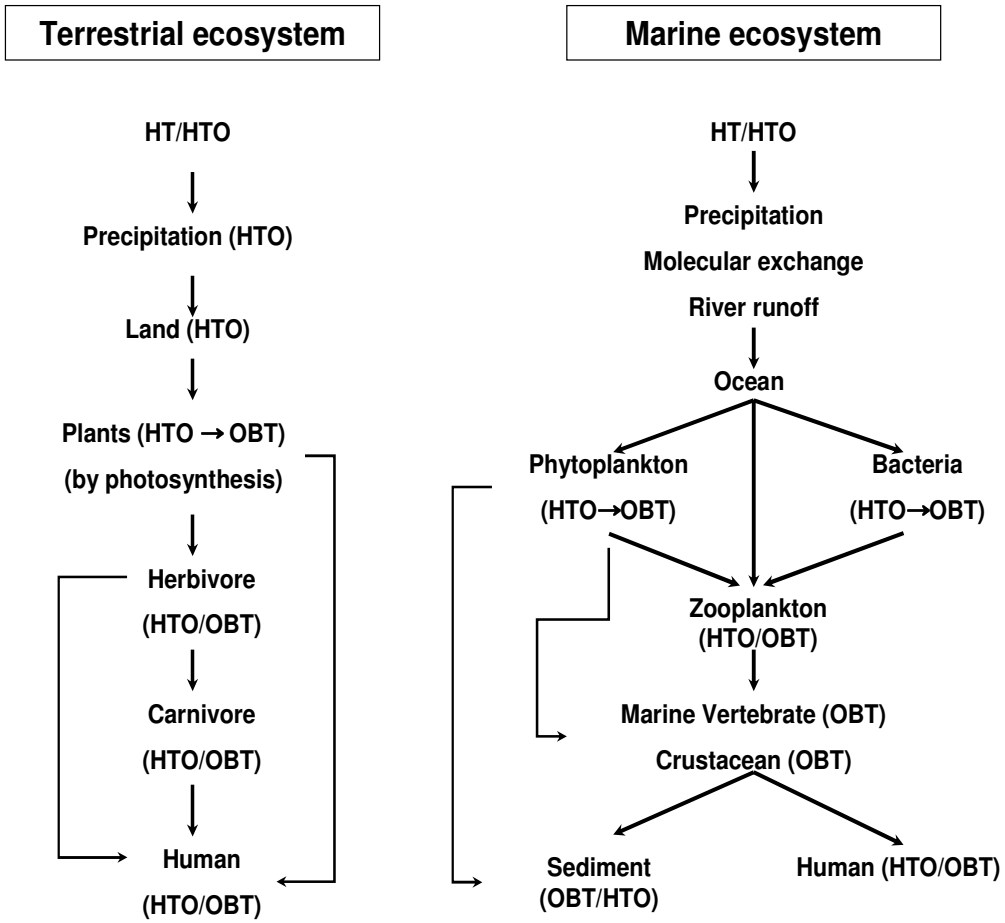

Figure 1.3: Comparison of terrestrial and marine ecosystems on ^{3}H circulation.

1.6 Radiological aspects of tritium

Recently internal tritium dosimetry has paid particular attention to tritiated water (HTO) and organic compound containing tritium (Harrison, 2009). Tritium has no gamma radiation and the low energy of the β particle suggests that there would be little radiation damage from the decay, although specific activity of tritium is high. However, tritium beta decay produces an average ionisation density significantly higher than that of high energy gamma (i.e. about 4.7 keV/μm compared to 0.22 keV/μm) (Lambert, 2009). Theoretical and experimental data suggest that tritium will be more biologically effective than either hard X-rays or gamma per unit dose (Lambert, 2009). Therefore, establishment of the effectiveness of tritium for human risk relative to reference radiation is required (Goodhead, 2009). For improving safety and reliability of tritium handling facilities, more investigation of the radiation hazards of tritium is required.

In order to appreciate the biological effects of ionizing radiation and associated hazards radiation dose or absorbed radiation dose is measured which is a measure of the energy, in joules, deposited per unit mass of tissue, in kilogrammes. The unit of absorbed dose is the **Gray (GY)**:

1 Gray = 1J in 1 kg.

However not all ionizing radiations cause the same biological damage. Different types of radiation have different effects on tissue (biological effectiveness) for the same amount of energy absorbed. Alpha particles and neutrons are more damaging than beta particles, gamma and X-rays. The equivalent dose is a measure of the radiation dose to allow different biological effects of radiation. To allow this, a radiation weighting factor (W_R, sometimes refereed to as quality factor, Q) is used which takes into account the ability of the radiation to produce biological damage. The unit of equivalent dose is the sievert (Sv) and takes account of the radiation weighting factor. For beta, gamma and X radiation, W_R is one and therefore for tritium, the equivalent dose is equal to the absorbed dose.

Equivalent dose (Sv) = absorbed dose × W_R

For protection purpose, effective dose is used which takes account of the sensitivity of different tissues to radiation and for this tissue weighting factors (W_T) is used. The sum of the effective doses of the various organs gives the effective whole body dose and the weighting factor (W_T) for whole body is one.

Effective dose (Sv) = equivalent dose × W_T

Tritium has some unusual features that increase average ionization density (linear energy transfer; LET), short ranges of electron tracks, non-uniformity of absorbed dose, cell hit frequencies per unit dose, nuclear transmutation (^{3}H to ^{3}He), isotopic mass difference ratio and different molecular form (e.g. HTO and OBT; exchangeable, non-exchangeable). Previously conventional radiation protection dosimetry have not incorporated most of these unusual features of tritium (Goodhead, 2009). However, experimental measurements of relative biological effectiveness (RBE) may incorporate some of these in various ways. The RBE is calculated as the dose of a reference radiation, usually 250 kV x rays or ^{60}Co gamma rays, required to produce the same biological effect as was seen with a test dose (D_T) of another radiation (NCRP, 1979). The major factors affecting RBE are absorbed dose, linear energy transfer (LET), dose rate, fractionation, distribution, oxygenation of the exposed tissue. The value of the RBE provides a quantitative index of the effectiveness per unit of absorbed dose of any radiation.

$$RBE = \frac{Dose\ from\ reference\ \ radiation}{Dose\ from\ test\ \ radiation, D_T}$$

Recent radiological research data however using relative biological effectiveness (RBE) indicate that the weighting factor (W_R) for tritium is higher than one, though the ICRP recommendation of weighting factors for tritium is one. Because the tritium effect in human organs may not only be considered as a beta irradiation effect (HPA, 2007; Goodhead, 2009; Harrison, 2009; Lambert, 2009). The decay of tritium incorporated with biological molecules (e.g. DNA and RNA) may produce more hazardous genetic and remote effects (NCRP, 1979; Alizadeh, 2006; Lambert, 2009). Therefore, weighting factor (W_R) of 2 is suggested for tritium (Harrison et al., 2002; HPA, 2007; Harrison and Day, 2008; Harrison, 2009).

In the environment, tritium can be taken up by all hydrogen-containing molecules, distributing widely on a global scale. Tritium can be incorporated into humans through respiration as HTO or in gaseous form, ingestion of HTO or OBT via food and drinking water, and diffusion through skin by exposure. When humans are exposed to tritium as tritiated water by inhalation ingestion or skin absorption, it is rapidly distributed to intracellular and extracellular water. The kinetics of tritium movement throughout the body follow those of water, a small fraction of the intake becomes organically bound tritium. The transfer of tritium to organic compounds following intake of tritiated water occurs mainly by exchange of tritium from body water with the labile hydrogen of organic fractions (Smith and Taylor, 1969). Due to the body's ready adsorption of tritium in the form of tritiated

water, exposure to tritiated water in air is up to 25,000 times more hazardous than exposure to gaseous tritium (HT, DT, and T_2); (Coyle, 1978; ICRP, 1979).

The effect of tritium in human organs and tissues may not only be considered as a beta-irradiation effect. Transformation of cell-incorporated tritium into inert helium breaks H-bonds in cells. For instance, it breaks H-bonds in such unique biological molecules as DNA and RNA, causing harmful genetic and remote consequences (Petti and McCarthy, 2000). To understand the dose distribution due to internal exposure following intake of tritium, the distribution of activity concentration and the decay behavior of tritium after exposure in human are required. However, it is difficult to measure the tritium directly, the tritium has to be estimated from tritium concentrations in bioassay samples (e.g. urine, blood, exhaled water, feces, hair etc). After consumption of tritium, as a HTO or OBT form, is excreted by humans as two or three components with half-times of around 10 days, 21 to 76 days and 280 to 550 days (NCRP, 1979; Harrison et al., 2002). The biological half-time of HTO and OBT are dependent on the ingestion path of tritium and the mass of biota which is related to the size of the body water pool (Hill and Johnson, 1993; Hodgson et al., 2005). ICRP (ICRP, 1993) have calculated a higher dose coefficient for OBT than HTO and the activity is excreted in two components of 10 days and 40 days half-time respectively (Table 1.14).

Table 1.14: Retention half-time and dose coefficients for tritium ingestion as HTO and OBT at different ages

Age	Retention half-time (day)		Dose coefficients (Sv $Bq^{-1}\times10^{-11}$)	
	HTO	OBT	HTO	OBT
3 months	3	8	6.3	12
1 year	3.5	15	4.8	12
5 years	4.6	19	3	7.3
10 years	5.7	26	2.3	5.7
15 years	7.9	32	1.8	4.2
Adults	10	40	1.8	4.2

These data were compiled from the Meeting of Radiological Protection of tritium (Harrison, 2009).

In most countries the guidelines for radionuclides in drinking water are based on international radiation protection methodologies, including recommendations of the International Commission on Radiological Protection (ICRP) and the World Health Organization (WHO). Current guidelines suggest that high concentrations of ^3H are required to constitute a radiological hazard (annual limit of intake is 3 GBq)(ICRP, 1979). The legal

limits for tritium in drinking water are variable depended on the country (Table 1.15) However, since appreciable quantities are released into the environment, monitoring of ^{3}H activity in effluent streams and environmental waterways is of considerable importance (Warwick et al., 2003).

Table 1.15: The legal limits for tritium in drinking water

Country	**Regulatory limits (Bq/L)**
Canada	7000
USA	740 (Safe Drinking Water Act, USA)
EU	Investigate limit of 100
UK	100
Finland	30,000
Australia	76,103
Russia	7,700
Switzerland	10,000
World Health Organization (WHO)	10,000

These data were compiled from World Nuclear Association reactor database (http://db.world-nuclear.org/reference/reactorsdb_index.php)

1.7 References

Alizadeh E. 2006. Environmental and safety aspects of using tritium in fusion. Journal of Fusion Energy 25: 47-55.

Alvarez LW, Cornog R. 1939. Helium and Hydrogen of Mass 3. Physical Review 56: 613.

Bonka H. 1979. Production and emission of tritium from nuclear facilities and the resulting problems. In Behaviour of tritium in the Environment, IAEA Report No. STI/PUB/498. IAEA, IAEA Report No. STI/PUB/498, Vienna, Austria.

Brudenell AJP, Collins CD, Shaw G. 1997. Dynamics of tritiated water (HTO) uptake and loss by crops after short-term atmospheric release. Journal of Environmental Radioactivity 36: 197-218.

Brudenell AJP, Collins CD, Shaw G. 1999. Rain and the effect of washout of tritiated water (HTO) on the uptake and loss of tritium by crops and soils. MAFF report for project RP 0175. Imperial College, London.

Camplin WC. 1992-1995. Radioactivity in surface and coastal waters of the British Isles, 1990 to 1994 (Annual reports). MAFF Directorate of Fisheries Research, Lowestoft.

Coyle PE. 1978. Proceeding of the symposium Behaviour of Tritium in the Environment, San Francisco, 1978, p. 139, IAEA-SM-232/102.

Craig H, Lal D. 1961. The production rate of natural tritium. Tellus 13: 85.

Daillant O, Kirchner G, Pigree G, Porstendorfer J. 2004. Lichens as indicators of tritium and radiocarbon contamination. Science of The Total Environment 323: 253-262.

DEFRA. 2002. DEFRA (2002). Radioactive Wastes in the UK: A summary of the 2001 inventory. Department for Environment, Food and Rural Affairs, London, UK, p14.

Diabate S, Strack S. 1993. Organically Bound Tritium. Health Physics 65: 698-712.

EA. 2003. Radioactive Substances Act 1993. Proposed decision document on the application made by Amersham plc for a variation to the authorisation to dispose of radioactive wastes from its premises at: The Maynard Centre, Foresr Farm, Whitchurch, Cardiff. Reference AB1363/BK3328., Environment Agency Wales, Cardiff.

EA, EHS, FSA, SEPA. 2003. Radioactivity in food and the environment, 2002. RIFE Report 8. Environment Agency, Environment and Heritage Service, Food Standards Agency and Scottish Environment Protection Agency, Preston, Belfast, London and Stirling.

EA, EHS, FSA, SEPA. 2004. Radioactivity in food and the environment, 2003. RIFE Report 9. Environment Agency, Environment and Heritage Service, Food Standards Agency and Scottish Environment Protection Agency, Preston, Belfast, London and Stirling.

EA, EHSNI, FSA, SEPA. 2006. Radioactivity in Food and the Environment, 2005. RIFE 11. Lowestoft, Centre for Environment, Fisheries and Aquaculture Science.

Eisenbud M, Gesell T. 1997. Environmental Radioactivity. Academic Press, London.

EPA. 1974. U.S. Environmental Protection Agency, Environmental Radiation Dose Commitment: An application to the nuclear power industry, Report No. EPA-520/4-72-002.

Epstein S, Yapp CJ, hall JH. 1979. The determination of the D/H ratio of non-exchangeable hydrogen in cellulose extracted from aquatic and land plants. Earth Planet. Sci. Lett. 30: 241-251.

FSA, SEPA. 1996. Radioactivity in food and the environment, 1995. RIFE Report 1. Food Standards Agency and Scottish Environment Protection Agency, London and Stirling.

FSA, SEPA. 1997. Radioactivity in food and the environment, 1996. RIFE Report 2. Food Standards Agency and Scottish Environment Protection Agency, London and Stirling.

FSA, SEPA. 1998. Radioactivity in food and the environment, 1997. RIFE Report 3. Food Standards Agency and Scottish Environment Protection Agency, London and Stirling.

FSA, SEPA. 1999. Radioactivity in food and the environment, 1998. RIFE Report 4. Food Standards Agency and Scottish Environment Protection Agency, London and Stirling.

FSA, SEPA. 2000. Radioactivity in food and the environment, 1999. RIFE Report 5. Food Standards Agency and Scottish Environment Protection Agency, London and Stirling.

FSA, SEPA. 2001. Radioactivity in food and the environment, 2000. RIFE Report 6. Food Standards Agency and Scottish Environment Protection Agency, London and Stirling.

FSA, SEPA. 2002. Radioactivity in food and the environment, 2001. RIFE Report 7. Food Standards Agency and Scottish Environment Protection Agency, London and Stirling.

Goodhead DT (2009) Should we be concerned about tritium? Radiological Protection of Tritium, Harwell, UK.

Grinsted MJ, Wilson AT. 1979. Hydrogen isotopic chemistry of cellulose and other organic material of geochemical interest. New Zeal. Journal of Science 22: 281-287.

Guen BL (2009) Impact of tritium around nuclear power plants in France Radiological Protection of Tritium, Harwell, UK.

Guenot J, Belot Y. 1984. Assimilation of ^{3}H in photosynthesizing leaves exposed to HTO. Health Physics 47: 849-855.

Guthrie DG. 1972. Self-powered emergency signs. Lighting Equipment News 6: 8,10-18,10

Harolf TPJ, Baker DA. 1985. Tritium production, release and populations doses at nuclear power reactors. Fusion Technology 8: 2544-2550.

Harrison J, Day P. 2008. Radiation doses and risks from internal emitters. Journal of Radiological Protection 28: 137-159.

Harrison JD (2009) Where do we stand? Radiological Protection of Tritium, Harwell, UK.

Harrison JD, Khursheed A, Lambert BE. 2002. Uncertainties in dose coefficients for intakes of tritiated water and organically bound forms of tritium by members of the public. Radiation Protection Dosimetry 98: 299-311.

Harteck P. 1954. The Relative Abundance of HT and HTO in the Atmosphere. The Journal of Chemical Physics 22: 1746-1751.

Hemmer BA. 1954. Ion-pair yield of the tritium-oxygen reaction. The Journal of Chemical Physics 22: 1555-1558.

Hill RL, Johnson JR. 1993. Metabolism and dosimetry of tritium. Health Physics 65: 628-647.

HMSO (1993) Radioactive Substances Act 1993 Substances of Low Activity (SoLA) Exemption order (London: HMSO). HMSO Publication Centre, pp 44.

Hodgson A, Scott JE, Fell TP, Harrison JD. 2005. Doses from the consumption of Cardiff Bay flounder containing organically bound tritium. Journal of Radiological Protection 25: 149-159.

Hou X. 2005. Rapid analysis of ^{14}C and ^{3}H in graphite and concrete for decommissioning of nuclear reactor. Applied Radiation and Isotopes 62: 871-882.

HPA. 2007. Review fo Risks from Tritium: Report of the independednt Advisory Group on ionising Radiation.

Hunt GJ. 1979-1989. Radioactivity in surface and coatal waters of the British Isles, 1977 to 1988 (Annual reports). MAFF Directorate of Fisheries Research, Lowestoft.

IAEA. 1994. Classification of radioactive waste, SAFETY SERIES No. 111-G-1.1.

IAEA. 2004. Technical reports series no. 421, Management of waste containing tritium and carbon-14 (printed by the IAEA, in Austria, 2004).

Ichimasa M, Ichimasa Y, Yagi Y, Ko R, Suzuki M, Akita Y. 1989. Oxidation of Atmospheric Molecular Tritium in Plant-Leaves, Lichens and Mosses. Journal of Radiation Research 30: 323-329.

ICRP. 1979. International Commission on Radiological Protection, Limits for intakes of radionuclides by workers, ICRP Publication 30, part 1, Annals ICRP 2 (3/4), 1979.

ICRP. 1993. Age-dependent doses to members of the public intakes of radionuclides: Part 2. Ingestion dose coefficients (publication 67). International Commision on Radiological Protection, Oxford.

Jenkins WJ, Rhines PB. 1980. Tritium in the Deep North-Atlantic Ocean. Nature 286: 877-880.

Johnson JR, Brown RM, Myers DK. 1992. An overview of research at CRNL on the environmental aspects, toxicity, metaboilism and dosimetry of tritium. Radiation Research 50: 197:211.

Kaufman S, Libby WF. 1954. The natural distribution of tritium. Physica Review 93: 1337-1344.

Kim SB, Workman WJG, Davis PA, Yankovich T. 2008. HTO and OBT concentrations in a wetland ecosystem. Fusion Science and Technology 54: 248-252.

Kullen BJ, Trevorrow LE, Steindler MJ. 1975. Tritium and noble-gas fissin products in the nuclear fuel cycle. II. Fuel Reprocessing Plants, Report No. ANL-8135 (Argonne National Laboratory, Lemont, Illinois).

Lambert B (2009) The risks from tritium: a review of the experimental data. Radiological Protection of tritium, Harwell, UK.

Lang ARG, Manson SG. 1960. Tritium exchange between cellulose and water accessibility measurements and effects of cyclic drying. Journal of Chem 38: 373-387.

Lockley WJS. 2007. Tritium chemistry: history, current status and future developments; a brief review. Journal of Labelled Compounds & Radiopharmaceuticals 50: 256-259.

Lucas LL, Unterweger MP. 2000. Comprehensive review and critical evaluation of the half-life of tritium. Journal of Research of the National Institute of Standards and Technology 105: 541-549.

Mann J. 1971. Deuteration and tritiation in: Bikales, N.M. and Segal, L., Editors, 1971. Cellulose and Cellulose Derivatives, Part IV, Wiley-interscience, New York, pp. 89-116.

McKay HAC (1980) "Background considerations in the immobilization of volatile radionuclides ", management of gaseous wastes from nuclear facilities. In: IAEA (ed). IAEA, pp 59-78.

Mitchell NT. 1968-1978. Radioactivity in surface and coastal waters of the British Isles, 1967 to 1978 (Annual reports). MAFF Directorate of Fisheries Research, Lowestoft.

Morris JE. 2006. Organically bound tritium in sediments from the Severn estuary, UK. Ocean and earth science, Southampton.

Murphy CE. 1993. Tritium Transport and Cycling in the Environment. Health Physics 65: 683-697.

NCRP. 1979. Tritium in the environment. National Council on Radiation Protection and Measurement, Bethesda, Maryland.

NCRP. 1985. A bandbook of radioactive measurements procedures. national Council on Radiation Protection and measurement, Bethesda, Maryland.

NDA, DEFRA. 2008. The 2007 UK Radioactive Waste Inventory.

NIREX, DEFRA. 2005. The 2004 UK Radioactive Waste Inventory.

Nishikawa M, Baba A, Kawamura Y. 1997. Tritium inventory in a LiAlO2 blanket. Journal of Nuclear Materials 246: 1-8.

Okada S, Momoshima N. 1993. Overview of Tritium - Characteristics, Sources, and Problems. Health Physics 65: 595-609.

Patzer RG, Moghissi AA, McNelis DN. 1974. Accumulation of tritium in various species of fish reared in tritiated water, Report No. EPA 680/4-74-001 (National Environmental Research Center, Las Vegas, Nevada).

Petti D, McCarthy K. 2000. Progress in US fusion safety and environmental activities over the last decade. Fusion Technology 37: 1-23.

Pointurier F, Baglan N, Alanic G. 2004. A method for the determination of low-level organic-bound tritium activities in environmental samples. Applied Radiation and Isotopes 61: 293-298.

Price AH. 1958. Vapour Pressure of Tritiated Water. Nature 181: 262-262.

Roesch WC. 1950. P-10 Chemical Equilibria, USAEC Report No. HW(Hanford Atomic Products Operation, Richland, Washington).

Rudran K. 1988. Significance of in vivo organic binding of tritium following intake of tritiated water. Radiation Protection Dosimetry 25: 5-13

Sinclair WK. 1987. Tritium in the environment, NCRP Report No. 62.

Sweet CW, Murphy C.E, Jr. 1984. Tritium deposition in pine trees and soil from atmospheric releases of molecular tritium. Environ. Sci. Technol. 18: 358-361.

Tarlton S. 2006. World nuclear industry Handbook. Wilmington Media Ltd.

UNSCEAR. 1977. Sources and effects of ionizing radiation. United Nation Publications, Vienna.

UNSCEAR. 2000. Sources and effects of ionising radiation. United Nations Scientific Committee on the Effects of Atomic Radiation. Report to the General Assembly, Volume 1: Sources. United Nations, Vienna.

Villa M, Manjon G. 2004. Low-level measurements of tritium in water. Applied Radiation and Isotopes 61: 319-323.

Waller EJ, Cole D, Jamieson T. 2007. Release limits and decontamination efficacy for tritium: Lessons learned outside nuclear power operations. Health Physics 93: S155-S159.

Ware A, Allott RW. 1999. Review of methods for the analysis of total tritium and organically bound tritium. National Compliance and Assessment Service, NCAS/TR/99/003, Lancaster.

Warwick PE, Croudace IW, Howard AG, Cundy AB, Morris J, Doucette K (2003) Spatial and temporal variation of tritium activities in coastal marine sediments of the Severn estuary (UK). In: Warwick P (ed) Environmental Radiochemical Analysis II, pp 92-103.

Wegemans C. 1991. The Nnuclear Fission Process. CRC Press.

Chapter 2

Review of method

2 Review of method

2.1 Introduction

Tritium is predominantly produced via neutron capture by stable deuterium or lithium or via ternary fission (0.01% fission yield). The nuclide is therefore associated with nuclear power stations and in particular with those reactors moderated using deuterated water (such as the Canadian CANDU and UK SGHWR reactors). In addition, ^{3}H is widely used as a radiolabel in radiopharmaceutical studies, as a fuel in nuclear fusion reactors and thermonuclear weapons. Tritium contamination of plant and laboratories is therefore widespread, with ^{3}H penetrating into most construction materials. Atmospheric releases of ^{3}H can result in a general low level contamination of buildings in the immediate vicinity of the plant. Authorised releases of ^{3}H from nuclear and radiopharmaceutical facilities occur and monitoring of foodstuffs and water effluent in the vicinity of establishments are required to protect human health and the environment from the contaminants due to direct exposure and bioaccumulation via food chain. In addition, the requirement for ^{3}H measurement in a wide range of materials has increased in recent years mainly as a result of accelerated nuclear decommissioning programmes with its associated waste sentencing requirements.

The measurement of a beta-emitting radionuclide may be performed either through the detection of the emitted beta particle (radiometric technique) or through direct measurement of the number of atoms of the specific radionuclide that are present in the sample (mass spectrometric technique). In general, radionuclides with relatively short half-lives and correspondingly high specific activity (activity per unit mass of the isotope in Bq/g) are best determined using a radiometric technique. Radionuclides with long half-lives and low specific activity are best determined using a mass spectrometric technique.

The decay energy of a pure beta-emitting radionuclide is shared between the emitted beta particle and an anti-neutrino. The beta particle emitted is not monoenergetic but may possess energies ranging from nearly the total decay energy (E_{max}) to near zero (L'Annunziata, 2003). Beta spectrometry is therefore of limited application in the quantitative determination of a mixture of beta-emitting radioisotopes. Qualitative detection and quantitative measurement of a pure beta emitter must therefore consist of a specific chemical separation of the element of interest followed by the measurement of the beta activity associated with that purified fraction (Warwick, 1999). Tritium is a pure low-energy beta emitter (E_{max} = 18.6 keV), quantitative measurement of ^{3}H must be therefore consist of collection of representative samples, isolation of ^{3}H from the sample and measurement of the ^{3}H activity. The detection

systems used to measure the beta activity of final purified fractions are discussed in Section 2.3. The specific chemical separations employed and sample preparations are reviewed further in Section 2.4.

A wide range of detectors has been used for the determination of total tritium activity. Detectors include ion chambers, soild scintillation detectors, surface barrier detectors and gas-flow proportional counters. The ^{3}He ingrowth method (Mass spectrometry) can also be used to determine ^{3}H activities in extremely low level samples (<0.1 TU; Clarke *et al.,* 1976); however, the lengthy ingrowth period of 3~6 months is a disadvantage of this method. One of the most versatile counting systems for the detection of tritium is liquid scintillation counting. Tritium activities are expressed in tritium units (TUs), Becquerels (Bq) (the SI unit of radioactivity) or Curies (Ci) (a pre-SI unit of radioactivity), where 1 TU = 1 ^{3}H atom per 10^{18} H atoms (Okada and Momoshima, 1993), which is equivalent to 0.118 Bq HTO per litre of H_2O, and 1 Ci = 3.7×10^{10} Bq (NCRP, 1979).

2.2 Analytical method for tritium analysis

2.2.1 Ionisation chambers

Ionisation chambers are the most widely used instruments for measuring gaseous forms of tritium in air (Pretzsch et al., 1985; Purghel and Valcov, 2000; Purghel et al., 2005; Worth et al., 2005); (Figure 2.1). This device requires an electrically polarized ionization chamber, suitable electronics and a method for moving the gas sample through the chamber, such as a pump (Colmenares, 1974). Tritium decays to ^{3}He by the ejection of a beta particle, generated by the decay of tritium, which ionizes the surrounding gas. The number of ions produced due to the loss of energy of the beta particle is a function of the type of gas. A sample of gas is collected in the ionization chamber and the ionization current is measured. The resulting chamber ionization current is proportional to the quantity of tritium in the gas. Chamber volumes typically range from a tenth to a few tens of litres, depending on the required sensitivity (L'Annunziata, 2003). Modern electronic technology has solved the problems of measuring small ionization currents in small volumes, as a result the volume of ionization chambers has been reduced over the years from 50 L down to 1 or 2 L (IAEA, 2004). Although most ionization chambers are the flow-through type that requires a pump to move the gas, a number of facilities use open window or perforated wall chambers. These chambers, which employ a dust cover to protect the chamber from particulates, allow the air or gas to penetrate through the wall to the inside chamber without a pump. These instruments are used as single point monitors to monitor rooms, hoods, glove boxes and ducts.

Figure 2.1: Ionisation chamber (Overhoff Tech. Corp)

2.2.2 Gas-flow proportional counters

Gas proportional counters can be used for tritium monitoring in air (Szarka et al., 1979; Aoyama and Watanabe, 1985; Aoyama, 1990; Sakuma et al., 2005; Tuo et al., 2007); (Figure 2.2). A sample of the gas to be monitored is mixed with a counting gas and passed through a proportional counter tube, in which the pulses caused by the decay of tritium are counted. Proportional counter monitors can be used for most gas monitoring applications and are also used to measure surface contamination. Disadvantages of the conventional proportional counters are the need for a counting gas and a rather short operation range. Aoyama (1990) demonstrated the tritium monitoring method in air by flow-through proportional counters using air as a counting gas. The counters need no counting gas other than the sampled air. The electronic equipment attached to the counting system comprises pulse height discrimination, anticoincidence shielding, and background compensation. With this way, it is possible to detect and measure tritium in an external gamma background and also in alpha and beta background originating from other gaseous radioactive materials in the air sample. It was reported that a lower detection limit of 0.005Bq/cm^3 in the presence of natural background can be obtained in a counting time of 1 minute. Also, a wide range up to 5000 Bq/cm^3 (up to six decades) can be managed by this system (L'Annunziata, 2003).

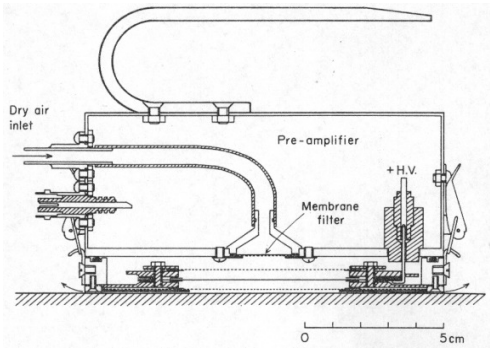

Figure 2.2: Prototype air proportional counter for ^{3}H on surfaces (Aoyama and Watanabe, 1985)

2.2.3 Mass spectrometers

Mass spectrometric techniques can be used for tritium measurement either by direct measurement of the tritium atoms or through indirect assessment of the ^{3}He produced by decay. Direct tritium analysis by mass spectrometry is limited to high activities involved in fusion and weapons research. In most cases, quadrupole mass spectrometers are utilized due to their favorable resolution at low mass units (IAEA, 2004). Magnetic sector, quadrupole and drift tube mass spectrometers are used to measure the individual components that make up the gas being measured. A sample of the gas is introduced at low pressure (approximately 1–5 kPa) into a chamber and ionized. The ions produced are then measured by a means that discriminates on ionized atom mass. The number of ions produced at each mass is measured and is proportional to the partial pressure of the component in the gas sample (IAEA, 2004). The limit of detection for tritium is 0.25ppm (55 MBq/g) (Price and Aslett, 1995). Accelerator mass spectrometry (AMS) is also used for quantitative tritium measurement (Suter et al., 2000). AMS has the advantage of requiring only small quantities of sample size in the mg range. The detection limit for a 2mg sample using AMS is approximately 70 TU (8.3Bq) although electrolytic enrichment would potentially allow further reduction. Measurement of ^{3}He ingrowth by mass spectrometry can also be used to determine ^{3}H activities in extremely low levels (<0.1TU) samples (Clarke et al., 1976; Beyerle et al., 2000). However, the lengthy ingrowth period of ~6 months is a major disadvantage to this method. A novel approach to ^{3}He measurement has been investigated using a less complex and cost effective helium leak detector mass spectrometer (Demange et al., 2002). The disadvantage of this method is that mass spectrometers require a large capital investment and in some cases may not be cost effective. Quadrupole mass spectrometer is much less expensive.

2.2.4 Scintillation crystal detectors

Scintillation crystal detector systems are used to measure the total mole percent of tritium in a gas sample, independent of the chemical composition of the tritium in the gas (HT, DT, T_2 and CH_xT_y) (Ellefson et al., 1995); (Figure 2.3). A gas sample is introduced into a measurement chamber at low pressure, generally less than a few torr (approximately 1–5 kPa). The chamber contains a scintillation crystal (CaF_2[Eu]) which is exposed to the tritium as it decays and emits light. The dynode photomultiplier or PMT is placed in direct contact with the solid scintillation crystal to ensure optimum light transmission from the scintillation crystal to the PMT. The PMT photocathode produces photoelectrons when bombarded with photons of visible light, which are accelerated toward a positively charged dynode in the PMT. A series of several additional dynodes in the PMT produce multiple secondary

electrons and the magnitude of the final current pulse collected after the series of dynode amplifications. The current is proportional to the mole percent tritium contained in the gas sample. Crystal scintillation detection is generally used to measure the mole percent of tritium in gases containing high concentrations of tritium.

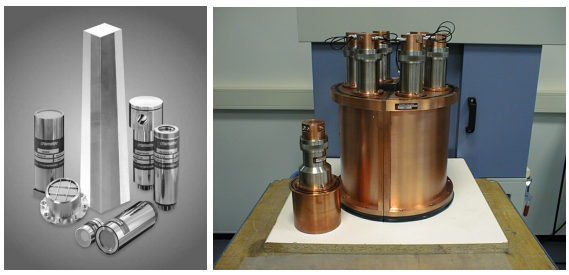

Figure 2.3: Various scintillation crystal (left) and detector (right)

2.2.5 Flow scintillation analysis (FSA)

Flow scintillation analysis (FSA) is the application of scintillation detection methods for the quantitative analysis of radioactivity in a flowing system (Figure 2.4). The advantage of the FSA is that can provide real-time analysis with minimal fluor cocktail consumption (L'Annunziata, 2003). Three basic detector types have been applied to flow scintillation analysis; (1) the liquid scintillator (homogeneous) flow cell (Sigg et al., 1994), (2) the solid scintillator (heterogeneous) flow cell (Hofstetter, 1995), and (3) the gamma-cell. The liquid scintillator (homogeneous) flow cell and the solid scintillator (heterogeneous) flow cell are used for ^{3}H measurement. The liquid scintillator (homogeneous) flow cell is the most commonly used for ^{3}H measurement due to high efficiency (20-60%) and absence of the liquid absorption of radionuclide-labelled compounds onto solid scintillator (L'Annunziata, 2003).

The liquid scintillator (homogeneous) cell consists of fine Teflon tubing coiled flat between two transparent windows at either side of the coiled tubing and the cell is inserted between the two photomultiplier tubes (PMTs) of the flow scintillation analyser. This has traditionally been referred to as the homogeneous method, because the effluent stream and fluor cocktail are homogeneously mixed, and the flow cell is referred to as a liquid cell. However, a previous study (Rapkin, 1993) comparing the sensitivity and accuracy of low-level analysis by liquid scintillation counting and flow scintillation analysis demonstrated that liquid scintillation counting of extracted ^{3}H provided more sensitivity and accuracy of radioactivity measurement compared to a flow scintillation analysis.

The solid scintillator (heterogeneous) flow cell consists of fine beads or particles of an insoluble solid scintillator placed within the Teflon tubing of the flow cell. The tubing is coiled flat between two transparent windows and placed between the faces of two PMTs. The HPLC (high performance liquid chromatography) radioactive effluent stream flows through the cell and makes intimate contact with the solid scintillator beads. This approach is referred to as the heterogeneous method, because the effluent stream and scintillator do not mix and the flow cell is called a solid cell (L'Annunziata, 2003). The photomultiplier tubes will detect and measure the scintillation light photons emitted from the solid scintillator, and the radioactivity determined during the sample residence time in the flow cell according to conventional liquid scintillation technology as described in Chapter 2.3.

Various types of solid scintillators are used to make up the heterogeneous cell including yttrium glass, polycrystalline cerium-activated yttrium silicate [YSi(Ce)], europium-activated calcium fluoride [CaF_2(Eu)], cerium-activated lithium glass, and plastic scintillator. The detection efficiency for α/β emitters will depend on the scintillator. The counting efficiencies are low for low energy β emitters (e.g. ^{3}H with 1.5-5%) and good for the intermediate energy β emitters such as ^{14}C (45-85%). High energy β emitters are detected with higher counting efficiency (L'Annunziata, 2003). A major advantage of the heterogeneous flow cell is that the sample in the HPLC (High Performance Liquid Chromatography) effluent is not mixed with flour cocktail. The whole effluent stream can be subsequently analysed by on-line nuclear magnetic resonance or mass spectrometry. In addition, chemical quench, which is a problem with the liquid homogeneous flow cell, does not occur with the solid (heterogeneous) cells. Therefore high salt, buffer solutions or pH gradients used in HPLC eluates will not affect counting efficiency. The only problem is that, due to the high surface area structure of the solid scintillator packed in these flow cells, compounds undergoing separation in the HPLC often bind reversibly or irreversibly onto the scintillator. This can result in high backgrounds and peak broadening.

Figure 2.4: Solid scintillation detector assembly (left) and flow scintillation analyser (PerkinElmer, model C150F00)

2.2.6 Solid state detectors

A range of solid-state based detectors have been designed specifically for surface tritium measurement and can broadly be split into two types (McGann et al., 1988), those intended for biomedical applications - imaging of tritium labelled compounds (Gordon et al., 1994; Barthe et al., 2004; Mettivier et al., 2004; Deptuch, 2005) and those designed for tritium monitoring in the environment (Shah et al., 1990; Wampler and Doyle, 1994; Shah et al., 1997; Scott Willms et al., 2005). The former are usually limited to detection of the high activities used in radiolabels. However the detector developed by Gordon et al. (1994) was tested with some low concentration standards of in the order of 2.66 Bq per spot and proved to be effective at measuring these concentrations. Instruments utilize either avalanche photodiodes (APDs) or PIN-photodiodes (Figure 2.5). McGann et al. (1988) produced an APD based tritium monitor with a detection limit of 33Bq/cm^2 (500 second count time) and a detection efficiency of 15%. More recent advances in the technology used to manufacture APDs have allowed increased detection efficiencies of 50% for tritium (Shah et al., 1997).

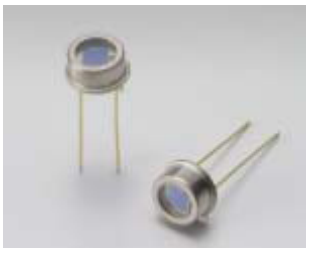

Figure 2.5: PIN-photodiodes

2.2.7 Liquid scintillation counting

Liquid scintillation counting was developed primarily to overcome the low counting efficiency problems associated with measurement low-level beta emitters in gas-filled detectors. However it is now widely used to measure both beta and alpha emitters (Figure 2.6). Beta-emitters may be measured with high counting efficiency, typically >90% for intermediate to high energy beta emitters and low backgrounds, typically a few cpm (counts per minute) for modern low-level instruments. It has the advantage over proportional counting in that advanced energy discrimination is possible which enables the accurate determination of the activity of the analyte in the presence of other beta emitters. LSC is now commonly used for the following applications: measurement of natural series radionuclides, monitoring the environment for radionuclide releases associated with nuclear fuel cycle activities (fuel enrichment, fuel fabrication, power generation, and fuel reprocessing facilities) and studying the rates of processes in the environment (e.g. ^{14}C dating and ground

water movement and dating using ^{3}H etc). More details of the liquid scintillation counting are reviewed further in Section 2.3.

Figure 2.6: Liquid scintillation counter (PerkinElmer 1220)

2.2.8 Miscellaneous

Portable room air monitors: Several portable room air monitors are used and their capabilities and ranges vary as a function of the manufacturer and the purpose for which they were designed (Figure 2.7). It is convenient in some activities to have the capability to connect a small hose to the monitor so that it may be used to detect tritium leaks around equipment.

Figure 2.7: Portable tritium monitor (Overhoff Tech. Corp, model 200SB)

Fixed station room air monitors: Fixed station monitors are designed to be installed in fixed locations and used to monitor the room air tritium concentration (IAEA, 2004). Depending on the manufacturer, they may have several ranges, may be equipped with one or two alarm set points and may have audible as well as visual alarms.

Glovebox atmosphere monitors: Glovebox monitors may be open mesh or closed ionization chambers and are designed to monitor the higher levels of tritium inside glovebox containment systems (IAEA, 2004). Ionization chambers operated in a dry glovebox environment have a tendency to become more contaminated with tritium than those operated in air, which can lead to false high readings and require frequent cleaning or the adjustment

of alarm set points. Gold plated and virtual wall ionization chambers have been used to reduce this tendency for monitor contamination.

Hood and exhaust duct air monitors: Hood and exhaust duct air monitors are similar to fixed station monitors in range and characteristics except that they generally have larger ionization chambers to increase the sensitivity of the monitor (IAEA, 2004).

2.2.9 Specialized instrumentation

Remote field tritium analysis system: The Field Deployable Tritium Analysis System (FDTAS) was developed for the remote, in situ analysis of tritium in surface waters and groundwater (Singh et al., 1985; Cable et al., 1997; Hofstetter et al., 1998; Hofstetter et al., 1999); (Figure2.8). The system uses automated liquid scintillation counting techniques and has sufficient sensitivity to measure tritium in water samples at environmental levels (10 Bq/L (~270 pCi/L) for a 100 min count) on a near real time basis. The prototype FDTAS consists of several major components: a multi-port, fixed volume sampler; an on-line water purification system using single use tritium columns; a tritium detector employing liquid scintillation counting techniques; and serial communications devices (IAEA, 2004). The sampling and water purification system, referred to as the autosampler, is controlled by a logic controller preprogrammed to perform a well defined sampling, purification and flushing protocol. The tritium analyser contains custom software in the local computer for controlling the mixing of the purified sample with a liquid scintillation cocktail, for counting and for flushing the cell. An external standard is used to verify system performance and for quench correction. All operations are initiated and monitored at the remote computer through standard telephone line communications (IAEA, 2004).

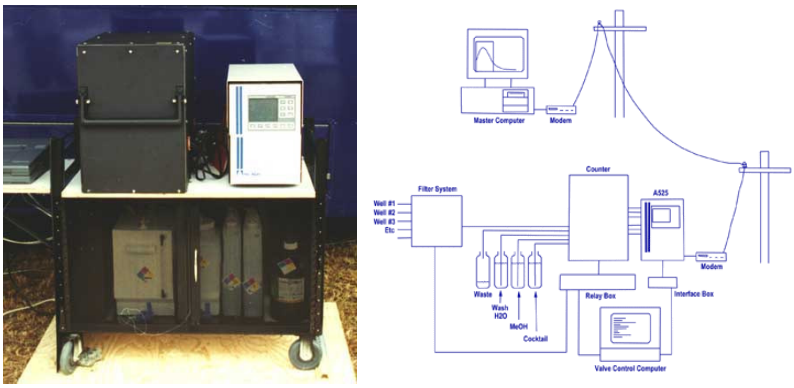

Figure 2.8: Field-deployable tritium analysis system and (left) and schematic diagram (right); (Cable et al., 1997).

Surface activity monitor (SAM): A new surface activity monitor (SAM) for measuring tritium on metal (electrically conducting) and non-metal (electrically non-conducting) surfaces has been recently developed (Shmayda et al., 1997; Shmayda et al., 2002); (Figure 2.9). The monitor detects tritium on the surface and in the near surface regions by means of primary ionization in air due to the outward electron flux from the contaminated surface. The resulting ion pairs are measured by imposing an electric field between the contaminated surface and a collector plate (IAEA, 2004). A simple theoretical model relates the total tritium concentration on the surface to the measured current. Application of the surface activity monitor on a variety of non-conducting surfaces (e.g. paper, concrete, granite and wood) has been demonstrated. Currently, the SAM is commercially available in two models, QP100 and QP200, which have measurement ranges of 0–200 nCi/cm^2 and 0–200 μCi/cm^2, respectively.

Figure 2.9: Surface activity monitor (TYNE engineering Inc., model 7001-SAM-001)

Breathalyser: It is an automatic monitor dedicated to health physics and radiation biology applications using ionization chamber (Figure 2.10). The tritium in breath monitor measures levels of exhaled tritium within 1 min of sampling, thus saving considerable time and effort in the monitoring process (IAEA, 2004). This rapid assessment has a sensitivity level of 0.3 μCi/m^3, which may be sufficient for identifying cautionary levels of in-body tritium.

Figure 2.10: Tritium breathalyzer (TYNE engineering Inc., model 7008-B-001). The breathalyser comprises a large (3 litre) ion chamber to maximize sensitivity while minimizing the time taken to fill with breath. It is compensated for gamma and background radiation by the provision of a second and identical chamber (http://www.tyne-engineering.com).

Table 2.1: Methods of tritium measurements

Method	Type of sample	Limit of detection	Brief details of method	Advantages	Disadvantages	References
Scintillation crystal detectors	Gas sample	3.7 Bq/ml	The light pulse produced in the scintillation crystal is either counted or is used to produce a current that is proportional to the mole percent tritium contained in the gas sample	High efficiency. Solid scintillator often re-usable	Producing a waste stream	Ellefson et al, 1995; Rathnakaran et al, 2000; Falter and Bauer, 1992
Proportional counter	Air monitoring	1-10 Bq/cm^2	A sample of the gas to be monitored is mixed with a counting gas and passed through a proportional counter tube, in which the pulses caused by the decay of tritium are counted	Real time ^{3}H measurement in air	Require a supply of counting gas	Szarka et al, 1979; Aoyama, 1990
Ionisation chamber	Air monitoring	0.003~0.037 Bq/cm^3	The number of ions produced due to the loss of energy of the beta particle is a function of the type of gas. A sample of gas is collected in the ionization chamber and the ionization current is measured.	Their design being relatively simple, cheap and compact	Chamber volumes range from a tenth to a few tens of litres, depending on the required sensitivity.	Purghel & Valcov, 2000; Worth et al, 2005
Liquid scintillation counting	Colourless liquids	~0.005 Bq/g	Samples and solvent are mixed with scintillators, which release energy as light in response to an α or β decay event. This light is measured by photomultiplier tubes.	Low background (~1 cpm). Relatively efficient detection of low energy β emitters such as ^{3}H	Interference by other radionuclides if present. Chemiluminescence. Quenching (self-absorption) can prevent ^{3}H detection.	Kallman, 1950; Reynolds et al, 1950; Dyer, 1974; L'Annunziata, 2003a
^{3}He ingrowth	Water samples	0.1 TU (for water samples (~40g) sealed for 6 months to 1 year)	Degassed water sample is sealed in a (low He permeability) glass bulb for a length of time. The ^{3}He/^{4}He ratio of the water is measured using a noble gas mass spectrometer. This allows the amount of ^{3}He attributed to tritium decay to be calculated.	Very low detection limit. Simple analytical procedure.	Length of time for in-growth of ^{3}He (~6 months).	Clarke et al, 1976

Remote field tritium analysis system	Water sample	10 Bq/L for a 100 min count	All operations are initiated and monitored at the remote computer through standard telephone line communications. The system uses automated liquid scintillation counting techniques	Remote, in situ analysis of tritium in surface waters and groundwater	Relatively high detection limit	Singh et al., 1985; Cable et al., 1997; Hofstetter et al., 1998, 1999
Flow scintillation analysis	Effluent water sample	4 Bq/ml	Application of scintillation detection methods for the quantitative analysis of radioactivity in a flowing system.	Real-time analysis with minimal fluor cocktail consumption	Relatively low sensitivity compared to the liquid scintillation counting. The solid scintillators provide limited detection sensitivity with a counting efficiency of only 0.185 for ^{3}H	Sigg et al, 1994
Solid state detector	Surface measurement	0.17 Bq/cm^2 (96 hrs count) ~33 Bq/cm^2 (500s count)	Instruments utilize either avalanche photodiodes (APDs) or PIN-photodiodes. McGann et al. (1988) produced an APD based tritium monitor with a detection limit of 33Bq/cm^2 and a detection efficiency of 15% (500 second count time).	More recent APDs have allowed increasing detection efficiencies of 50% for tritium.	Long counting time required to increase detection limit.	McGann et al., (1988); Shah, 1997
Surface activity monitor (SAM)	Surface measurement (e.g. metal etc)	0–200 nCi/cm^2	The monitor detects tritium on the surface and in the near surface regions by means of primary ionization in air	A variety of non-conducting surfaces (e.g. paper, concrete, granite and wood) has been demonstrated.	Only surface monitor for tritium	Shmayda et al., 1997, 2002
Breathalyser	Breath monitor	0.3 μCi/m^3	It is an automatic monitor dedicated to health physics and radiation biology applications using ionization chamber.	This rapid assessment of ^{3}H in breath <1 min of sampling, thus saving considerable time and effort in the monitoring process.	Limited usage for breath monitoring	IAEA, 2004

2.3 Liquid scintillation counting (LSC)

2.3.1 Basic theory

Liquid scintillation counting (LSC) is suitable for the quantitative measurement of alpha, beta and some electron capture radionuclides. The development of liquid scintillation counting is attributed to Kallman (Kallman, 1950) and Reynold (Reynolds, 1950), who demonstrated that homogeneous solutions of samples with organic scintillators or fluors emit light photons on interaction with α and β-particles which can be measured (Dyer, 1974). A sample containing radioactivity is mixed with scintillation cocktail which contains solvent, scintillator and emulsifier. Since the majorities of radionuclides are present in aqueous solution and are not miscible with aromatic solvents, the emulsifier provides a homogeneous mixture of solvent and aqueous phases allowing efficient energy transfer. The aromatic solvent absorbs most of the energy which enables energy associated with radioactive decay to be converted into light photons that are subsequently detected by photomultiplier tube (PMT) as an electric pulse (L'Annunziata, 2003). Energy from radiation associated with the sample, construction material or background/cosmic radiation excites the scintillant solvent. This solvent molecule then interacts with an aromatic organic compound known as a scintillator. The excitation energy is transferred to the scintillator molecule raising the molecule to an excited energy state and de-exciting the solvent molecule. The scintillator then de-excites to produce the ground state scintillator molecules and a photon of light with a wavelength between 350 and 400 nm. The intensity of the light pulse is proportional to the original particle energy (L'Annunziata, 2003). Most modern counters incorporate a sample changing mechanism allowing the counter to be used continuously with limited operator interaction. The incorporation of a multi-channel analyser (MCA) allows spectrometric information to be recorded that can aid in the identification of the radioisotopes as well as permitting the deconvolution of signals from relatively simple mixtures of radioisotopes.

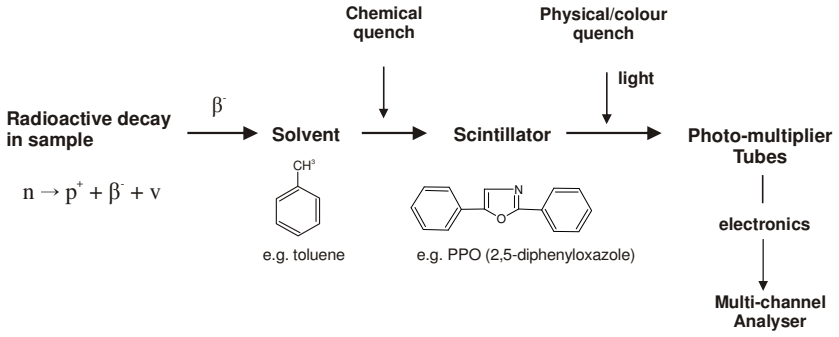

Figure 2.11: The basic mechanism of liquid scintillation counting (after Dyer, 1974). This figure compiled from Morris (2006)

Counting is usually carried out in borosilicate glass, plastic or quartz vials and the choice of vial affects the counting characteristics. Any natural radioactivity in the vial will increase the background count rate and for this reason, glass vials with a low ^{40}K content are desirable. Silica and Teflon vials are commonly used for radiocarbon dating and have been demonstrated that to produce significant background reductions. However, their main disadvantage is the comparatively high cost compared to low ^{40}K glass vial. Plastic vials are commonly used and produce a lower background count than glass vials, but have the disadvantage that the solvents used in scintillants may permeate the vials resulting in variation in counting efficiencies during long counting times.

Liquid scintillation counters count the number of scintillation events to provide a count rate (CPM) of the sample. The sample count rate is dependent on efficiency of converting decay energy into light flashes. The most common interferences affecting the count rate in liquid scintillation counting are associated with quench and chemiluminescence. Chemiluminescence is the emission of light photons within a scintillation cocktail due to a chemical reaction rather than nuclear radiation. This is short lived and declines with time (typically 1-4 hours), therefore it can be eliminated by careful choice of scintillant or by leaving the samples in the dark following preparation prior to counting to permit the decay of the luminescence.

2.3.2 Quench in liquid scintillation counting

Quench affects the scintillation photon intensity and efficiency of detection of radionuclides in the liquid scintillation cocktail. The effects of quenching (chemical, physical and colour) require that the counting efficiency should be determined for each sample (see Section 2.3.3) and the effects of each type of quenching need to be corrected for separately. The detection of light photons produced from the interaction of ionizing radiation with the scintillant cocktail can be adversely affected by the photons interacting with other compounds, contaminants present prior to reaching the photomultiplier tubes. In addition, the energy of the solvent can be lost as heat before scintillation process. This reduction in efficiency of the detection system is known as quench. The effect of quench is to decrease the number of decay events registered by the photomultiplier tubes and to shift the energy spectrum of a nuclide to a lower energy region as fewer photons are registered for a given particle energy and hence decrease counting efficiency. Quenching most strongly affects weak β-emitters such as ^{3}H and ^{14}C (L'Annunziata, 2003). There are three main types of quenching: (1) chemical quench, the presence of one or more chemicals in the fluor cocktail that is mixed

with the sample, (2) color quench, a colored substance that comes from the sample and (3) physical quench, physical interference. The collective effect of quench is a reduction in the number of photons detected or produced.

(1) Chemical quench

Chemical quench occurs when non-fluorescent molecules absorb the energy of the solvent molecules instead of the scintillant molecules where the energy is lost as heat instead of light. Chemical quench results in the excitation energy being absorbed before it can produce light in the scintillation process and reduced the number of light flashes. Any compound without an aromatic structure will produce quench, but the strongest quenching agents are halogenated compounds; salts, bases, acids, alcohols and water have less quenching effect and are described as diluters (L'Annunziata, 2003).

A wide range of compounds can induce chemical quench. Chemical quench due to dissolved oxygen can be removed by bubbling nitrogen through the sample. However, when using after-pulsing corrections a reduction rather than an increase in counting efficiency may be observed after purging of the O_2. In most other cases quenching is limited by sample purification prior to liquid scintillation measurement and by correction of the final measurement for any unavoidable quenching that is still occurring.

(2) Colour quench

The colour quench occurs after the fluorescence stage by absorbing photons of light in the scintillation vial before they can be detected by the PMT. Colour can be produced either by reactions between the scintillator solution and the sample, or by the introduction of a coloured sample (Dyer, 1974). These quench phenomena is an attenuation of the photons of light and reduce the number scintillation event of the sample that are detected by the LSA. As scintillators usually emit in the blue region of the visible spectrum the greatest quenching is observed with red compounds.

(3) Physical quench

Another cause of quench occurs when the light photon is produced but is physically prevented from reaching the detector by an obstruction such as particulate matter suspended in the mixture. In physical quenching the light photons produced are prevented from reaching the photomultiplier tubes by a physical barrier. Physical quench also occurs if the sample adsorbs onto the surface of the vial and is therefore not intimately mixed with the solvent. Any ionising radiation emitted cannot interact with the solvent under these

conditions. Furthermore, if the adsorbed sample is in intimate contact with the scintillant, the counting efficiency will still be significantly reduced as only those radiations emitted towards the contents of the vial will excite the solvent molecule whereas those radiated towards the vial wall are lost.

2.3.3 Counting efficiency of LSC

Even following chemical separation and purification of an analyte the degree of quench may still vary from sample to sample. The lower the energy of the decay, the greater is the effect of quench on the counting efficiency for beta emitting radionuclide. The degree of quench associated with each sample and hence the counting efficiency of each sample may be determined using one of a range of techniques. The most direct way of determining the counting efficiency for a sample is internal standard method; counts sample, then the sample is re-counted with a known amount of standard radionuclide spiked into the sample. The increase in count rate coupled with the activity of the added spike can be used to calculate the counting efficiency and then to determine the activity of the sample using the initial count-rate data. It is the most accurate way for environmental sample containing low activity. Disadvantage that the sample is counted twice and hence the technique is not suitable for large number of samples. For samples containing relatively high activities, the initial count rate of the sample may be used to determine the degree of quench using techniques such as the sample channels ratio (SCR) and spectral quench parameter of the isotope spectrum (SQP(I)) to determine counting efficiency. However, this is not readily applicable to low-level environmental samples where insufficient counts are detected to permit such a correction procedure or long counting time will be required to achieve acceptable levels of statistical accuracy.

Other quench correction methods include use of external standards to create Compton-derived events in the solvent which subsequently lead to scintillation. The apparent maximum (E_{max}) observed on the liquid scintillation Compton spectrum is dependent on the gamma photon energy (E_γ) of the external standard. The intensity of the scintillation depends on the degree of sample quench. By positioning an external gamma source adjacent to the sample vial and measuring the effect of the radiation from the external source on the scintillation mixture a measure of quench which is independent of the sample activity may be made. Liquid scintillation counters having multichannel analyzers generally use external standard quench correction methods using sample spectrum quench-indicating parameters. In Wallac instruments the External Standard Spectral Quench Parameter, SQP(E), is determined. The spectrum of the external standard is stored in a 1024 channel MCA and the

SQP(E) is described as the channel number which is the upper boundary to the spectrum containing 99.5% of the total counts of the spectrum. The SQP(E) value can then be used to determine the counting efficiency of the sample by comparison with standards of known counting efficiency and quench level. The advantages of this way are that many samples can be handled in a short time, original sample not altered and completely instrumental.

2.3.4 Liquid scintillation counter (used for present study)

Most commercial scintillation counters consist of two photomultiplier tubes that detect photons emitted from the vial via the scintillation process. The two photomultiplier tubes permit coincidence counting technique which reduces background counts significantly by eliminating thermal and electrical noise (L'Annunziata, 2003). The associated electronics register both the number of counts detected within a specified time (related to the total activity of the sample) and also the intensity of each photon burst. The intensity of the burst is directly related to the energy of the beta particle that initiated the scintillation process. By incorporating a multichannel analyser (MCA) into the electronic circuitry, the number of events with a given intensity can be recorded separately allowing an energy spectrum to be derived. In addition to the two photomultiplier tubes monitoring the sample vial, the Wallac 'Quantulus' has a further two photomultiplier tubes monitoring a chamber of scintillant gel (the guard chamber) directly above the sample chamber (Figure 2. 12). These are set to count in anti-coincidence with the sample photomultiplier tubes. Any cosmic events that would normally trigger the sample photomultiplier tubes will also initiate a scintillation event in the guard chamber. When an event is registered in both sets of photomultiplier tubes it is regarded as a cosmic background event and subsequently rejected. In this way the Wallac 'Quantulus' liquid scintillation counter can differentiate between genuine decay events originating in the sample and cosmic background events originating outside the counter. For these reasons the observed background for the Quantulus counter is superior to that provided by the Packard 2250CA and Wallac 1410 counters. Finally all liquid scintillation counters have associated lead shielding to reduce background derived from external radiation sources, sample changing mechanisms to permit the automatic counting of sample batches, and associated electronics and software to permit signal processing, data collection and manipulation.

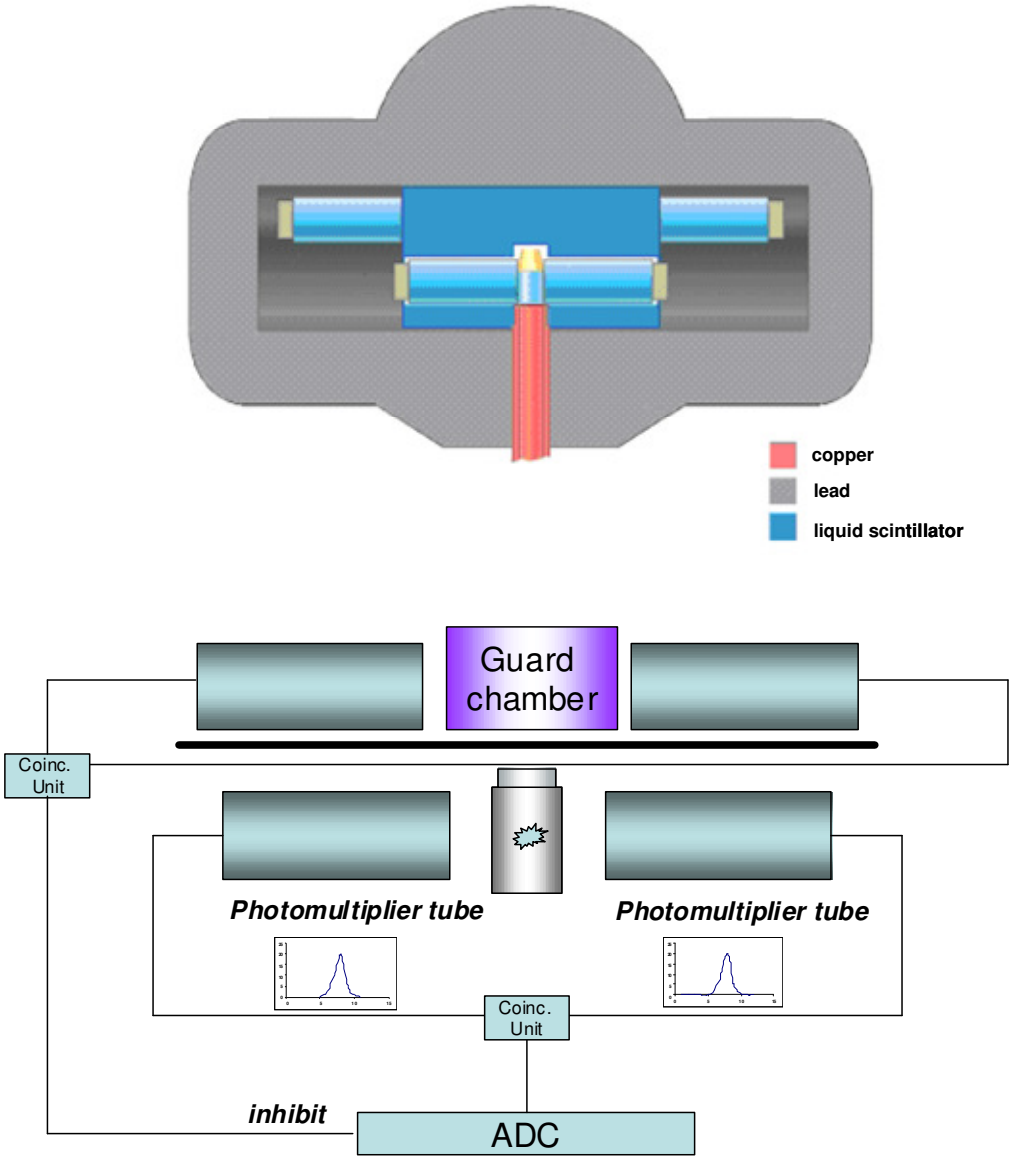

Figure 2.12: Anticoincidence guard detector and lead shield (above) and configuration of the Wallac 1220 'Quantulus' liquid scintillation counter. The diagrams are compiled from PerkinElmer and P E Warwick (pers.comm).

2.4 Preparation of sample for ^{3}H measurement by LSC

2.4.1 Sample preparation

Tritium in liquid or solid samples cannot be easily determined quantitatively by any kind of non-destructive analysis because its beta radiation energy is so low. Most non-aqueous samples must be treated chemically or physically to be suitable for liquid scintillation counting. Typically, three methods of preparation are employed for environmental tritium analysis of water which are direct addition, electrolytic enrichment and benzene synthesis. The method of sample preparation depends on the type of analysis to be performed. The primary objective of all sample preparation methods is to obtain a stable homogeneous solution suitable for analysis by liquid scintillation counting.

Direct addition or filtering

Relatively pure water samples (e.g. drinking water) can be counted without any purification steps. However, purification is required for samples with colour, organic present sample and contains interfering chemicals. The purified water sample is mixed with a scintillation cocktail and counted. Filtering of unclean water samples can produce clean water that is suitable for counting. This should be used only when the source of the sample is well known, such as a routinely sampled streams or wells where there is little chance of the presence of interferences. This type of cleanup should be used for samples in which mud or silt is suspended. An alternative would be to allow the suspended material to settle out and then decant the clean sample.

Electrolytic enrichment

This technique is based on the principle of selective isotopic enrichment using electrolysis. Water samples are distilled, then made slightly alkaline and placed in an electrolysis cell (Bogen et al., 1973b; Stencel et al., 1995). A constant current is applied to the cell, and electrolytic decomposition of the water reduces the sample to about 5% of the initial volume. Isotopic fractionation, due to the higher binding energy for ^{3}H compared with H, typically concentrates over 90% of the tritium in the remaining water. The concentrated sample is purified by distillation or vacuum distillation and counted by the direct addition method. This procedure usually takes 5 to 7 days to complete. Electrolytic enrichment is used for measuring low-level activity concentrations of tritium in environmental waters using a liquid scintillation counter because most tritium levels in water are lower than 1 Bq/l (Kim et al., 1996; Villa and Manjon, 2004; Plastino et al., 2007). The minimum detectable ^{3}H activity in water using electrolytic enrichment is 0.95 Bq/kg (Plastino et al., 2007).

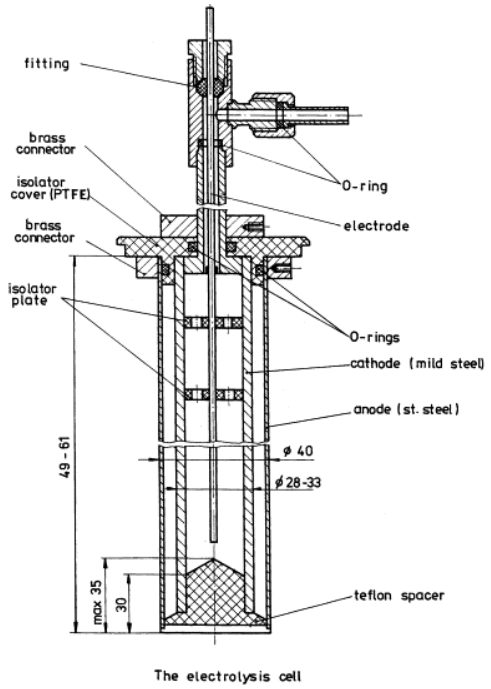

Figure 2.13: Longitudinal section through the electrolytic cell (Plastino et al., 2007)

Benzene synthesis

The water sample is added to calcium carbide in an evacuated reaction vessel and acetylene (C_2H_2) is generated (De Filippis and Noakes, 1991). The acetylene is then cyclotrimerized to high-purity benzene using a chromium or vanadium catalyst. For liquid scintillation counting of benzene, there is no requirement for a scintillation cocktail, as the fluors can be dissolved in solid form directly into the benzene. One sample per day can be handled, with the production of 8-15 ml of high-purity benzene. The method is only marginally more sensitive than direct addition and is not generally used.

2.4.2 Tritium purification/extraction method

A number of methods including freeze-drying, sub-boiling distillation, combustion and pressurised oxidative combustion (oxygen bomb) have been used for ^3H extraction of wide range of radioactive samples. Sample type (e.g. aqueous, metal, soil, concrete and plastics) and ^3H form of the sample are significant factors to decide method to extract ^3H from the sample. For solid samples contaminated with HTO, a rapid screening of ^3H activity can be achieved by leaching the sample with water and determining the ^3H activity in the leachate. However, for quantitative analysis and where the ^3H is present as a species other than free HTO a more aggressive approach is required to liberate the ^3H.

Freeze drying

Freeze-drying is used, both to analyse the condensate for tritiated water (Wickenden, 1993), and to obtain a dry residue for organically bound tritium extraction (Bogen et al., 1973a; Kim et al., 1992). Freeze drying is the process whereby a sample is frozen and then exposed to high vacuum (Figure 2.14). The water contained in the sample goes from the solid phase directly to a vapour (sublimation), and if the vapour is drawn through a cold trap, this vapour can be collected as pure water. Routine application of this process, for the purpose of extracting pure water for tritium analysis, is generally accomplished using custom glassware and cryogenic (liquid nitrogen, LN_2) cooling. The sample is first frozen solid using a dewar of LN_2; the dewar is then moved to a collecting flask (cold trap) and a high vacuum applied. The ambient room temperature supplies sufficient heat to accelerate the sublimation process, which may take several hours depending on the volume of water required. The water sample is collected in the cold trap as deposited ice and is melted and recovered for analysis.

Figure 2.14: Freeze drying system (SciQuip, model BETA 1.8 LD)

Distillation

Enrichment of tritium by distillation has been attempted. Water samples for ^{3}H determination normally require distillation prior to analysis. Typical or vacuum distillation is used to extract trititated water from liquids or solids with high water content (Figure 2.15). The sample is placed in the bottom of distillation rig and heated to 100°C. Discard the initial fraction of distillate (i.e. up to ca 20ml) because this fraction may contain low boiling point tritium-containing compounds. When the temperature has stabilized collect approximately 30 ml of distillate. Discard the remaining solution in the distillation flask because this fraction may contain high boiling point tritium-containing compounds (EA, 1999). The distillation carried out in the presence of sodium carbonate and sodium thiosulphate to prevent the transfer of inorganic ^{14}C and radioiodine respectively (IAEA, 1989).

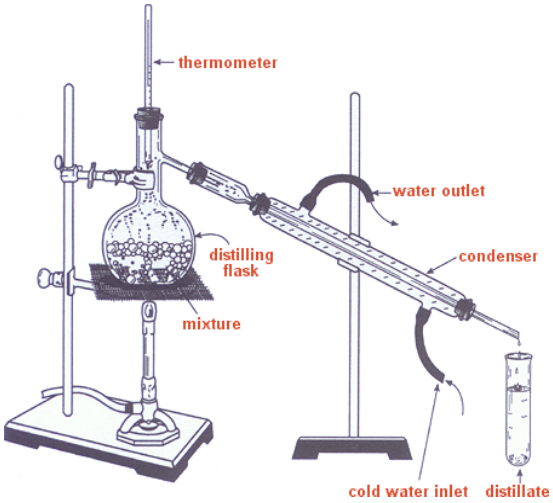

Figure 2.15: Typical distillation apparatus

Azeotropic distillation

An azeotropic is a liquid mixture that has a constant boiling point and whose vapour has the same composition as the liquid. Several compounds, such as toluene, benzene, and cyclohexane, form suitable azeotropes with water. Each is compatible with scintillation cocktails, immiscible in water, and cyclic in structure, making them resistant to exchange with external hydrogen. Azeotropic distillation provides a simple method for extracting water from a wide range of media (e.g. honey, milk, vegetation, soil, fish), for tritium analysis using liquid scintillation counting (Moghissi et al., 1973; Wickenden, 1993). This method allows the sample to be distillated at a lower temperature than conventional distillation (69~81°C compared to 100°C) and reduces the isotopic effects produced by the incomplete removal of water; isotopic exchange between HTO and H_2O can occur. However, there are significant health risks associated with benzene therefore, cyclohexane is the preferred compound due to the least hazardous and provides a suitable level of performance.

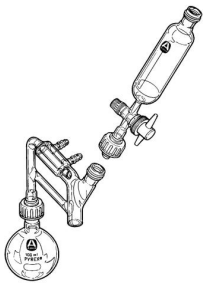

Figure 2.16: Azeotropic distillation apparatus (http://www.sigmaaldrich.com)

Table 2.2: Sample sizes and the quantity of benzene required for azeotropic distillation of various sample types (Moghissi et al., 1973)

Sample type	Mass (g) of sample	Volume (ml) of benzene
Soil	200	1300
Hay	50	400
Green chop	30	70
Urine	20	50
Animal & human tissue	30	150

Sub-boiling distillation

Sub-boiling distillation (Warwick et al., 1999) is used for the purification of river and effluent water samples prior to the determination of tritium by liquid scintillation counting (Figure 2.17). The outer annulus is filled with raw aqueous sample (ca 1cm depth), a watch glass is placed over the top and the whole unit is placed on a warm surface such as a hot plate (40-80°C) or oven. Water evaporates from the outer vessel, condenses on the underside of the cooler watch glass where it runs to the lowest point of the watch glass surface and subsequently collects in the inner vessel. To produce sufficient distillate for HTO analysis, 2-3 hours are needed. The technique requires less analyst set-up and supervision time than conventional distillation techniques. However it cannot be used for vegetation samples where azeotropic distillation, freeze drying or combustion are more appropriate. If samples are likely to be contaminated, they can either be distilled with $KMnO_4$ and Na_2O_2 to oxidise organic residues and remove trace contaminants, or hold back carriers can be incorporated into a conventional distillation rig to trap other radionuclides (Ware and Allott, 1999).

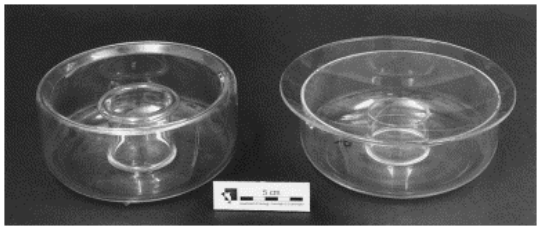

Figure 2.17: Diagram showing the annular sub-boiling distillation unit (Warwick et al., 1999).

Wet oxidation

Wet oxidation has been employed for the determination of organically bound tritium (Ware and Allott, 1999). A previous study has reviewed the use of strong acids and bases in this

method (Mahin and Lofberg, 1970). Acrylamide gels, frequently used for electrophoretic separation of proteins and nucleic acids, may be digested with hydrogen peroxide. Blood, which is troublesome in scintillation counting because of the strong colour quenching of the pigment, may be digested with perchloric acid-hydrogen peroxide (Mahin and Lofberg, 1966). Chromic acid digestions have also been routinely used for ^{3}H in biological materials (McCubbin et al., 2001; Leonard et al., 2007). The method using H_2O_2 in the presence of Fe^{2+} ion, is also applicable for oxidizing samples for tritium analysis (Sansoni and Kracke, 1971). However, wet oxidation is not suitable for analysis requiring great accuracy or sensitivity because losses of tritium are inevitable and because other hydrogenous compounds are added to the sample. Residues of strong oxidizing agents remain in the sample causing chemiluminescence in the subsequent liquid scintillation counting (NCRP, 1976). The sample size is restricted compared to combustion way.

Combustion (oxidation)

Combustion is the most aggressive way to extract any ^{3}H from solid samples where all tritiated compounds are converted to trititiated water and counted by liquid scintillation counting (Braet and Bruggeman, 2005; Torikai et al., 2007). As the products of combustion are water and carbon dioxide, colour quenching and chemiluminescene effectively can be eliminated (L'Annunziata, 2003). In addition, the combustion method is the only technique to physically separate ^{3}H and ^{14}C. During combustion the organic portion of the sample is completely converted to water (H_2O) and carbon dioxide (CO_2). Sample combustion is suitable for any organic and inorganic samples; the selection of this method is typically decided by the number of samples that need to be processed. Plasma combustion (using oxygen plasma gas) has been used for tritium extraction however, which took *ca* 23 hours and did not always completely combust the organic matter in the sample (Momoshima et al., 1996). Advanced plasma combustion apparatus (modified model of Yanaco LTA-154, Japan; using methane free pure oxygen gas 99.9995%) was developed where the combustion water was collected in a cold trap cooled by liquid nitrogen (Fuma and Inoue, 1995). It takes *ca* 8 hours to combust a sample of 25g completely. For routine applications, there are four principal oxidizer systems in use today: (1) the PerkinElmer Sample Oxidizer, (2) the Harvey Oxidizer (also known as R.J. Harvey Biological Oxidizer), (3) Carbolite systems and (4) Pyrolyser system. All these are able to both combust and separate ^{3}H and ^{14}C quantitatively, however the mechanisms of those are slightly different which are combustion chamber, plumbing, heating techniques, timing cycles, and regents.

(1) The PerkinElmer Sample Oxidizer (Model 307)

The PerkinElmer Sample Oxidizer (Model 307) is an automatic preparation and oxidization system for both single and dual radiolabeled samples containing ^{3}H and/or ^{14}C for use in liquid scintillation counting (Figure 2.18). This system ensures reliable combustion of biological, environmental and industrial samples. The sample oxidizer combusts sample materials in an oxygen-enriched atmosphere with a continuous flow of oxygen to constituent water vapor and carbon dioxide using a patented process to achieve physical separation of ^{3}H and ^{14}C radionuclides. This system includes the following features (Table 2.3).

Figure 2.18: The PerkinElmer Sample Oxidizer (Model 307; www.perkinelmer.com)

Table 2.3: General characteristics of the PerkinElmer Sample Oxidizer

Model	Sample Oxidizer 307
Radionuclide	Single or dual labeled samples, ^{3}H & ^{14}C
Combustion temperature	Up to 1300°C
Capacity	60 sample/hour
Sample type	wet, dry of freeze-dried (any sample can be combusted)
Sample size	up to 1.5g
Recovery	97%
Memory effect	<0.08%
Catalyst	Non-catalytic combustion
Advantages	Robotic sample processing is possible. Sample processing time is rapid. There is no loss of radioactivity by volatilization, colour quench and chemiluminescence. Observation of combustion allows for visual inspection during sample combustion Sample placed into a Combusto-Cone™ is placed into the platinum ignition basket
Disadvantages	Expensive instrument and need gas supply (O_2 and N_2) Must be operated in a fume hood Reagents are corrosive and flammable

Source: www.perkinelmer.com

(2) The Harvey Oxidizer (R.J. Harvey Biological Oxidizer)

The Harvey oxidizer is automated system for combustion tritium and carbon-14 labeled samples at 900°C (Figure 2.19).

Figure 2.19: The Harvey Oxidizer (model OX-700; left and OX-500 & OX-600; right, Source: http://www.rjharveyinst.com)

Table 2.4: Characteristics of the Harvey Oxidizer

Model	OX-500,OX-600 and OX-700
Radionuclide	Single or dual labeled samples, ^{3}H and ^{14}C
Combustion temperature	900°C
Sample type	Wet or dry sample and liquid (Ideal for soil or high ash content materials and fatty samples)
Sample size	Up to 300mg (e.g. Feces or tissue homogenates or 0.50 ml whole blood).
Recovery	98% (with reproducibility within ± 1%)
Features	Rapid start, less than 20 minutes from cold. Continuous sample combustion and determinations (model OX-700). No sample preparation required. Catalytic oxidation ensures removal of quenching agents (e.g. SO_2, NO_2 etc). Easy access, to all parts of the unit A sample presentation method that prevents residue buildup common to other systems. No need to run blanks to purge residual activity. Easily exhaust vented without a hood. Low memory effect

Source: http://www.rjharveyinst.com

(3) Carbolite system

The Carbolite combustion furnace (model MTT) employs for the determination of tritium or carbon-14 in combustible materials (Figure 2.20). The sample combustion tube, gas bubbler train and associated connectors are fabricated entirely from glass and easily decontaminated, thereby avoiding analytical memory effects. The Carbolite furnace permits oxygen to be delivered to the catalyst to operate at its optimum at all stages of the sample combustion. In addition, since the gas delivery tube runs through the heated catalyst there is no possibility of thermal decomposition products condensing out on the outside surface of the gas delivery tube. The oxygen is also ejected at right angles to the main gas flow therefore reducing opportunities for the back flow of sample combustion gases/products into the gas delivery tube. The temperature control of the sample zone can be programmed via a linked PC. This has the advantage that different sample combustion protocols can be created and conveniently stored on disc. A number of furnaces can be daisy-chained together to a single PC hence permitting their individual operation; each can be running a different protocol, from a single PC or workstation. This would also allow a furnace and its associated equipment to be placed in a hazardous environment and operated remotely if so required.

Figure 2.20: Carbolite system (http://www.carbolite.com)

Table 2.5: Sample mass capability of the Carbolite system (Wickenden, 2002)

Sample type	**Typical sample size (dry wt[a]; g)**	**Wet/Dry ratio**	**^{3}H (OBT) LOD[b] (Bq/g wet)**	**^{14}C LOD (Bq/g wet)**
Soil	20	1.3	0.02	0.023
Grass	5	3.9	0.031	0.031
Sediment	20	1.5	0.018	0.02
Carrot	5	8.3	0.015	0.014
Potato	4	4.3	0.033	0.035
Cabbage	5	20.2	0.006	0.006

[a]; weight, [b]; limit of detection

Table 2.6: Characteristics of the Carbolite Oxidizer

Model	Tube furnace (MTT)
Radionuclide	Single or dual labeled samples, ^{3}H and ^{14}C
Combustion temperature	Up to 1000°C
Sample type	Wet or dry sample and liquid (Ideal for soil or high ash content materials and fatty samples)
Recovery	>98% (with reproducibility ± 1%)
LOD	0.02-0.60 Bq/g (wet weight)
Oxidant	Copper oxide (CuO) heated to 750°C
Advantages	Computer control to precisely control the combustion and reproducibility. Different sample combustion protocols can be created and permitting their individual operation; each can be running a different protocol, from a single PC or workstation. A furnace and its associated equipment to be placed in a hazardous environment and operated remotely if so required. Unique design of an oxygen gas delivery system to the catalyst to ensure optimum performance during the initial carbonisation of the sample in dried compressed air prior to full combustion in oxygen All-glass construction removing the possibility of tritium migration into plastic fittings and allowing effective decontamination.
Disadvantages	Single tube furnace

Source: (http://www.carbolite.com)

(4) Pyrolyser System

In the present study, all samples were analysed using a Pyrolyser system which is modified version of the combustion furnace method (Figure 2.21). This method is cost effective, rapid (8 to 12 samples per day were analysed) and reproducible. The application of the furnace are represented depend on the sample species (Table 2.8). The combustion furnace method reduces the loss of activity through evaporation and can fully combust larger sample sizes than the wet chemical oxidation method. Further explanation of the Pyrolyser System will be given in Chapter 3.

Figure 2.21: Pyrolyser system; prototype (left) and MARK II (http://www.raddec.com/).

Table 2.7: Characteristics of the Pyrolyser System

Model	Raddec Pyrolyser-4 and Pyrolyser-6
Radionuclide	Single or dual labeled samples, ^{3}H and ^{14}C
Combustion temperature	Up to 900°C
Sample type	Wet or dry sample (see Table 2.8)
Recovery	98%
Memory effects	3% (immediately after run)
LOD	0.01Bq/g
Catalyst	Platinum alumina catalyst (Pt-Al_2O_3) heated to 800°C
Features	The Pyrolyser is multi-tube system fully integrated into a single space-efficient instrument. Each system incorporates controllable heating, metered air and oxygen gas flows A catalytic oxidation zone and a bubbler chain to extract and quantitatively trap fully-oxidised sample decomposition products. Up to 6 samples can be extracted at one time over a period. The Pyrolyser designed for the extraction of total tritium and carbon-14 in almost any sample type simultaneously.

Source: http://www.raddec.com

Table 2.8: Sample mass capability of the Pyrolyser System

Material	Mass extractable
Concrete from reactor bioshields	Up to 40g
Metal work from reactors (e.g. SGHWR and Magnox)	Up to 40g
Asbestos lagging from Magnox reactor systems	Up to 10g
Graphite from reactors	Up to 20g
Desiccants	Up to 40g
Oils	Up to 2g
Soft-wastes (plastics, paper etc)	Up to 10g
Ion-exchange resins	Up to 5g
Biota	Up to 10g
Sediment	Up to 40g
Soil	Up to 40g
Sewage pellets	Up to 10g

Note: SGHWR (Steam Generated Heavy Water Reactor, Winfrith UK, now decommissioned); Magnox, pressurized, carbon dioxide cooled, graphite medorated reactors using natural uranium as fuel and magnox alloy as fuel cladding. Boron-steel control roads were used. (Source: http://www.raddec.com)

Pressurised oxidative combustion (the oxygen bomb)

Combustion with oxygen in a sealed bomb is a reliable procedure whose effectiveness stems from its ability to treat analytical samples quickly and conveniently within a closed system without losing any of the sample or its combustion products (Moghissi et al., 1975). Combustion is rapid, releasing all of the heat obtainable from the sample and oxidizing all elements in the sample to soluble forms which are easily recovered for chemical analysis.

The oxygen bomb method can produce similar yields to the furnace combustion method (Bogen et al., 1973a; Moghissi et al., 1973) and is good for combustible materials. However the sample size for the oxygen bomb method is restricted and depends on the bomb capacity for safety reason - collection of the oxidized gases (HTO and CO_2) can be difficult. One example of an oxygen bomb is the PARR BOMB (1121 oxygen combustion bomb) which is designed to burn large samples of slow burning materials such as grain, wood fibre, paper and other vegetable matter (Figure 2.22). Slow burning, combustible samples weighing up to 10 grams can be burned in the bomb using oxygen charging pressures up to 300 psig (~20 bar), but these limits vary and must be checked experimentally for each sample. The sample size must be adjusted to an amount which will give complete combustion with peak pressures held in the range from 1000 to 1200 psig. The pressure should never exceed 1500 psig as an absolute maximum.

Figure 2.22: PARR BOMB (1121 oxygen combustion bomb)

Table 2.9: Methods of analysis for tritiated water and organically bound tritium (Morris, 2006)

Method	Type of sample	Level of activity	Details of method	Reference
Aqueous sample				
Conventional distillation	Aqueous samples	Low/high	Samples placed in bottom of distillation rig and heated to 100°C. Water vapour, which will include HTO, is condensed and collected for analysis	Ware and Allott, 1999
Sub-boiling distillation	Aqueous samples	Low/high	Water in the outer ring of an annular distillation unit is covered with a watch glass and gently warmed (40~80°C). Tritiated water evaporates onto the watch glass and runs into the centre, where it is collected for analysis.	Warwick *et al*, 1999
Freeze-drying	Milk and pureed foodstuffs	Low/high	Known mass of sample is weighed into round-bottom flask, frozen in liquids nitrogen and evacuated using a high vacuum pump. The receiving vessel is then cooled and the sample allowed to reach room temperature. An aliquot of the collected water is analyed.	Wickenden, 1993
Azeotrophic distillation with benzene	Biological, environmental and soil	Low	Samples were covered with dry thiopene-free benzene and distilled at 69°C for 2~4 hours.	Moghissi *et al*, 1973
Environmental sample (wet and solid form) to measure tritiated water and organically bound tritium (OBT)				
Freeze-drying & combustion	Environmental and biological	Low	Freeze-dried sample was placed in low pressure chamber with CuO catalyst in O_2-Air flow. Combustion water was collected in a dry ice-cooled trap.	Bogen *et al*, 1973
Freeze-drying conventional & plasma combustion	Environmental (leaf litter and humus)	Low	Free water is removed by freeze-drying in a vacuum, distilled and eletrolytically enriched. Thin layer of freeze-dried sample is spread across glass plates in a glass chamber and oxygen plasma induced. Pt-alumina catalyst in combustion tube is held at 450°C, and the sample is heated with a gas burner for 2 hours. Resulting water vapour is trapped in dry-ice cooled trap and distilled with $KMnO_4$ and Na_2O_2.	Momoshima *et al*, 1994

Method	Type of sample	Level of activity	Details of method	Reference
Split combustion	Environmental and effluent	Low/high	Dual-zone combustion furnace with Pt-alumina catalyst at 750°C. Sample is initially held at 100°C for 2 hours in mixed N_2/O_2 flow and combustion water is trapped in cooled distilled water bubblers. Then bubblers are changed and the sample is heated to 700°C, gas is changed to O_2 only at 450°C.	Verral and Odell, 2002
Freeze-drying and combustion	Environmental	Low	Free water removed by freeze-dried samples are combusted in mixed N_2/O_2 flow and combustion water collected. Purified by double-distillation after adding $KMnO_4$ and Na_2O_2.	Kim *et al*, 1992; Kim and Han, 1999
Combustion	Vegetation	Low/ background	Pretreatment by drying at 40°C and grinding. Dry samples are mixed with tritium-free water for 2 days to remove exchangeable OBT, then filtered and freezedried. Dual zone furnace with CuO (oxidant) and quartz beads at 850°C. Samples are gradually combusted to ash by a mobile heating unit at 450°C in a pure oxygen flow. The combustion water is collected in a cold trap and distilled after pH adjustment with Na_2O_2	Pointurier *et al*, 2003
Oxygen bomb combustion	Environmental	Low	Up to 10 g of sample was placed into a vessel, which was sealed and pressurided to 250 psi with oxygen, which was then ignited with two electrodes joined by a Ni-Cr wire. Combustion gases were subsequently passed through a dry ice and alcohol cooled trap, collecting tritiated water, which was counted by liquid scintillation counting	Moghissi *et al*, 1975
Wet chemical digestion	Filtered effluent	High	Tritiated water is determined separately by direct distillation of the sample under alkaline conditions at 100°C. Total tritium is then extracted by refluxing the sample with chromium trioxide and sulphuric acid to oxidise the organic fraction to HTO, followed by alkaline distillation at 100°C.	Ware and Allott, 1999
Plasma combustion and distillation	Environmental	Low/high	Dried sample of 5-25 g was combusted automatically in an oxygen plasma combustion apparatus with methane free pure oxygen gas (99.9995%), and the resulting combustion water was collected in a cold trap cooled by liquid nitrogen. It took about 8h to combust a sample of 25 g completely. The collected water was purified by single distillation under atmospheric pressure after pH adjustment with Na202 and $PbCI_2$.	Fuma and Inoue, 1995

2.5 References

Aoyama T. 1990. A tritium-in-air monitor with compensation and additional recording of alpha, beta and gamma backgrounds. IEEE Transactions on Nuclear Science 37: 885-891.

Aoyama T, Watanabe T. 1985. A New Type of H-3 Surface-Contamination Monitor. Health Physics 48: 773-779.

Barthe N, Chatti K, Coulon P, Maitrejean S, Basse-Cathalinat B. 2004. Recent technologic developments on high-resolution beta imaging systems for quantitative autoradiography and double labeling applications. Nuclear Instruments and Methods in Physics Research Section A: Accelerators, Spectrometers, Detectors and Associated Equipment 527: 41-45.

Beyerle U, Aeschbach-Hertig W, Imboden DM, Baur H, Graf T, Kipfer R. 2000. A Mass Spectrometric System for the Analysis of Noble Gases and Tritium from Water Samples. Environmental Science & Technology 34: 2042-2050.

Bogen DC, Henkel CA, White CGC, Welford A. 1973a. A method for the determination of tritium distribution in environmental and biological samples. Journal of Radioanalytical Chemistry 13: 335-341.

Bogen DC, Henkel CA, White CGC, Welford GA. 1973b. Method for Determination of Tritium Distribution in Environmental and Biological Samples. Journal of Radioanalytical Chemistry 13: 335-341.

Braet J, Bruggeman A. 2005. Oxidation of tritiated organic liquid waste. Fusion Science and Technology 48: 188-193.

Cable PR, Hofstetter KJ, Beals DM, Jones JD, Collins SL, Noakes JE, Spaulding JD, Neary MP, Peterson R. 1997. A remotely operated, Field Deployable Tritium Analysis System for surface and ground water measurement. Field Analytical Methods for Hazardous Wastes and Toxic Chemicals: 345-352.

Clarke WB, Jenkins WJ, Top Z. 1976. Determination of tritium by mass spectrometric measurement of 3He. The International Journal of Applied Radiation and Isotopes 27: 515-522.

Colmenares CA. 1974. Bakeable ionization chamber for low-level tritium counting. Nuclear Instruments and Methods 114: 269-275.

De Filippis S, Noakes JE. 1991. Sample preparation of environmental samples using benzene synthesis followed by high-performance LSC. Transactions of the American Nuclear Society 64: 79-80.

Demange D, Grivet M, Pialot H, Chambaudet A. 2002. Indirect tritium determination by an original (3)he ingrowth method using, a standard helium leak detector mass spectrometer. Analytical Chemistry 74: 3183-3189.

Deptuch G. 2005. Tritium autoradiography with thinned and back-side illuminated monolithic active pixel sensor device. Nuclear Instruments and Methods in Physics Research Section A: Accelerators, Spectrometers, Detectors and Associated Equipment 543: 537-548.

Dyer A. 1974. An introduction to liquid scintillation counting. Heyden and Son Ltd, London

EA. 1999. The determination of tritium (tritiated water) activity concentration by alkaline distillation and liquid scintillation counting 1999. Environment Agency North West Region, Warrington.

Ellefson RE, Price BR, West DS. 1995. Tritium inventory measurement by beta scintillation detection. 16th IEEE/NPSS Symposium Fusion Engineering, SOFE '95. Seeking a New Energy Era (Cat. No.95CH35852): 1018-1021 vol.1012.

Fuma S, Inoue Y. 1995. Simplified and sensitive analysis of organically bound tritium in tree rings to retrospect environmental tritium levels. Applied Radiation and Isotopes 46: 991-997.

Gordon JS, Farrell R, Daley K, Oakes CE. 1994. Solid state tritium detector for biomedical applications. IEEE Transactions on Nuclear Science 41: 1494-1499.

Hofstetter KJ. 1995. Continuous Aqueous Tritium Monitoring. Fusion Technology 28: 1527-1531.

Hofstetter KJ, Cable PR, Beals DM. 1999. Field analyses of tritium at environmental levels. Nuclear Instruments & Methods in Physics Research Section a-Accelerators Spectrometers Detectors and Associated Equipment 422: 761-766.

Hofstetter KJ, Cable PR, Beals DM, Noakes JE, Spaulding JD, Neary MP, Peterson R. 1998. Field deployable tritium analysis system for ground and surface water measurements. Journal of Radioanalytical and Nuclear Chemistry 233: 201-205.

IAEA. 1989. Measurement of radionuclides in food and the environment, Vienna.

IAEA. 2004. Technical reports series no. 421, Management of waste containing tritium and carbon-14 (printed by the IAEA, in Austria, 2004).

Kallman H. 1950. Scintillation counting with solutions. Physica Review 78: 621-622.

Kim CK, CHo YW, Han MJ, Pak CK. 1992. Tritium distribution in some environmental sample - Rice, chinese cabbage and pine needles in Korea. Journal of the Korean Association of Radiation Protection 17: 25-35.

Kim CK, Cho YW, Kim KH. 1996. Tritium concentrations in surfaces seawater around Korean peninsular. Journal of Korean Association for Radiation protection 21: 107-115.

L'Annunziata MF. 2003. Liquid scintillation analysis: principles and practice. In *Handbook of radioactivity analysis* (Edited by M. F. L'Annunziata). Academic Press, Sandiego.

Leonard KS, Shaw S, Wood N, Rowe JE, Runacres SM, McCubbin D, Cogan SM. 2007. Independent radiological monitoring; Results of a recent intercomparison exercise. Environmental Radiochemical Analysis Iii: 162-168.

Mahin DT, Lofberg RT. 1966. A simplified method of sample preparation for determination of tritium, carbon-14, or sulfur-35 in blood or tissue by liquid scintillation counting. Analytical Biochemistry 16: 500-509.

Mahin DT, Lofberg RT. 1970. Determinatiom of several isotopes in tissue by oxidation, page 212 in The current status of Liquid Scintillation Counting, Bransome, E., Jr., Ed. Grune and Stratton, New York.

McCubbin D, Leonard KS, Bailey TA, Williams J, Tossell P. 2001. Incorporation of Organic Tritium (^{3}H) by Marine Organisms and Sediment in the Severn Estuary/Bristol Channel (UK). Marine Pollution Bulletin 42: 852-863.

McGann WJ, Entine G, Farrell RF, Clapp A, Squillante MR. 1988. Solid-state nuclear detectors for monitoring low levels of tritium. Fusion Technology 14: 1041-1046.

Mettivier G, Cristina Montesi M, Russo P. 2004. Tritium digital autoradiography with a Medipix2 hybrid silicon pixel detector. Nuclear Instruments and Methods in Physics Research Section A: Accelerators, Spectrometers, Detectors and Associated Equipment 516: 554-563.

Moghissi AA, Bretthauer EW, Compton EH. 1973. Seperation of water from biological and environmental samples for tritium analysis. International Journal of Applied Radiation and Isotopes 26: 339-342.

Moghissi AA, Bretthauer EW, Whittaker EL, McNelis DN. 1975. Oxygen Bomb Combustion of Environmental and Biological Samples for Tritium Analysis. International Journal of Applied Radiation and Isotopes 26: 339-342.

Momoshima N, Tjahaja PI, Okai T, Takashima Y. 1996. Measurement of tritium in forest soil. Liquid Scintillation Spectrometry 1994: 89-96.

Morris JE. 2006. Organically bound tritium in sediments from the Severn estuary, UK. Ocean and earth science, Southampton.

NCRP. 1976. Tritium measurement techniques. National Council on Radiation Protection and Measurement, Bethesda, Maryland.

NCRP. 1979. Tritium in the environment. National Council on Radiation Protection and Measurement, Bethesda, Maryland.

Okada S, Momoshima N. 1993. Overview of Tritium - Characteristics, Sources, and Problems. Health Physics 65: 595-609.

Plastino W, Chereji I, Cuna S, Kaihola L, De Felice P, Lupsa N, Balas G, Mirel V, Berdea P, Baciu C. 2007. Tritium in water electrolytic enrichment and liquid scintillation counting. Radiation Measurements 42: 68-73.

Pretzsch G, Dorschel B, Seifert H, Streil T, Seeliger D. 1985. Measurement of Tritium Activity Concentration in Air by Means of the Electret Ionization-Chamber. Radiation Protection Dosimetry 12: 345-349.

Price GPJ, Aslett T. 1995. Performance of a Vg 30-38 Mass-Spectrometer During Initial Testing. Fusion Technology 28: 1061-1066.

Purghel L, Calin MR, Bartos D, Serbia L, Lupu A, Lupu F, Lupu D. 2005. Portable intelligent tritium in air monitor. Fusion Science and Technology 48: 390-392.

Purghel L, Valcov N. 2000. Statistical discrimination based monitor for radioactive gases and vapors. Romanian Journal of Physics 45: 371-374.

Rapkin E. 1993. Î²-Particle Detection in HPLC by Flow-Through Monitoring vs. Liquid Scintillation Counting. Journal of Liquid Chromatography & Related Technologies 16: 1769 - 1781.

Reynolds GT. 1950. Liquid scintillation counters. Nucleonics 6: 68-69.

Sakuma Y, Iida T, Koganezawa T, Ogata Y, Aoyama T, Torikai Y, Ohta M, Takami M. 2005. Development of a low-level tritium air monitor. Fusion Science and Technology 48: 397-400.

Sansoni B, Kracke W. 1971. Rapid determination of low-level alpha and beta activities in biological material using wet ashing by OH radicals, pp 217-231 of Rapid Methods for Measuring Radioactivity in the Environment. International Atomic Energy Agency, Vienna (1971).

Scott Willms R, Dogruel D, Myers R, Farrell R. 2005. A new solid state tritium surface monitor. Fusion Science and Technology 48: 409-412.

Shah KS, Gothoskar P, Farrell R, Gordon J. 1997. High efficiency detection of tritium using silicone avalanche photodiodes. IEEE Transactions on Nuclear Science 44: 774-776

Shah KS, Squillante MR, Entine G. 1990. HgI2 low energy beta particle detector. Nuclear Science, IEEE Transactions on 37: 152-154.

Shmayda CR, Shmayda WT, Kherani NP. 2002. Monitoring tritium activity on surfaces: Recent developments. Fusion Science and Technology 41: 500-504.

Shmayda WT, Kherani NP, Stodilka D. 1997. Evaluation of the tritium surface activity monitor. Fusion Technology 1996. Proceedings of the 19th Symposium on Fusion Technology 2: 1245-1248.

Sigg RA, McCarty JE, Livingston RR, Sanders MA. 1994. Real-Time Aqueous Tritium Monitor Using Liquid Scintillation-Counting. Nuclear Instruments & Methods in Physics Research Section a-Accelerators Spectrometers Detectors and Associated Equipment 353: 494-498.

Singh AN, Ratnakaran M, Vohra KG. 1985. An Online Tritium-in-Water Monitor. Nuclear Instruments & Methods in Physics Research Section a-Accelerators Spectrometers Detectors and Associated Equipment 236: 159-164.

Stencel JR, Griesbach OA, Ascione G. 1995. Practical aspects of environmental analysis for tritium using enrichment by electrolysis. Radioactivity and Radiochemistry; Vol. 6; ISSUE 2; PBD 1995: pp. 40-49.

Suter M, Jacob SWA, Synal HA. 2000. Tandem AMS at sub-MeV energies - Status and prospects. Nuclear Instruments & Methods in Physics Research Section B-Beam Interactions with Materials and Atoms 172: 144-151.

Szarka J, Usacev S, Povinec P. 1979. A new type of proportional counter for the measurement of low tritium activities. Acta Facultatis Rerum Naturalium Universitatis Comenianae, Physica 19: 199-215.

Torikai Y, Murata D, Penzhorn RD, Akaishi K, Watanabe K, Matsuyama M. 2007. Migration and release behavior of tritium in SS316 at ambient temperature. Journal of Nuclear Materials 363-365: 462-466.

Tuo X, Mu K, Lei J, Li X, Yang X. 2007. A tritium measuring instrument with high detection efficiency. Nuclear Techniques 30: 388-390.

Villa M, Manjon G. 2004. Low-level measurements of tritium in water. Applied Radiation and Isotopes 61: 319-323.

Wampler WR, Doyle BL. 1994. Low-energy beta spectroscopy using pin diodes to monitor tritium surface contamination. Nuclear Instruments and methods in Physics Research Section A: Accelerators, Spectrometers, Detectors and Associated Equipment 349: 473-480.

Ware A, Allott RW. 1999. Review of methods for the analysis of total tritium and organically bound tritium. National Compliance and Assessment Service, NCAS/TR/99/003, Lancaster.

Warwick PE. 1999. The determination of pure beta-emitters and their behaviour in a salt-marsh environment. Chemistry, Southampton.

Warwick PE, Croudace IW, Howard AG. 1999. Improved technique for the routine determination of tritiated water in aqueous samples. Analytica Chimica Acta 382: 225-231.

Wickenden DA. 1993. Determination of Tritiated-Water in Biological Matrices. Science of the Total Environment 130: 121-128.

Wickenden DA. 2002. Carbolite Process Manual: Analysis of tritium and carbon-14 in combustible materials using the Carbolite/AEA technology combustion furnace and associated apparatus.

Worth LBC, Pearce RJH, Bruce J, Banks J, Scales S. 2005. Development of a novel contamination resistant ion chamber for process tritium measurement and use in the JET first trace tritium experiment. Fusion Science and Technology 48: 370-373.

Chapter 3

Methods used in this research

3 Methodology

3.1 Introduction

The requirement for ^{3}H measurement in a wide range of materials has increased in recent years mainly as a result of accelerated decommissioning programmes with its associated waste sentencing requirements. However, as ^{3}H is a pure low-energy beta emitter, any analytical procedure usually involves collection of representative samples, isolation of ^{3}H from the sample and measurement of the ^{3}H activity using liquid scintillation counting (LSC). A number of techniques are routinely used for isolation of ^{3}H. For solid samples contaminated with HTO, a rapid screening of ^{3}H activity can be achieved by leaching the sample with water and determining the ^{3}H activity in the leachate. However, for quantitative analysis and where the ^{3}H is present as a species other than free HTO a more aggressive approach is required to liberate the ^{3}H. Typically, this involves the combustion of the sample and the conversion of all liberated ^{3}H species to HTO which is subsequently trapped and counted by liquid scintillation counting. Sample oxidation has been effected using a range of techniques including chemical oxidation and combustion in O_2 atmospheres at elevated pressures. The most widespread technique is ambient pressure combustion where the sample is thermally oxidised in air or O_2-enriched air within a tube furnace assembly (Payne et al., 1952; Lockyer and Lally, 1993; Kim et al., 2008). The sample is slowly heated using a predetermined heating cycle to a maximum temperature. Often oxygen is introduced at some stage during the heating cycle to enhance sample combustion. All combustion products are normally passed over a heated catalyst such as Pt-alumina or oxidant such as CuO to ensure that all tritiated species are converted to HTO. This approach relies on effective optimisation of the combustion profile.

Complete oxidation of diverse sample types is always a critical issue of any combustion method because it will directly affect the extraction of ^{3}H or ^{14}C from specific samples and ultimately the accurate measurement. The factors affecting the oxidation rate include maximum temperature, oxidant gas (i.e. oxygen or air) and total combustion time. In the case of organic samples, these are particularly important factors because rapid heating or incorrect oxidant gas supply result in incomplete oxidation or uncontrolled combustion; when organic samples are incompletely oxidized, a strong odour may be generated and brown-yellow coloration formed in the trapping solution which will cause colour or chemical quench when using LSC. Carbon monoxide (CO) can be generated also rather than CO_2. Therefore optimized combustion strategies must be established for each sample material. For some materials complete decomposition may take as long as 4-6 hours where the ramping time

taken is controlled to allow slow oxidation of samples which inhibits any pressure excursions which could cause blow outs or glass breakage.

3.2 Tritium extraction by combustion

Total tritium ($^3H_{total}$) was quantitatively extracted from samples using a Raddec Pyrolyser Trio™ System that provides simultaneous oxidation of up to six samples (Figure 3.1). The systems comprises six alumina (or silica) liner tubes that pass through the furnaces, each holding 30 mm ID silica-glass work tubes that narrow at one end to accommodate a catalyst pellet bed. Originally, the early Pyrolysers incorporated two independent furnaces (isolated by an insulated air gap) allowing the sample and catalyst to be heated separately. The variation in temperature throughout the sample zone was small. A third, mid-zone furnace was later incorporated to remobilise any combustion condensates that may have formed in the cooler region between the two main furnaces. The presence of a middle zone separating the sample and catalyst zones effectively isolated the sample zone from the high temperature catalyst zone, preventing premature radiative heating of the sample zone.

The catalyst zone is loaded with 0.5% Pt-alumina catalyst (3 mm pellets, 10g) and heated to 800°C which promotes the oxidation of any organic compounds in the gaseous combustion products to CO_2 and H_2O. Samples are loaded into silica-glass boats which are then placed into each work tube before fitting a borosilicate end socket with a spigot for admitting the air or air/O_2 mix. The other end of the tube has a spigot for connecting a short section of silicone rubber tubing that carries the gaseous decomposition products to a dilute nitric acid bubbler trap. The sample zone is gradually heated from room temperature to either 500°C or 900°C depending on the defined ramping profile. The sample zone is heated from 50 to 200°C at a rate of 3 °C/minute and held for 20 minutes before being heated to 500°C at 5 °C/minute with further holding stages at 300 and 500°C. A modified ramping cycle was also developed where the final temperature was increased to 900°C at a rate of 10 °C. An air flow is passed through the system at a rate of 200 ml/min carrying the combustion products over the Pt catalyst and results in the production of water and CO_2. At these flow rates, it takes approximately 2 minutes to completely sweep a tube volume. Once the sample zone has reached 500°C, pure oxygen is introduced to accelerate combustion and the mid-zone is heated to drive off any condensates. Temperatures in the sample and catalyst zone are monitored using thermocouples placed within the furnace chamber and have been validated through additional measurements of temperature profiles within the silica tube (Figure 3.2).

Tritium, as tritiated water, is subsequently trapped in a 0.1M HNO_3 bubbler which contains all of the tritium activity and effectively prevents co-trapping of CO_2.

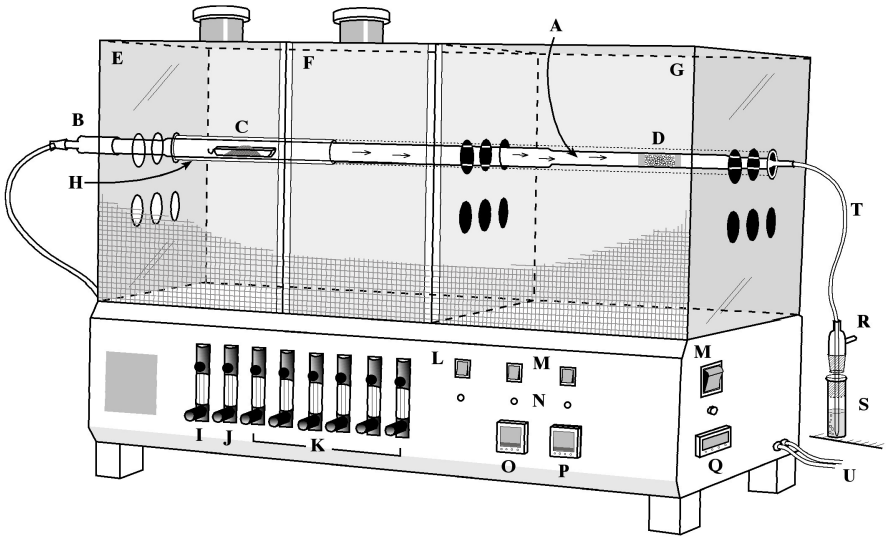

Key

A. Silica glass work tube
B. Borosilicate glass end cap
C. Silica glass sample boat
D. Pt-alumina catalyst
E. Sample zone furnace
F. Mid-zone furnace (optional)
G. Catalyst zone furnace
H. Silica tube liner
I. Primary air flow control
J. Primary oxygen flow control
K. Flow controllers for tubes 1-6
L. Sample furnace cooling switch
M. Elements isolated switch
N. Element isolated indicators
O. Sample zone furnace temperature controller
P. Catalyst zone furnace temperature controller
Q. Mid zone furnace temperature controller (optional)
R. Bubbler head (borosilicate)
S. Bubbler bottle (borosilicate)
T. Silicone tube connector
U. Compressed air/oxygen inlet connectors

Figure 3.1: Schematic diagram showing the main components of the Pyrolyser furnace (http://www.raddec.com)

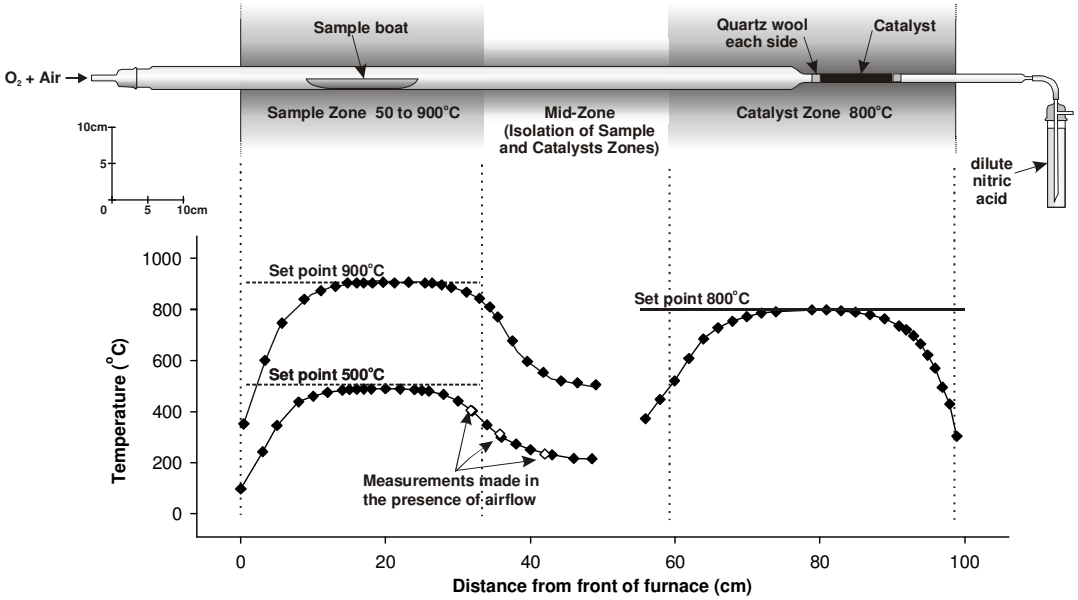

Figure 3.2: Temperature profiles measured within the silica tube along the furnace.

3.3 Method validation

3.3.1 The role of the catalyst

The decomposition of some hydrogenated products can be slow, therefore a catalyst is required for ^{3}H extraction using a combustion system (Burger, 1979). Platinum (Pt) and palladium (Pd) are well known as effective catalysts for oxidizing hydrogen and carbon compounds to water and CO_2 respectively (Munakata et al., 1998; Munakata et al., 2002). Copper oxide (CuO) is also commonly used as an oxidant to ensure complete oxidation of all molecular hydrogen isotopes and hydrocarbons released during the combustion (Penzhorn et al., 2000). Platinum alumina catalysts were used in the Pyrolyser combustion system because they are widely considered to effectively convert a higher proportion of a wide range of tritiated compounds to trititated water. The speciation of the tritiated compounds also affects the furnace recoveries; volatile compounds are released at lower temperatures whilst oxidation of more refractory compounds (such as glutamic acid, leucine, sucrose and thymidine) that only decompose at higher temperature will be slow. An air flow is supplied through the system at a rate of 200 ml/min. At these flow rates, it takes approximately 2 minutes to completely flush the work tube. The effectiveness and role of platinised alumina catalyst was investigated under a range of temperatures and compared with different materials or other oxidant beds.

Materials

The effectiveness of Pt-alumina (0.5% Pt-Al_2O_3) and CuO for the oxidation of combustion products was compared to non-active materials such as quartz glass and alumina beads which simply provide a more tortuous path and increase transit times through the catalyst zone. Approximately 10g of test material were loaded in the catalyst zone to give a bed length of approximately 7cm. However, 30g of copper oxide (CuO; oxidant) granules was required to produce a corresponding bed length because CuO has relatively smaller diameter than the other materials investigated (Table 3.1). Platinum catalyst, Pt-free aluminum pellet and CuO (oxidant) were changed over at each evaluated temperatures and whilst other materials including re-used platinum alumina catalyst were used at all ranges temperatures without recharging (200-800°C).

Table 3.1: Catalyst and catalytic material examined

Catalyst/oxidant	Particle size in diameter (mm)	Mass (g)	Variation of catalyst zone temp. (°C)
Platinum alumina pellet (0.5% Pt-Al_2O_3)	~3.0±0.2	10	200-800
Alumina pellet (platinum-free)	~3.0±0.2	10	200-800
CuO (oxidant) granules	0.8-2.0	30[a]	200-800
Quartz glass fragments [b]	~3.0±0.3	10	200-800
No catalyst	-	-	200-800
Re-used platinum alumina pellet [c]	~3.0±0.2	10	200-800

[a] *To set a catalyst zone length with others, 30g of CuO was used to achieve a 10cm length*
[b] *Sieved fragments is similar size with alumina pellet, ~3mm*
[c] *Catalyst were reused at all temperature variations without changing*

Catalyst function and temperature

Freeze-dried fish powder 5.28 ± 0.34 Bq/g (reference value at 31/03/2001) and milk powder 5.04 ± 0.32 Bq/g (reference value at 31/03/2001) spiked with ^{3}H-thymidine were used to investigate the catalyst function with temperature. These materials were originally supplied as part of a Ministry of Agriculture, Fisheries and Food intercomparison exercise 2003 (Toole, 2003). Thymidine is difficult to isolate from the matrix and exhibits more complex combustion characteristics with slow oxidation. Replicate measurements of the two samples using the combustion system with platinised alumina catalyst heated to 800°C showed good reproducibility confirming that the samples were homogeneously spiked. The average ^{3}H concentration measured and standard deviation were 3.61 ± 0.05 Bq/g for fish and 3.15 ± 0.15 Bq/g for milk, respectively (Table 3.2). MAFF fish and milk were heated to 900°C for ^{3}H extraction with a preset ramping cycle (Table 3.3). After combustion of the samples under the range of conditions, the physical appearance of the bubbler solution was recorded and the ^{3}H activity and quench levels were measured.

Table 3.2: Comparison of $^3H_{total}$ (Bq/g) of present study with intercomparison exercise results

Sample	Reference values calculated to 31/03/2001	Reference results decay corrected (Ref_{DC}) to 31/01/2006	Measured results (31/01/2006)
MAFF fish (Plaice)	5.28 ± 0.34	4.02 ± 0.26	3.61 ± 0.05
MAFF milk	5.04 ± 0.32	3.83 ± 0.24	3.15 ± 0.15

Note: Total ^{3}H analysis of two MAFF standards sample were performed at 31/01/2006. Both materials spiked ^{3}H thymidine were tested for homogeneity before distribution of the sample for intercomparison exercise (Toole, 2003).

Table 3.3: Ramping profile for sample combustion

Stage	Description	Ramp rate (°C/min)	Target temperature (°C)	Hold time (min)
1	Ramp	3	200	
2	Hold		200	20
3	Ramp	5	300	
4	Hold		300	20
5	Ramp	5	500	
6	Hold		500	90
7	Ramp	10	900	
8	Hold		900	120
9	End	cooled	50	

Tritium recoveries from fish and milk were relatively low when the catalyst was heated to low temperature (200~300°C). Increasing the catalyst zone temperature resulted in an increase in ^{3}H recovery for all evaluated materials (Table 3.4-3.5 & Figure 3.3-3.4). No significant difference was observed in ^{3}H recoveries for the range of catalyst zone materials tested. There was also no significant difference between a re-used catalyst and a new platinum catalyst. An intense coloration of the bubbler solution (0.1 M HNO_3) with an accompanying odour was noted when the catalyst zone was heated to low temperatures (<500°C) for all catalyst zone loading types except Pt-alumina catalyst. This was related to incomplete oxidation of organic rich materials (e.g. fish, milk and sewage) which could adversely affect ^{3}H measurement by liquid scintillation counting. The typical colour of the condensate was yellow and brown which results in significant colour quench (L'Annunziata, 2003). In addition, incompletely oxidized organic compounds may be trapped in the bubbler solution (0.1 M HNO_3), potentially resulting in chemical quench of liquid scintillation counting. However, no significant coloration and odour was produced using platinum catalyst at all catalyst zone temperatures (200-800°C). This is demonstrable evidence that most organic compounds can be oxidized effectively by platinum catalyst (Figure 3.5). The most significant coloration of bubbler solution trapping ^{3}H was produced by CuO at 200°C, and quartz and no catalyst condition up to 500°C. The sample solution having intense coloration showed significantly low SQPE values (Figure 3.6). No visible condensations and odour were produced with any of the materials with catalyst zone temperatures >600°C. A cloudiness associated with low temperature catalyst zone occurred with quartz (~300°C), alumina (at 200°C) and no catalyst condition (~ 300°C).

Table 3.4: ^{3}H determination in fish at different catalyst zone temperatures.

Catalyst zone temp. (°C)	No catalyst		Quartz glass fragments		Alumina pellet New		CuO granules New		Re-used Pt-Al_2O_3 at 800°C		Pt-Al_2O_3 New	
	^{3}H (Bq/g)	2sd	^{3}H (Bq/g)	2sd	^{3}H (Bq/g)	2sd	^{3}H (Bq/g)	2sd	^{3}H (Bq/g)	2sd	^{3}H (Bq/g)	2sd
200	2.5	0.3	2.5	0.4	2.7	0.3	2.9	0.5	2.6	0.3	2.9	0.3
300	2.2	0.3	2.2	0.3	2.3	0.3	3.2	0.4	2.6	0.3	2.4	0.3
400	2.7	0.4	3.0	0.4	2.8	0.3	3.9	0.4	3.3	0.5	3.4	0.5
500	3.1	0.6	2.8	0.5	3.1	0.7	3.7	0.7	3.6	0.5	3.5	0.7
600	4.6 4.7	0.5 0.7	3.8	0.6	3.8	0.6	3.9	0.5	4.1	0.6	4.2	0.6
700	3.8	0.5	3.8	0.6	3.6	0.5	4.0	0.6	3.9	0.6	3.7	0.5
800	3.7	0.4	3.8	0.4	3.4	0.4	4.1	0.6	4.1	0.6	3.6	0.4
Linear equation	y = 0 .3169x + 1.9617 (R^2=0.6245)		y = 0.2952x + 1.946 (R^2=0.8275)		y = 0.2038x + 2.28 (R^2=0.6469)		y = 0.1768x + 2.9561 (R^2=0.8086)		y = 0.274x + 2.3617 (R^2=0.8635)		y = 0.1966x + 2.5973 (R^2=0.5343)	

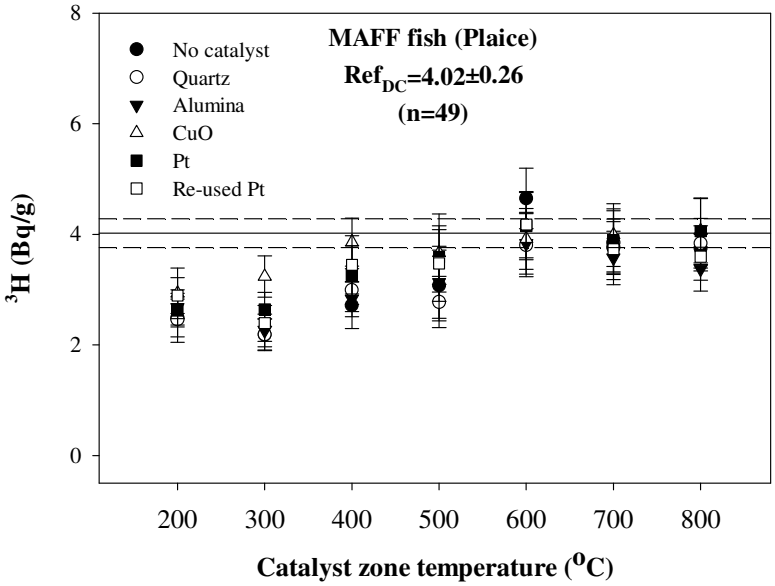

Figure 3.3: ^{3}H in fish depend on the types of catalyst and its temperature. Ref_{DC} is the decay corrected reference value. The reference value is shown as a solid line and the upper and lower limits as dashed lines.

Table 3.5: ^{3}H determination in milk at different catalyst zone temperatures.

Catalyst zone temp. (°C)	No catalyst		Quartz glass fragments		Alumina pellet New		CuO granules New		Re-used $Pt\text{-}Al_2O_3$ at 800°C		$Pt\text{-}Al_2O_3$ New	
	^{3}H (Bq/g)	2sd	^{3}H (Bq/g)	2sd	^{3}H (Bq/g)	2sd	^{3}H (Bq/g)	2sd	^{3}H (Bq/g)	2sd	^{3}H (Bq/g)	2sd
200	1.8	0.3	2.1	0.3	1.9	0.2	3.2	0.4	2.1	0.2	2.3	0.2
300	3.3	0.4	4.0	0.5	2.7	0.3	2.8	0.3	3.3	0.5	2.4	0.4
400	3.1	0.4	2.7	0.4	2.7	0.3	3.7	0.4	3.5	0.5	2.7	0.4
500	3.1	0.4	3.0	0.4	3.3	0.5	3.5	0.5	2.8	0.4	2.6	0.4
600	3.7	0.4	3.3	0.4	3.7	0.4	3.7	0.4	3.3	0.5	3.5	0.5
700	3.7	0.5	3.8	0.4	2.9	0.3	2.9	0.3	2.6	0.3	3.0	0.3
800	4.3	0.5	3.9	0.4	3.2	0.4	4.0	0.6	3.8	0.4	3.8	0.6
Linear equation	$y = 0.3261x + 1.9797$ (R^2=0.7932)		$y = 0.2021x + 2.4292$ (R^2=0.3855)		$y = 0.1996x + 2.1077$ (R^2=0.5158)		$y = 0.0975x + 3.0029$ (R^2=0.2244)		$y = 0.1371x + 2.509$ (R^2=0.2578)		$y = 0.234x + 1.9584$ (R^2=0.7914)	

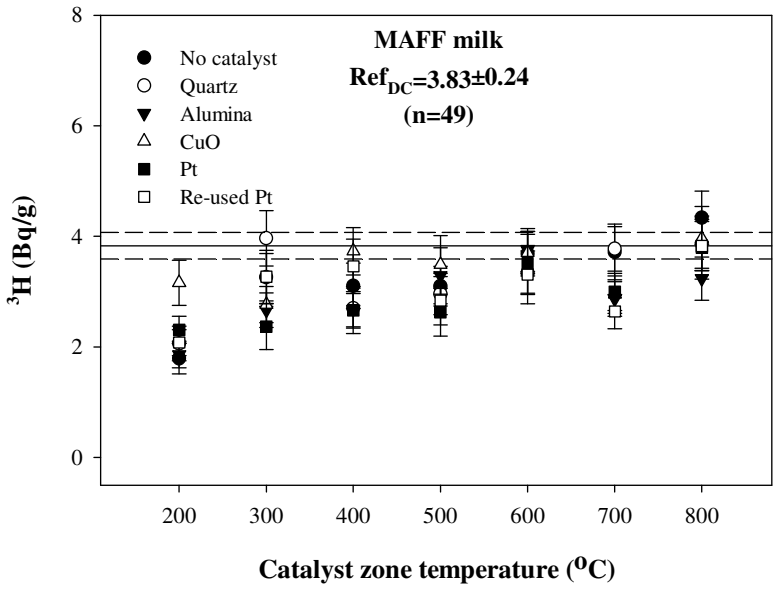

Figure 3.4: ^{3}H in milk depend on the types of catalyst and its temperature. Ref_{DC} is the decay corrected reference value. The reference value is shown as a solid line and the upper and lower limits as dashed lines.

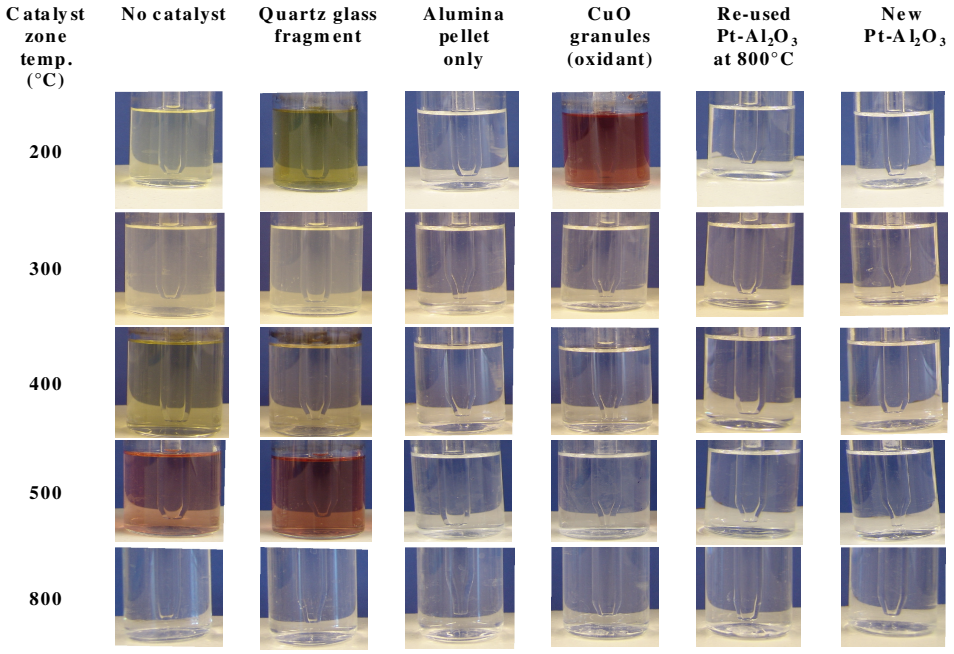

Figure 3.5: Images of aqueous sample after combustion of fish with temperatures and materials loaded in the catalyst zone. Similar results were obtained from milk however, less condensation was observed compared to the fish sample.

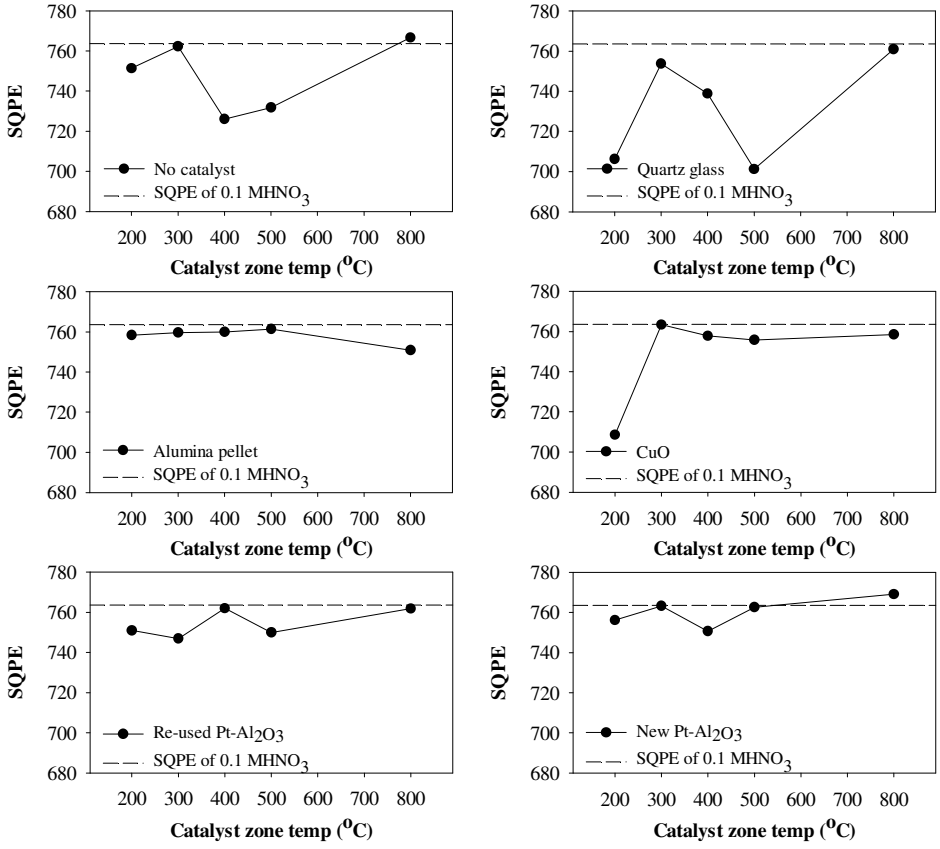

Figure 3.6: The SQPE levels of each samples under a range of conditions tested.

GC-MS analysis of combustion products

The gas chromatography mass spectrometer (GC-MS) analysis of the bubbler solution can provide information on the identity of any unoxidised species that are trapped in the bubbler solution. Two reference samples (MAFF fish and milk) were used for this investigation; similar masses (*ca* 1g) of fish and milk were heated up to 900°C in the quartz glass tube loaded with either new platinum alumina catalyst or quartz glass fragment. The catalyst zone was heated to 400°C. The mass (*ca* 10g) and particle size (*ca* 3 mm in diameter) of Pt-alumina and quartz glass were similar.

On completion of combustion, 3 mL of bubbler solution (0.1 M HNO_3), which contained all the combustion products and tritium activity, were taken and extracted with 6ml of solvent (Diethyl ether or dichloromethane) in a glass vial (22 ml) in an auto-mixer for 6 hours. The separated solvent from the aqueous sample was transferred to a 5ml glass vial for GC-MS analysis (Figure 3.7). Sample preparation of fish and milk sample for GC-MS analysis was carried out by D J Kim, GC-MS analysis was performed by Dr John Langley, School of Chemistry, University of Southampton and final data analysis was performed by D J Kim and Dr Phillip E Warwick. A Thermo Trace GC-MS system (model: ThermoQuest Trace MS, single quadrupole type GC-MS) with electron ionisation source and helium was used as a carrier gas. Column Type is Restek Stabilwax 30m × 0.25mm and 0.25 micron film thickness

A range of oxidation products were identified in the bubbler solution following combustion with quartz glass fragments in the catalyst zone. For instance, 3-furaldehyde and butyrolactone were identified following combustion of milk which may be typical partial decomposition products of sugar (e.g. sucrose and fructose). Similarly, for fish various incomplete oxidized compounds were identified. However, such compounds were not observed when platinised alumina catalyst was used. These results clearly demonstrated that combustion product from organic rich samples can be more effectively oxidized by platinum alumina catalyst. Some of combustion products (e.g. 1-[2-Methyl-3-(methylthio)allyl]cyclohex-2-enol and 8-Hexadecenal, 14-methyl-, (Z)-) were also identified following combustion of fish and milk using Pt-alumina catalyst. These are considered as a cross contamination from the wax component of used glass vial lid (Table 3.6).

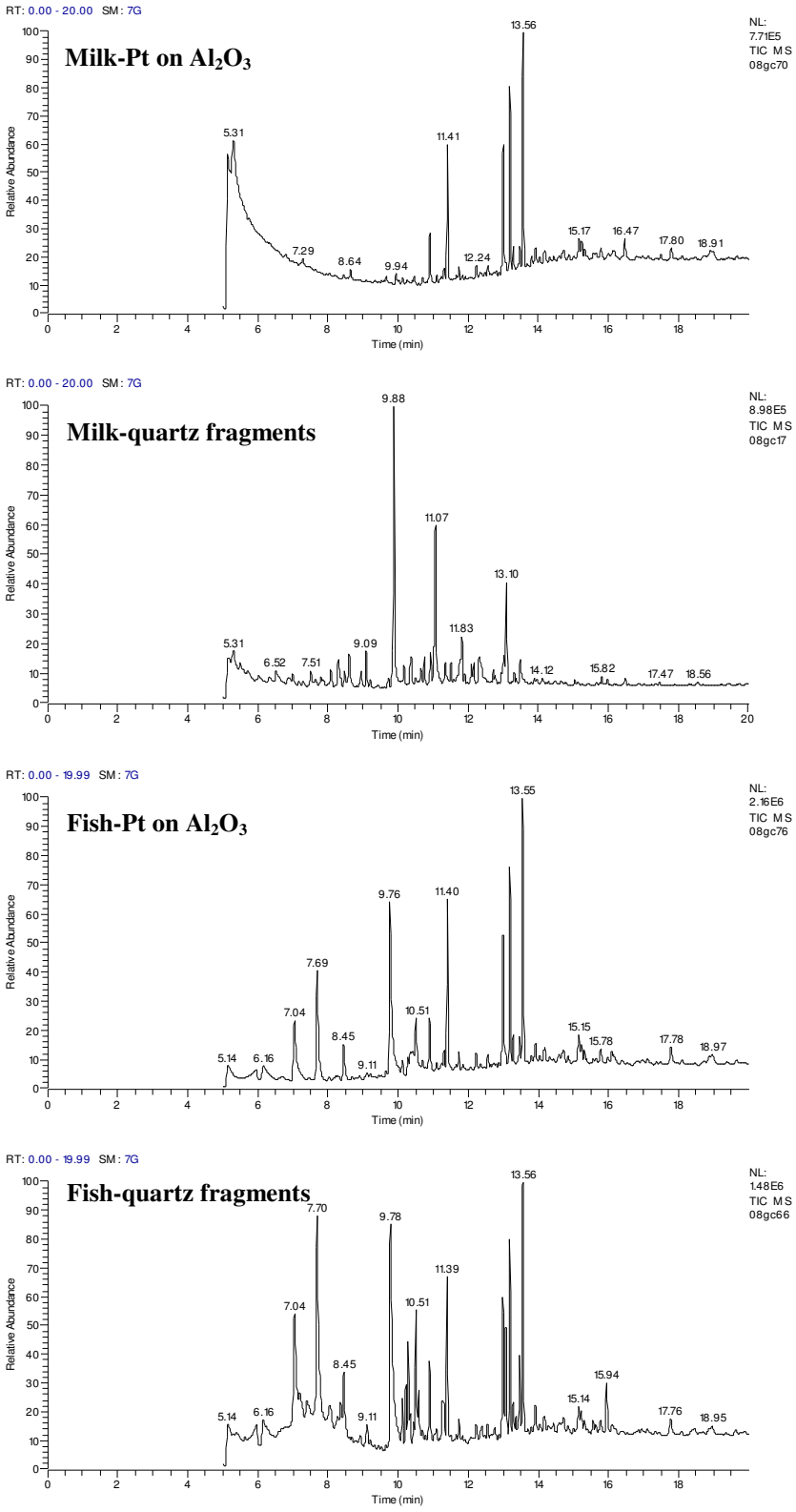

Figure 3.7: Chromatograms obtained for the analysis of MAFF milk and fish analysed by GC-MS. Platinum alumina catalyst (above spectrum) and Quartz glass fragments (below spectrum) were loaded in the catalyst zone heated to 400°C

Table 3.6: Comparison of compounds in solvent identified by GC-MS

	Milk (MAFF reference sample) Compounds structure	**Fish (MAFF reference sample) Compounds structure**
0.5% Pt on Al_2O_3	Acetic acid, dichloro- 1-[2-Methyl-3-(methylthio)allyl]cyclohex-2-enol 8-Hexadecenal, 14-methyl-, (Z)-	1-Octyn-3-ol, 4-ethyl- 2,2,4,4,5,5,7,7-Octamethyloctane
Quartz fragments	Propanoic acid Butanoic acid Phenol 2-Cyclopenten-1-one 3-Furaldehyde Butyrolactone 2(5H)-Furanone	7,8-Epoxylanostan-11-ol, 3-acetoxy- 2-Butanone, 4-hydroxy- Pyridine Ethane, 1,1-diethoxy- Thiocyanic acid, methyl ester 2-Butanol, 3-methoxy- Pyrrole Pentanoic acid, 3-methyl- Methoxyacetic acid, 3-tridecyl ester Phenol 1-Octanol, 2-butyl- Phenol, 3-methyl- 1H-Pyrrole-2-carbonitrile

Thermal impact on platinum catalyst

Platinum alumina catalyst contains 0.5% of platinum evenly distributed throughout cylindrical alumina pellets (3 mm in diameter), and it is difficult to detect the spatial distribution of Pt on the alumina pellet by scanning electron microscope (SEM); (Figure 3.8). This suggests that individual particles are likely to be <1μm in size (nano-particle size). In addition, it is difficult to distinguish any differences in platinum distribution for catalyst pellets heated to different temperatures (200-800°C).

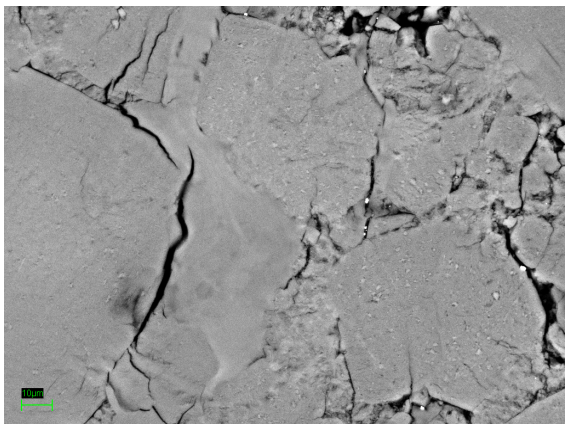

Figure 3.8: SEM image of the platinum alumina catalyst. Sample preparation for SEM analysis was done by Robert Jones, and the SEM image was produced by Dr Richard Pearce, National Oceanography Centre, University of Southampton.

X-ray fluorescence (XRF) analysis is a well established rapid method for determining the concentration of both major and trace elements in a sample. X-ray analysis and elemental mapping of platinum-alumina pellets was performed using a μXRF EAGLE III to investigate the change in distribution of platinum and any disintegration of the pellet after heating the platinum-alumina catalyst at different temperature (200-800°C). Although the X-Ray analysis (spot size ~50μm) has a lower resolution than SEM (1μm), X-Ray analysis provides a more effective method to find specific elements. It is clearly demonstrated that the platinum of the Pt-alumina catalyst was evenly distributed on the surface of cylindrical pellet and no significant visible change in its distribution or evidence for physical breakdown for all temperatures at the resolution provided ~50μm (Figure 3.9). There is also no significant difference between new Pt-alumina catalyst and platinum catalyst routinely used before this test at 800°C for ^{3}H extraction and at a range of temperature over 50 runs with a range of sample types including fish, milk, sludge, concrete and metals.

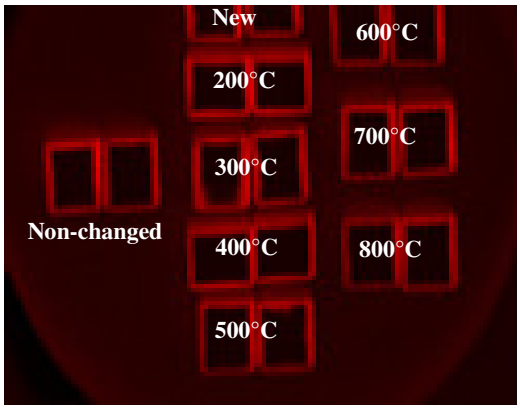

Figure 3.9: X-ray map (PtLα) of platinum distribution on the cylindrical Pt-alumina pellet (Cut through the middle and polished; shows Pt is only on the surface of the alumina). Platinum alumina catalyst preparation for X-ray map was done by Robert Jones and this image was produced by Dr Ian Croudace with μXRF EAGLE III.

3.3.2 Summary of catalyst function

Total ^{3}H activity of fish and milk were analysed using the combustion furnace method where platinum alumina catalyst and different materials (e.g. quartz glass fragments and alumina pellet) were loaded in the catalyst zone heated to a range of temperatures (200-800°C). Samples were heated up to 900°C using a preset ramping cycle. The tritium activity is not significantly different between using platinum alumina catalyst and other materials (e.g. quartz glass and alumina pellet) loaded in the catalysts zone of the combustion furnace

system. However, it is clearly demonstrated that platinum catalyst can effectively oxidize combustion products of organic compounds via GC-MS analysis of ^{3}H trapping solution. Incompletely combusted organic compounds and oxidized combustion products can produce chemical or colour quench which is significant factor to affect to efficiency of liquid scintillation counting for ^{3}H measurement.

Tritium recovery increased with increasing catalyst zone temperature, and coloration or odor of bubbler solution were removed at >600°C. There is no visible change to Pt distribution in catalysts heated up to 800°C. Therefore, for quantitative ^{3}H analysis of organic rich compounds through complete oxidation using combustion furnace method, platinum alumina catalyst heated to 800°C is appropriate.

3.4 Thermal evolution profiles of various materials

3.4.1 Introduction

The temperature at which ^{3}H is liberated from the sample may depend on the origin of tritium, the chemical form of ^{3}H in the sample and the sample composition. Tritium is most often encountered as tritiated water adsorbed onto the surface of the sample. Tritium as HTO may be rapidly liberated from the sample at temperatures around 100°C. However, ^{3}H may also be adsorbed as non-aqueous species or be intimately incorporated in the bulk sample matrix as water of crystallisation, structural H in organic minerals or as organic species. In these cases, higher temperatures will be required to liberate the ^{3}H and in such instances, complete decomposition of the sample may be necessary to ensure quantitative recovery of ^{3}H.

In this study, the temperature dependence of ^{3}H release from a range of tritiated materials commonly encountered during decommissioning and environmental surveys was investigated. Evolution profiles provide valuable information which can provide insights into the association and form of tritium. These studies can help to develop robust analytical analysis and sample preservation (storage) procedures for a range of waste types.

3.4.2 Method and materials

Tritium evolution profiles were determined for a range of contaminated materials which were either artificially spiked with tritiated compounds or which had become contaminated as a results of nuclear reactor operations and direct neutron activation or exposure to tritiated organic compounds from radiopharmaceutical manufacturers (e.g. Amersharm plc now GE

Healthcare at Cardiff). Evolution profiles were also determined for ^{3}H-thymidine in water (92.14 Bq/g, reference date is 07/12/1999 supplied by GE Healthcare Ltd). The specimens used for this study are classified into two groups; i) organic materials; sewage sludge, milk and fish, ii) construction materials; structural concrete, brick, metal and graphite (Table 3.7).

The sample was heated from 50°C to 500 or 900°C depending on the defined ramping profile (see Table 3.3). Thermal evolution profiles were determined by changing the bubbler at 30 min intervals throughout the run with each bubbler being analysed separately to determine the point at which tritium liberation occurred. The gas supply was isolated during the bubbler changeover. All tritium measurements were performed using a 1220 liquid scintillation counter (Wallac Quantulus™). Eight milliliters of aqueous sample were mixed with 12ml Gold Star™ (Meridian) scintillation cocktail in a 22ml polythene vial.

Table 3.7: Materials used in thermal evolution profile tests

Material	Origin	Origin of ^{3}H	Probable form of ^{3}H
^{3}H thymidine	^{3}H standard	Labelling	Thymidine
Fish	Lab preparation	Artificial spike	Thymidine
Milk	Lab preparation	Artificial spike	Thymidine
Cardiff East STW Sewage sludge	Waste water treatment works	Radiopharmaceutical	HTO/OBT
Structural concrete	Nuclear site (Winfrith)	Environmental exposure	HTO or structural H
Metal	Nuclear site (Winfrith)	Atmospheric exposure	HTO
Graphite (Reactor moderator)	[a]GLEEP (1 g) [b]COSORT (1 g) [c]DMTR (0.5 g)	Neutron capture	Structural H/ strongly bound
Brick	MOD site	Atmospheric exposure	HTO

[a]**GLEEP (Graphite Low Energy Experimental Pile)** was the first reactor in Europe and was built at the Atomic Energy Research Establishment near Harwell, Oxfordshire in an aircraft hangar in 1946. Generally operating at 3kW, GLEEP was used for initial investigations into reactor design and operation, and later used as an international standard for materials testing and calibration of instruments for measuring neutron flux. After continuous operation for 43 years, GLEEP was closed in 1990. The fuel was removed in 1994 and the control rods and external equipment the following year. A project to completely dismantle the reactor was started in 2003 and completed in October 2004.

[b]**CONSORT** was 100kW research reactor operated by Imperial College at a site near Ascot

[c]**DMTR**: Dounreay Material Test Reactor; DMTR reactor was used to test the performance of materials under intense neutron irradiation, particularly those intended for fuel cladding and other structural uses in a fast neutron reactor core. DMTR was closed in 1969.

3.4.3 Results

Evolution of ^{3}H-thymidine and a range of samples demonstrated different profile depending on sample types and ^{3}H form (Figure 3.10). Release of ^{3}H from samples could be grouped into two categories. Tritium liberation from concretes and brick was rapid with initial release of ^{3}H occurring at around 100°C and complete recovery of ^{3}H occurring below < 300°C. For all other sample types studied, the release of ^{3}H was delayed with quantitative recovery only being achieved at temperatures in excess of 500°C. The most delayed release of ^{3}H was observed for graphite where quantitative recovery of ^{3}H was only achieved following the complete decomposition of the graphite at temperatures exceeding 850°C.

^{3}H thymidine

Recoveries for ^{3}H in thymidine spiked into cellulose filter paper were over 95% using the combustion technique. Rapid initial liberation of ^{3}H occurred at low temperature (<100°C) due to the presence of tritiated water arising from decomposition of the ^{3}H thymidine during storage. Liberation of ^{3}H bound as C-H in thymidine was significantly slower than tritiated water and rapid liberation occurred between 300°C and 400°C in temperature. Tritium-labelled thymidine is routinely used as a standard material to evaluate furnace recovery.

Cardiff East STW sewage sludge

For sewage sludges contaminated with organic ^{3}H, ^{3}H evolution increased with temperature and achieved a peak at 500°C; over 97% of tritium was recovered within 4 hours. There was no rapid ^{3}H release in the early stages of combustion cycle or ^{3}H release at temperatures in excess of 500 °C. This implies that there is no significant quantity of tritiated water in this sewage sludge. Approximately, 1.0 g of sewage sludge pellets with 0.3- 0.5 cm in diameter was used in this study for ^{3}H evolution profile. If the sewage sludge size is reduced by grinding, more rapid oxidation could be achieved via an increased surface area (Penzhorn et al., 2000).

The sewage sludge used in this study contains organically bound tritium (OBT) originating from the Cardiff East Sewer Treatment Waste where liquid wastes containing variable tritiated organic compounds arose from radiopharmaceutical manufacture at Amersham plc Cardiff (now GE Healthcare). The wastes contained a wide range of uncharacterized ^{3}H intermediates, target compounds and by-products, whereas those from the nuclear power plants probably consist almost entirely of HTO (McCubbin et al., 2001). A commonly adopted definition of organically bound tritium (OBT) is a non-exchangeable ^{3}H form bound to a carbon atom (Pointurier et al., 2004), thus it is tightly held to the organic structure due to

the stable C-^{3}H bounds (Diabate and Strack, 1993) and has been shown to be persistent in the environment over decadal timescale (Warwick et al., 2003). Therefore, the evolution profile is being controlled by the form of ^{3}H contamination adsorbed to the sample substrate rather than incorporation of the ^{3}H into structural H groups within the sample matrix.

MAFF Fish and milk

Similar ^{3}H evolution profiles were observed for ^{3}H thymidine spiked into a matrix of either fish or milk. There was no rapid release of ^{3}H at low temperatures associated with HTO arising from decomposition of thymidine which differs from that observed for pure thymidine evolution profile. Tritiated thymidine spiked into fish/milk matrix and stored in a freezer does not appear to have degraded in the same way as ^{3}H thymidine in solution. Most tritium was evolved at <500°C and took 3 hours for both milk and fish to achieve 93% of recovery.

Structural concrete

Rapid evolution of ^{3}H was observed from the structural concrete at low temperatures and >95% of total tritium extraction was achieved at <350°C. The lack of ^{3}H in the evolution profile at temperatures >400°C confirms that no significant proportion of ^{3}H is associated with the mineral portlandite. In a separate experiment, it was demonstrated that drying the structural concrete for 3 days at 80°C resulted in the loss of >95% of ^{3}H, confirming that ^{3}H was not significantly associated with structural H. Concretes, along with many other structural materials become contaminated with ^{3}H during routine operation as a result of the wide spread presence of tritiated water vapour in reactor buildings coupled with its rapid diffusion into relatively porous materials (Furuichi et al., 2006).

Metal (mild steel)

Tritium evolution commenced at *ca* 200°C and the most vigorous ^{3}H evolution was observed at 300-500°C where the peak ^{3}H liberation was achieved at 350°C. A previous study (Kikuchi et al., 2006) carried out similar experiment with stainless steel by thermal desorption method (TDS) where a sample was heated up to 1000°C (constant ramp rate of 10°C/min) and a mixture of nitrogen and hydrogen (<2% volume) was used as a carrier gas. Tritium in stainless steel was released above 250°C and achieved a peak at about 400°C which is similar to that seen for the metal evolution profile obtained in this study. There was no additional tritium release from stainless steel at >400°C.

The mechanism for the retention of ^{3}H in metals following exposure to atmospheric tritiated water vapour is unclear. Previous studies have demonstrated that the ^{3}H is predominantly confined to the top 40μm (Lewis et al., 2005). One mechanism for ^{3}H retention could therefore be hydration of the surface Fe_2O_3 oxidation layer which forms at surface grain boundaries of mild steel. Such hydration has been shown to produce OH layers on α-Fe_2O_3 at $pH_2O > 10^{-4}$ Torr (Liu et al., 1998). Thermal decomposition of iron oxyhydroxides occurs at 200-300°C (Mitov et al., 2002) which coincides with the commencement of ^{3}H evolution in the sample. The absence of ^{3}H evolution at low temperatures has implications in sample preparation where filings or turnings are often produced in an attempt to obtain a representative sub-sample for ^{3}H analysis. The ^{3}H evolution profile would indicate that the heat generated during filing is unlikely to be sufficient to prematurely liberate the ^{3}H from the sample.

Moderator graphite

The graphite sample used in the study was sub-sampled from the moderator graphite removed from the GLEEP (Harwell), CONSORT (Imperial College) and DMTR (Dounreay) research reactor. Tritium evolution from graphite commenced at *ca* 600°C which is the highest temperature of all the materials tested. The commencement of ^{3}H evolution coincides with the onset of thermal decomposition of graphite at 645°C and continues up to 900°C (Bushuev et al., 1992; Pang et al., 1993; Bisplinghoff et al., 2000). Tritium is produced within the graphite structure via neutron activation of trace Li impurities via the $^{6}Li(n,\alpha)^{3}H$ reaction (σ_{th} = 940 b) and is effectively trapped within the graphite grains. However, some fraction of the tritium generated near to grain boundaries may penetrate through pore or gaps to be released. A significantly smaller proportion of ^{3}H is also produced via $^{2}H(n,\gamma)^{3}H$ and $^{3}He(n,p)^{3}H$ reactions (Hou, 2005). As such, the ^{3}H will only be released following decomposition of the graphite matrix.

Acid digestion using H_2SO_4, HNO_3, $HClO_4$ or mixture of them has also been used to decompose graphite and release ^{3}H (Goodall et al., 1989; Raymond, 1990) however, this method showed lower analytical results than the combustion technique (Hou, 2005) suggesting incomplete oxidation of the sample. Combustion is the most common method for decomposition of graphite where for the quantitative analysis of ^{3}H in graphite heating up to 900 °C is required and grinding of the sample recommended because combustion rate will be increased by the enhanced surface area exposed to heat (Penzhorn et al., 2000).

Brick

Tritium evolution from brick, sampled from MOD (Military of Defence) site, commenced at the early stages of combustion cycle (~120°C) and >90% of tritium extraction was achieved at <200°C. This is more rapid evolution of ^{3}H than structural concrete and confirms that most tritium originated from tritiated water form via atmospheric adsorption and no significant proportion of structurally-bound ^{3}H. Brick is a porous and permeable material consisting mainly of clay minerals (kaolinite, montmorillonite/smectitie, illite and chlorite) and variable amounts of water in the mineral structure by polar attraction (Guggenheim and Martin, 1995; Calabria et al., 2009). The porosity of brick may be higher than concrete consisting various sizes of several materials (e.g. Portland cement, sand, water and rock aggregates). Porosity is a significant factor that influences the physical-chemical interaction between solids and the gases and liquids that may absorb to the material (Calabria et al., 2009). The more rapid ^{3}H evolution from brick compared to that of structural concrete is most probably due to the higher porosity of the brick.

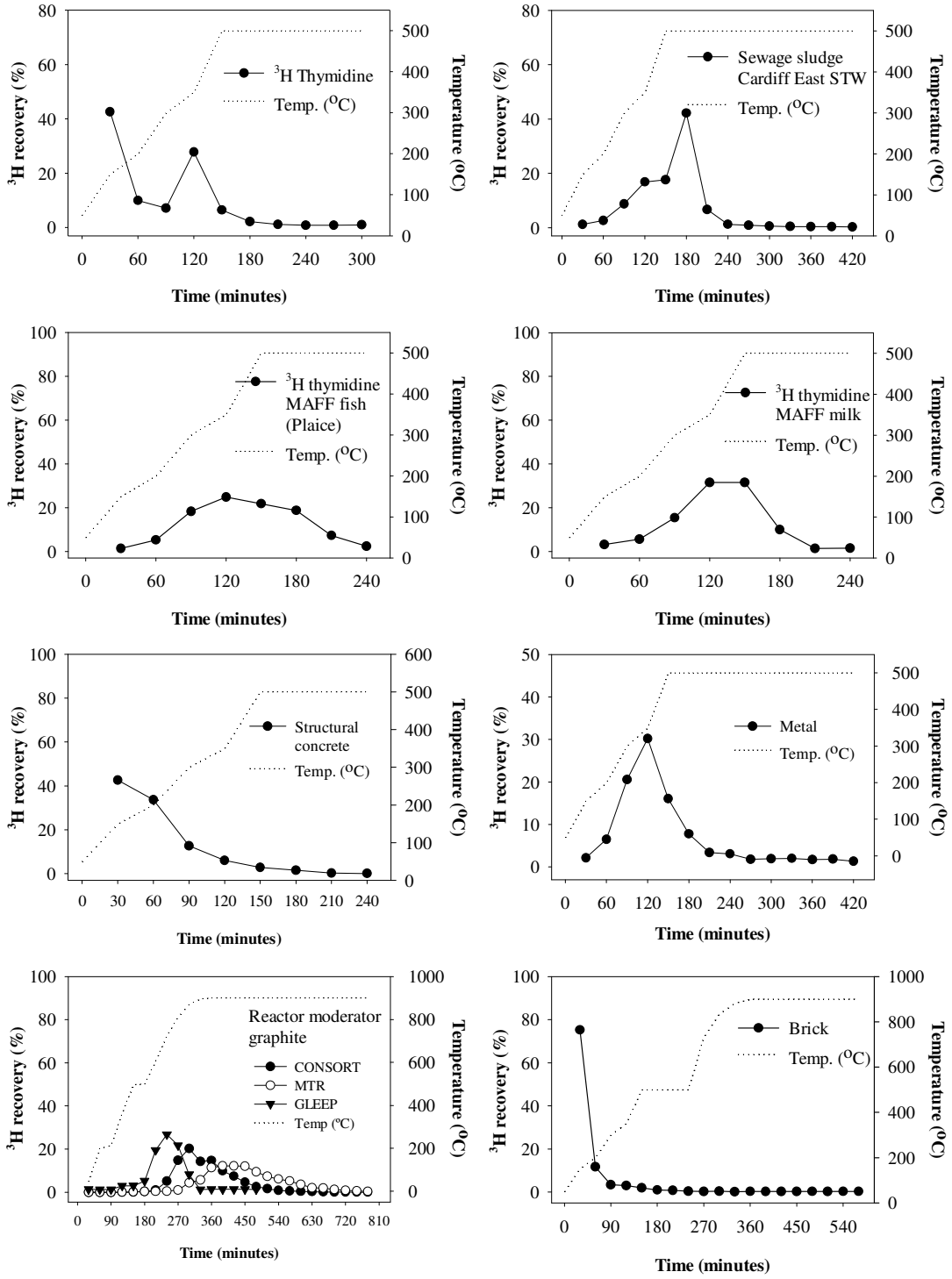

Figure 3.10: ^{3}H evolution depend on materials

3.4.4 Summary

For the majority of materials investigated in this study, the ^{3}H evolution temperatures were dictated by the initial form of ^{3}H contamination and the mechanism of adsorption of these tritiated species to the sample substrate. There was no evidence for in situ formation of ^{3}H or ^{3}H isotopic exchange involving structural hydrogen. The one exception to this is graphite, where ^{3}H production occurs in situ within the graphite lattice via neutron irradiation of trace Li impurities and where the ^{3}H evolution temperatures are related to the decomposition temperatures of the graphite matrix. These findings provide valuable information that can be used in assessing the ^{3}H evolution temperatures of other materials during combustion and help in developing heating profiles. In addition, the measurement of ^{3}H evolution profiles helps in assessing the potential for ^{3}H loss during sampling. The elevated temperatures required to liberate ^{3}H from metals would indicate that cutting/grinding during metal sampling is not problematic whereas for concrete samples, heat generation could easily result in the loss of ^{3}H and such loss must be taken into account during subsequent sample treatment and sub-sampling.

3.5 Precision and accuracy

As it is not possible to determine the specific chemical recovery for each sample analysis, it is vital that the efficiency of the combustion procedure is frequently assessed through the analysis of certified standards. The furnace recovery was assessed regularly with ^{3}H-thymidine standard (Amersham plc) which is difficult to combust compared to tritiated water but may reflect more precisely the furnace recovery when analyzing unknowns. The average furnace recovery for ^{3}H during this study was 90 ± 9.7 % (2 SD n = 131). This recovery and associated uncertainty was used in all subsequent calculations. Standard runs were performed after every five samples run and blank were analysed in each quartz glass tube after every standard analysis. Results were only accepted if their associated measured standard recoveries were between 80 and 110 (Figure 3.11). If measurable activity (>0.01Bq/g) was detected in the furnace blank the tube was cleaned before the next analysis by heating to high temperature (>600°C) until background tritium activities dropped to below the limit of detection of the liquid scintillation counter. Furnace blank samples are also run at regular intervals to confirm that no contamination in the following batch of samples especially after using the furnace for samples with high levels of ^{3}H.

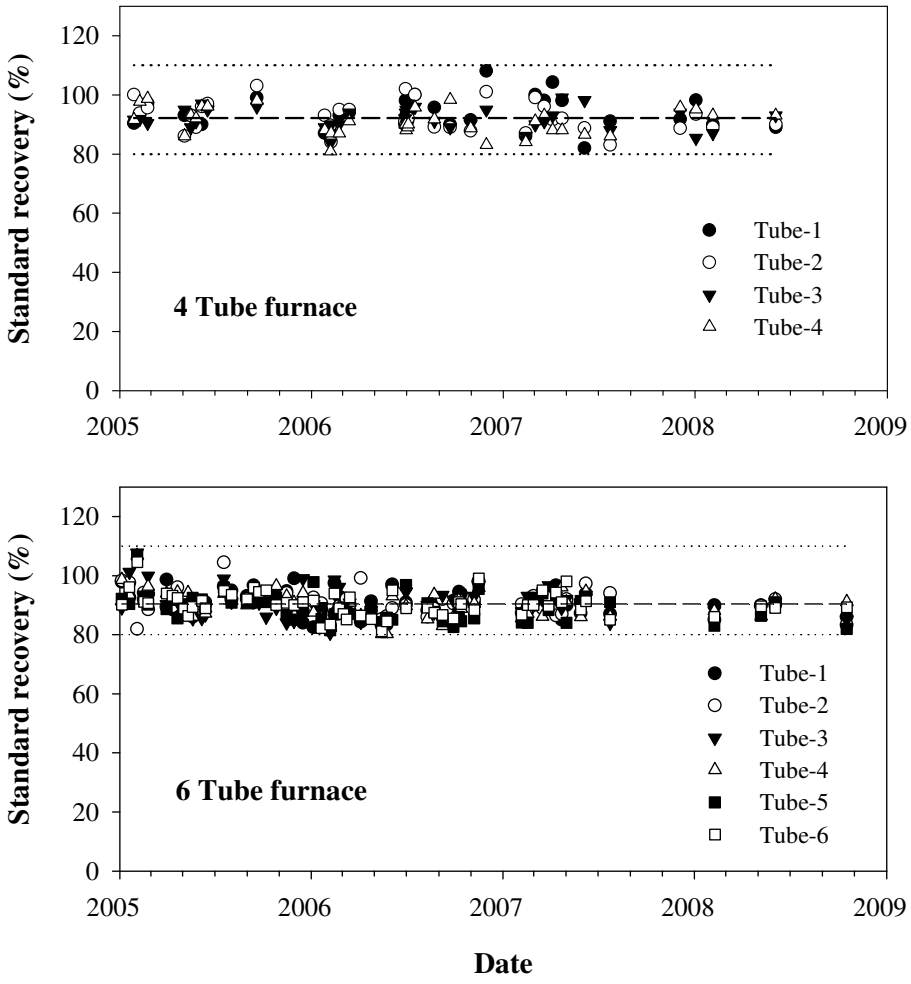

Figure 3.11: Control charts showing standard recoveries for the four tube furnace and six tube furnaces throughout the present study. Data are presented as the percentage of the standard recovered by the furnace and measured by the LSC. The mean furnace recovery (90%) is shown as a dashed line and the upper (110%) and lower (80%) limits as dotted lines.

The method reproducibility was assessed by replicate analysis of a ^{3}H thymidine standard (Try-44, Nycomed Amersham plc, Bucks, UK) and four different sample types which had a range of ^{3}H activity. Reference materials included MAFF (Ministry of Agriculture, Fisheries and Food) fish and milk powder. The tritium added to the materials was in the form of [methyl 1', 2'-^{3}H] thymidine, (supplied from Amersham plc) which was chosen to present a greater degree of difficulty to isolate from matrix as it exhibited more complex combustion characteristics compared with HTO (also stability of the standard). Sample preparation was carried out by Harwell Scientifics Ltd. The calculated reference values for MAFF fish and milk are 5.28±0.34 Bq/g and 5.04±0.32 Bq/g, respectively and to a reference date of 31 March 2001. All results were within 2σ uncertainty of the mean $^{3}H_{total}$ activity (Figure 3.12).

These results demonstrate that the combustion furnace method is rigorously reproducible for ^{3}H analysis. The measured reproducibility is greater than the predicted method uncertainty as the measured reproducibility does not include certain uncertainty factors (e.g. decay correction, speciation, LSC calibration and standard activity).

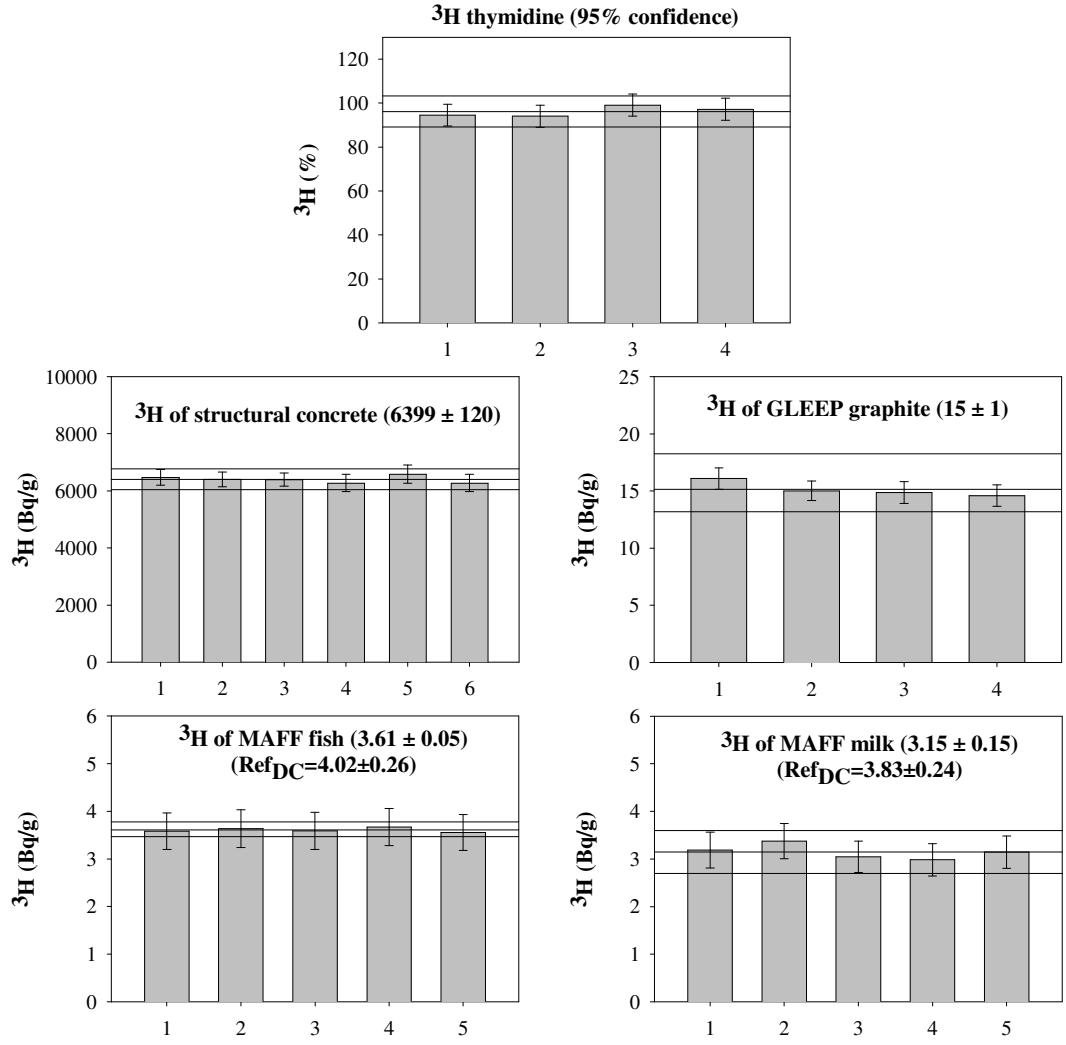

Figure 3.12: Method reproducibility determined from replicate analyses of ^{3}H thymidine and four different sample types. The values in the blanket are measured mean and standard deviation of total ^{3}H activity of each samples obtained from replicate analysis.

The results of the present study using MAFF fish and milk powder were compared with results from a MAFF-funded tritium intercomparison exercise in 2003 (Toole, 2003). This allowed the combustion furnace method to be compared with a range of other methods. The results, measured and decay corrected, were close to the reference value which are shown as

dashed line (Figure 3.13). Analytical method used in the intercomparison exercise in 2003 for tritium extraction included combustion, wet chemical oxidation using chromic acid and a sealed combustion bomb with high pressure oxygen. Combustion bomb method provided precise and accurate result for the milk, but not for the fish. Combustion furnace method provided results that were consistent with the assigned values. Most results presented varying degrees of negative bias (as much as 16% for plaice and 32% for milk) indicating incomplete recovery of the tritium following oxidation. A wet chemical oxidation method showed that it can perform at least as well as the dry combustion method, although one laboratory using this method had erratic results. One laboratory using a dry combustion method showed a large excess of tritium indicating a contamination problem. The results of the present study show negative biases indicating 10% for fish and 18% for milk. Given the sample type and scatter of data for all laboratories, this bias is considered acceptable.

Another intercomparison exercise in 2002 and 2004 results, originated by the National Physical Laboratory, provide measurement accuracy of combustion furnace (Pyrolyser system) and liquid scintillation counting for ^{3}H measurement (Table 3.8).

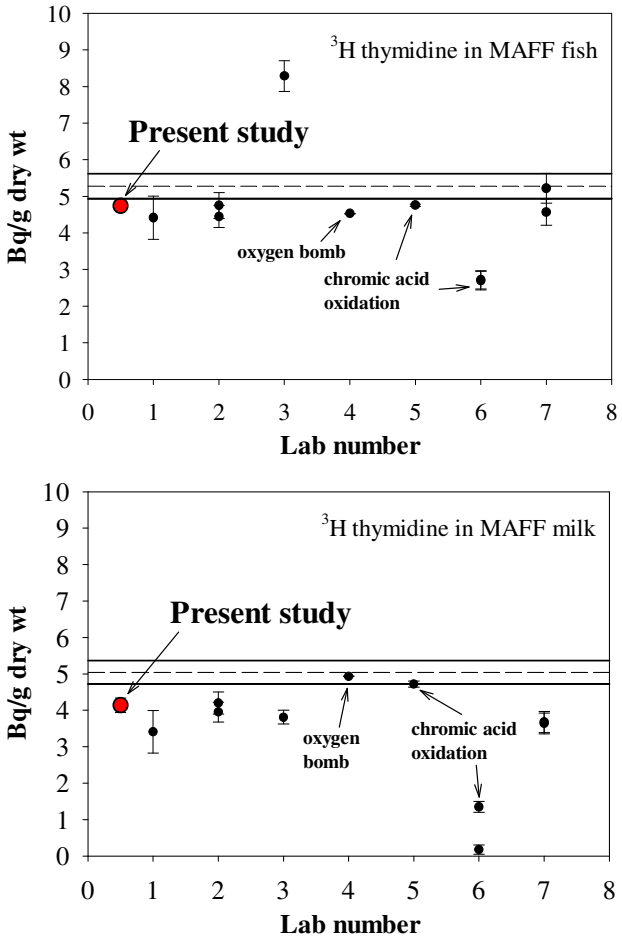

Figure 3.13: Comparison of ^{3}H activity of present study with intercomparison exercise results. The MAFF standards sample reference values are shown as a dash line (for MAFF fish and milk are 5.28±0.34 Bq/g and 5.04±0.32 Bq/g, respectively) and uncertainties (95%) as solid lines. These data were compiled from a total ^{3}H intercomparison exercise (Toole, 2003) and plotted with the present results. The analytical technique used is shown for each result, where no technique is specified, the result was obtained using a combustion furnace approach.

Table 3.8: Results ^{3}H in water for 2002 and 2004 NPL intercomparison exercise

Sample type	Supplier	Contaminant	Measured value (Bq/g±1σ)	Reference value (Bq/g±1σ)
Water	National Physical Laboratory	^{3}H water	20 ± 1 19 ± 1	20.04 ± 0.18
Water	National Physical Laboratory	^{3}H water	0.536 ± 0.042	0.539 ± 0.006

These data were compiled from measurements by GAU-Radioanalytical, University of Southampton using Pyrolyser system and LSC which used for the present study.

3.5.1 Method uncertainty

The method uncertainty was calculated by propagating the uncertainties associated with both sub-sampling and analysis of the sample (Table 3.9). Weighing of samples, standards and water bubblers and pipetting solutions into vials, introduced quantitative uncertainties in the final result. The variability in furnace recovery introduced the largest uncertainty with a spread from 90 to 110% (2SD) of the measured standard activity (results associated with recoveries outside this range were discarded). Counting statistical uncertainties are incorporated into the total method uncertainty on a sample-by-sample basis. All uncertainties are quoted at the 95% confidence level and refer to propagated method uncertainties.

Table 3.9: Calculation of a propagated uncertainty for the total tritium method

Measurement	**Uncertainty (%)**	**Relative standard deviation (1σ)**
Weighing	0.1	0.001
Decay correction	0.2	0.002
Furnace recovery	4.9	0.049
Speciation	2.5	0.025
LSC calibration	1	0.01
Standard activity (certified)	0.67	0.0067
Total (1σ)	5.6	0.056
Total (2σ)	11.2	0.112

This uncertainty was evaluated by GAU-Radioanalytical

Total uncertainty (%) is calculated by

$$Total\,(1\sigma) = \sqrt{(0.1)^2 + (0.2)^2 + (4.9)^2 + (2.5)^2 + (1)^2 + (0.67)^2} = 5.6\,\%$$

3.6 Tritium measurement

All tritium measurements were performed using a 1220 liquid scintillation counter (Wallac Quantulus™). The Wallac 1220 Quantulus has a further two photomultiplier tubes monitoring a chamber of scintillation gel (the guard chamber) directly above the sample chamber. These are set to count in anticoincidence with the sample photomultiplier tubes which reduces background counts significantly by eliminating thermal and electrical noise (L'Annunziata, 2003). The counter has associated lead shielding to reduce background derived from external radiation sources. The Quantulus 1220 applies the Spectral Quench Parameter of the External Standard method to correct for quenching effects. A γ-ray source (37000 Bq of ^{152}Eu) placed next to the vial irradiates the sample, producing Compton electrons with a constant spectrum of energies. This allows the effect of quench (measured as the position of 99.5% of the endpoint of the external standard spectrum) to be quantified.

Eight milliliters of aqueous sample were mixed with 12ml Gold Star™ (Meridian) scintillation cocktail in a 22ml polythene vial. Glass vials are normally avoided as they contain potassium which contributes to the measurement background. For ^{3}H measurements, cocktails with high aqueous loadings such as Gold Star and Ultima Gold LLT are most appropriate. It is usually advisable to reduce the aqueous loading to improve source stability. An aqueous : scintillant loading of 8 : 12 is recommended for Gold Star cocktail. Figure of merits plots (Figure 3.14) can be used to determine the optimum aqueous : cocktail ratios (where figure of merits are calculated as E^2V^2/B; E = efficiency, V = volume of sample and B is the background count rate)

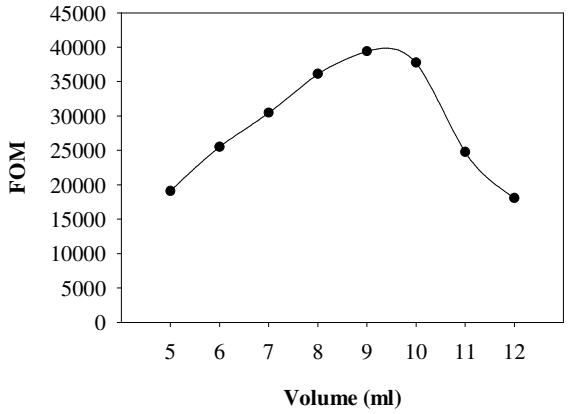

Figure 3.14: Figure of merit versus sample volume for ^{3}H (0.1M HNO_3 + Gold Star). Total volume = 20ml.

The vial was dark adapted for 8 hours to eliminate chemiluminescence and then counted for 1 hour (3 × 20 minutes) which can prevent sporadic counting events and provide a practical counting uncertainty. The total tritium activity (Bq/g) was then calculated using the equation:

$$A = \frac{C - B}{60} \cdot \frac{100}{E} \cdot \frac{1}{V_m} \cdot \frac{V_t}{M} \cdot \frac{100}{R_s}$$

, where C = the sample count rate (CPM); B = the background count rate (CPM); E = efficiency; V_t = Total volume of bubbler; V_m = Measured volume; M = Sample mass; and R_s = Standard recovery.

Blank sample (8 ml of 0.1 M HNO_3 into a scintillation vial along with 12 ml of Goldstar scintillation cocktail) was also used to determine the instrument background count rate. The background count rate is subtracted from the gross sample count rate to give the net count rate (or background-subtracted count rate) used for activity calculations. The efficiency was calculated using an empirically-defined calibration curve, which corrected for the amount of quench in the samples. The counter was calibrated for ^3H using a traceable tritiated water standard (TRY-44, Nycomed Amersham PLC, Bucks, UK); the standard calibration curve used was for 4 to 10 ml of Milli-Q water spiked with a certified tritiated water source (TRY-44, Nycomed Amersham PLC, Bucks, UK), mixed with the appropriate volume of Goldstar scintillation cocktail to give a total volume of 20 ml in a 22 ml polythene scintillation vial and counted for 1 hour (Figure 3.15). The limit of detection for this technique was 0.01 Bq/g, based on 1.3 cpm background and 60 minutes count time. Limits of detection is quoted as L_D as defined by Currie (Currie, 1968).

$$L_D(Bq/g) = \frac{2.71 + 4.65\sqrt{C}}{t} \times \frac{100}{E} \times \frac{100}{R} \times \frac{1}{M_g}$$

, where *C* is the total background count, *t* is the measurement time in seconds, *E* is the ^3H counting efficiency, *R* represents the chemical recovery (where appropriate) and *M* is the mass of sample in grams.

For all samples, the measured quench levels (SQP(E)) ranged from 700 to 850 which correspond to ^3H counting efficiencies of 17 - 31%. All uncertainties are quoted at the 95% confidence level and refer to propagated method uncertainties

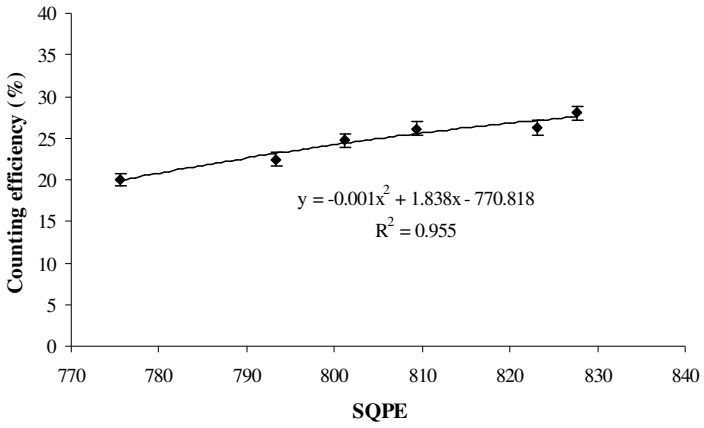

Figure 3.15: The standard calibration curve for ^{3}H measurement on the Quantulus 1220 liquid scintillation counter (instrument Q3). Aqueous samples, ranging in volume from 5 to 10 ml, were spiked with a tritiated water standard (from Amersham plc, Cardiff), then made up to 20 ml in a 22 ml polythene scintillation vial, dark adapted and counted for 1 hour.

Carbon-14 is a potential interference because it can also dissolve in water in the ^{3}H trapping bubbler and the tail of the ^{14}C energy spectrum would overlap with the ^{3}H energy spectrum. To counteract this, a solution of 0.1 M HNO_3 was used for trapping tritium because the acid reduced the solubility of CO_2. The presence of certain volatile radionuclides may interfere with the determination of tritium and ^{14}C. Specifically, high levels of ^{99}Tc, ^{106}Ru and ^{210}Po may result in spurious $^{3}H/^{14}C$ results. To test this, 9000Bq of ^{99m}Tc was transferred to filter paper strips in a sample boat. The filter paper was combusted using the standard procedure. The dilute HNO_3 bubbler was counted by gamma spectrometry to determine the total quantity of ^{99m}Tc that had been volatilized and trapped in the bubbler. The activity of ^{99m}Tc in the water bubbler was, 0.07Bq showing that 0.001% of the Tc was transferred to the bubbler. Analysis of ^{3}H and ^{14}C in water sample also containing ^{35}S (supplied as part of the 2002 NPL intercomparison exercise) gave results for both radionuclides that were good agreement with the certified values and confirmed that ^{35}S did not interfere with the measurement of either ^{3}H of ^{14}C.

Chemiluminescence, or the emission of light from chemical reactions, is a major interference for tritium because it produces peaks with similar energies to the ^{3}H energy spectrum. It is often produced by exposure of the scintillation cocktail to UV light or by reaction with basic samples (pH 8 to 14). To prevent chemiluminescence, samples can either be acidified or stored in a cool dark place overnight (L'Annunziata, 2003); in the present study samples were dark adapted for 8 hours before counting. However, for organic samples (e.g. MAFF

fish and milk reference samples), vials were dark adapted for 24 hours before counting to eliminate chemiluminescence.

3.7 Summary

Tritium extraction by Pyrolyser furnace system from various sample types was evaluated and showed high and reproducible recovery. For quantitative ^{3}H analysis using the combustion method, optimization of heating profiles and effective oxidation of volatile combustion products are essential. The ramping cycle is dependent on the sample matrix types and ^{3}H form present in the sample where maximum heating temperature and total combustion time can be determined by evolution profile of each sample type. Therefore, investigation of evolution profile of each sample prior to routine analysis for ^{3}H from various sample types is essential. Tritium evolution profile of specific materials depends on the form of ^{3}H in the sample, the origin of ^{3}H and the material composition. Tritiated water is rapidly liberated from the sample at lower temperature around 100°C whilst ^{3}H bound to structural H in organic minerals or organic species require high temperature (>300°C). However, for ^{3}H produced via neutron activation of trace Li impurities within the lattice (e.g. graphite) require higher temperature (>600°C).

The oxidation efficiency of platinised alumina catalyst is more effective than other tested materials (e.g. CuO, quartz and alumina pellet) although there is no significant difference in final ^{3}H measurement. Combustion using platinum catalyst can also effectively remove coloration (yellow and brown) of bubbler solution arisen from incomplete oxidation of organic rich materials which provide significant quench (colour and chemical) decreasing counting efficiency of LSC. The function of the platinum alumina catalyst in the furnace system is more effective when the catalyst is heated to high temperature (~800°C). There is no significant physical degradation or change of Pt distribution on the cylindrical pellet.

3.8 References

Bisplinghoff B, Lochny M, Fachinger J, Brucher H. 2000. Radiochemical characterization of graphite from Julich experimental reactor (AVR). Nuclear Energy-Journal of the British Nuclear Energy Society 39: 311-315.

Burger LL (1979) Distribution and reactions of tritiated hydrogen and methane. In: (IAEA) IAEA (ed) Proceedings of the International Symposium on the Behaviour of Tritium in the environment. IAEA, Vienna, pp 47-63.

Bushuev AV, Verzilov YM, Zubarev VN, Kachanovskii AE, Matveev OV, Proshin IM, Bidulya LV, Ivanov AA, Kalugin AK. 1992. Quantitative-Determination of the Amount of H-3 and C-14 in Reactor Graphite. Atomic Energy 73: 959-962.

Calabria JA, Vasconcelos WL, Boccaccini AR. 2009. Microstructure and chemical degradation of adobe and clay bricks. Ceramics International 35: 665-671.

Currie LA. 1968. Limits for qualitative detection and quantitative determination. Application to radiochemistry. Analytical Chemistry 40: 586-593.

Diabate S, Strack S. 1993. Organically Bound Tritium. Health Physics 65: 698-712.

Furuichi K, Takata H, Motoshima T, Satake S, Nishikawa M. 2006. Study on behavior of tritium in concrete wall. Journal of Nuclear Materials 350: 246-253.

Goodall DHJ, McCracken GM, Coad JP, Causey RA, Sadler G, Jarvis ON. 1989. Measurement of tritium distribution in JET. Journal of Nuclear Materials 162-164: 1059-1064.

Guggenheim S, Martin RT. 1995. Definition of Clay and Clay Mineral - Joint Report of the Aipea Nomenclature and Cms Nomenclature Committees. Clays and Clay Minerals 43: 255-256.

Hou X. 2005. Rapid analysis of ^{14}C and ^{3}H in graphite and concrete for decommissioning of nuclear reactor. Applied Radiation and Isotopes 62: 871-882.

Kikuchi K, Nakamura H, Tsujimoto K, Kobayashi K, Yokoyama S, Saitoh S, Yamanishi T. 2006. Evaluation of residual tritium in stainless steel irradiated at SINQ target 3. Journal of Nuclear Materials 356: 157-161.

Kim DJ, Warwick PE, Croudace IW. 2008. Tritium Speciation in Nuclear Reactor Bioshield Concrete and its Impact on Accurate Analysis. Anal. Chem. 80: 5476-5480.

L'Annunziata MF. 2003. Liquid scintillation analysis: principles and practice. In *Handbook of radioactivity analysis* (Edited by M. F. L'Annunziata). Academic Press, Sandiego.

Lewis A, Warwick PE, Croudace IW. 2005. Penetration of tritium (as tritiated water vapour) into low carbon steel and remediation using abrasive cleaning. Journal of Radiological Protection 25: 161-168.

Liu P, Kendelewicz T, Brown GE, Nelson EJ, Chambers SA. 1998. Reaction of water vapor with [alpha]-Al2O3(0001) and [alpha]-Fe2O3(0001) surfaces: synchrotron X-ray photoemission studies and thermodynamic calculations. Surface Science 417: 53-65.

Lockyer JF, Lally AE. 1993. The Determination of Tritium, C-14 and S-35 in Milk and Crop Samples Using a Combustion Technique. Science of the Total Environment 130: 337-344.

McCubbin D, Leonard KS, Bailey TA, Williams J, Tossell P. 2001. Incorporation of Organic Tritium (^{3}H) by Marine Organisms and Sediment in the Severn Estuary/Bristol Channel (UK). Marine Pollution Bulletin 42: 852-863.

Mitov I, Paneva D, Kunev B. 2002. Comparative study of the thermal decomposition of iron oxyhydroxides. Thermochimica Acta 386: 179-188.

Munakata K, Baba A, Nishikawa M, Penzhorn RD. 1998. Development of an improved ceramic tritium breeder-ceramic breeder with catalytic function. Journal of Nuclear Science and Technology 35: 511-514.

Munakata K, Yokoyama Y, Koga A, Nakashima N, Beloglazov S, Takeishi T, Nishikawa M, Penzhorn RD, Kawamoto K, Moriyama H. 2002. Effect of catalytic metals on tritium release from ceramic breeder materials. Journal of Nuclear Materials 307-311: 1451-1455.

Pang LSK, Saxby JD, Chatfield SP. 1993. Thermogravimetric Analysis of Carbon Nanotubes and Nanoparticles. Journal of Physical Chemistry 97: 6941-6942.

Payne PR, Campbell IG, White DF. 1952. The combustion of tritium-labeled organic compounds. Biochem. J. 50: 500-502.

Penzhorn RD, Bekris N, Hellriegel W, Noppel HE, Nagele W, Ziegler H, Rolli R, Werle H, Haigh A, Peacock A. 2000. Tritium profiles in tiles from the first wall of fusion machines and techniques for their detritiation. Journal of Nuclear Materials 279: 139-152.

Pointurier F, Baglan N, Alanic G. 2004. A method for the determination of low-level organic-bound tritium activities in environmental samples. Applied Radiation and Isotopes 61: 293-298.

Raymond A. 1990. Analyse des radioisotopes emetteurs beta purs (^{3}H, ^{14}C, ^{36}Cl, ^{63}Ni) dans le graphite irradie. Rapport Techniques, CEA-RT-DSD-20, CEA, France.

Toole J. 2003. A proficiency testing scheme for the measurement of tritiated thymidine in milk and fish. Harwell Scientifics Ltd, Didcot, UK.

Warwick PE, Croudace IW, Howard AG, Cundy AB, Morris J, Doucette K (2003) Spatial and temporal variation of tritium activities in coastal marine sediments of the Severn estuary (UK). In: Warwick P (Ed) Environmental Radiochemical Analysis II, pp 92-103.

Chapter 4

Paper: Tritium (^{3}H) speciation in nuclear reactor bioshield concrete and its impact on accurate analysis

Analytical Chemistry, 80, 5476-5480 (2008)

4 Paper in Analytical Chemistry, 80, 5476-5480 (2008):

Tritium (^{3}H) speciation in nuclear reactor bioshield concrete and its impact on accurate analysis

Dae Ji Kim, Phillip E.Warwick and Ian W. Croudace

GAU-Radioanalytical, National Oceanography Centre, University of Southampton, European Way, Southampton SO14 3ZH, UK

4.1 Abstract

Tritium (^{3}H) is produced in nuclear reactors via several neutron induced reactions [^{2}H(n,γ)^{3}H, ^{6}Li(n,α)^{3}H, ^{10}B(n, 2α)^{3}H, ^{14}N(n, ^{3}H)^{12}C and ternary fission (fission yield <0.01%)]. Typically, ^{3}H is present as tritiated water (HTO) and can become adsorbed into structural concrete from the surface inward where it will be held in a weakly-bound form. However, a systematic analysis of a sequence of sub-samples taken from a reactor bioshield using combustion and liquid scintillation analysis has identified two forms of ^{3}H, one weakly bound and one strongly bound. The strongly bound tritium, which originates from neutron capture on trace lithium (^{6}Li) within mineral phases, requires temperatures in excess of 350°C to achieve quantitative recovery. The weakly bound form of tritium can be liberated at significantly lower temperatures (100°C) as HTO and is associated with dehydration of hydrous mineral components. Without an appreciation that two forms of tritium can exist in reactor bioshields the ^{3}H content of samples may be severely underestimated using conventional analytical approaches. These findings exemplify the need to develop robust radioactive waste characterization procedures in support of nuclear decommissioning programmes.

4.2 Introduction

A wide range of early generation nuclear facilities (military and civil) are undergoing decommissioning worldwide. These include research reactors, civil nuclear power plants, isotope production plants, particle accelerators, experimental fusion facilities and isotopic enrichment facilities. In the UK in particular, most first and second generation nuclear research sites and nuclear power plants are being decommissioned or are scheduled to begin decommissioning within the next decade.

The nature of decommissioning works varies from site to site but typically involves the extensive clean out, refurbishment or demolition of buildings and other facilities, and remediation of the land. As a result, large volumes of potentially radioactive waste materials will be generated which require accurate characterization prior to waste sentencing. In many instances, novel radioanalytical approaches must be developed and validated to permit quantification of radionuclides in diverse and complex matrices. Concrete, cements and other cementitious materials account for 21% of the total weight of low level radioactive waste (LLW) and 12 % of the total weight of intermediate level waste (ILW) in the UK (DEFRA, 2002). Concrete has been widely used in the nuclear industry due to its strength, durability, low cost and good radiation shielding characteristics. Concretes, along with many other structural materials become contaminated with ^{3}H during routine operations as a result of the widespread presence of tritiated water (vapour) in reactor buildings coupled with its rapid diffusion into relatively porous materials. The high diffusivity of ^{3}H makes prediction of activity concentrations difficult and there is therefore a need to directly determine ^{3}H in concretes. In certain types of reactor design using D_2O, such as CANDU reactors and the now decommissioned SGHW reactor (Winfrith, UK) significant quantities of tritium were produced via neutron activation of deuterium (D_2O moderator) or lithium and ternary fission (0.01% fission yield). The quantities of tritium produced in Heavy Water Reactors by neutron activation of deuterium exceeds that in Light Water Reactors by almost 100 times (Harolf and Baker, 1985; Johnson et al., 1992). Reactor bioshield concrete will also be directly exposed to neutrons resulting in the *in-situ* formation of a range of radionuclides including ^{3}H, ^{14}C, ^{63}Ni, ^{60}Co, ^{36}Cl, ^{55}Fe, ^{41}Ca, ^{152}Eu, and ^{133}Ba (Hou, 2005). Of these, tritium is considered to be one of the critical radionuclides (Bushuev et al., 1992; Bisplinghoff et al., 2000; Kinno et al., 2002a). Previous studies of tritium in concrete (Numata et al., 1990a; Numata et al., 1990b; Hou, 2005; Furuichi et al., 2006; Furuichi et al., 2007), have mainly focused on structural concretes exposed to HTO and have not specifically considered bioshield concrete. Neutron activation of trace Li impurities in bioshield concrete provides an alternative mechanism for ^{3}H production and such ^{3}H produced *in-situ* may be expected to be present in a different, potentially less-available, form since it may be locked/trapped inside mineral lattices.

Direct non-destructive detection of ^{3}H at low activity concentrations is difficult given the low energy pure beta emission of the radionuclide (E_{max} = 18.6 keV). Therefore standard laboratory procedures for the determination of ^{3}H in solid matrices will liberate ^{3}H by aqueous leaching, distillation, freeze drying, azeotropic distillation or via chemical / thermal

oxidative decomposition prior to quantification of the liberated ^{3}H usually by liquid scintillation counting. With the exception of oxidative decomposition, the techniques depend on the ^{3}H being present as tritiated water which is readily extractable. The efficacy of these methods could be significantly affected by the form of ^{3}H present and in particular may not quantitatively recover ^{3}H produced *in situ* via neutron activation of Li. There has been no previous attempts to compare the extractability of ^{3}H in bioshield and structural concretes and to assess the impact that this may have for accurate analytical measurements, although measurement of total ^{3}H in bioshield concrete has been previously reported using oxidative combustion (Hou, 2005). This investigation aimed to determine whether different analytical approaches are required for these two concrete types, if a single method would be effective for all types and to consider the implications for improper waste characterization prior to waste sentencing.

4.3 Experimental Section

A cylindrical concrete core, traversing the reactor bioshield, was taken from the 100 MWe Steam Generating Heavy Water Reactor (SGHWR) which was operated by the United Kingdom Atomic Energy Authority at Winfrith, Dorset from 1967-1990 (Figure 4.1). The core was sectioned at 10cm intervals and its outer surface, which may have been compromised during coring, was removed and discarded. Core sub-sections were crushed to ensure a homogenous sample suitable for analysis and 30g of sample were transferred to a 20 ml polythene vial. Gamma emitting radionuclides were determined using a Canberra 40% well-type HPGe gamma spectrometer previously calibrated against a matrix-matched mixed radionuclide standard of identical geometry (QCYK8563). Spectral deconvolution was performed using Fitzpeaks™ software (JF Computing). Additional corrections for cascade-summing effects were applied for ^{152}Eu. Total tritium activity concentrations and ^{3}H thermal evolution profiles were determined on each of the sub-sections.

Structural concrete samples and other construction materials used in the leaching trials were taken from the nuclear reactor site (Winfrith) and from other non-nuclear sites for comparative purposes. These materials had not been exposed to a neutron flux and the ^{3}H present originated from exposure to tritiated water vapour only.

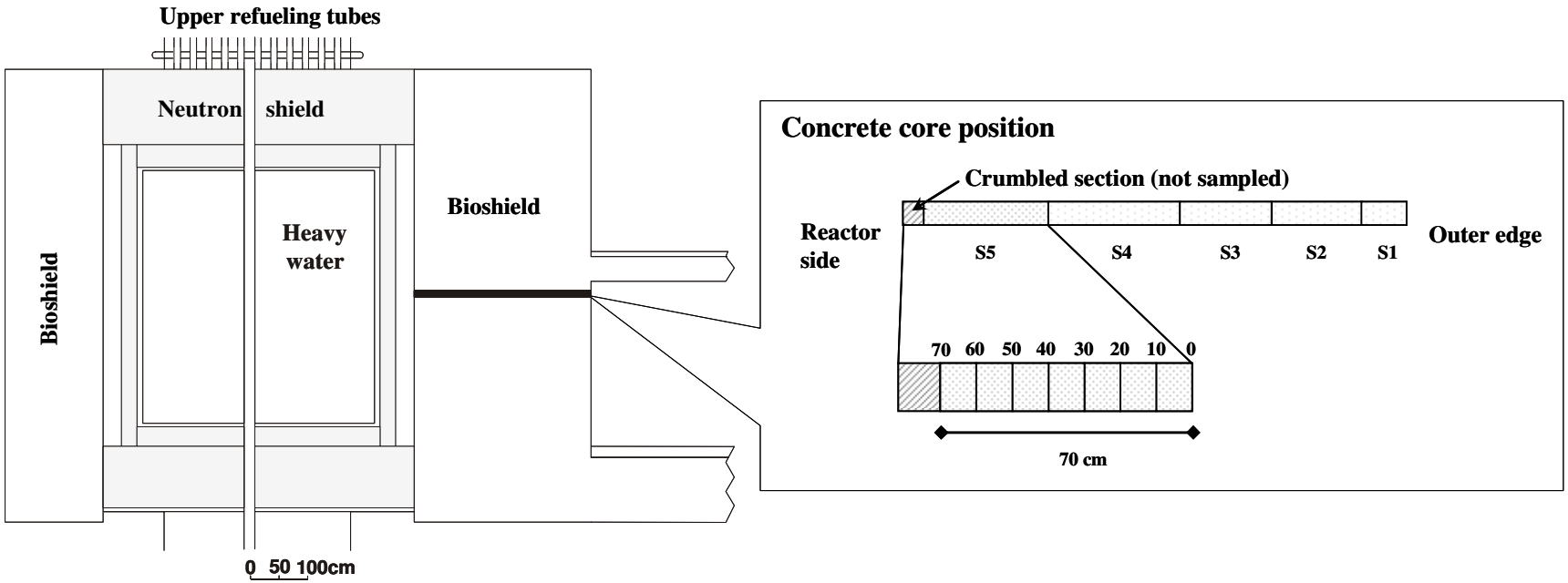

Figure 4.1: Sampling of bioshield concrete

Tritium extraction was achieved using a Raddec Pyrolyser Trio™ System (Figure 4.2) which permits simultaneous extraction/oxidation of up to six samples. This system was designed specifically for quantitative extraction of tritium and ^{14}C from nuclear and environmental samples.

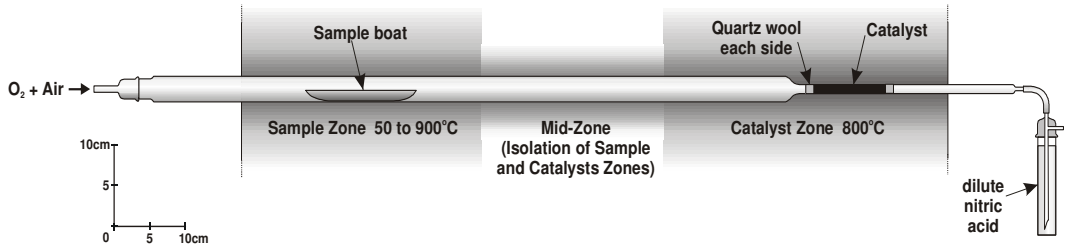

Figure 4.2: Schematic diagram of the Pyrolyser triple zone furnace

Each sample was heated using a preset heating cycle (Figure 3) in its own silica glass work-tube that carried a stream of air/oxygen. The liberated gases pass through a zone containing 10 g of platinised alumina catalyst that oxidizes any organic combustion products to CO_2 and H_2O (and HTO). Any water vapour, including HTO, is trapped in a bubbler containing 20 ml of 0.1 M HNO_3. Bubblers are changed every 30 minutes to determine the ^3H evolution profile and the gas supply is isolated during the bubbler changeover. Reported temperatures refer to that recorded by the furnace thermocouple and the sample temperature is typically 10 – 20% lower than the furnace temperature during the ramping stages but < 5% lower during the hold stages.

The amount of tritium emanated at various temperatures was also investigated by heating sub-samples of concrete to set temperatures for 12 hours and then allowing the samples to cool to room temperature. The ^3H content and evolution profile of the ^3H remaining in the sample after this heating stage was then determined as described previously.

The aqueous leachability of ^3H from the bioshield concrete was compared with that from a range of other building materials sampled from the SGHWR reactor building and also from a non-nuclear HTO handling facility that had been exposed to HTO vapor *in situ* (but which were not exposed to a reactor neutron flux). Approximately 1g of solid material was mixed with 10ml of water for a defined time with constant agitation. Bioshield concretes were

leached for 12 hours whilst all other materials were leached for 2 hours. The samples were then filtered and the ^{3}H content of the filtrate determined by liquid scintillation counting.

All tritium measurements were performed using a 1220 liquid scintillation counter (Wallac Quantulus™). 8ml of aqueous sample were mixed with 12ml Gold Star™ (Meridian) scintillation cocktail in a 22ml polythene vial. The counter was calibrated for ^{3}H using a traceable tritiated water standard (TRY-44, Nycomed Amersham PLC, Bucks, UK). For all samples, the measured quench levels (SQPE) ranged from 700 to 850 which correspond to ^{3}H counting efficiencies of 17 - 31%. All uncertainties are quoted at the 95% confidence level and refer to propagated method uncertainties.

Lithium concentrations in the bioshield concrete sub-sections were measured to allow calculation of the theoretical quantity of ^{3}H produced via the $^{6}Li(n,\alpha)^{3}H$ reaction. Stable Eu was also determined to permit the calculation of theoretical ^{152}Eu production and hence the expected $^{3}H/^{152}Eu$ ratio. Approximately 1g of concrete was accurately weighed and completely digested using a combination of HNO_3 and HF. The residue was dissolved in 2% HNO_3 and diluted to reduce the total dissolved solid content. Li concentrations in the digest were determined using ICP-AES whilst Eu concentrations were determined by ICP-MS. Measurement uncertainties were typically ±3% relative standard deviation (2σ).

4.4 Results and discussion

Two distinct stages of ^{3}H loss were identified for the bioshield concrete. In concrete located further away from the reactor core (outer bioshield), where neutron fluxes would have been relatively low, tritium was liberated in the early stages of the combustion cycle at < 350°C. The tritium evolution profile was similar to that seen for structural concrete (non-irradiated concrete) where ^{3}H contamination arose from exposure of the concrete to HTO vapor. For the concrete sub-samples located nearer to the reactor core (inner bioshield) and which had been exposed to higher neutron fluxes, the tritium evolution mostly occurred over a 500-900°C temperature range (Figure 4.3). The two distinct forms of tritium are subsequently referred to as ‘weakly bound ^{3}H’ and ‘strongly bound ^{3}H’ respectively.

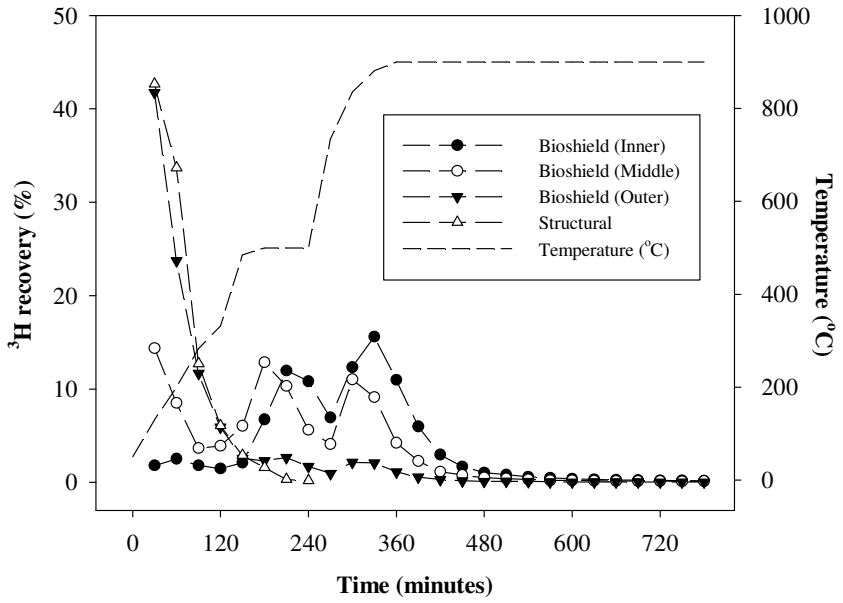

Figure 4.3: Tritium evolution profiles for structural and bioshield concrete

The temperature of ^{3}H evolution will depend on whether the ^{3}H is present in the concrete as free water, water of crystallization, structural OH groups or otherwise lattice-bound ^{3}H. Some earlier studies (Alarcon-Ruiz et al., 2005) have identified that water loss from concrete occurs in three key transition stages at approximately 105°C, 170°C and 300°C. In the present study the ^{3}H evolution profiles of the concrete sub-samples previously heated to these key temperatures for 12 hours were compared with that for non-thermally treated bioshield concrete (Figure 4.4). Heating the concrete to 105°C resulted in the complete loss of the weakly bound tritium component which is dominantly present in outer bioshield concrete. However, the strongly bound tritium, which is the main component of the inner bioshield concrete, was not significantly affected by any preliminary heating to 105°C or 170°C. The quantitative removal of weakly bound ^{3}H, following drying of the sample at 105°C, suggests that the more prolonged release of ^{3}H observed up to 300°C in the evolution profile arises from a slow rate of release as opposed to a strongly bound form of ^{3}H requiring higher temperatures to effect decomposition and indicates that the weakly bound ^{3}H is present as adsorbed water.

The total ^{3}H concentration in bioshield concrete is highest near the reactor core and decreases exponentially with distance from the reactor. However, when the tritium species in the

bioshield concrete are considered, the relative proportion of strongly bound tritium decreases exponentially while the weakly bound tritium increases with increasing distance from the core (Figure 4.5). The activity concentration of weakly bound ^{3}H, however, remains approximately constant throughout the core. The different proportions of the two forms of tritium identified suggest different origins.

A simple aqueous leach test is often employed to assess the level of ^{3}H contamination in a solid sample. A comparison of leached ^{3}H versus total ^{3}H ($^{3}H_{total}$) highlights three different relationships. For the majority of sample types exposed to HTO (including structural concrete), the leached ^{3}H compares very well with the $^{3}H_{total}$ as determined by combustion (Figure 4.6 zone B). Similar results are also observed between leaching and the weakly bound ^{3}H component of the bioshield concrete samples (Figure 4.6 ●). For certain materials (notably brick, plaster and sealant), the ^{3}H leach results were lower than the $^{3}H_{total}$ although a correlation still existed between the two measurements (Figure 4.6 zone A). The low bias may indicate a slow leach rate and may be improved by extending the leach time. However, no correlation was observed between the leached ^{3}H and the total ^{3}H as measured by combustion (Figure 4.6 zone C) suggesting that the leaching technique was not capable of extracting the strongly bound ^{3}H fraction in the bioshield concrete.

The systematic analysis of a sequence of sub-samples taken from the examined core showed tritium evolution profiles that varied with distance from the reactor. In concrete sampled further away from the reactor (outer bioshield) rapid tritium loss at lower temperature occurs that is similar to that seen for structural concrete (non-bioshield concrete). Conversely, for the concrete closer to the reactor (inner bioshield concrete) the rate of HTO lost at low temperature is considerably reduced and temperatures in excess of 860°C were required to completely liberate the ^{3}H.

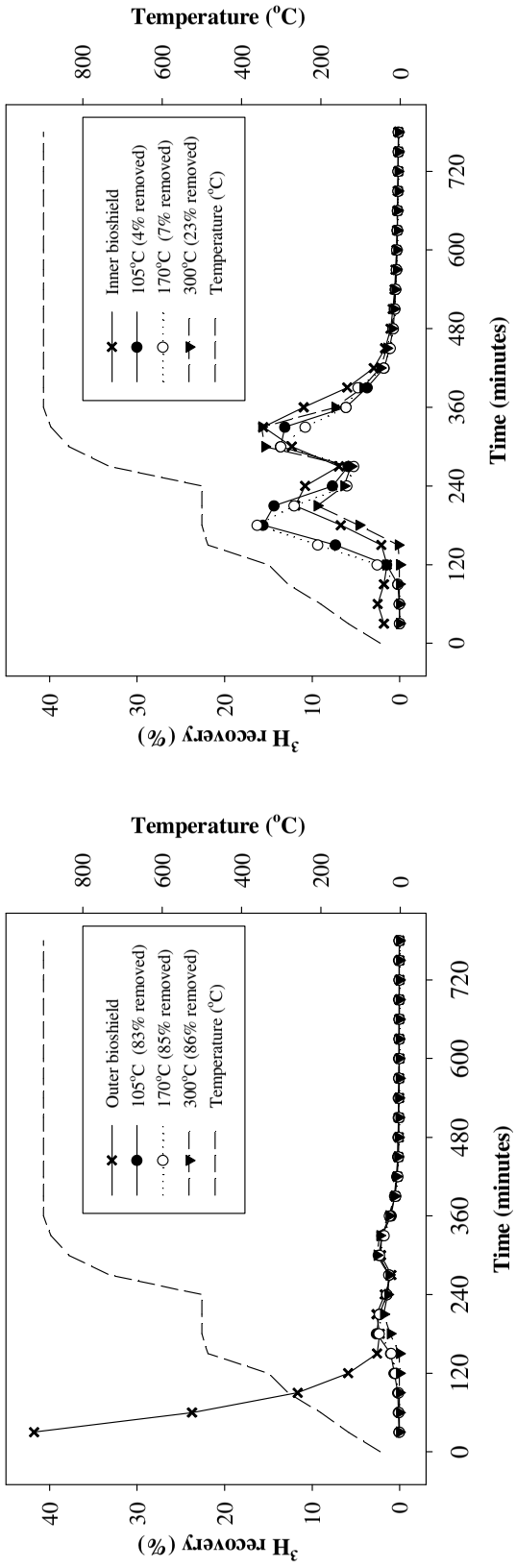

Figure 4.4: Thermal profiles showing the proportion of weakly bound tritium in inner and outer bioshield concrete.

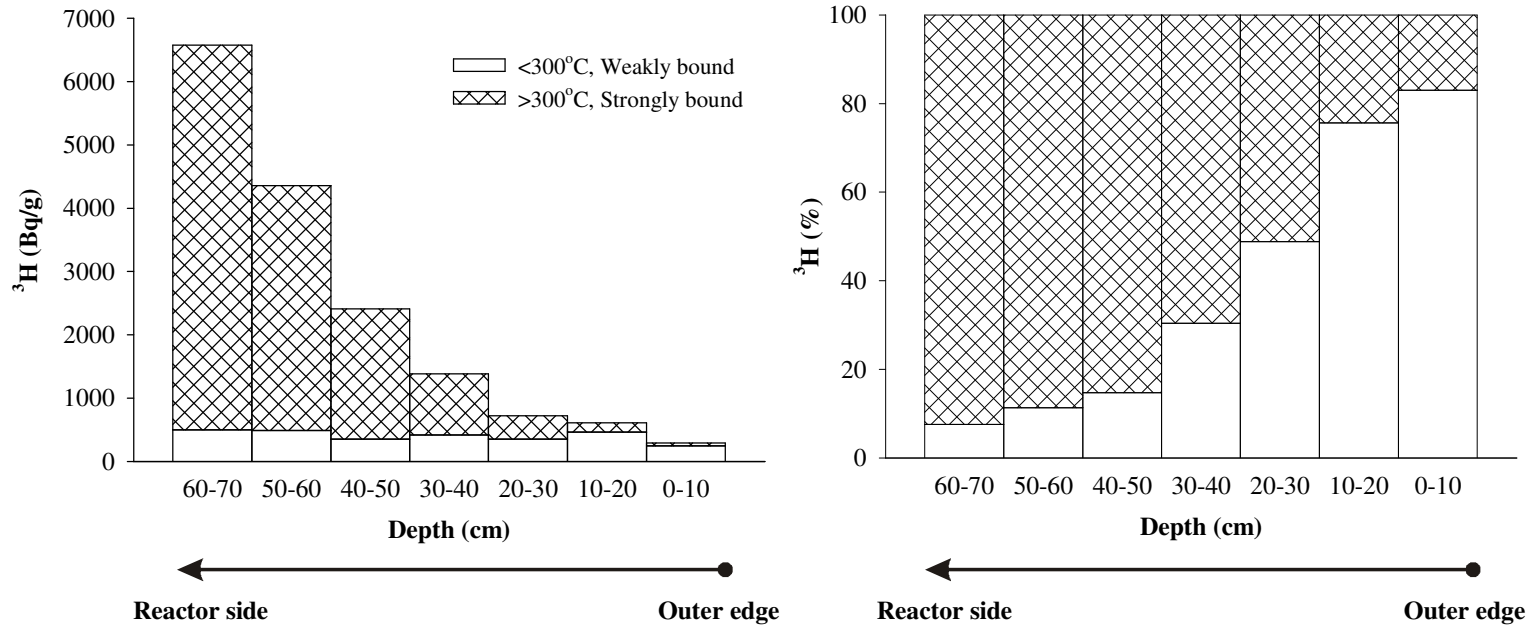

Figure 4.5: Proportions of different types of tritium along a section of bioshield concrete.

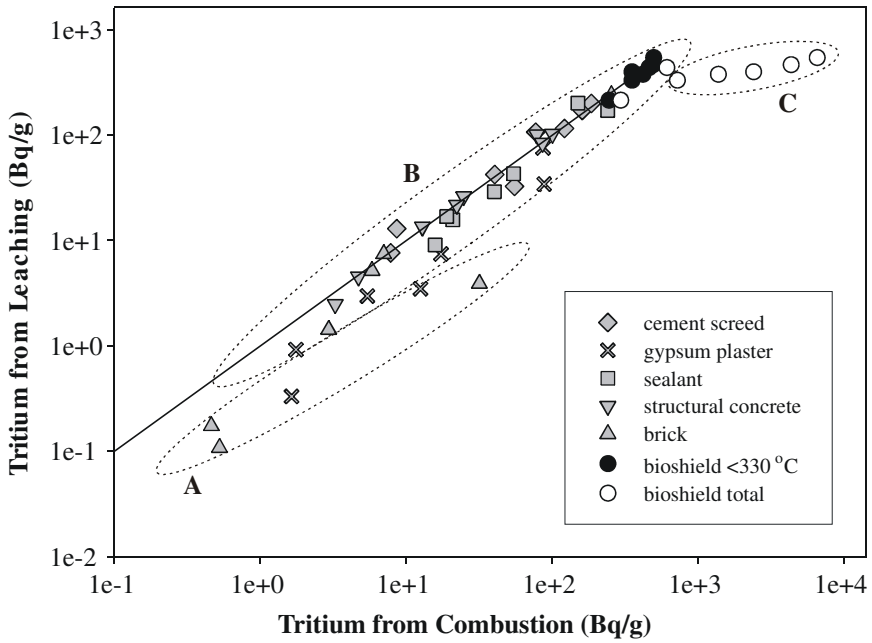

Figure 4.6: Relationship between ^{3}H extracted from various construction materials by aqueous leaching and combustion**:** Zone A - Partial ^{3}H leaching correlating with total ^{3}H; Zone B - Quantitative leaching of ^{3}H correlating with total ^{3}H; Zone C – Partial leach not correlating with total ^{3}H (bioshield samples)

Concrete is a permeable hydrophilic material typically formed from reacting Portland cement, sand, water and rock aggregates. However, in terms of the tritium capacity of concrete, the cement is the most significant component owing to its abundant structural water capable of trapping tritium by isotopic exchange (Furuichi et al., 2007). The hydrated cement is composed of four major compound classes: tricalcium silicates (C_3S), dicalcium silicate (C_2S), tricalcium aluminate (C_3A) and tetracalcium aluminoferrite (C_4AF). The most important products of the hydration reactions are the calcium silicate hydrate (C-S-H) and portlandite (also called calcium hydroxide, CH) (Sha et al., 1999). Thermogravimetric analysis (TGA) and differential thermo-analysis (DTA) curves for the Portland cement, show major mass losses in the temperature range < 200°C (release of free water), 200 - 450°C (release of water of crystallization), 450 - 550°C (decomposition of $Ca(OH)_2$), and 600 - 850°C (decomposition of hydrated calcium silicates) (Numata et al., 1990b; Alarcon-Ruiz et al., 2005). The proportions of ^{3}H lost at the key transition temperatures from inner and outer bioshield concrete were compared with other published data (Table 4.1) (Numata et al., 1990b). The relative proportion of ^{3}H in cement exposed to HTO vapour, and of ^{3}H in outer bioshield lost at < 200°C and 200 - 450°C agrees well with previously published data

indicating that the weakly bound ^{3}H is distributed as expected between free water and water of crystallization. However, the proportion of ^{3}H lost at key transition temperatures in inner bioshield concrete does not correlate with that observed for concretes exposed to HTO with ~90% of the ^{3}H being liberated at > 485°C.

Table 4.1: Comparison of ^{3}H and water in concrete and cements

Water group	Numata *et al.*[9]			Present study		
	Temperature (°C)	% of ^{3}H in cement material	% of total water liberated	% of ^{3}H of Outer (0-10cm)	% of ^{3}H of Inner (60-70cm)	Temperature (°C)
Liquid water (Free & capillary water)	**< 200**	**77**	**65**	**66**	**4**	**< 200**
Water of crystallization	**200-450**	**15**	**20**	**20**	**5**	**200-485**
Water constituent (Calcium hydroxide)	**450-550**	**7**	**12**	**7**	**29**	**485-500**
Water constituent (Calcium silicate hydrate)	**600-850**	**1**	**3**	**8**	**61**	**500-900**

** ^{3}H data obtained from cement contaminated by tritiated water vapour (Numata et al., 1990b)*

The strongly bound ^{3}H is inferred to originate from the $^{6}Li(n,\alpha)^{3}H$ reaction (σ_{th} = 940 b) which has been previously suggested as the dominant mechanism for ^{3}H production in bioshield concrete (Kinno et al., 2002a; Kinno et al., 2002b). Though this reaction has been previously identified this is the only study that has examined the relative behaviour (through thermal loss patterns) of different tritium types in concrete and considered the impact. The concretes analysed in this study typically contain 12 ± 1 mg/kg Li which is comparable with previously reported values (Kinno et al., 2002a). Conversion of ^{2}H to ^{3}H is not considered significant given the low thermal neutron capture cross section of 0.508 ± 0.015 mb for this reaction (Jurney et al., 1982). Predicted maximum ^{3}H activity concentrations arising from $^{2}H(n,\gamma)^{3}H$ (based on MCNP model neutron flux data supplied by UKAEA) for the 60 – 70cm fraction are <0.01 Bq/g compared with 15000 Bq/g via Li activation. Previous studies (Kinno et al., 2002a) have investigated the theoretical correlation between ^{3}H and ^{152}Eu in neutron irradiated concretes. Europium-152 is produced via neutron activation of stable ^{151}Eu (47.7% of natural Eu) with a high thermal neutron capture cross section of 5900 barns and provides a good indicator of neutron flux. The comparable half-life of ^{152}Eu (13.54 years)

and ^{3}H (12.33 years) means that the $^{3}H/^{152}Eu$ ratio should be predictable for a given [Li] /[Eu] ratio irrespective of the irradiation time. Strongly bound ^{3}H activity concentrations measured in the bioshield concrete correlate with ^{152}Eu and hence neutron flux (Figure 4.7) which further supports the proposition that the $^{3}H_{strong}$ originated from neutron activation. The $^{3}H_{strong}/^{152}Eu$ ratio of 8.6 is low compared with the value of ~27 reported for materials with a similar stable Li/Eu concentration ratio (Kinno et al., 2002a) (mean [Li]/[Eu] = 44). This may indicate that not all ^{3}H formed in this manner is strongly-bound or that the strongly-bound ^{3}H slowly converts to the more loosely bound form (e.g. via migration out of mineral lattices) with time and which subsequently diffuses through the bioshield. The weakly-bound ^{3}H probably arises from a combination of diffusion of HTO from the reactor core into the concrete as well as a slow conversion of strongly-bound ^{3}H to a more weakly-bound form. The presence of significant quantities of weakly-bound ^{3}H at distance from the neutron flux confirms that diffusion controls the distribution of this form of ^{3}H. Furuichi et al (2006) observed a pronounced ^{3}H diffusion profile in cement pastes exposed to tritiated water vapour after 5 days which flattened to a more evenly dispersed profile to depths of 8cm after only 318 days. Given the operational period of the reactor and the time that has elapsed since shutdown, it is feasible that ^{3}H originating from the reactor has had sufficient time to diffuse to relatively uniform concentration throughout the bioshield.

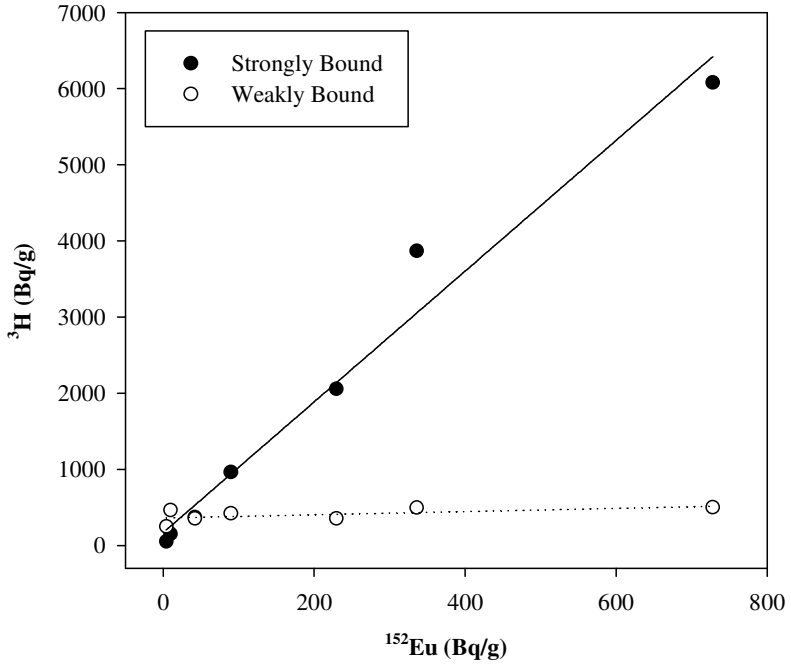

Figure 4.7: Relation between measured ^{3}H and ^{152}Eu activity concentrations

The presence of a hitherto uncharacterised, strongly-bound component of ^{3}H in bioshield concretes has significant implications for accurate analytical characterization of ^{3}H in such materials. For quantitative analysis of ^{3}H in bioshield concretes, a thermally aggressive treatment is required to quantitatively liberate the ^{3}H. Typically, this should involve heating samples up to 900°C. For other sample types, the temperature that ^{3}H is completely liberated from the sample will depend on the chemical form of the ^{3}H and the physical properties of the sample material. The necessity for determining thermal evolution profiles for specific materials prior to commencing routine analysis is clearly highlighted from these studies. The study also demonstrates that although a simple leaching technique can be used to provide rapid screening of ^{3}H activity concentrations in a range of matrices, it is not appropriate in all instances and should be used with caution.

4.5 Acknowledgements

The authors would like to thank Dr Jung Suk Oh for radioanalytical support and discussions, Dr N G Holland (GAU-Radioanalytical) for production of figures and graphs and UKAEA Winfrith for the provision of the SGHWR bioshield core.

4.6 References

Alarcon-Ruiz L, Platret G, Massieu E, Ehrlacher A. 2005. The use of thermal analysis in assessing the effect of temperature on a cement paste. Cement and Concrete Research 35: 609-613.

Bisplinghoff B, Lochny M, Fachinger J, Brucher H. 2000. Radiochemical characterization of graphite from Julich experimental reactor (AVR). Nuclear Energy-Journal of the British Nuclear Energy Society 39: 311-315.

Bushuev AV, Verzilov YM, Zubarev VN, Kachanovskii AE, Matveev OV, Proshin IM, Bidulya LV, Ivanov AA, Kalugin AK. 1992. Quantitative-Determination of the Amount of H-3 and C-14 in Reactor Graphite. Atomic Energy 73: 959-962.

DEFRA. 2002. DEFRA (2002). Radioactive Wastes in the UK: A summary of the 2001 inventory. Report DEFRA/RAS/02.003. Department for Environment, Food and Rural Affairs, London, UK, p14.

Furuichi K, Takata H, Katayama K, Takeishi T, Nishikawa M, Hayashi T, Kobayashi K, Namba H. 2007. Evaluation of tritium behavior in concrete. Journal of Nuclear Materials 367-370: 1243-1247.

Furuichi K, Takata H, Motoshima T, Satake S, Nishikawa M. 2006. Study on behavior of tritium in concrete wall. Journal of Nuclear Materials 350: 246-253.

Harolf TPJ, Baker DA. 1985. Tritium production, release and populations doses at nuclear power reactors. Fusion Technology 8: 2544-2550.

Hou X. 2005. Rapid analysis of ^{14}C and ^{3}H in graphite and concrete for decommissioning of nuclear reactor. Applied Radiation and Isotopes 62: 871-882.

Johnson JR, Brown RM, Myers DK. 1992. An overview of research at CRNL on the environmental aspects, toxicity, metaboilism and dosimetry of tritium. Radiation Research 50: 197:211.

Jurney ET, Bendt PJ, Browne JC. 1982. Thermal neutron capture cross section of deuterium. Phys Rev. C 25: 2810-2811.

Kinno M, Kimura K, Ishikawa T, Miura T, Ishihama S, Hayasaka N, Nakamura T. 2002a. Correlation between tritium and ^{152}Eu induced in various types of concrete by thermal neutron irradiation. Journal of Nuclear Science and Technology 39: 215-225.

Kinno M, Kimura K, Nakamura T. 2002b. Raw materials for low-activation concrete neutron shields. Journal of Nuclear Science and Technology 39: 1275-1280.

Numata S, Amano H, Minami K. 1990a. Diffusion of Tritiated-Water in Cement Materials. Journal of Nuclear Materials 171: 373-380.

Numata S, Amano H, Okamoto M. 1990b. Tritium inventory in portland cement exposed to trttiated water vapor. Journal of Nuclear Materials 171: 350-359.

Sha W, O'Neill EA, Guo Z. 1999. Differential scanning calorimetry study of ordinary Portland cement. Cement and Concrete Research 29: 1487-1489.

Chapter 5

Draft paper: The analytical impact of sample storage on tritium analysis

5 Paper in preparation:

The analytical impact of sample storage on tritium analysis

5.1 Abstract

Tritium contamination and behaviour during storage is significantly dependent on the form of ^{3}H present in the material. Tritium contamination can be grouped into weakly-bound and strongly-bound ^{3}H depending on its rate of release. Weakly-bound tritium is easily exchanged with atmospheric hydrogen in the form of water vapour at room temperature. However, the loss of strongly bound tritium is not significant even at room temperature. Strongly bound ^{3}H has significantly slow exchange and diffusion rates as the ^{3}H is trapped within mineral phase. The characteristics of the contaminated material are a significant factor affecting the degree of ^{3}H contamination. Porous hydrophilic materials will be more contaminated by absorption and isotopic exchange reaction and the magnitude will increase with time. As samples may contain different forms of ^{3}H, cross contamination and loss of ^{3}H may be a concern during storage and sampling procedures. The degree of ^{3}H loss and cross-contamination can be reduced significantly by careful selection of the storage conditions. For quantitative ^{3}H analysis and correct nuclear waste sentencing strategies, reliable sample storage and sampling strategies are required. These involves (1) storing samples in airtight and vapour tight containers at the point of sampling, (2) storing samples in a freezer (3) and segregation of samples with different ^{3}H activity concentrations to prevent cross contamination.

5.2 Introduction

Tritium is produced naturally in the upper atmosphere through fast neutron reactions (with the natural inventory of tritium in the world is 1.3×10^{18} Bq) and is a by-product of civil and military nuclear fission and fusion programmes. In 1950s and 1960s, atmospheric nuclear weapon tests were the main contributors of anthropogenic tritium in the environment and with the injection of 2.0×10^{20} Bq into the atmosphere (UNSCEAR, 1977). However, reprocessing of nuclear fuels, the operation of nuclear reactors (fission reactor) and radiopharmaceutical manufacture are a more significant tritium source at present. Tritium, produced as a by-product of the nuclear industry, is mainly discharged into the sea and atmosphere as tritiated water (HTO) and tritium gas (HT) which becomes part of the water

cycle in the environment. As a consequence, 2.97×10^{17} Bq of ^{3}H from nuclear reactor and reprocessing plants, and 1.26×10^{17} Bq of ^{3}H from reprocessing plants have been released worldwide to the atmosphere and ocean (UNSCEAR, 2000).

Tritium is produced in nuclear reactors via several neutron induced reactions [$^{2}H(n,\gamma)^{3}H$, $^{6}Li(n,\alpha)^{3}H$, $^{10}B(n, 2\alpha)^{3}H$, $^{14}N(n, ^{3}H)^{12}C$ and ternary fission (fission yield <0.01%)]. This ^{3}H may become incorporated into the fabric of reactor building materials (e.g. structural concrete and metals). Tritium (mostly HTO) incorporation into permeable and porous building materials (e.g. concrete) mainly occurs by physical absorption, diffusion and chemical reaction (isotope exchange) beyond the reactor core and will be held in a weakly-bound form (Numata et al., 1990a; Numata et al., 1990b; Furuichi et al., 2006; Kim et al., 2008). However, neutron capture on the trace lithium (^{6}Li) within mineral phase is the principle mechanism of tritium contamination of certain reactor components (e.g. bioshield concrete, graphite moderator and desiccant of reactor gas dryer system) (Hou, 2005; Kim et al., 2008) where the ^{3}H mostly is held in a strongly-bound form (Kim et al., 2008).

Decommissioning of nuclear facilities will generate large volumes of wastes (e.g. concrete, asbestos, wood, desiccants, reactor metal work, graphite blocks and tiles, soft wastes etc). These may contain widely varying tritium activity concentrations and need to be characterized prior to waste sentencing. Careful consideration needs to be given to their sampling and storage if reliable analytical data are to be obtained. For this characterization, it is essential to take samples, store and transport before finally analyzing and during each stage there is a potential for cross contamination if care is not taken. ^{3}H trapping capacity (Furuichi et al., 2007), diffusion (Numata et al., 1990a; Munakata et al., 2003; Furuichi et al., 2006) and release (Surette and McElroy, 1988; Ono et al., 1995; Shu et al., 2002; Munakata et al., 2003; Torikai et al., 2005; Chubarov and Krivosheev, 2006; Torikai et al., 2007) from a range of materials has been previously reported. However, there has been no previous attempt to evaluate the importance of ^{3}H form, storage temperature, and materials composition on ^{3}H loss and cross-contamination rates and to assess the impact that this may have for accurate analytical measurements. This study aimed to determine ^{3}H emanating behaviour and degree of cross contamination under various storage conditions (e.g. ^{3}H form and origin, storage temperature and materials composition) and to consider the implication for sample storage and sampling strategy resulting in accurate ^{3}H analysis for decommissioned material prior to waste sentencing and the waste management.

5.3 Experimental section

A range of materials derived from various nuclear decommissioning sites, having different forms of ^{3}H, were used as tritium emanation source materials (Table 5.1). A cylindrical concrete core, traversing the reactor bioshield, was taken from the 100 MW steam generating heavy water reactor (SGHWR), which was operated by the United Kingdom Atomic Energy Authority at Winfrith, Dorset, from 1967 to 1990. The closest bioshield concrete core section (10cm interval) to the reactor exposed highest neutron flux was used as tritium emanating source material. A structural concrete was taken from the nuclear reactor site (Winfrith, UK) building material away from any neutron source. This structural concrete had not been exposed to a neutron flux and the ^{3}H present originated from exposure to tritiated water vapour only. Concrete samples were crushed to produce a homogeneous concrete powder (<125 μm) for subsequent trials. Active granular desiccant (0.4mm in diameter, *ca* 0.5g) used in a reactor gas dryer system in the Magnox reactor (Hinkley A, UK) and mild steel operationally exposed to HTO vapour (Winfrith, UK) were also used for tritium emanating source materials.

A range of tritium free materials were used as potential receivers, including RO water, cellulose filter paper, polyethylene, metal wire (mild steel), and various drying agents (e.g. silica gel, Drierite™ ($CaSO_4$) and zeolite).

A range of construction materials used in the leaching trials were taken from a nuclear site (Borehamwood, UK). These materials had not been exposed to a neutron flux and it is assumed that the ^{3}H present originated from exposure to tritiated water vapour only.

Table 5.1: Description of ^{3}H of structural and bioshield concrete

Materials	Location	Origin of ^{3}H	Form of ^{3}H	^{3}H (kBq/g)
Structural concrete	Nuclear site building materials (Winfrith)	Adsorbed tritiated water (HTO)	Weakly bound ^{3}H (HTO mainly)	~9.0±0.9
Bioshield concrete	*SGHWR bioshield	Neutron activation of ^{6}Li	Strongly bound ^{3}H (mainly bonded with structural OH groups/ lattice-bound)	~6.0±0.6
Desiccant (4mm long)	Magnox reactor gas dryer system (Hinkley)	Activated tritium gas and tritiated water (HTO)	Weakly and strongly bound ^{3}H	~310.0±30
Metal	Nuclear site building materials (Winfrith)	Adsorbed tritiated water (HTO)	Weakly bound ^{3}H (mainly) and structural OH groups	~0.1±0.01

** Steam generating heavy water reactor which was built at Winfrith site, UK*

Initial sample characterization was performed using a Raddec Pyrolyser Trio System (Figure 5.1), which permits simultaneous extraction/oxidation of up to six samples. This system was designed specifically for quantitative extraction of tritium and ^{14}C from nuclear and environmental samples. Each sample was heated using a preset heating cycle in its own silica glass work-tube that carried a stream of air/oxygen. The liberated gases passed through a zone containing 10 g of platinised alumina catalyst that oxidizes any organic combustion products to CO_2 and H_2O (and HTO). Any water vapour, including HTO, was trapped in a bubbler containing 20 ml of 0.1 M HNO_3. Bubblers were changed every 30 minutes to determine the ^3H evolution profile and the gas supply was isolated during the bubbler changeover. The quantities and proportion of ^3H present as weakly bound and strongly bound were inferred from the evolution profile.

The amount of tritium transferred to water from concretes perhaps having different forms of ^3H was compared at various storage temperatures. Bioshield concrete powder (*ca* 1g, ~6 kBq/g) contained in a sealable polythene bag was placed in one of eighteen Kilner jars fitted with airtight rubber seals. Ten millilitres of RO water in an open and closed vial were placed in each of the jars and the jars stored in a fridge, a freezer and at room temperature for 1 day, 5 days, 10 days, 15 days, 20 days and 30 days, respectively. At the end of each pre-defined storage time the ^3H in the RO water was measured by LSC. The experiment was repeated with active structural concrete powder (*ca* 4g, ~9kBq/g).

The transfer of ^3H at different storage temperatures was further investigated using an adaptation of the above experiment. A known amount of active structural (~1 kBq) and bioshield (~6.6 kBq) concrete powder (<125μm, 1g) in a sealable polythene bag was placed into a Kilner jar (635ml volume) modified with inlet and outlet ports which permitted the measurement of ^3H activity in the air of the container (Figure 5.1). Ten milliliters of RO water in an open and a closed vial were placed in each of the Kilner jars and the jars sealed and stored in a freezer and at room temperature for 2 weeks. After 2 weeks, dry air was introduced into the container for 10 minutes. The flush gas was then passed through the pre furnace bubbler to trap HTO and then through a furnace containing Pt-alumina catalyst to convert other forms of ^3H into HTO which was subsequently trapped in the post furnace bubbler. The total ^3H activity (Bq) measured in the flushed air was used to calculate ^3H concentrations of the water vapour in the Kilner jar. Tritium activities were also determined in the RO water, card supports and all container surfaces by rinsing with water. Finally the quantity of ^3H remaining in the concrete was determined by combustion / LSC.

The relative magnitudes of contamination for different absorber materials exposed to a tritiated atmosphere were investigated. A range of non-tritiated materials (e.g. silica gel, Drierite™ ($CaSO_4$), zeolite, concrete, metal and plastic in open vial) were stored with active structural concrete powder (~28 kBq) in a airtight Kilner jar. All samples types were prepared in a triplicate and stored under three different storage conditions (fridge, freezer and at room temperature) over a 2 weeks period. The same procedure was performed using different tritium emanating source materials (e.g. desiccant, metal and structural concrete) and other absorber materials (silica gel, cellulose filter paper and water). Active structural concrete powder (~37 kBq), desiccant pellet (~170 kBq) and metal (~310 Bq) in sealable polythene bags were used as tritium emanating source materials. Silica gel (in open vial, single polythene bag and double polythene bag, *ca* 5g each), cellulose filter paper (in open vial, *ca* 0.15g each) in open vial and RO water (10ml in an open and closed vial) were used as the absorbers.

The importance of storage conditions on ^3H preservation during a real sampling campaign was assessed. Immediately after sample collection, sub-samples of building materials were transferred to vials containing water to leach ^3H. The activity of ^3H leached was then determined by liquid scintillation counting. Separate samples were stored and transferred to the laboratory either at room temperature or refrigerated. The ^3H activity in these samples was then determined by combustion.

All tritium measurements were performed using a 1220 liquid scintillation counter (Wallac Quantulus™). Eight milliliters of aqueous sample were mixed with 12ml of Gold Star™ (Meridian) scintillation cocktail in a 22ml polythene vial. The counter was calibrated for ^3H using a traceable tritiated water standard (TRY-44, Nycomed Amersham PLC, Bucks, UK). For all samples, the measured quench levels (SQPE) ranged from 700 to 850 which correspond to ^3H counting efficiencies of 17 - 31%. All uncertainties are quoted at the 95% confidence level and refer to propagated method uncertainties. The typical detection limit for ^3H using this method is 0.01 Bq/g.

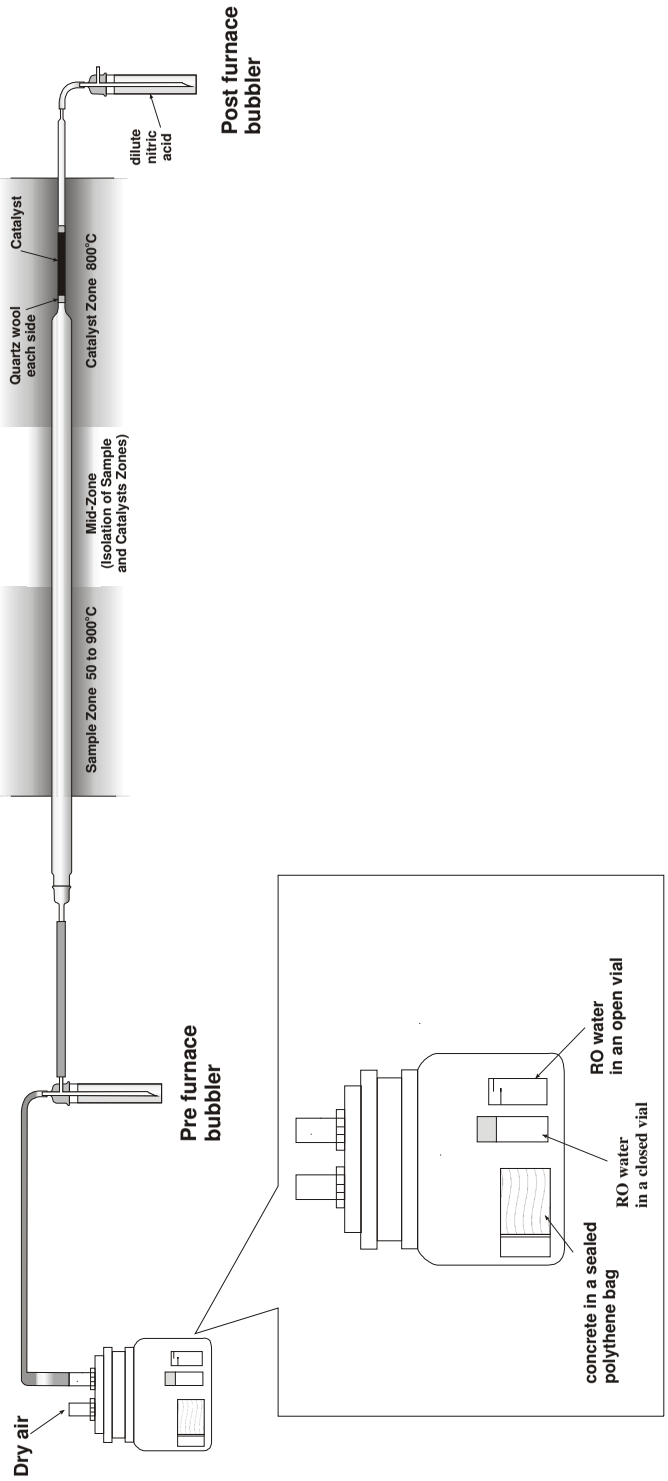

Figure 5.1: Modified apparatus used to determine ^{3}H in water vapour following storage of ^{3}H-contaminated materials.

5.4 Results and discussion

The magnitude of tritium emanation is dependent on the form of ^{3}H in the contaminated material and storage temperature. The most significant ^{3}H loss occurred at room temperature from structural concrete (nonirradiated concrete) where ^{3}H contamination arose from exposure of the concrete to HTO vapour (Table 5.2). For the bioshield concrete which had been exposed to a neutron flux, ^{3}H loss is not significant. The greatest contamination transfer occurred to water in open vial from structural concrete at room temperature. Another non-negligible ^{3}H contamination transfer occurred to the cardboard which was used to support the open vial containing RO water. However, the proportions of ^{3}H activity transfers to water and cardboard from bioshield concrete were significantly less even at room temperature. For both structural and bioshield concrete, ^{3}H loss and cross-contamination is low for jars stored in the freezer.

Table 5.2: Tritium distribution after storage depend on ^{3}H form and storage conditions

^{3}H contaminated into	**Activity (Bq) of ^{3}H (% of ^{3}H)**			
	Structural concrete		**Bioshield concrete**	
	Room temp.	**Freezer**	**Room temp.**	**Freezer**
Air in the Kilner jar	45.9 (4.1)	4.4 (0.4)	18.5 (0.3)	2.7 (< 0.1)
Jar walls	0.7 (0.1)	0.1 (< 0.1)	0.2 (< 0.1)	0.1 (< 0.1)
Polythene bag (inside wash)[a]	5.2 (0.5)	9.8 (0.9)	8.0 (0.1)	5.8 (0.1)
Polythene bag (outside wash)[b]	0.1 (< 0.1)	0.1 (< 0.1)	0.1 (< 0.1)	0.1 (< 0.1)
RO water (open vial)	377.1 (33.9)	0.4 (< 0.1)	282.4 (4.3)	0.1 (< 0.1)
RO water (closed vial)	0.2 (< 0.1)	0.1 (< 0.1)	0.2 (< 0.1)	0.1 (< 0.1)
Out of scintillation vial	0.1 (< 0.1)	0.1 (< 0.1)	0.1 (< 0.1)	0.1 (< 0.1)
Cardboard[c]	146.3 (13.2)	17.7 (1.6)	33.8 (0.5)	5.2 (0.1)
^{3}H remaining in the concrete	499 (45)	1046 (94)	6148 (94)	6383 (97)
Total	**1075 (97)**	**1078 (97)**	**6491 (99)**	**6397 (97)**
Original ^{3}H (Bq) in Concrete	1112 (100)	1112 (100)	6577 (100)	6577 (100)

[a] *^{3}H activity inside of polyethylene bag which contained concrete*
[b] *^{3}H activity outside of polyethylene bag which contained concrete*
[c] *Cardboard support used with the open vial containing RO water*

Systematic measurement of ^{3}H activity transferred from two different sources of concrete to water with storage time showed significantly different variation depended on storage temperature. The greatest contamination transfer occurred to water in an open vial from structural concrete where the quantities exponentially increased with time at room temperature (Figure 5.2, Appendix 11). Systematically less contamination occurs to water in

open vials stored in a fridge and freezer. For water stored in closed vial at room temperature and in a fridge, ^{3}H contamination is significantly less (0.03% of the $^{3}H_{total}$), though measurable, over the 30 day duration whilst the samples in the freezer showed minimal contamination (with ^{3}H activity concentrations approaching the limit of detection of 0.01Bq/ml). However, contamination arising from bioshield concrete was significantly less, although slight increases in ^{3}H contamination were observed at room temperature and fridge temperature.

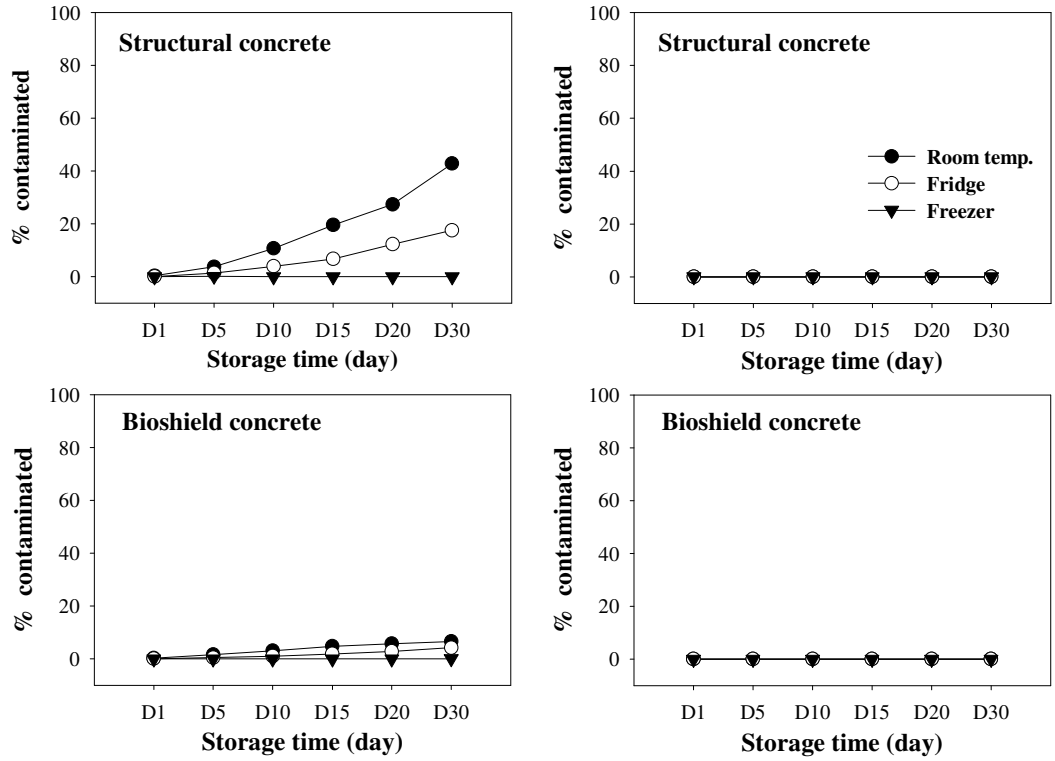

Figure 5.2: Variations of ^{3}H contamination in RO water from different sources of materials (Ao of structural concrete and bioshield concrete are ~9kBq/g and ~6kBq/g, respectively)

Significant quantities of ^{3}H contamination in water is due to the high isotopic exchange rate of tritium with water vapour where the reaction is significantly decreased as temperature is decreased (Numata et al., 1990b; Munakata et al., 2003; IAEA, 2004; Furuichi et al., 2007). Tritium cross-contamination and its emanation behaviour depend significantly on the form of ^{3}H in the material and also on storage temperature. A previous study by the author identified two distinct forms of tritium from concrete which are referred to as weakly bound ^{3}H and strongly bound ^{3}H (Kim et al., 2008). The bioshield concrete and the structural concrete used

in the present study have significantly different proportions of the two forms of ^{3}H (Figure 5.3). The structural concrete mainly consisted of tritiated water (weakly bound form) which exists as labelled free water or crystallization water (Numata et al., 1990b) and is coupled with its rapid diffusion into relatively porous hydrophilic materials. This form rapidly equilibrates with water vapour in air. Conversely, bioshield concrete dominantly contains a strongly bound form of ^{3}H within mineral phases arising from neutron activation of trace lithium-6 (Kim et al., 2008). This ^{3}H form is potentially less-available since it may be locked/trapped inside mineral lattices and interacts slowly with atmospheric water vapour (Kim et al., 2008). Therefore most of the ^{3}H loss and contamination from both structural and bioshield concrete would be derived from weakly bound ^{3}H (HTO) by absorption and isotopic exchange. This has significant implications for sample storage and waste management strategies in nuclear decommissioning work.

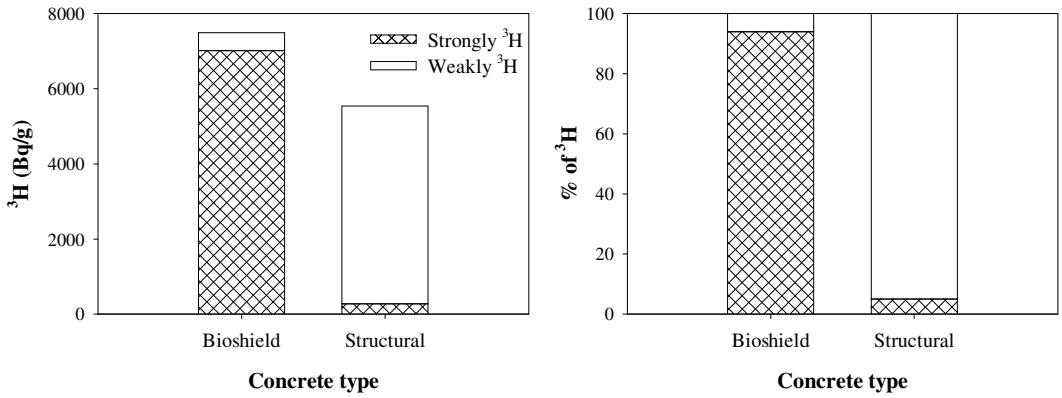

Figure 5.3: Total ^{3}H activity (left) and the ratio of ^{3}H form in the concrete (right).

Most of tritium was trapped in the pre furnace bubbler and the tritium measurement in the post furnace bubbler was below the limit of detection. This implies that most tritium emanated from the sample was as HTO. During storage, ^{3}H loss and transfer to other materials occurs through exchange with atmospheric water vapour. Non-negligible quantities of ^{3}H were observed in the air of the container (Kilner jar) within which structural concrete was stored at room temperature. Theoretically $1m^3$ of air has a mass of 1.17 kg and 22g H_2O/kg air present at normal temperature (25°C), therefore the mass of air in the Kilner jar (635×10^{-6} m^3 in volume) is 0.74g and the mass of water vapours in the Kilner jar is 16 mg. Tritium activity determined in the air of the Kilner jar by purging of dry air during 10 minutes was 8.2 Bq, therefore the ^{3}H concentration of the water vapour in the container is 501.7 Bq/g. This is significantly higher than ^{3}H concentration of water (37.7Bq/g) in the

open vial. This implies that ^{3}H equilibrium within the container was not reached during the storage time used.

Previous studies have demonstrated persistent tritium release from various materials (e.g. stainless steel, cement and ceramic breeder materials) exposed to tritiated water vapour (Surette and McElroy, 1988; Ono et al., 1995; Munakata et al., 2003; Torikai et al., 2005; Torikai et al., 2007). Similar significant ^{3}H loss (mainly HTO, weakly bound) also occurred from the structural concrete in the present study; with ~9 kBq/g of ^{3}H activity of used structural concrete decreasing to ~1 kBq/g in 20 months. The degree of ^{3}H contamination is dependent on the physical and compositional characteristics of source materials emanating tritium. Significantly different ^{3}H cross-contamination occurred for a given absorber from different tritium emanating materials. The greatest ^{3}H loss occurred from concrete (structural) though desiccant contains the highest activity (Table 5.3). The highest ^{3}H contamination ratio (contaminated ^{3}H by absorber/original ^{3}H of emitter) occurred from metal at room temperature. ^{3}H loss and contamination decrease significantly for samples stored in a fridge and freezer with the exception of desiccant. For the desiccant, the highest ^{3}H contamination occurred for samples stored in the fridge, although the ^{3}H activity was comparatively low. This may relate to condensation of water vapour in the fridge because isotopic exchange reaction is enhanced by increasing the water concentration (Oya et al., 2001).

Desiccant used in this study derived from the Magnox reactor gas (carbon dioxide) dryer system (Hinkley, UK) where the desiccants absorb tritiated water from carbon dioxide gas coolant. Tritium gas produced by neutron induced reaction in the reactor core can be adsorbed to desiccant where isotopic exchange reaction occur with water and hydroxyl groups in the desiccant (Rosson et al., 1998). The tritium present in the desiccant as HTO, which absorbed by water and hydroxyl groups of the desiccant, exchanges slowly with water vapour in ambient air and the inferred exchangeable water from desiccant is *ca* 6% (Rosson et al., 1998). This explains the significantly low ^{3}H contamination from high active desiccant to other materials.

Table 5.3: ^{3}H cross-contamination of depend on material types and temperatures

Source materials	Storage condition	$^{3}H_{total}$ (Bq) of source materials	$^{3}H_{total}$ (Bq) contaminated (% contaminated)					
			silica gel (open)	silica gel (single bag)	silica gel (double bag)	Cellulose paper (open)	RO water (open)	RO water (closed)
Concrete (structural)	Room	36632	3234 (8.8)	1738 (4.7)	1081 (3.0)	4 (0.01)	12496 (34.1)	15 (0.04)
	Fridge	37116	3402 (9.2)	165 (0.4)	93 (0.3)	35 (0.1)	2620 (7.1)	6.1 (0.02)
	Freezer	36829	23 (0.1)	1.3 (<0.01)	1.0 (<0.01)	6.8 (0.02)	4.3 (0.01)	0.1 (<0.01)
Desiccant	Room	171120	306 (0.2)	184 (0.1)	46 (0.03)	6 (<0.01)	543 (0.3)	0.7 (<0.01)
	Fridge	181660	4175 (2.3)	333 (0.2)	146 (0.1)	52 (0.03)	3392 (1.9)	1.3 (<0.01)
	Freezer	157790	16 (0.01)	1.1 (<0.01)	1.0 (<0.01)	3 (<0.01)	2 (<0.01)	0.1 (<0.01)
Metal	Room	263	57 (21.8)	33 (12.6)	11 (4.1)	1 (0.2)	155 (59.0)	0.3 (0.1)
	Fridge	357	22 (6.1)	2.6 (0.7)	1.0 (0.3)	2.0 (0.6)	15 (4.1)	0.1 (0.02)
	Freezer	319	1.6 (0.5)	0.6 (0.2)	1.0 (0.3)	0.1 (0.04)	0.3 (0.1)	0.1 (0.02)

Note: All absorber (silica gel and cellulose filter paper) were stored together with each source material except for RO water which stored separately with same conditions.

During storage, ^{3}H is lost from samples and can potentially cross-contaminate other samples or any proximal materials by physical and chemical reactions (e.g. absorption, diffusion and isotopic exchange) depended on temperature. The magnitude of ^{3}H contamination is dependent on the material being contaminated. The greater ^{3}H contamination from an active structural concrete occurred with drying agent materials (e.g. silica gel, Drierite™ ($CaSO_4$) and zeolite) and to a lesser extent concrete (Figure 5.4). The highest contamination by the absorber occurred at fridge which is same result to that seen at Table 5.3 and Figure 5.4. This can be explained by the condensation effect of water vapour in the fridge resulting in increased transfer of tritiated water. However ^{3}H contamination of plastic and metals was negligible at all investigated storage temperatures.

Tritium in the chosen source material (structural concrete) mainly consisted of tritiated water (HTO) held in a weakly bound form (Kim et al., 2008). Previous studies demonstrated persistent tritium (HTO) release from structural concrete (Ono et al., 1995; Furuichi et al., 2007) and similar significant ^{3}H (mainly HTO form) loss was observed in the present study. Most of tritiated water becomes adsorbed physically on the surface of the solid materials and

undergoes exchange with trace water in the absorber materials. The extent of tritium contamination on is mainly dependent on physical and compositional characteristics of materials being contaminated (Oya et al., 2001; Harms and Jerome, 2004). Typically porous hydrophilic material (e.g. concrete) will be more easily contaminated (Ono et al., 1995). This can explain the high observed ^{3}H contamination by porous hydrophilic concrete at room temperature compared to metal and plastic. However, exchange reactions become slower at low temperature (Rosson et al., 1998) by which cross contamination is significantly decreased at freezer.

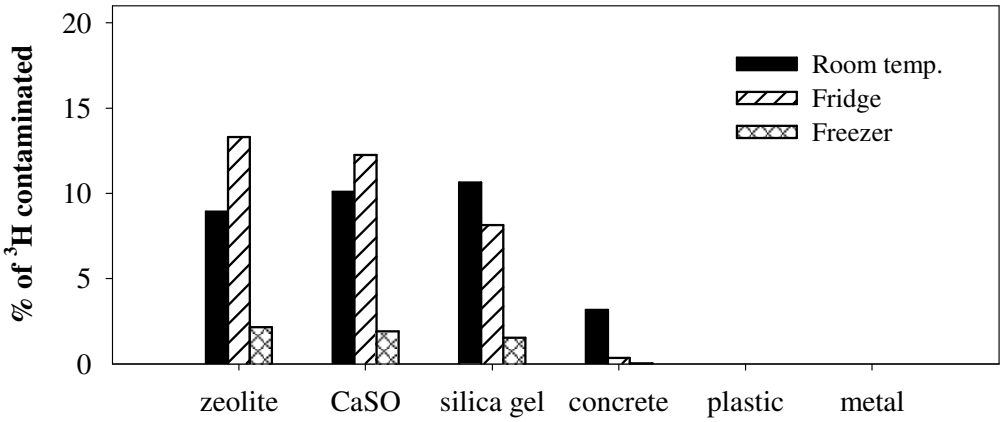

Figure 5.4: ^{3}H contamination of various materials from high active structural concrete (~28kBq) for 2 weeks storage.

An aqueous leach test may be used to rapidly assess the level of ^{3}H contamination in a leachable solid sample at the point of sampling. A comparison of leached ^{3}H determined immediately following sampling and total ^{3}H ($^{3}H_{total}$) measured in the laboratory after a period of storage / transport showed poor correlation in measured ^{3}H activity concentrations for samples stored at room temperature (Figure 5.5 non-solid symbols). Where samples were refrigerated immediately after sampling, the leached ^{3}H compared well with the $^{3}H_{total}$ as determined by combustion (Figure 5.5 solid symbols). This further confirms the importance of storing samples at low temperature following sample collection.

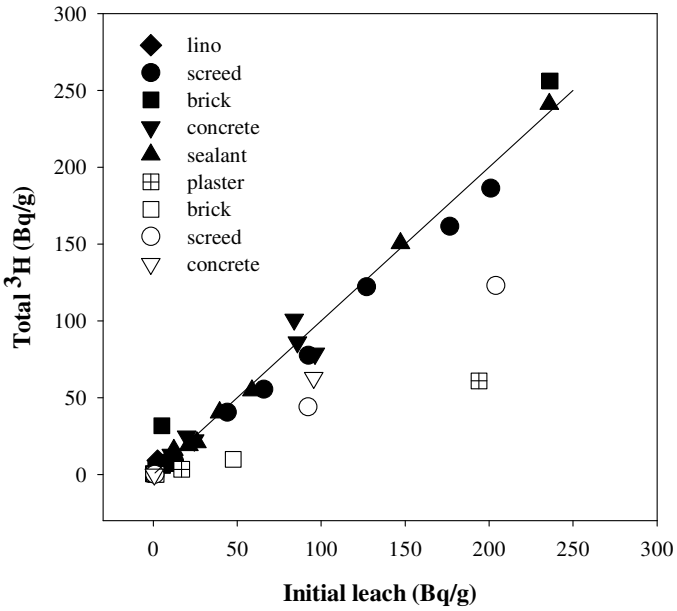

Figure 5.5: Relationship between ^{3}H extracted from various construction materials by aqueous leaching immediately following sampling and combustion for samples stored under different conditions. The solid symbol represents refrigerated samples at the point of sampling. On the other hand, the non-solid symbol stored at room temperature at the point of sampling.

Careful consideration must be given to strategies for sample preservation in order to ensure that a representative sample is supplied for analysis. Sample should be sealed in vapour tight containers (glass or high density plastic is preferred) to avoid cross contamination and tritium loss, as the hydrogen from water or water-bearing samples is readily exchanged with atmospheric water vapour. Samples should be frozen to limit ^{3}H release and cross contamination. Low temperature can effectively reduce the tritium emanating rate therefore storing sample at freezer is the most secure and recommended way to preserve sample integrity. However, frozen samples should be thawed completely before tritium extraction and any sublimed water within the container recombined with the sample prior to sub-sampling. The external areas of the container must be dried prior to opening in order to minimize sample exposure to condensation of atmospheric water (onto the sample) or isotopic exchange with water vapor in the air. When samples are exposed, it should be assumed that contamination is a possibility, and steps to prevent or monitor this are required. Finally, suspected low activity samples should be segregated from high activity samples to further reduce the possibility of cross contamination.

5.5 References

Chubarov MN, Krivosheev MV. 2006. Behaviour of tritium released into the working rooms of the International Thermonuclear Experimental Reactor. Plasma Devices and Operations 14: 201-213.

Furuichi K, Takata H, Katayama K, Takeishi T, Nishikawa M, Hayashi T, Kobayashi K, Namba H. 2007. Evaluation of tritium behavior in concrete. Journal of Nuclear Materials 367-370: 1243-1247.

Furuichi K, Takata H, Motoshima T, Satake S, Nishikawa M. 2006. Study on behavior of tritium in concrete wall. Journal of Nuclear Materials 350: 246-253.

Harms AV, Jerome SM. 2004. Development of an organically bound tritium standard. Applied Radiation and Isotopes 61: 389-393.

Hou X. 2005. Rapid analysis of ^{14}C and ^{3}H in graphite and concrete for decommissioning of nuclear reactor. Applied Radiation and Isotopes 62: 871-882.

IAEA. 2004. Technical reports series no. 421, Management of waste containing tritium and carbon-14 (printed by the IAEA, in Austria, 2004).

Kim DJ, Warwick PE, Croudace IW. 2008. Tritium Speciation in Nuclear Reactor Bioshield Concrete and its Impact on Accurate Analysis. Anal. Chem. 80: 5476-5480.

Munakata K, Koga A, Yokoyama Y, Kanjo S, Beloglazov S, Ianovski D, Takeishi T, Penzhorn RD, Kawamoto K, Moriyama H. 2003. Effect of water vapor on tritium release from ceramic breeder material. Fusion Engineering and Design 69: 27-31.

Numata S, Amano H, Minami K. 1990a. Diffusion of Tritiated-Water in Cement Materials. Journal of Nuclear Materials 171: 373-380.

Numata S, Amano H, Okamoto M. 1990b. Tritium inventory in portland cement exposed to trttiated water vapor. Journal of Nuclear Materials 171: 350-359.

Ono F, Tanaka S, Yamawaki M. 1995. Tritium sorption by cement and subsequent release. Fusion Engineering and Design 28: 378-385.

Oya Y, Kobayashi K, Shu W, Higashijima T, Hayashi T, O'Hira S, Obara K, Nishi M, Shibanuma K, Koizumi K. 2001. Tritium contamination and decontamination study on materials for ITER remote handling equipment. Fusion Engineering and Design 55: 449-455.

Rosson R, Jakiel R, Kahn B. 1998. Isotopic Exchange and Vapor Pressure Isotope Effect in Tritium Oxide Adsorption on Silica Gel. The Journal of Physical Chemistry B 102: 10342-10346.

Shu WM, Gentile CA, Skinner CH, Langish S, Nishi MF. 2002. The effect of oxygen on the release of tritium during baking of TFTR D-T tiles. Fusion Engineering and Design 61-62: 599-604.

Surette RA, McElroy RGC. 1988. Regrowth, Retention and Evolution of Tritium from Stainless-Steel. Fusion Technology 14: 1141-1146.

Torikai Y, Murata D, Penzhorn RD, Akaishi K, Watanabe K, Matsuyama M. 2007. Migration and release behavior of tritium in SS316 at ambient temperature. Journal of Nuclear Materials 363-365: 462-466.

Torikai Y, Penzhorn RD, Matsuyama M, Watanabe K. 2005. Chronic release of tritium from SS316 at ambient temperature: Correlation between depth profile and tritium liberation. Fusion Science and Technology 48: 177-181.

UNSCEAR. 1977. Sources and effects of ionizing radiation. United Nation Publications, Vienna.

UNSCEAR. 2000. Sources and effects of ionising radiation. United Nations Scientific Committee on the Effects of Atomic Radiation. Report to the General Assembly, Volume 1: Sources. United Nations, Vienna.

Chapter 6

Tritium speciation in metals from nuclear sites

6 Tritium speciation in metals from nuclear sites

6.1 Introduction

The worldwide rise in nuclear decommissioning and the demands of the regulators mean there is a need to characterize waste for reactor materials properly prior to final sentencing. Fundamental studies of different materials from reactor sites can provide significant insights that lead to improved radioanalytical practices and more accurate data. This study has focused specifically on tritium in metals and follows from an earlier study where tritium loss and speciation in concrete were examined (Kim et al., 2008).

Tritium is produced to varying degrees in nuclear reactor materials via several neutron induced reactions [$^{2}H(n,\gamma)^{3}H$, $^{6}Li(n,\alpha)^{3}H$, $^{7}Li(n,\alpha)^{3}H$, $^{10}B(n,2\alpha)^{3}H$, $^{14}N(n,^{3}H)^{12}C$ and ternary fission (fission yield <0.01)]. When considering the origin of tritium in metals and other materials there are two main routes to its formation. It may be formed externally followed by ingress or it may be formed *in situ* through activation of impurities in the metals. Of the reactions listed the most significant producers of tritium in steels would be via ^{6}Li activation (Westall et al., 2007). It is notable that Westall et al. (2007) found that Li was associated with Al inclusions in steel and they provisionally estimated a Li concentration of 0.4 ng/g in Magnox pressure vessel steels and that such a concentration could lead to tritium activities of up to 12 Bq/g following 26 years of integrated neutron exposure. Clearly the activity formed depends on the Li content and integrated neutron flux. Boronated metals might generate tritium via ^{10}B activation. Deuterium-derived lithium is generally only significant as an external contaminator of metals and other reactor materials. It is most significantly produced in nuclear power stations where deuterated water is or has been used as a moderator (e.g. CANDU reactors and the prototype SGHWR reactor) and it will contaminate a wide range of materials in reactor buildings mostly via HTO ingress. Tritium can also be produced *in situ* in materials that are exposed to a neutron flux though neutron capture reactions on trace ^{6}Li, ^{7}Li and ^{10}B impurities (e.g. structural metalwork, reactor components, graphite and concrete).

Tritium as tritiated water, HTO (NCRP, 1985) can become absorbed into the structure of any materials with high diffusion coefficients (Alizadeh, 2006). Following its initial absorption and its later redistribution and ageing the tritium in the sample matrix will exist as free water, water of crystallization or as structural OH groups. Another form of tritium may be lattice bound as deduced from a study of bioshield concrete (Kim et al., 2008) where two discrete forms of ^{3}H were identified. By studying the variation in tritium evolution in concretes with

increasing temperature it became apparent that a weakly bound and strongly bound form existed. The weakly bound form was liberated around 100°C as HTO and was associated with dehydration of hydrous mineral components or adsorbed water. The strongly bound form of tritium originated from neutron capture on trace lithium (^{6}Li) residing in mineral lattices and required temperatures of 350-800°C to achieve quantitative evolution. That study demonstrated that the accurate characterisation of tritium activities in samples required heating up to 900°C to ensure that all tritium was liberated. It also showed the value of thermal evolution profiles for understanding the nature of tritium speciation in different materials. Tritium contamination in metals can also originate by its *in situ* formation via one or more neutron capture reactions; studies on irradiated metals have received less systematic attention (see however Westall et al 2007).

Metals, like concrete, are important construction materials in reactors and reactor buildings and account for 22% of the total weight of low-level waste (LLW) and 35% of intermediate level waste (ILW) in the UK (DEFRA, 2002). The issue of ILW disposal will also be of particular concern for deuterium-tritium burning fusion reactors (e.g. JET and ITER) because their long-term operation will involve use of large activities of tritium and will lead to potentially large volumes of contaminated metals such as Inconel, stainless steel, copper, beryllium and aluminum alloys (Kalinin et al., 2000; Perevezentsev et al., 2005; Penzhorn et al., 2006; Perevezentsev et al., 2008).

Determination of tritium requires specialized methods of extraction and measurement because of the low-energy pure β emission of the radionuclide (E_{max} = 18.6 keV). Also since it is a relatively mobile species it cannot be estimated using a fingerprint approach. A number of limited non-destructive (*in situ*) methods have been used for quantifying ^{3}H in metals. These include surface activity monitoring (Shmayda et al., 1997; Shmayda et al., 2002), spectroscopy based on Bremsstrahlung and X-rays induced by interaction of tritium β particles with materials (BIXS method); (Matsuyama et al., 1998). However, these methods are relatively insensitive because the detection of ^{3}H at low activity concentration is difficult. Destructive methods are widely used and more readily allow for quantitative determination. The two main methods involve acid dissolution (Hirabayashi et al., 1985; Masaki et al., 1989; Perevezentsev et al., 2002a; Torikai et al., 2005; Torikai et al., 2007) and thermal oxidation (Payne et al., 1952; Lockyer and Lally, 1993; Lewis et al., 2005; Kikuchi et al., 2006; Kim et al., 2008). Whichever extraction method is used for metals it is necessary to be confident that the ^{3}H is effectively liberated regardless of its speciation and the combustion

technique is known to be capable of quantitatively extracting tritium in all solid materials tested (Kim et al., 2008).

Several studies of tritium behaviour in metals have been reported (Hayashi et al., 1988; Yukhimchuk and Gaevoy, 1996; Nishikawa et al., 2000; Perevezentsev et al., 2005; Torikai et al., 2007; Perevezentsev et al., 2008) and these have mainly focused on non-irradiated metal exposed to tritiated water (HTO). The mechanism for the retention of ^{3}H in metals following exposure to atmospheric tritiated water vapour could be hydration of the surface Fe_2O_3 oxidation layer which forms at surface grain boundaries of metals (Liu et al., 1998).

There have been few previous reports dealing with the extractability of ^{3}H in irradiated and non-irradiated metal and the impact on accurate analytical measurements. This investigation has therefore used the most widely applied approach of thermal decomposition under a stream of oxygen. By taking multiple sub-samples of the evolved products it has been possible to examine the thermal evolution profiles to provide insights into the timing of tritium loss from metals and hence to infer the breakdown of tritium-holding phases. Such insights then provide practical feedback on effective analytical methods to ensure accurate waste characterization prior to waste sentencing.

6.2 Methods

6.2.1 Metal types

A range of irradiated and non-irradiated metals from two nuclear reactors undergoing decommissioning (the Material Test Reactor MTR, Dounreay, UK and the Steam Generating Heavy Water Reactor SGHWR Winfrith) were investigated in detail. The irradiated metals had been exposed to a significant neutron flux in the MTR and included Boral, aluminum, cadmium, lead and steel (Table 6.1). Boral® is a precision hot-rolled composite plate material consisting of a core of mixed aluminum and boron carbide particles with an aluminum cladding on both external surfaces. It was used to fabricate neutron absorbing components in reactor systems (control blades, beam-port shutters, and thermal column liners). Non-irradiated metals, mostly from the SGHWR reactor building, included stainless steel, copper, steel and aluminum and were exposed to tritiated water vapour (Table 6.1). All metals were carefully filed or drilled prior to tritium extraction by combustion to ensure a homogenous sample suitable for analysis. The filing procedure was performed gently to avoid significant heat generation which could potentially result in the loss of weakly bound tritium.

A subsample was transferred to a scintillation vial and counted on a well-type HPGe detector previously calibrated with a mixed nuclide standard of identical geometry. The resulting

spectrum was analysed using Fitzpeaks spectral analysis software. All detected anthropogenic radionuclides were identified and quantified.

Lithium and boron concentrations in metals were measured to allow calculation of the theoretical quantity of ^{3}H produced via the neutron activation. Lithium and boron concentrations were determined using X-ray fluorescence (XRF) and ICP-MS.

Table 6.1: Total ^{3}H activities for the metals investigated

Material	Location	Reactor environment	Total ^{3}H (Bq/g) [a]
Stainless steel	Nuclear site (Winfrith)	Exposure to HTO	777 ± 24
Copper	Nuclear site (Winfrith)	Exposure to HTO	109 ± 5
Aluminum	Nuclear site (Winfrith)	Exposure to HTO	13.0 ± 1
Steel	Nuclear site (Winfrith)	Exposure to HTO	4.9 ± 0.3
Aluminum	MTR[b]	Exposure to neutrons and HTO	8230 ± 209
Boral™	MTR	Exposure to neutrons and HTO	4280 ± 116
Steel	MTR	Exposure to neutrons and HTO	313 ± 15
Lead	MTR	Exposure to neutrons and HTO	9.4 ± 0.8
Cadmium	MTR	Exposure to neutrons and HTO	4.9 ± 0.3

[a] *Sample heated from 50-900°C with a standard ramping cycles*
[b] *Materials Test Reactor (Dounreay, UK); Winfrith is the site of the SGHWR*

6.2.2 Tritium thermal evolution profiles

Tritium thermal evolution profiles were determined for all the metal samples and in some cases profiles were also determined from selected samples (e.g. stainless steel, Boral and copper) taken at different depth increments. One example was Boral, which consisted of two 1 mm thick layers sandwiching a 6 mm thick layer; each layer was sampled by filing and/or drilling to obtain sub-samples. Tritium extraction was achieved using a Pyrolyser furnace system (Raddec Ltd., Southampton UK) which is a multi-sample, flow-through, oxidative heating/combustion system. The Pyrolyser consists of three contiguous furnace zones through which pass six separate, metre-long, silica work tubes. The controllable furnace zones can be heated up to 900^{o}C. Samples are heated in silica boats that are inserted into silica glass work-tubes that carry a stream of air/oxygen using a preset (user adjustable)

heating cycle (Figure 6.1). For metal samples that melt the sample is loaded onto silica sand in the boat to prevent possible breakage. The liberated decomposition products pass through an intermediate zone and then into a zone containing 10 g of platinised alumina catalyst heated to 800° that is designed to oxidise any surviving organic combustion products to CO_2 and H_2O. Any water vapour, including HTO, is trapped in a bubbler containing 20 mL of 0.1 M HNO_3. For the determination of tritium evolution profiles only the bubblers are changed every 30 minutes with sub-samples of the bubbler solution being taken for ^3H counting. The gas supply is isolated during the bubbler changeover. To confirm the features seen in tritium emanation profiles samples were heated to selected set temperatures for 24 hours and then increasing the temperature to 900°C to determine remained ^3H in the metal. The purpose of this approach was to ensure that ramp rates did not obscure any kinetic controls on tritium loss.

6.2.3 Tritium measurement

All tritium measurements were performed using Wallac 1220 Quantulus ultra low level background liquid scintillation counters. The standard approach mixed 8 mL of aqueous sample with 12mL Gold Star™ (Meridian) scintillation cocktail in a 22mL polythene vial. The counters were calibrated for ^3H using a traceable tritiated water standard (TRY-44, Nycomed Amersham PLC, Bucks, UK). For all samples, the measured quench levels (SQPE) ranged from 700 to 850 which correspond to ^3H counting efficiencies of 17–31%. All uncertainties are quoted at the 95% confidence level and refer to propagated method uncertainties.

6.3 Results

The effective liberation of tritium from a metal in an oxidizing flow-through combustion furnace depends on several factors. These include the physical form of the metal (e.g. lumps or fine grained particles), the temperature that metal samples are heated to, the composition and location of tritium-bearing phases, the neutron irradiation history of the metal and on any HTO exposure. Tritium may be associated with compounds such as tritides (unlikely to survive after ageing of the metal) or oxide phases (hydrated oxides) that could occupy sites along grain boundaries. It may also exist in mineral lattices (including defect sites) where original Li was transformed to tritium following neutron capture. The thermal decomposition of oxyhydroxides is expected to occur at 200-300°C (Mitov et al., 2002) which coincides with the commencement of ^3H evolution found for many of the metals examined here except for irradiated Boral (Figure 6.1-A). Since temperatures of 200-300°C are needed to liberate

tritium from metals it can be assumed that the normally used sampling procedures (careful drilling and filing) will not lead to any significant losses and this is borne out by the results of this study. The determination of thermal evolution profiles provide an insight into the origin of the tritium found in metals. That which is lost at temperatures around 100°C is indicative of HTO loss or similarly weakly-bound tritium. That which is lost around 300°C indicates breakdown of oxide or oxyhydroxide phases and that lost at 800-900°C indicates release of Li-derived (or boron) tritium from metal lattices.

Some of the irradiated metal examined (e.g. steel, aluminum and Boral; Figure 6.1-A) appears to have relatively significant quantities of ^{3}H produced via neutron induced reactions whereas others (e.g. cadmium and lead) did not contain significant quantities of ^{3}H originating from neutron activation (Table 6.2). This implies that ^{3}H produced via neutron activation may depend on the metallic composition and/or impurity elements (e.g. ^{6}Li, ^{7}Li and ^{10}B). Another control would be the integrated neutron flux seen by the sample. Therefore for the metal located further away from reactor core, ^{3}H will be more likely to be contaminated by absorption and diffusion of ^{3}H as HTO rather than neutron activation. Negligible ^{3}H loss at high temperature (>500°C) from irradiated metal except for Boral and aluminum can be interpreted in this way. On the other hand, most ^{3}H loss from non-irradiated metals occurs at <500°C except for stainless steel. Significant quantities of ^{3}H loss from non-irradiated stainless steel occurred at high temperature (>500°C) (Figure 6.1-C) which is controversial to the typical HTO speciation that will be held in a weakly bound form and liberate at lower temperature (<100°C) (Kim et al., 2008). This result is interpreted that absorbed and diffused HTO into bulk metal will be hydrated to the metal surface oxidation layer and required high temperatures due to the strong retention along grain boundaries of metal (Liu et al., 1998).

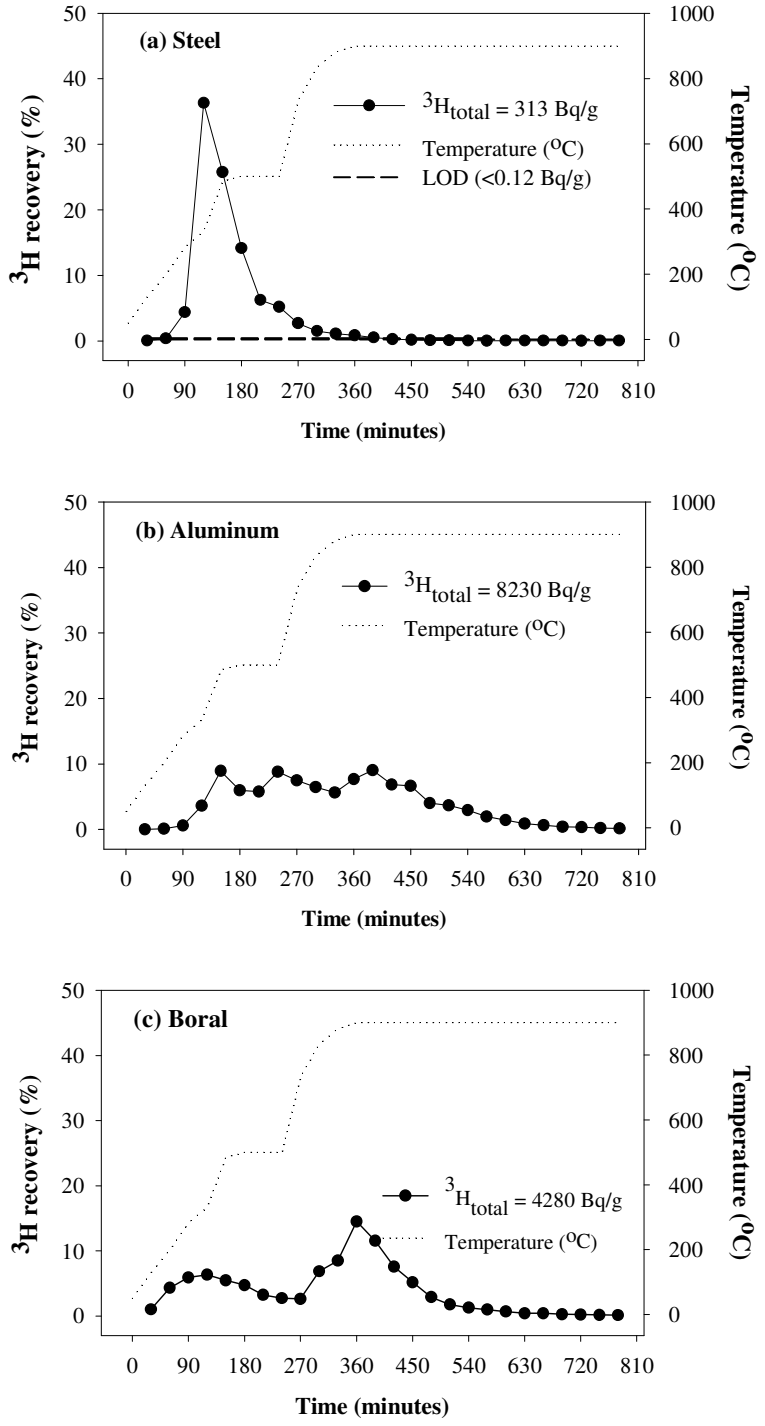

Figure 6.1-A: ^{3}H evolution for irradiated metals (using standard ramp rates)

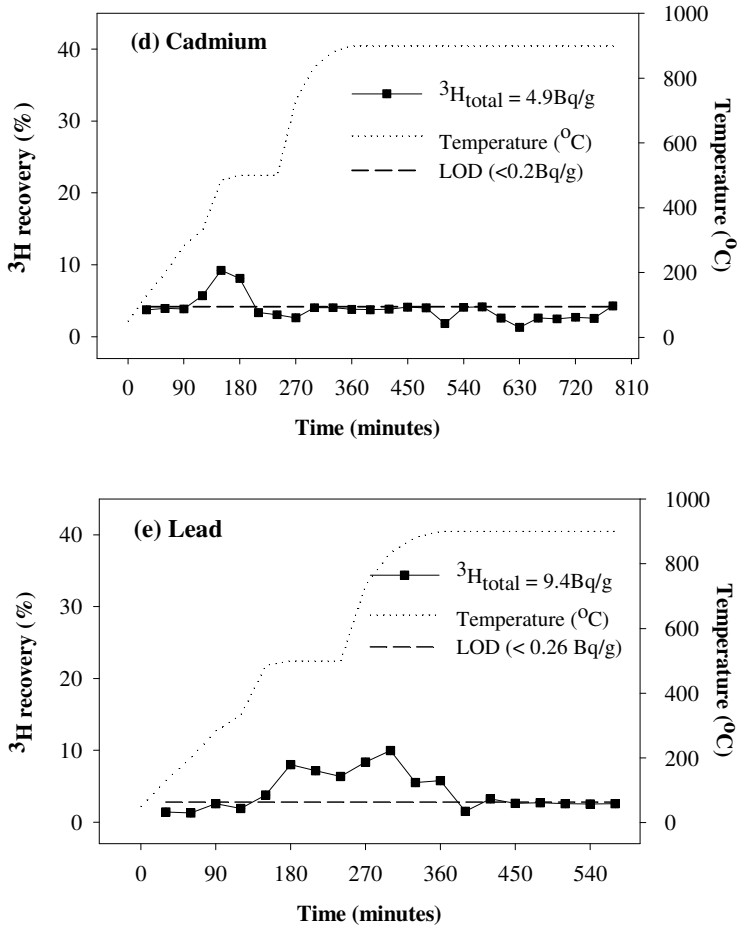

Figure 6.1-B: ^{3}H evolution for irradiated metals (using standard ramp rates)

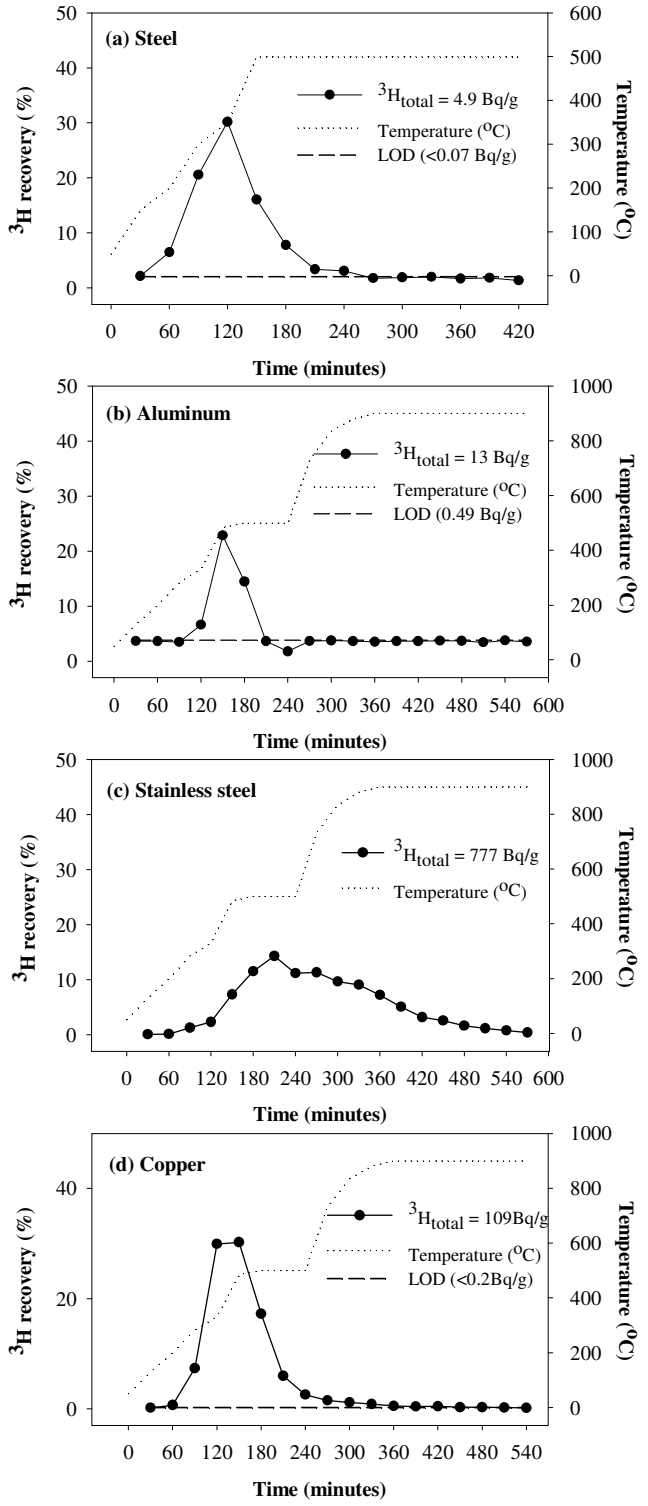

Figure 6.1-C: ^{3}H evolution for non-irradiated metals (using standard ramp rates)

Table 6.2: Gamma spectrometry (Bq/g) of metal samples and concentration of ^{6}Li and ^{10}B

Sample	^{241}Am	^{60}Co	^{139}Ce	^{137}Cs	^{152}Eu	^{154}Eu	^{155}Eu	^{54}Mn	^{22}Na	^{233}Pa	^{65}Zn	^{6}Li	^{10}B
Irradiated metal													
Boral	< 0.1	110 ± 10	-	4.3 ± 0.3	35 ± 1	9.4 ± 1.3	-	< 0.3	1.1 ± 0.2	-	< 1		
Aluminium	9.9	3300 ± 200	0.26 ± 0.14	340 ± 20		350 ± 20	19 ± 3	< 2	16 ± 2	4.1 ± 0.6	< 4		
Steel	< 0.06	78 ± 4	-	< 0.1	-	-	-	< 0.1	-	-	< 0.3		
Cadmium	< 0.4	21 ± 1	-	< 0.1	-	-	-	< 0.2	-	-	< 0.4		
Iron shot	< 0.02	16 ± 1	-	< 0.04	-	-	-	< 0.04	-	-	< 0.1		
Lead	< 0.2	1.3 ± 0.1	-	-	< 2	< 2	< 0.2	< 0.09	< 0.1	-	< 0.2		
Non-irradiated metals													
Copper	< 0.01	< 0.01	-	< 0.01	< 0.2	< 0.1	< 0.01	< 0.01	< 0.01	-	< 0.02		
Stainless steel	< 0.01	< 0.02	-	< 0.01	< 0.3	< 0.2	< 0.01	< 0.01	< 0.02	-	< 0.02		
Aluminium	< 0.01	< 0.02	-	< 0.01	< 0.2	< 0.1	< 0.01	< 0.01	< 0.01	-	< 0.02		
Steel	< 0.01	< 0.01	-	< 0.01	< 0.1	< 0.04	< 0.01	< 0.01	< 0.01	-	< 0.01		

6.4 Discussion

6.4.1 Tritium loss according to metal type and origin

Tritium in non-irradiated metals is likely to originate from the absorption of HTO from the ambient air of nuclear facilities (Hirabayashi and Saeki, 1984; Surette and McElroy, 1988; Perevezentsev et al., 2002b). In irradiated metals there are two potential contributions, namely HTO adsorption and neutron-induced tritium formation via activation of lithium or boron. The ^{3}H activity of the irradiated steel samples studied were notably higher than the non-irradiated steel samples although both the^{3}H evolution profiles were quite similar with most tritium being liberated at <500°C (Figure 6.1-a&b). This implies that the ^{3}H in both steels was held in similar phases or similar sites. A study by Torikai et al. (2007) argued that ^{3}H in steel was trapped in hydroxyl groups that would thermally decompose to yield releasable tritiated water [$2FeO(OH) \rightarrow Fe_2O_3 + H_2O$].

The ^{3}H evolution profiles for aluminum were significantly different from that of steels (Figure 6.1-c&d). Santos et al. (2000) described the thermal transformation sequence for aluminum hydroxides and indicated that gibbsite ($Al + 3H_2O \rightarrow Al(OH)_3 + 3H$) was formed when temperatures increased up to 300-400 K. With increasing temperature, gibbsite was subjected to the reactions of $Al(OH)_3 \rightarrow AlO(OH) + H_2O$ transforming it to boehmite and to γ-alumina by the reaction $2AlO(OH) \rightarrow Al_2O_3 + H_2O$. Gamma alumina could be expected to form on the top layer of the oxide film. Boehmite (AlO(OH)) decomposed into γ-alumina after the gibbsite was heated in air for 24 h at 803 K (Novák et al., 2005). The thermogravimetric analysis (TGA) curve of the pure aluminum showed a weight gain at 832K due to the transformation of gibbsite to diaspore (Shih and Liu, 2006). This implies that dehydration and oxidation of aluminum occurs at relatively high temperatures. Therefore, if ^{3}H was produced within the lattice or lattice edges in aluminum via neutron activation (of Li or B) then it is likely that it will require a high temperature to be extracted.

6.4.2 ^{3}H distribution depend on metal depth and composition

Previous studies have demonstrated that ^{3}H is predominantly confined to the top surface layer and decrease significantly inward bulk of the metal (Austin and Elleman, 1972; Nishikawa et al., 2000; Lewis et al., 2005; Perevezentsev et al., 2005; Penzhorn et al., 2006; Torikai et al., 2007; Perevezentsev et al., 2008) which agrees with the present study except for irradiated Boral (Figure 6.2). The Boral examined in this study has a sandwich type construction of aluminum enclosing aluminium plus boron carbide (Bale and Schafer, 1990; Abe et al., 1995; Paffett et al., 2002; Kharfi et al., 2005). The highest amount of ^{3}H was

found in the middle layer implying that it was formed via neutron induced reaction of $^{10}B(n,2\alpha)^{3}H$. Of all the materials studied here the highest tritium activity was observed in the irradiated Boral. In case of non-irradiated stainless steel, though highest ^{3}H contamination was confined to the surface layer, significant quantities of ^{3}H activity was observed at subsurface layer. Similar results demonstrated from other study where the stainless steel was exposed to hydrogen containing ^{3}H (Perevezentsev et al., 2008). This can be explained with the rapid ^{3}H absorption rate which was demonstrated previously where gaseous tritium penetrated more than 30 μm into SS316 after 35 days of exposure time at 13.3 kPa and 298K (Hirabayashi and Saeki, 1984). All other studies that investigated ^{3}H distribution with depth in metals mainly examined metals exposed to tritiated gases or tritiated water vapour. Therefore, most tritium was more likely to be confined to the surface layer and the quantities of tritium absorbed into the metal increased with exposure time via rapid absorption of ^{3}H at ambient or elevated temperature. However, if the metal received a high neutron flux and contains specific tritiogenic elements (e.g. ^{6}Li, ^{7}Li and ^{10}B), then the highest ^{3}H concentration will be found in those layers (Perevezentsev et al., 2008).

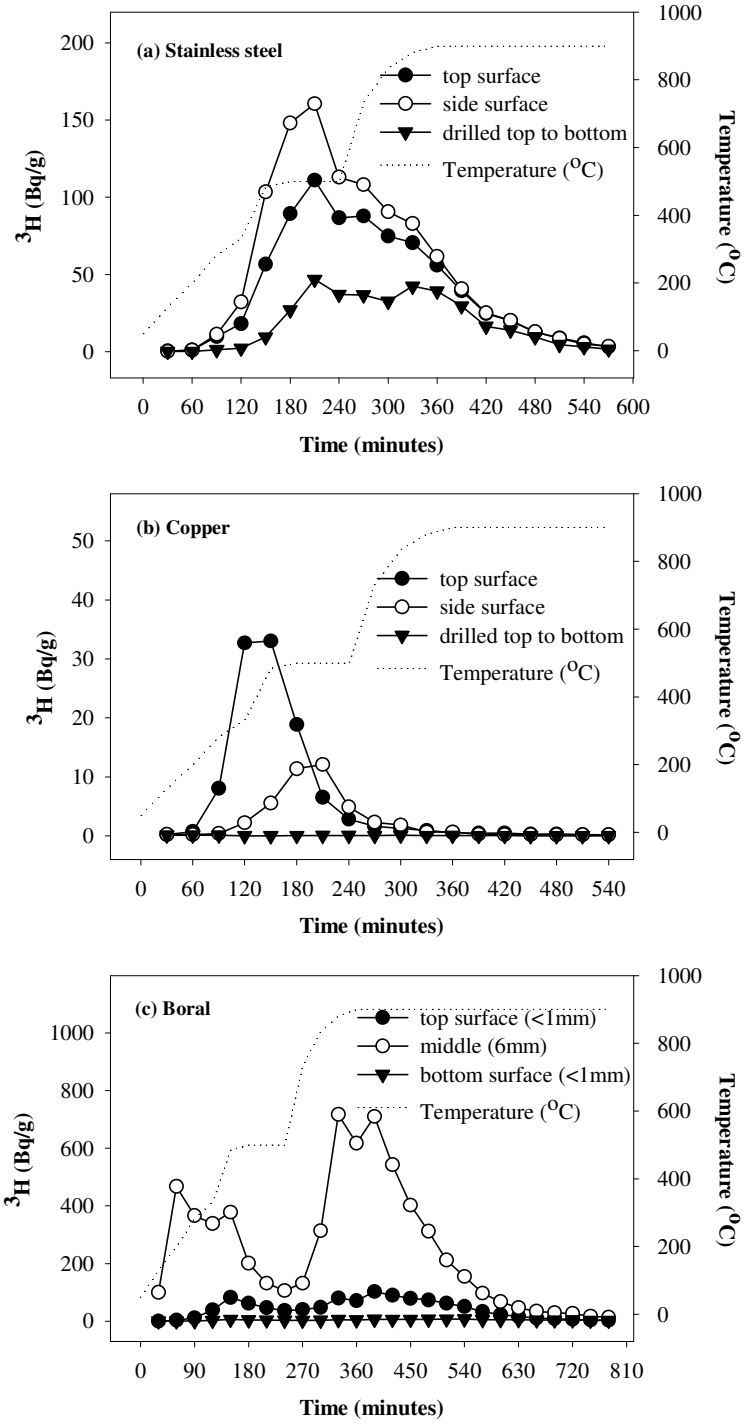

Figure 6.2: ^{3}H evolution depend on metal depth and composition

6.4.3 ^{3}H variations with temperature

The temperature of ^{3}H evolution will depend on whether it is present in the metals as free water, water of crystallization, surface oxyhydroxides layer, structural OH groups or trapped along grain boundaries ^{3}H. Previous studies (Nishikawa et al., 1989; 2000) demonstrated that non-negligible quantities of water or –OH present on the various metal surface (e.g. stainless steel, copper and aluminum) play an important role in trapping tritium via absorption and isotopic exchange reactions. This surface water can be physically or chemically adsorbed water or structural water (Nishikawa et al., 2000). The structural water represents any chemically adsorbed water, crystal water and some chemical groups containing hydrogen (e.g. –OH bases) which are strongly connected with surface, and tritium is exchanged with hydrogen in the structural water through the isotope exchange reaction. The study identified that water loss from some metals (e.g. stainless steel, copper and aluminum) occurs in specific stages at approximately 120 and 200 °C (Nishikawa et al., 2000). In the current study the quantities of ^{3}H evolved for some metals (non-irradiated stainless steel, -copper, irradiated aluminum, -Boral, and -steel) previously heated to these key temperatures for 24 hours were compared with that of typical evolution of the metals. Three types of ^{3}H evolution were identified (Table 6.3); group-A (non-irradiated stainless steel and irradiated aluminum), increased ^{3}H evolution with increasing temperatures and significant ^{3}H liberation at high temperatures (>300°C); group-B (irradiated Boral), significant ^{3}H liberation at low (<120°C) and high (>300°C) temperature; group-C (non-irradiated copper and irradiated steel), non-significant ^{3}H evolution at high temperatures (>300°C).

Table 6.3: The proportion of ^{3}H evolved in different metals according to temperature

		% of ^{3}H (% of ^{3}H in conventional evolution)					
		120°C	**200°C**	**300°C**	**120-300°C**	**300-900°C**	**Total**
Group A	**Stainless steel (non-irradiated)**	5.8±0.4 (0.1±0.03)	16.9±0.9 (0.2±0.04)	17.6±1.5 (3.8±0.2)	40.3±1.7 (4.1±0.3)	59.7±6.0 (95.9±3.1)	100
	Aluminum (irradiated)	5.7±0.5 (0.01±0.002)	19.1±1.1 (0.1±0.01)	33.5±1.7 (4.3±0.4)	58.3±2.1 (4.4±0.4)	41.7±4.2 (95.6±2.5)	100
Group B	**Boral (irradiated)**	47.6±4.5 (1.5±0.2)	5.3±0.3 (8.7±0.7)	4.5±0.3 (19.5±1.1)	57.4±4.5 (29.7±2.0)	42.6±4.2 (70.3±2.4)	100
Group C	**Copper (non-irradiated)**	30.0±2.3 (0.2±0.01)	39.9±3.4 (0.9±0.2)	15.7±1.4 (38.2±3.2)	85.5±4.3 (39.3±3.4)	14.5±1.1 (60.7±3.8)	100
	Steel (irradiated)	14.2±0.6 (0.04±0.001)	52.4±2.4 (0.4±0.1)	31.7±2.5 (41±0.5)	98.3±3.6 (41.4±1.0)	1.7±1.1 (58.6±3.1)	100

Note: Each metal was combusted at specific temperature (120, 200 and 300°C) for 24 hours, respectively and then heated up to 900°C.

Heating the irradiated Boral to 120°C for 24 hours resulted in significant ^{3}H loss, which arose from a slow rate of release of ^{3}H and may indicate that significant quantities of ^{3}H were present in the weakly bound form (mainly as HTO). Similar result was occurred from the irradiated steel where complete loss of ^{3}H was occurred after heating to 120, 200 and 300°C (Figure 6.3). The quantitative removal of tritium suggests that most ^{3}H in steel (both irradiated and non-irradiated because of its similar ^{3}H evolution) may be present in a weakly bound form. On the other hand, significant quantities of ^{3}H loss from non-irradiated stainless steel at high temperature (>300°C) demonstrated that the presence of strongly bound tritium via absorption and isotopic exchange depended on metal types. A previous study (Perevezentsev et al., 2008) demonstrated that the quantities of tritium absorbed into metals depends on the chemical form of the tritium, the surface conditions and history (e.g. heat treatment, polishing or forging) of the metal prior to exposure to tritium. Therefore, for analytical security it should be assumed that ^{3}H in metals from nuclear sites may be retained in different physico-chemical forms and a high temperature treatment should be considered normal to ensure accurate analytical data.

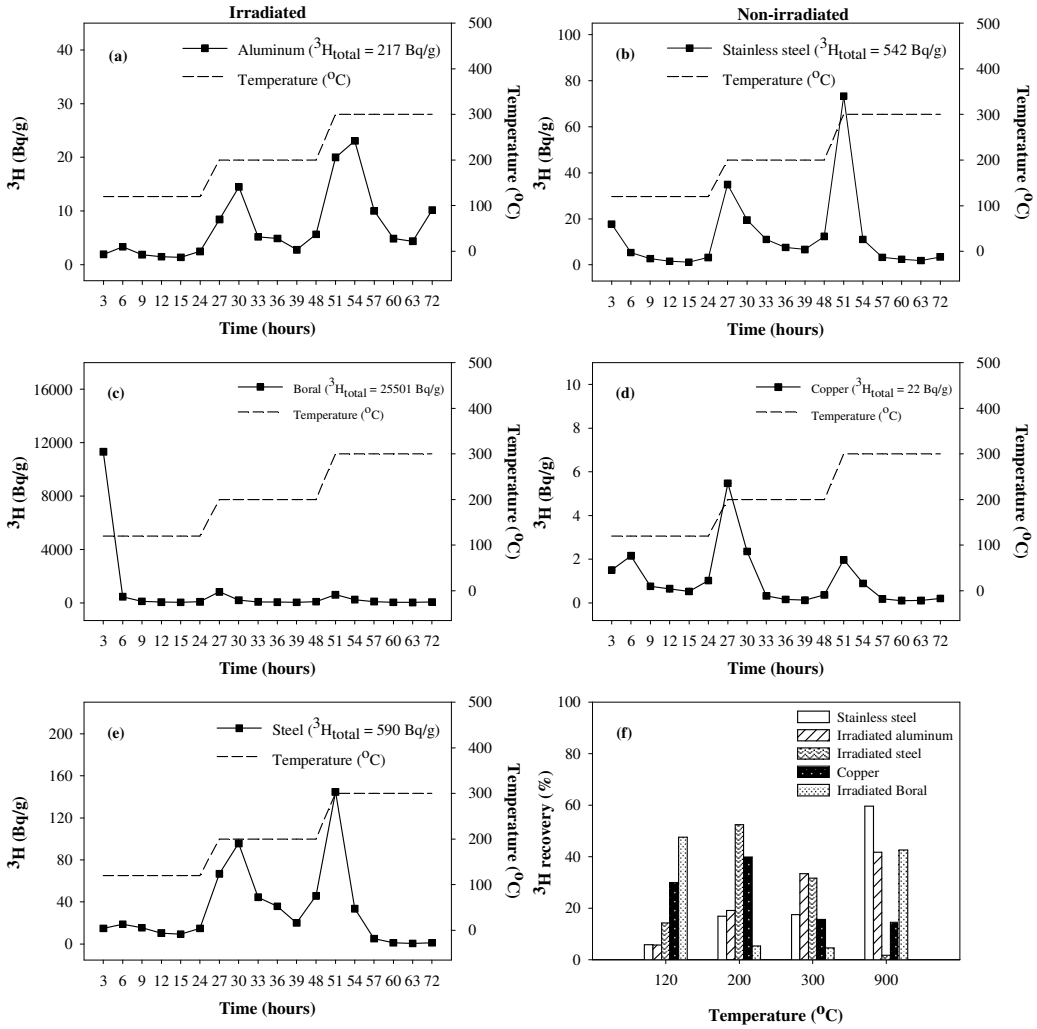

Figure 6.3: ^3H evolution using very slow ramping profiles

6.4.4 ^3H retention mechanisms in metal

Tritium retention in metals are most likely to be via absorption of free water (HTO) (Kikuchi et al., 2006), hydration of the surface oxidation layer (Liu et al., 1998), HT ingress into bulk metal (e.g. along grain boundaries) and lattice bound tritium produced *in-situ* via neutron activation (Austin and Elleman, 1972; Sugai et al., 1995; Westall et al., 2007).

Tritium, incorporated on and into stainless steel at ambient or higher temperature following expose to HT, is predominantly desorbed as tritiated water (Hirabayashi and Saeki, 1984;

Surette and McElroy, 1988; Perevezentsev et al., 2002b). This may be explained by the existence on the metal surface as well as in the inter-granular bulk zone of an oxide (probably Cr_2O_3) with its associated OH (OT) and O groups (Castle and Clayton, 1977; Abraham et al., 1978; Matsuyama et al., 1998). Desorbed water can conceivably be formed from a reaction between adjacent adsorbed OH/OT groups, via oxidation reactions taking place during desorption of hydrogen in the presence of air (Surette and McElroy, 1988) or from a combination between OH (or OT) groups with dissolved atomic H (or T) (Hirabayashi et al., 1984). The mechanism for the retention of ^3H in metals following exposure to atmospheric tritiated water vapour is unclear. One possible mechanism for ^3H retention could be hydration of the surface Fe_2O_3 oxidation layer which forms at surface grain boundaries of mild steel. Such hydration has been shown to produce OH layers on α-Fe_2O_3 at $pH_2O > 10^{-4}$ Torr and on α-Al_2O_3 at $pH_2O > 1$ Torr (Liu et al., 1998). However, prolonged exposure of the metal samples to atmosphere at low temperature (~120°C) can be lead to significant ^3H loss from the metal which was demonstrated via heating of the metals at key transition stage for prolonged heating time (Figure 6.3 and Table 6.3).

Nishikawa et al (2000) quantified tritium trapping capacity on the metal surface (e.g. stainless steel, copper and aluminum) via surface water. The surface water is defined as amount of water or OH bases present on the metal surface and consists of physically adsorbed water, chemically adsorbed water and structural water. Non-negligible amount of surface water exists on the metal surface, and this water plays an important role in trapping of tritium via adsorption and isotopic exchange reaction (Nishikawa et al., 1989; Shiraishi et al., 1997). The amount of surface water may vary with thickness and chemical composition of the oxide layer (Nishikawa et al., 2000). When the metal is exposed to tritiated water, tritium is trapped on the surface as physically or chemically adsorbed water at first and then, the isotope exchange reaction between tritiated water in the gas phases and water on the surface supplies tritium to the surface until the T/H ratio in the surface water becomes the same as T/H ratio in the gas phase. Copper gives the smallest tritium trapping capacity compared with stainless steel and aluminum and almost no chemically adsorbed water is observed on the copper surface (Nishikawa et al., 2000). The contribution of chemically adsorbed water becomes negligible when the temperature is above 100°C.

Alternative ^3H retention mechanisms of the metal can arise from nuclear reactors via several neutron-induced reactions [$^2H(n,\gamma)^3H$, $^6Li(n,\alpha)^3H$, $^7Li(n,\alpha)^3H$, $^{10}B(n, 2\alpha)^3H$, $^{14}N(n, ^3H)^{12}C$]. Previous studies (Sugai et al., 1995; Sugai, 2007) demonstrated that the dominant irradiation

effects on β-LiAl are due to the $^{6}Li(n,\alpha)^{3}H$ reaction induced by thermal neutrons. The increase of lithium concentration reduces the tritium diffusion coefficients owing to the increase in the number of trapping sites and raises the activation energy for ^{3}H escape from a trap in β-LiAl owing to the attractive interaction with Li-atoms in lithium sub-lattices around the nearest neighbor of tritium (Hayashi et al., 1988; Sugai, 2007). There are two typical diffusion mechanisms in solids; one is an interstitial mechanism and the other is a vacancy mechanism (Shewmon, 1963). Tritium in β-LiAl diffuses through interstitial mechanism, because there is a repulsive interaction between tritium and lithium. The dominant origin of the large activation energy in the interstitial mechanism is attributed to the impeded diffusion due to the strong attractive interaction between tritium and Li in β-LiAl. In the tritiated species released above the melting point of β-LiAl (*ca* 700°C) (Yahagi, 1980), the other gaseous tritiated species except HT was negligible and the percentage of HTO was less than 2% for the total tritium released from β-LiAl. The origin of HTO was due to the presence of oxygen that existed in the oxide layer on the surface of β-LiAl (Sugai et al., 1992). The surface of β-LiAl crystal is active to react with oxygen and nitrogen; oxides and nitrides might be formed on the surface of crystals heated. The oxides and nitrides on the surface lead to depression of tritium release, because the tritium release rates of oxides (Okuno and Kudo, 1986) and nitrides (Kudo et al., 1983) are smaller than that of β-LiAl. Since the surface reaction of β-LiAl with oxygen and nitrogen was accelerated with increasing the temperature. The contribution of the oxides and nitrides to the tritium diffusion in β-LiAl crystals is negligibly small (Sugai, 2007).

Tritium penetration rate into metals will vary dependent on the metal type and the nature of the metals. The significant factors impacting on tritium penetration into the metals are temperature, pressure, metal surface conditions and tritium concentration exposed to the metals where tritium penetration depth will be deeper with increasing of those (Perevezentsev et al., 2005). Absorbed tritium into the metal shows tendency even at room temperature to migrate to the surface and either remain trapped there, most probably as a hydroxyl group, or recombine with an already existing hydroxyl group to yield tritiated water releasable into the atmosphere (Torikai et al., 2007). Persistent tritium release from stainless steel exposed to tritium at ambient temperature was demonstrated (Surette and McElroy, 1988; Torikai et al., 2005). Similar results were observed in this study for non-irradiated stainless steel; ^{3}H activity decreased from ca 777 Bq/g to 542 Bq/g; the stainless steel was stored at room temperature after the first ^{3}H measurement for over one year. The early study by the author demonstrated significant ^{3}H loss from metal at room temperature

for 2 weeks (Kim et al., 2007). The chronic release of tritium originates not only from the metal surface or subsurface but also from the bulk (Torikai et al., 2005). Tritium will migrate both to the surface as well as to the bulk (Torikai et al., 2007), therefore collecting reliable sub samples from bulk metals and heating at elevated temperatures is the most adequate approach to extract tritium from metals.

6.5 Conclusions

A range of metals from two nuclear sites have been investigated for their tritium content and their tritium evolution profiles. These metals have had different exposure histories to tritiated water, tritium gas and neutrons and these variations have led to their different tritium content. Irradiated and non-irradiated metals show different tritium thermal loss profiles and this reflects the relative ease of thermally decomposing hydrated oxides trapped along grain boundaries or the greater difficulty in mobilizing tritium trapped in the metal lattice. Significant quantities of ^{3}H contamination were observed from non-irradiated metals (e.g. stainless steel and copper) which implies that exposure of the metal to tritiated water vapour or gases near the nuclear facilities is a significant source of tritium contamination. Tritium contamination into the metals via atmospheric absorption is mainly confined to the surface layer or paint layer. Tritium penetrates into the metal surface by diffusion with a rate controlled by the metal types and the surface condition of the metal (painted, unpainted).

Tritium contamination of metals via neutron activation is not mainly confined to the surface layer. It will be affected by the distribution of some elements (e.g. ^{6}Li or ^{10}B) presented in the metal. Tritium in metals mainly presented two different forms including a weakly bound ^{3}H (inferred to be an HTO form) and a strongly bound form (inferred to be a non-HTO form) that required a high temperature to liberate it. However, the HTO form of the metal has different thermal decomposition behaviour indicating a slow evolution rate at low temperature (~120°C). This is significantly different thermal decomposition behavior of HTO isolated rapidly at low temperature (~100°C). Therefore, the effective and quantitative extraction of ^{3}H from metals requires prolonged heating at a high temperature (900°C for 4-5 hours).

6.6 References

Abe AY, Lee JC, Burn RR. 1995. Neutronic analysis of boral plate irradiation experiments. Transactions of the American Nuclear Society 73: 388-390.

Abraham PM, Elleman TS, Verghese K. 1978. Diffusion and trapping of tritium in grainboundaries of 304L stainless steel. Journal of Nuclear Materials 73: 77-88.

Alizadeh E. 2006. Environmental and safety aspects of using tritium in fusion. Journal of Fusion Energy 25: 47-55.

Austin JH, Elleman TS. 1972. Tritium diffusion in 304- and 316-stainless steels in the temperature range 25 to 222°C. Journal of Nuclear Materials 43: 119-125.

Bale MG, Schafer K. 1990. Observations on hydrogen generation in boron carbide/aluminum/water systems. Transactions of the American Nuclear Society 62: 248-249.

Castle JE, Clayton CR. 1977. The use of in the x-ray photo-electron spectroscopy analyses of passive layers on stainless steel. Corrosion Science 17: 7-26.

DEFRA. 2002. DEFRA (2002). Radioactive Wastes in the UK: A summary of the 2001 inventory. Report DEFRA/RAS/02.003. Department for Environment, Food and Rural Affairs, London, UK, p14.

Hayashi T, Okuno K, Kudo H, Amano H. 1988. Tritium diffusion and trapping associated with lithium in Al-Li systems. Journal of the Less Common Metals 141: 169-176.

Hirabayashi T, Saeki M. 1984. Sorption of gaseous tritium on the surface of type 316 stainless steel. Journal of Nuclear Materials 120: 309-315.

Hirabayashi T, Saeki M, Tachikawa E. 1984. A thermal desorption study of the surface interaction between tritium and type 316 stainless steel. Journal of Nuclear Materials 126: 38-43.

Hirabayashi T, Saeki M, Tachikawa E. 1985. Chemical Decontamination of the Tritium-Sorbing Surface of Type-316 Stainless-Steel. Journal of Nuclear Materials 136: 179-185.

Kalinin G, Barabash V, Cardella A, Dietz J, Ioki K, Matera R, Santoro RT, Tivey R. 2000. Assessment and selection of materials for ITER in-vessel components. Journal of Nuclear Materials 283-287: 10-19.

Kharfi F, Boukerdja L, Attari A, Abbaci M, Boucenna A. 2005. Implementation of neutron tomography around the Algerian Es-Salam research reactor: preliminary studies and first steps. Nuclear Instruments and Methods in Physics Research Section A: Accelerators, Spectrometers, Detectors and Associated Equipment 542: 213-218.

Kikuchi K, Nakamura H, Tsujimoto K, Kobayashi K, Yokoyama S, Saitoh S, Yamanishi T. 2006. Evaluation of residual tritium in stainless steel irradiated at SINQ target 3. Journal of Nuclear Materials 356: 157-161.

Kim DJ, Croudace IW, Warwick PE (2007) The analytical impact on tritium data from storing nuclear decommissioning samples under different conditions. In: Warwick P (Ed) Environmental Radiochemical Analysis III, pp 108-115.

Kim DJ, Warwick PE, Croudace IW. 2008. Tritium Speciation in Nuclear Reactor Bioshield Concrete and its Impact on Accurate Analysis. Anal. Chem. 80: 5476-5480.

Kudo H, Kushita K, Okuno K. 1983. Chemical behavior of tritium in neutron-irradiated Li3N. Journal of Nuclear Materials 116: 78-81.

Lewis A, Warwick PE, Croudace IW. 2005. Penetration of tritium (as tritiated water vapour) into low carbon steel and remediation using abrasive cleaning. Journal of Radiological Protection 25: 161-168.

Liu P, Kendelewicz T, Brown GE, Nelson EJ, Chambers SA. 1998. Reaction of water vapor with [alpha]-Al2O3(0001) and [alpha]-Fe2O3(0001) surfaces: synchrotron X-ray photoemission studies and thermodynamic calculations. Surface Science 417: 53-65

Lockyer JF, Lally AE. 1993. The Determination of Tritium, C-14 and S-35 in Milk and Crop Samples Using a Combustion Technique. Science of the Total Environment 130: 337-344.

Masaki NM, Hirabayashi T, Saeki M. 1989. Study on Sorption of Tritium on Various Material-Surfaces and Its Application to Decontamination of Tritium Sorbing Materials. Fusion Technology 15: 1337-1342.

Matsuyama M, Watanabe K, Hasegawa K. 1998. Tritium assay in materials by the bremsstrahlung counting method. Fusion Engineering and Design 39-40: 929-936.

Mitov I, Paneva D, Kunev B. 2002. Comparative study of the thermal decomposition of iron oxyhydroxides. Thermochimica Acta 386: 179-188.

NCRP. 1985. A bandbook of radioactive measurements procedures. national Council on Radiation Protection and measurement, Bethesda, Maryland.

Nishikawa M, Nakashio N, Shiraishi T, Odoi S, Takeishi T, Kamimae K. 2000. Tritium trapping capacity on metal surface. Journal of Nuclear Materials 277: 99-105.

Nishikawa M, Takeishi T, Matsumoto Y, Kumabe I. 1989. Ionization chamber system to eliminate the memory effect of tritium. Nuclear Instruments and Methods in Physics Research Section A: Accelerators, Spectrometers, Detectors and Associated Equipment 278: 525-531.

Novák C, Pokol G, Izvekov V, Gál T. 2005. Studies on the reactions of aluminium oxides and hydroxides Journal of Thermal Analysis and Calorimetry 36: 1895-1909.

Okuno K, Kudo H. 1986. Diffusion-controlled tritium release from neutron-irradiated [gamma]-LiAlO2. Journal of Nuclear Materials 138: 210-214.

Paffett MT, Willms RS, Gentile CA, Skinner CH. 2002. Surface characterization of TFTR first wall graphite tiles used during DT operations. Fusion Science and Technology 41: 934-938.

Payne PR, Campbell IG, White DF. 1952. The combustion of tritium-labeled organic compounds. Biochem. J. 50: 500-502.

Penzhorn R-D, Torikai Y, Matsuyama M, Watanabe K. 2006. Detritiation of type 316 stainless steel by treatment with liquids at ambient temperature. Journal of Nuclear Materials 353: 66-74.

Perevezentsev A, Watanabe K, Matsuyama M, Torikai Y. 2002a. Contamination of stainless steel type 316 by tritium. Fusion Science and Technology 41: 746-750.

Perevezentsev A, Watanabe K, Matsuyama M, Torikai Y. 2002b. Screen test of tritium recovery from stainless steel type 316. Fusion Science and Technology 41: 706-710

Perevezentsev AN, Bell AC, Rivkis LA, Filin VM, Gushin VV, Belyakov MI, Bulkin VI, Kravchenko IM, Ionessian IA, Torikai Y, Matsuyama M, Watanabe K, Markin AI. 2008. Comparative study of the tritium distribution in metals. Journal of Nuclear Materials 372: 263-276.

Perevezentsev AN, Rivkis LA, Gushin VV, Filin VM, Bulkin VI, Dmitrievskaya EV, Markin AI, Ryasantseva NN, Belyakov MI. 2005. Study of tritium distribution in various metals. Fusion Science and Technology 48: 208-211.

Santos PS, Santos HS, Toledo SP. 2000. Standard transition aluminas. Electron microscopy studies. Materials Research 3: 104-114.

Shewmon PG. 1963. Diffusion in Solids. McGraw-Hill, New York.

Shih T-S, Liu Z-B. 2006. Thermally-Formed Oxide on Aluminum and Magnesium. MATERIALS TRANSACTIONS 47: 1347-1353.

Shiraishi T, Odoi S, Nishikawa M. 1997. Adsorption and desorption behavior of tritiated water on the piping materials. Journal of Nuclear Science and Technology 34: 687-694.

Shmayda CR, Shmayda WT, Kherani NP. 2002. Monitoring tritium activity on surfaces: Recent developments. Fusion Science and Technology 41: 500-504.

Shmayda WT, Kherani NP, Stodilka D. 1997. Evaluation of the tritium surface activity monitor. Fusion Technology 1996. Proceedings of the 19th Symposium on Fusion Technology 2: 1245-1248.

Sugai H. 2007. Diffusion of tritium in intermetallic compound [beta]-LiAl: Relation to the defect structure. Solid State Ionics 177: 3507-3512.

Sugai H, Miao Z, Kato M, Kudo H. 1992. Tritium Diffusion Behavior in Neutron-Irradiated Lial Crystal. Fusion Technology 21: 818-820.

Sugai H, Tanase M, Yahagi M, Ashida T, Hamanaka H, Kuriyama K, Iwamura K. 1995. Defect structure in neutron-irradiated beta -6LiAl and beta -7LiAl: Electrical resistivity and Li diffusion. Physical Review B 52: 4050.

Surette RA, McElroy RGC. 1988. Regrowth, Retention and Evolution of Tritium from Stainless-Steel. Fusion Technology 14: 1141-1146.

Torikai Y, Murata D, Penzhorn RD, Akaishi K, Watanabe K, Matsuyama M. 2007. Migration and release behavior of tritium in SS316 at ambient temperature. Journal of Nuclear Materials 363-365: 462-466.

Torikai Y, Penzhorn RD, Matsuyama M, Watanabe K. 2005. Chronic release of tritium from SS316 at ambient temperature: Correlation between depth profile and tritium liberation. Fusion Science and Technology 48: 177-181.

Westall WA, Streatfield RE, Hebditch DJ. 2007. Determination of tritium radionuclide and lithium precursor in Magnox reactor steels. Environmental Radiochemical Analysis III: 137-146.

Yahagi M. 1980. Single crystal growth of LiAl. Journal of Crystal Growth 49: 396-398.

Yukhimchuk AA, Gaevoy VK. 1996. Study of hydrogen isotope permeation through some construction materials. Journal of Nuclear Materials 237: 1193-1197.

Chapter 7

Overall conclusions

7 Overall conclusions

7.1 Tritium determination using thermal extraction

a. A multi-tube combustion furnace system, incorporating a platinised alumina pellet catalyst bed, was thoroughly evaluated and used to extract tritium from a wide range of sample types sampled from UK sites undergoing nuclear decommissioning.

b. Tritium may exist

- in a wide range of radioactive samples found in nuclear reactor buildings (e.g. metal, soil, concrete, wood, graphite and plastics).
- in a range of chemical forms (HT, HTO and OBT) and in different structural positions in materials.
- in weakly and/or strongly-bound chemical associations

c. Tritium speciation will have an impact

- on the temperature range and rate of release from different materials.
- on the extraction methodology used. For quantitative extraction of species other than free HTO (weakly bound form) an aggressive thermal approach is required to liberate it. In this study this has involved the combustion of the sample and the conversion of all liberated ^{3}H species to HTO which is subsequently trapped and measured by liquid scintillation counting. The combustion method is effective at extracting all species of ^{3}H form including strongly bound form (e.g. organic species and lattice bound ^{3}H).

d. This study has shown the value of determining thermal evolution profiles as they provide insights into tritium association/location in various materials. The evolution profile also guides the maximum combustion temperature and time needed for efficient combustion. Prior to commencing an analytical run for total tritium extraction and measurement in new materials it is desirable to determine the (tritium loss) thermal evolution profiles. This clearly has important implications for radioactive waste sentencing of decommissioning materials.

7.2 ^{3}H in reactor bioshield concrete

Tritium (^{3}H) is produced in nuclear reactors via several neutron induced reactions [$^{2}H(n,\gamma)^{3}H$, $^{6}Li(n,\alpha)^{3}H$, $^{7}Li(n,\alpha)^{3}H$, $^{10}B(n,2\alpha)^{3}H$, $^{14}N(n, ^{3}H)^{12}C$ and ternary fission (fission yield <0.01%)]. Typically, ^{3}H is present as tritiated water (HTO) in the environment and can become adsorbed into structural concrete from the surface inward where it will be held in a weakly-bound form.

Systematic analysis of a sequence of sub-samples taken from a reactor (SGHWR) bioshield identified two forms of ^{3}H, one weakly bound and one strongly bound.

The total ^{3}H concentration in bioshield concrete is highest near the reactor core and decreases exponentially with distance from the reactor. However, when tritium species in the bioshield concrete are considered, the relative proportion of strongly bound tritium decreases exponentially while the weakly bound tritium increases with increasing distance from the reactor core. The activity concentration of weakly bound ^{3}H, however, remains approximately constant throughout the core due to the rapid diffusion coefficient of ^{3}H in the concrete. The different proportions of the two forms of tritium identified suggest different origin.

Strongly bound tritium originates from neutron capture by trace lithium (^{6}Li) held within mineral phases and requires temperatures of 350-900 °C to achieve quantitative recovery. Strongly bound ^{3}H activity concentrations measured in the bioshield concrete correlates highly with the activity of ^{152}Eu and hence neutron flux, which supports the proposition that the strongly bound ^{3}H originates from neutron activation. The strongly-bound ^{3}H slowly converts to the more loosely bound form (e.g. via migration out of mineral lattices) with time and which subsequently diffuses through the bioshield.

Weakly-bound ^{3}H probably arises from a combination of diffusion of HTO from the reactor core into the concrete as well as a slow conversion of strongly-bound ^{3}H to a more weakly-bound form. The presence of significant quantities of weakly-bound ^{3}H at distance from the neutron source confirms that diffusion controls the distribution of this form of ^{3}H. The weakly bound form of tritium can be liberated at significantly lower temperatures (100°C) as HTO and is associated with dehydration of hydrous mineral components.

Without an appreciation that two forms of tritium can exist in reactor bioshields the ^{3}H content of samples may be underestimated using conventional (moderate thermal treatment) analytical approaches. These findings exemplify the need to develop robust radioactive waste characterization procedures in support of nuclear decommissioning programmes. For quantitative analysis of ^{3}H in bioshield concretes, a thermally aggressive treatment is required to quantitatively liberate the ^{3}H. Typically, this should involve heating samples up to 900°C. For other sample types, the temperature that ^{3}H is completely liberated from the sample will depend on the chemical form of the ^{3}H and the physical properties of the sample material.

7.3 The analytical impact of storage on tritium analysis

Tritium emanation from materials can lead to cross-contamination if samples are not individually stored. The main tritium loss originates from weakly bound tritium which is dominantly present as tritiated water (HTO). This form of ^{3}H is easily exchanged with atmospheric hydrogen in the form of water vapour at room temperature. However, the loss of strongly bound ^{3}H produced by neutron activation is not significant even at room temperature.

The physical and compositional characteristics of materials that emanate tritium and those being contaminated along with storage temperature control the magnitude of ^{3}H contamination. Typically, porous hydrophilic materials can be more readily contaminated. The rate of loss of ^{3}H and any associated cross-contamination can be significantly reduced by storing sample in an air/water tight container in a freezer.

Proper sampling and storage are significant factors in achieving accurate tritium activity measurements and impact on correct nuclear waste sentencing strategies. Sample taken for tritium analysis need to be taken with care to retain their authenticity and should be rapidly and individually packed and frozen (-18°C) as quickly as possible. Packing in airtight containers (glass or high density polyethylene bottles or plastic bags) avoids cross contamination and freezing limits tritium loss. Finally, suspected low activity samples should be segregated from high activity samples by double bagging.

7.4 ^{3}H speciation in metals from nuclear sites

Metals derived from nuclear facilities are frequently contaminated with tritium via atmospheric exposure to HTO at nuclear sites and *in situ* production via neutron activation of Li and B (specifically ^{6}Li, ^{7}Li and ^{10}B). The irradiated metals investigated typically showed high ^{3}H concentrations compared with non-irradiated metals. However, although not all irradiated metals produce high quantities of ^{3}H via neutron activation and its production will be affected by the total received neutron flux, metal location in the reactor building and the presence of tritium precursor nuclides (e.g. ^{6}Li, ^{7}Li and ^{10}B) in the metal.

- Tritium contamination in metals arising from atmospheric absorption is mainly confined to the surface layer and decreases significantly inward. Tritium retention would be by absorption of free water, hydration of the metal surface oxidation layer, HT ingress into bulk metal (e.g. along grain boundaries) and in intergranular locations.

- Any absorbed ^{3}H would be expected to penetrate into metal surfaces by diffusion where the diffusion rate will be affected by metal types and surface condition or treatment. This has some implication for ^{3}H analysis of metal via sub-sampling from bulk metal.

- Where metals have been exposed to a significant neutron flux and contains specific nuclides (e.g. ^{6}Li, ^{7}Li and ^{10}B), then tritium will be produced and there should be an exponential decline in ^{3}H concentration with depth away from the neutron source. For heterogeneous materials (e.g. Boral which has a core of B_4C pressed into aluminium) then the highest ^{3}H concentration can be expected in the materials that will generate tritium.

- The temperature of ^{3}H evolution will depend on whether the ^{3}H is present in the metals as free water, water of crystallization, surface oxyhydroxides layer, structural OH groups, grain boundaries or intra-lattice ^{3}H. Tritium in metal exists in two forms, a weakly bound HTO form and a (non-HTO) strongly bound form. For accurate and effective isolation of any ^{3}H in metals (when using a Pyrolyser furnace) a rapid and sustained temperature (~900°C) for about 2 hours is required.

Appendices

Appendices

Appendix.1 Conference presentations given during the tenure of the PhD

1. 2006 Environmental radiochemical analysis 10th International symposium of Royal Society of Chemistry (RSC): Poster presentation of "The analytical impact on tritium data from decommissioning samples stored under different conditions", Oxford, United Kingdom (13-15 Sep 2006)
2. 2007 7th Meeting of the tritium users group: Oral presentation "^{3}H storage and analysis", Basingstoke, United Kingdom (9-10 May 2007)
3. 2007 Liquid Scintillation User's Forum (Tuesday 18th September 2007; CS6/CS7, Module 16, NPL; National Physical Laboratory): Invited talk of "Characteristics of ^{3}H speciation in bioshield concrete", United Kingdom (18th September 2007).
4. 2007 5th Korean Radioactive Waste Society Conference: Oral presentation of " Study of tritium (^{3}H) speciation in a reactor bioshield concrete", Busan, South korea (15-16 May 2007).
5. 2007 33rd Korean Scientists and Engineers Association in the UK Conference: Oral presentation of "^{3}H speciation in bioshield concrete", Imperial College, London, UK (24 November 2007)
6. 2008 8th Meeting of the tritium users group: Oral presentation "Tritium (^{3}H) speciation in nuclear reactor bioshield concrete and its impact on accurate analysis", Imperial College, London, UK (28-29 February 2008).
7. 2008 The role of radiochemistry in the sentencing and disposal of radioactive waste, Atkins Axis Office, Birmingham, UK (7 April 2008)
8. 2008 Liquid Scintillation Spectrometry: Oral presentation of "^{3}H speciation in bioshield concrete", Davos, Switzerland (25-30 May 2008).
9. 2008 Korea Atomic Energy Research Institute (KAERI); as part of a delegation from GAU-Radioanalytical.
10. 2008 Korea Institute of Nuclear Safety (KINS); as part of a delegation from GAU-Radioanalytical
11. 2008 Korea research Institute of Standards and Science (KRISS)
12. 2008 Royal Society of Chemistry/ Tritium Users Group Meeting: Oral presentation of "Characterisation of tritium in decommissioning wastes", National Oceanography Centre, University of Southampton, UK (23 October 2008).
13. 2009 The Society for Radiological Protection Meeting: Radiological protection of Tritium, Rutherford Appleton Laboratory Lecture Theatre, Harwell, UK (8 January 2009).

Appendix.2 Courses attended

1. Analysis of total tritium & ^{14}C and Processing of liquid scintillation raw data using LSC+ software (4^{th} Jan~25^{th} Feb 05)
2. Environmental Radioactivity & Radiochemistry (28^{th} Feb~19^{th} Mar 05)
3. X-ray and radioisotope users courses at Southampton University (23^{rd} November 2005)
4. SOES6023 Intensive Course

Appendix.3 Publications in journals and Proceedings

1. **Kim, D. J.**, Croudace, I. W. & Warwick, P. E. (2007) The analytical impact on tritium data from decommissioning samples stored under different conditions. In Warwick P (Ed) Environmental Radiochemical Analysis III, Special Publication, Royal Society of Chemistry, 108-115.
2. Oh, J-S, Warwick, P. E & Croudace, I. W., **Kim, D. J.** (2007) An efficient and optimised total combustion method for total H-3 & C-14 in environmental & decommissioning samples. In Warwick P (Ed) Environmental Radiochemical Analysis III, Special Publication, Royal Society of Chemistry, 101-107.
3. **Kim, D. J.**, Warwick, P. E & Croudace, I. W. (2008) Tritium (^{3}H) speciation in reactor bioshield concrete and its implication for accurate analysis. Analytical Chemistry 80, 5476-5480

Appendix.4 **RSC 2007 (Oxford) proceeding paper** in Warwick P (Ed) Environmental Radiochemical Analysis III, Special Publication, Royal Society of Chemistry 2006 RSC(2007), 108-115.

The analytical impact on tritium data from storing nuclear decommissioning samples under different conditions

Dae Ji Kim, Ian W Croudace and Phillip E Warwick

GAU-Radioanalytical, National Oceanography Centre, University of Southampton, European Way, Southampton SO14 3ZH, UK

Introduction

Tritium is a by-product of civil and military nuclear fission and fusion programmes and radiopharmaceutical production and commonly occurs, though not exclusively, as HTO or organically-bound tritium. During the lifetime of nuclear (involving heavy water) or other active sites tritium compounds may become variably incorporated into the fabric of the buildings. When decommissioning works and environmental assessments are undertaken it is necessary to evaluate tritium activities in a wide range of materials to evaluate waste sentencing options. Compositionally diverse materials (e.g. concrete bioshields, asbestos, wood, desiccants, reactor metal work, graphite blocks and tiles, softwastes etc) will often require characterization and careful consideration needs to be given to their sampling and storage if reliable analytical data are to be achieved. This study represents initial results from a range of simple experiments carried out to investigate tritium emanation rates for several sample types derived from some common reactor waste materials (bioshield concrete, desiccant, and steel). The effects of storing samples at room temperature, in a fridge and in a freezer were considered. All tritium determinations were made using a well-tested combustion method employing a purpose-designed tube furnace followed by LSC.

Methods

Total tritium ($^3H_{total}$) was quantitatively extracted from samples using a Raddec Pyrolyser-6 Trio™ System that provides simultaneous oxidation of six samples. The sample in a silica boat was placed in a tube in the centre of the sample zone. The tube end cap was replaced and oxygen-enriched air was passed over the sample. The sample was heated from 50°C to 500°C at a rate of 5°C/minute for 4 hours, with holding stages at 200°C and 300°C for 30 minutes. Pure oxygen was passed through each furnace tube when the sample zone reached 500°C. When required the sample zone was taken to 800°C, such as during decomposition of graphite. The catalyst zone contained 10g of Pt-coated alumina catalyst, held at 800°C,

which oxidizes any organic compounds in the combustion products to CO_2 and H_2O. The combustion gases are bubbled through a tube containing 20 ml of 0.1 M HNO_3 to trap the combustion water, which contained all of the tritium activity. These methods have been developed and validated by GAU-Radioanalytical at the University of Southampton (www.gau.org.uk).

All tritium measurements were performed using a 1220 liquid scintillation counter (Wallac Quantulus™). 8ml of aqueous sample were mixed with 12ml Gold Star™ (Meridian) scintillation cocktail in a 22ml polythene vial. The counter was routinely calibrated for ^3H using a traceable tritiated water standard. In this paper, all uncertainties are quoted at the 90% confidence level except for RO water.

A range of experiments were set up that used active desiccant (310,000Bq/g), concrete (8,950 Bq/g) and metal (110Bq/g) as tritium emanating source materials. RO water, silica gel, cellulose filter paper, plastic, metal, and various desiccants were used as potential receivers. The interaction with drying agents such as silica gel, zeolites and Drierite™ ($CaSO_4$) were also examined.

Figure 1: Design of the Pyrolyser-6 Trio combustion furnace

Tritium emanation with time from active concrete onto various receptor materials

Experiment 1: Contamination of water by emanation from concrete

Active concrete powder (~ 9 kBq of tritium) was placed in a sealable polythene bag and put in one of eighteen Kilner jars which had very effective rubber lid seals. An open and a closed scintillation vial containing 10 ml each of RO water were added to each of the jars which

were then stored in a fridge, a freezer and at room temperature for 1 day, 5 days, 10 days, 15 days, 20 days and 30 days, respectively. At the end of each pre-defined emanation time the respective Kilner jars were opened and the contents removed. 8 ml of each RO water vial (open and closed) was taken and transferred to clean scintillation vials with 12ml of scintillation cocktail (Goldstar) and counted by LSC for 1 hour. Similarly 50 ml of tritium-free RO water was added to the Kilner jar and shaken to collect any tritium (as HTO) that had adsorbed on the walls of the glass jars. An 8ml sample of this was also mixed with scintillant and counted.

Experiment 2: Tritium emanation from active concrete, desiccant and metal

Samples of active concrete powder, desiccant pellets and metal were placed in sealable polythene bags and then placed in one of nine Kilner jars each having an open and a closed scintillation vial containing 10 ml each of RO water. The jars were each stored in a fridge, a freezer and at room temperature for 2 weeks before being opened after which the scintillation vials were sampled and measured for tritium ingress. Any tritium that had adsorbed on the surface of the Kilner jars was also collected using a 50 ml wash and measured as previously described.

Experiment 3: Contamination of non-active silica gel, metal, plastic, zeolite and $CaSO_4$

A similar approach to that described above was applied to a range of other materials (silica gel, metal, plastic, zeolite and $CaSO_4$). A known amount of active concrete powder (~ 9 kBq of tritium) was placed in a sealable polythene bag and put in one of fifteen Kilner jars. Each jar contained an open and a closed scintillation vial holding approximately 5g samples of one of the non-active materials. All sample types were prepared in triplicate so that three different storage conditions (freezer, fridge and at room temperature) could be investigated over a 2 week period. At the end of the experiment, each Kilner jar was washed with 50 ml of tritium-free RO water to collect any tritium (as HTO) that had adsorbed on the walls of the glass jars and 8ml of this wash was mixed with scintillant and counted.

Experiment 4: Tritium emanation from active desiccant

Active desiccant (nominally 170 kBq tritium) was placed in each of twelve sealable plastic boxes having an O-ring lid seal. Samples of (i) silica gel in sealable polythene bag, (ii) silica gel in a double sealed bag, (iii) silica gel in an open scintillation vial and (iv) cellulose filter paper in an open scintillation vial were individually placed in each of the boxes. These were

stored for 2 weeks in a fridge, a freezer and at room temperature before opening, sampling and measuring.

Results and discussion

Experiment 1: Contamination of water by emanation from concrete powder

The contamination of RO water (open and closed vials) stored with bagged active concrete, under three different storage conditions, was investigated (Figure 2). The greatest contamination transfer occurred to open vials stored at room temperature. Systematically less contamination occurs to open vials stored in a fridge and freezer respectively. Water stored in closed vials at room temperature and in a fridge show significantly less, though measurable, contamination over the 30 day duration of the experiment while the samples in the freezer show no contamination.

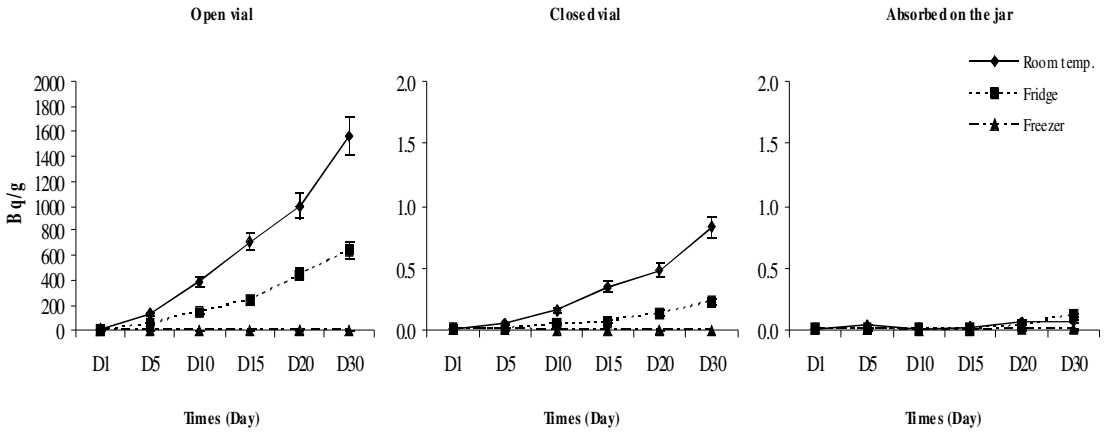

Figure 2: Variations of cross contamination of tritium from concrete (~9 kBq/g) with the passage of time (Expt. 1). *RO water in open and closed scintillation vials were stored in airtight Kilner Jars with a bagged sample of active concrete at room temperature, in a fridge and in a freezer for 1 day, 5 days, 10 days, 15 days, 20 days and 30 days.*

Table 1: Comparison of cross contamination with source materials and storage temperature (Expt. 1)

	% contamination transfer to RO water in an open vial			% contamination transfer to RO water in a closed vial		
	Rt	Rf	Fr	Rt	Rf	Fr
Day 1	0.1	<0.1 (0.04)	< 0.007	8.9E-05	8.9E-05	8.9E-05
Day 5	1.5	0.6	< 0.007	5.3E-04	1.0E-04	7.8E-05
Day 10	4.4	1.6	< 0.007	1.8E-03	5.5E-04	5.6E-05
Day 15	8.0	2.7	< 0.007	3.9E-03	7.6E-04	5.6E-05
Day 20	11.2	5.0	< 0.007	5.4E-03	1.6E-03	3.4E-05
Day 30	17.4	7.2	< 0.007	9.2E-03	2.5E-03	5.6E-05

Experiment 2: Tritium emanation from active concrete, desiccant and metal

Cross contamination of RO water in an open vial following exposure to different materials (bagged) shows a higher contamination than in a closed vial (Table 2). The greatest relative emanation occurs from concrete powder stored but it was also found (checked by triplicate experiments) that the greatest contamination of RO in vials occurred when the Kilner jars were stored in a fridge. This is a different outcome than that found with the concrete from Expt. 1 where RO water stored at room temperature became more contaminated at room temperature than in a freezer and a fridge. All jars containing RO water samples that were stored in a freezer (open and closed scintillation vial) showed very low contamination (Table 2).

Table 2: Comparison of cross contamination with source materials and storage temperature (Expt. 2)

Source materials	Storage condition	Activity of source materials (Bq)	Contaminated activity (Bq/g) of RO water					
			RO water open vial	2sd	% contamination transfer to the RO water	RO water closed vial	2sd	% contamination transfer to the RO water
Desiccant	Rt	171120	34.96	3.50	0.2	0.02	0.01	9.9E-05
	Rf	181660	187.19	18.73	1.0	0.09	0.01	4.9E-04
	Fr	157790	0.30	0.03	< 0.1 (0.02)	0.01	-	3.8E-05
Concrete	Rt	24558	66.34	6.64	2.7	0.04	0.01	1.6E-03
	Rf	24882	144.32	14.45	5.8	0.06	0.01	2.2E-03
	Fr	24690	0.70	0.07	< 0.1 (0.03)	0.01	-	2.4E-04
Metal	Rt	263.34	8.61	0.87	32.7	0.01	-	3.0E-02
	Rf	356.62	9.68	0.97	27.1	0.02	0.01	5.0E-02
	Fr	319.33	0.02	0.01	0.1	0.01	-	1.9E-02

Figures in bracket are the relative standard deviation %, Exposure time 2 weeks. Rt: Room temperature, Re: Refrigerator, F: Freezer, - measured values are below the limit of detection; all tests were conducted in triplicate.

Experiment 3: Contamination of non-active silica gel, metal, plastic, zeolite and $CaSO_4$ by active concrete

Different materials became contaminated to different extents when stored with a tritium emanator such as active concrete (Figure 3). The absorbers used, silica gel, zeolite and Drierite™ ($CaSO_4$), were contaminated to a greater extent than were metal and plastic, especially in an open scintillation vial. Zeolite and Drierite™ ($CaSO_4$) were more contaminated in the fridge (Figure 3). Plastic and metal, however, were relatively little

contaminated which implies physical and compositional controls on the extent of contamination [5, 9]. All samples stored in closed vials showed very low contamination.

Experiment 4: Tritium emanation from active desiccant

Contamination of silica gel and cellulose filter paper stored in a polythene box (having an O-ring lid seal) exposed to emanations from active desiccant were studied (Figure 4). The results show that no significant contamination occurred when containers are stored in a freezer. The same materials stored in a fridge or at room temperature did show increased contaminated with time. These results (Table 2 and Figure 3) show that samples stored in a fridge are more easily contaminated than when stored at room temperature or in a freezer.

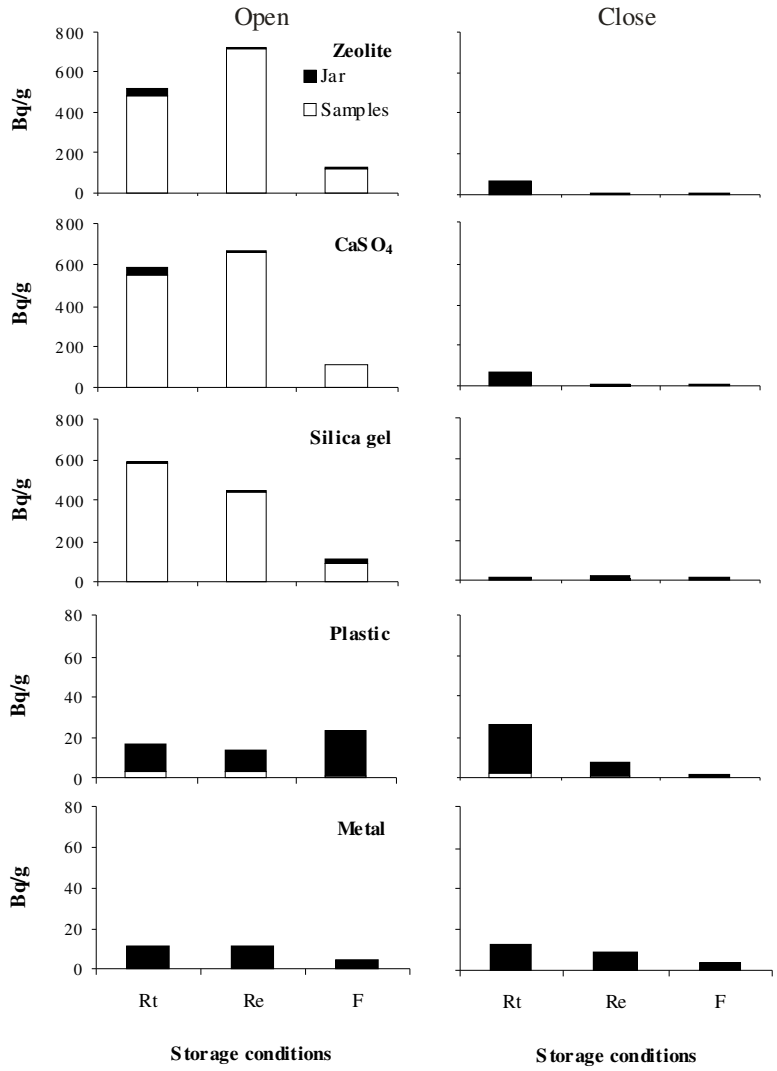

Figure 3: Comparison of cross contamination of various samples from active concrete (nominally 9 kBq tritium) stored in a fridge, a freezer and room temperature - (Expt. 3)

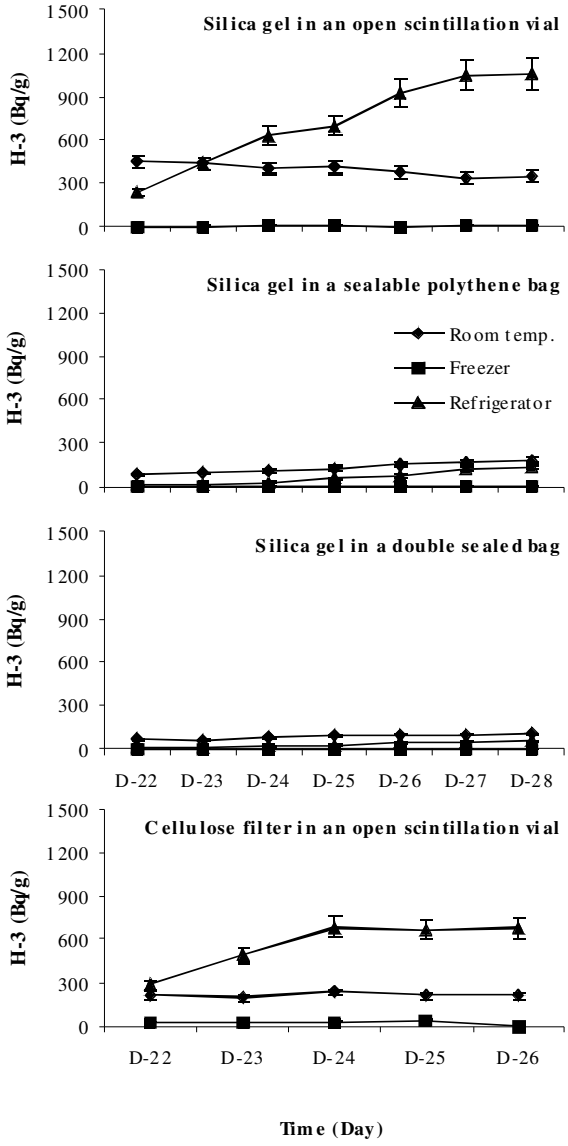

Figure 4: Variation of cross contamination of silica gel and cellulose filter-paper exposed to an active desiccant emanator (nominally 158 kBq tritium) with time. Storage occurred in a fridge, a freezer and at room temperature; Expt. 4.

Conclusions

A set of simple emanation and trapping experiments have shown the extent of cross contamination that can occur with emitter composition and packaging, storage temperature and exposure time.

1. Significant contamination of desiccants (silica gel, zeolite and $CaSO_4$) was observed in unsealed containers exposed to tritiated concrete powder at room temperature and in a refrigerator. This contamination was not seen for metals and plastics.
2. Contamination of desiccants exposed to tritiated concrete was significantly reduced by storing the samples in a freezer or within sealed vials.
3. Emanation of tritium was most significant from metals (nominally 30% loss over 2 weeks storage) and to a lesser extent concretes stored at room temperature (6% loss) and in a refrigerator. Emanation from desiccants was considerably lower. Again storage in sealed containers and in a freezer effectively eliminated the potential for cross contamination.

The recommended approaches for storing samples intended for tritium analysis are :-

- Store samples in a freezer in double plastic bags to avoid cross-contamination
- Store samples in vapour tight jars or boxes
- Segregate low activity samples from high activity samples where possible

References

1. UNSCEAR, *Sources and effects of ionizing radiation: sources and biological effects, 1982. Report to the General Assembly, with Annexes, United Scientific Committee on the Effects of Atomic Radiation. UN, New York, 1993.*
2. Villa, M. and G. Manjon, *Low-level measurements of tritium in water.* Applied Radiation and Isotopes, 2004. **61,** 319-323.
3. Fabre, A., et al., *On the correlation between mechanical and TEM studies of the aging of palladium during tritium storage.* Journal of Nuclear Materials, (2005) **342,** 101-107.
4. Evans, E.A., *Guide to the Self-Decompositon of Radiochemicals*. 1992, Chalfont, UK: Amersham International plc.
5. Harms, A.V. and S.M. Jerome, *Development of an organically bound tritium standard.* Applied Radiation and Isotopes, (2004) **61,** 389-393.
6. Ware, A. and R.W. Allott, *Review of methods for the analysis of total tritium and organically bound tritium*. 1999, National Compliance and Assessment Service: Lancaster.
7. Pointurier, F., N. Baglan, and G. Alanic, *A method for the determination of low-level organic-bound tritium activities in environmental samples.* Applied Radiation and Isotopes (2004) **61,** 293-298.
8. Warwick, P.E., I.W. Croudace, and A.G. Howard, *Improved technique for the routine determination of tritiated water in aqueous samples.* Analytica Chimica Acta, (1999) **382,** 225-231.
9. Oya, Y., et al., *Tritium contamination and decontamination study on materials for ITER remote handling equipment.* Fusion Engineering and Design (2001) **55,** 449-455.

Appendix.5 Determination of lithium in samples by ICP-AES

No	ID	Used mass	sample volume (mL)	Li in solution (mg/L)	Li in sample (mg/kg)
STD1	JSd-3	0.1087	21.5918	0.835	165.9
STD2	JR-2	0.1035	21.1708	0.413	84.5
BLK2	$HClO_4$ add	0	21.5328	<0.006	
BLK1	HF	0	20.1891	<0.006	
Concrete 1	0-10cm	0.1042	20.1243	0.060	11.6
Concrete 2	10-20cm	0.1063	20.0224	0.061	11.5
Concrete 3	20-30cm	0.1045	20.0495	0.061	11.7
Concrete 4	30-40cm	0.1031	19.7781	0.059	11.3
Concrete 5	40-50cm	0.1005	19.5496	0.056	10.9
Concrete 6	50-60cm	0.1006	21.3530	0.055	11.7
Concrete 7	60-70cm	0.1048	20.0062	0.076	14.5

Lithium concentration of JSd-3 (STD1) and JR-2 are 163ppm and 83ppm.
Uncertainty: The uncertainty about the data is ± 3% relative or the LOD, whichever is the greater

Appendix.6 ^{3}H evolution from bioshield concrete core sections with temperatures

Min	Temp. (°C)	0-10 cm			10-20 cm			20-30 cm			30-40 cm			40-50 cm			50-60 cm			60-70 cm		
		H-3 (Bq/g)	2sd	Acc. %	H-3 (Bq/g)	2sd	Acc. %	H-3 (Bq/g)	2sd	Acc. %	H-3 (Bq/g)	2sd	Acc. %	H-3 (Bq/g)	2sd	Acc. %	H-3 (Bq/g)	2sd	Acc. %	H-3 (Bq/g)	2sd	Acc. %
30	**130**	123.6	12.4	41.8	263.3	26.4	43.0	161.5	16.2	22.3	198.4	19.9	14.4	110.6	11.1	4.6	189.3	19.0	4.3	118.5	11.9	1.8
60	**200**	70.2	7.1	65.5	128.8	13.0	64.0	107.1	10.8	37.1	117.2	11.8	22.8	116.4	11.7	9.4	167.4	16.8	8.2	165.0	16.6	4.3
90	**283**	34.5	3.5	77.1	50.6	5.1	72.3	53.1	5.4	44.5	50.4	5.1	26.5	74.7	7.5	12.5	74.9	7.5	9.9	118.0	11.9	6.1
120	**332**	17.4	1.8	83.0	20.4	2.1	75.6	31.8	3.2	48.8	53.9	5.5	30.4	52.0	5.3	14.7	61.2	6.2	11.3	96.1	9.7	7.6
150	**485**	7.6	0.8	85.6	11.5	1.2	77.5	29.4	3.0	52.9	83.4	8.4	36.4	80.8	8.1	18.0	163.7	16.4	15.1	137.5	13.8	9.7
180	**500**	6.8	0.7	87.9	26.6	2.7	81.8	48.0	4.9	59.6	177.3	17.8	49.3	196.0	19.7	26.2	565.9	56.6	28.0	441.9	44.3	16.4
210	**500**	7.8	0.8	90.5	23.7	2.4	85.7	60.5	6.1	67.9	142.3	14.3	59.6	298.7	29.9	38.6	543.0	54.4	40.5	785.6	78.6	28.3
240	**500**	5.0	0.6	92.2	13.0	1.3	87.8	38.7	3.9	73.3	77.3	7.8	65.2	234.2	23.5	48.3	328.9	32.9	48.0	710.1	71.1	39.1
270	**733**	2.8	0.3	93.2	8.8	0.9	89.3	26.8	2.7	77.0	56.3	5.7	69.2	150.9	15.1	54.6	234.0	23.4	53.4	455.9	45.6	46.0
300	**835**	6.3	0.7	95.3	23.0	2.4	93.0	51.5	5.2	84.1	152.1	15.3	80.2	331.8	33.2	68.4	666.8	66.7	68.7	810.2	81.1	58.4
330	**881**	6.1	0.7	97.4	19.5	2.0	96.2	47.8	4.8	90.7	126.1	12.7	89.4	340.3	34.1	82.5	630.4	63.1	83.2	1024.4	102.5	73.9
360	**900**	3.3	0.4	98.5	9.2	1.0	97.7	28.6	2.9	94.6	58.3	5.9	93.6	203.7	20.4	90.9	305.8	30.6	90.2	721.7	72.2	84.9
390	**900**	1.6	0.2	99.0	4.7	0.5	98.5	14.6	1.5	96.6	31.4	3.2	95.9	86.7	8.7	94.5	164.4	16.5	94.0	393.5	39.4	90.9
420	**900**	0.8	0.1	99.3	2.8	0.3	98.9	7.4	0.8	97.7	15.7	1.6	97.0	40.3	4.1	96.2	82.3	8.3	95.9	193.9	19.4	93.9
450	**900**	0.4	0.1	99.4	1.7	0.2	99.2	4.5	0.5	98.3	10.5	1.1	97.8	23.7	2.4	97.2	49.4	5.0	97.0	109.2	11.0	95.5
480	**900**	0.3	0.1	99.5	1.0	0.2	99.4	2.7	0.3	98.7	6.6	0.7	98.2	14.8	1.5	97.8	28.7	2.9	97.6	68.0	6.8	96.5
510	**900**	0.3	0.1	99.6	0.7	0.1	99.5	2.2	0.3	99.0	5.1	0.6	98.6	11.6	1.2	98.3	20.8	2.1	98.1	52.0	5.3	97.3
540	**900**	0.2	0.1	99.7	0.6	0.1	99.6	1.7	0.2	99.2	4.2	0.5	98.9	7.7	0.8	98.6	16.9	1.7	98.5	37.9	3.8	97.9
570	**900**	0.2	0.1	99.8	0.5	0.1	99.7	1.3	0.2	99.4	2.5	0.3	99.1	6.5	0.7	98.9	11.8	1.2	98.8	30.9	3.2	98.4
600	**900**	0.1	0.1	99.8	0.4	0.1	99.7	1.1	0.2	99.5	2.6	0.3	99.3	5.6	0.6	99.1	11.4	1.2	99.0	23.8	2.4	98.7
630	**900**	0.1	0.1	99.8	0.4	0.1	99.8	0.8	0.1	99.6	2.1	0.3	99.4	4.9	0.5	99.3	9.1	1.0	99.3	19.5	2.0	99.0
660	**900**	0.1	0.1	99.9	0.3	0.1	99.8	0.7	0.1	99.7	1.9	0.2	99.6	4.1	0.5	99.5	7.8	0.8	99.4	16.7	1.7	99.3
690	**900**	0.1	0.1	99.9	0.3	0.1	99.9	0.6	0.1	99.8	1.6	0.2	99.7	3.7	0.4	99.6	7.1	0.8	99.6	14.0	1.5	99.5
720	**900**	0.1	0.1	99.9	0.3	0.1	99.9	0.5	0.1	99.9	1.7	0.2	99.8	3.0	0.4	99.8	6.8	0.7	99.7	11.6	1.2	99.7
750	**900**	0.1	0.1	100.0	0.2	0.1	100.0	0.4	0.1	99.9	1.2	0.2	99.9	2.9	0.4	99.9	5.2	0.6	99.9	11.1	1.2	99.9
780	**900**	0.1	0.1	100	0.2	0.1	100	0.4	0.1	100	1.4	0.2	100	2.6	0.3	100	5.8	0.6	100	9.7	1.0	100
Total		295.9	14.9		612.5	30.4		723.5	23.9		1381.5	41.4		2408.3	72.6		4358.5	136.3		6576.8	201.5	

(Acc. %: Accumulation %)

Appendix.7 ^{3}H evolution after heating of concrete to set temperature for 12hours

Min	Temp. (°C)	Outer bioshield (0-10cm, Ao is 296Bq/g)									Inner bioshield (60-70cm, Ao is 6877 Bq/g)								
		105ºC			170ºC			300ºC			105ºC			170ºC			300ºC		
		H-3 (Bq/g)	2sd	% of Ao	H-3 (Bq/g)	2sd	% of Ao	H-3 (Bq/g)	2sd	% of Ao	H-3 (Bq/g)	2sd	% of Ao	H-3 (Bq/g)	2sd	% of Ao	H-3 (Bq/g)	2sd	% of Ao
30	**130**	0.2	0.1	0.07	0.1	0.1	0.02	0.1	0.1	0.02	0.6	0.1	0.01	0.7	0.1	0.01	0.8	0.1	0.01
60	**200**	0.4	0.1	0.13	0.2	0.1	0.07	0.1		0.03	1.2	0.2	0.02	1.0	0.2	0.02	1.7	0.2	0.03
90	**283**	0.7	0.1	0.22	0.3	0.1	0.10	0.1		0.03	13.8	1.4	0.21	11.1	1.2	0.17	1.0	0.1	0.02
120	**332**	1.8	0.2	0.62	1.4	0.2	0.49	0.1		0.03	97.5	9.8	1.48	168.1	16.9	2.56	0.8	0.1	0.01
150	**485**	3.0	0.4	1.01	2.8	0.3	0.96	0.1	0.1	0.03	481.7	48.2	7.32	614.2	61.5	9.34	10.8	1.1	0.16
180	**500**	7.8	0.8	2.65	7.0	0.8	2.35	3.2	0.4	1.09	1025.7	102.6	15.60	1071.0	107.2	16.28	305.5	30.6	4.64
210	**500**	6.9	0.8	2.33	6.7	0.7	2.26	5.5	0.6	1.84	943.1	94.4	14.34	792.2	79.3	12.05	620.2	62.1	9.43
240	**500**	4.3	0.5	1.45	4.3	0.5	1.44	4.0	0.5	1.35	504.7	50.5	7.67	397.2	39.8	6.04	419.2	42.0	6.37
270	**733**	3.5	0.4	1.18	3.6	0.4	1.21	3.6	0.4	1.20	386.2	38.7	5.87	344.1	34.5	5.23	365.3	36.6	5.55
300	**835**	7.1	0.8	2.40	6.8	0.7	2.29	7.7	0.8	2.59	894.1	89.5	13.59	893.3	89.4	13.58	1014.1	101.5	15.42
330	**881**	5.9	0.7	2.01	5.2	0.6	1.76	6.8	0.7	2.28	862.3	86.3	13.11	708.8	70.9	10.78	1036.8	103.8	15.76
360	**900**	2.9	0.4	0.98	3.4	0.4	1.14	3.6	0.4	1.21	403.7	40.4	6.14	402.3	40.3	6.12	485.7	48.6	7.38
390	**900**	1.6	0.2	0.55	1.3	0.2	0.44	1.7	0.2	0.58	244.9	24.6	3.72	311.6	31.2	4.74	276.2	27.7	4.20
420	**900**	1.0	0.2	0.32	0.6	0.1	0.20	1.0	0.2	0.35	116.6	11.7	1.77	118.1	11.9	1.80	145.7	14.6	2.22
450	**900**	0.6	0.1	0.22	0.4	0.1	0.13	0.6	0.1	0.21	76.8	7.7	1.17	70.4	7.1	1.07	96.5	9.7	1.47
480	**900**	0.5	0.1	0.17	0.3	0.1	0.11	0.4	0.1	0.14	49.1	5.0	0.75	47.3	4.8	0.72	56.7	5.7	0.86
510	**900**	0.4	0.1	0.13	0.2	0.1	0.05	0.3	0.1	0.10	37.1	3.8	0.56	34.8	3.5	0.53	42.2	4.3	0.64
540	**900**	0.4	0.1	0.13	0.2	0.1	0.06	0.3	0.1	0.10	30.5	3.1	0.46	28.8	2.9	0.44	34.4	3.5	0.52
570	**900**	0.3	0.1	0.10	0.1	0.1	0.05	0.2	0.1	0.05	22.8	2.3	0.35	21.9	2.2	0.33	25.4	2.6	0.39
600	**900**	0.3	0.1	0.09	0.1	0.1	0.03	0.2	0.1	0.06	20.3	2.1	0.31	19.0	2.0	0.29	23.1	2.4	0.35
630	**900**	0.2	0.1	0.07	0.1	0.1	0.03	0.2	0.1	0.06	16.5	1.7	0.25	15.7	1.6	0.24	19.0	2.0	0.29
660	**900**	0.2	0.1	0.08	0.1	0.1	0.03	0.1	0.1	0.05	15.8	1.7	0.24	14.7	1.5	0.22	17.1	1.8	0.26
690	**900**	0.3	0.1	0.09	0.1	0.1	0.03	0.2	0.1	0.05	11.8	1.2	0.18	11.0	1.2	0.17	13.1	1.4	0.20
720	**900**	0.2	0.1	0.06	0.1	0.1	0.03	0.1	0.1	0.05	11.1	1.2	0.17	10.5	1.1	0.16	12.1	1.3	0.18
750	**900**	0.2	0.1	0.08	0.1	0.1	0.03	0.1	0.1	0.02	9.2	1.0	0.14	8.8	0.9	0.13	10.3	1.1	0.16
780	**900**	0.2	0.1	0.05	0.1	0.1	0.02	0.1	0.1	0.03	8.7	0.9	0.13	8.5	0.9	0.13	9.7	1.0	0.15
Total		50.9	1.8	17.2	45.4	1.7	15.34	40.1	1.6	13.57	6285.4	209.4	95.57	6124.9	201.2	93.13	5043.4	180.2	76.68

Appendix.8 ^{3}H evolution from a range of material with temperatures

Min	Temp. (°C)	^{3}H thymidine			Sewage sludge			Fish (Plaice)			Milk			Structural concrete			Graphite (GLEEP)			Brick		
		H-3 (Bq/g)	2sd	Acc. %	H-3 (Bq/g)	2sd	Acc. %	H-3 (Bq/g)	2sd	Acc. %	H-3 (Bq/g)	2sd	Acc. %	H-3 (Bq/g)	2sd	Acc. %	H-3 (Bq/g)	2sd	Acc. %	H-3 (Bq/g)	2sd	Acc. %
30	**50**	268.3	28.4	42.6	1.9	0.4	1.2	0.1	0.1	2.4	0.1		2.8	2363.4	236.7	42.6	0.2		1.4	25.3	2.6	75.3
60	**150**	62.9	8.1	52.6	4.2	0.6	3.8	0.3	0.1	10.2	0.1	0.1	4.8	1867.2	187.0	76.3	0.2		2.7	3.9	0.4	86.9
90	**200**	44.9	6.1	59.7	14.0	1.6	12.5	1.2	0.2	44.0	0.7	0.1	21.5	703.1	70.5	89.0	0.2		4.0	1.1	0.2	90.3
120	**297**	175.0	19.1	87.5	27.1	3.0	29.4	0.5	0.1	57.7	1.0	0.1	45.2	336.5	33.8	95.1	0.5	0.2	7.0	1.0	0.2	93.3
150	**342**	40.6	5.4	94.0	28.3	3.1	47.0	0.7	0.2	78.7	1.1	0.2	70.8	159.8	16.1	98.0	0.5	0.2	10.1	0.6	0.1	95.2
180	**497**	13.9	3.0	96.2	67.7	7.1	89.2	0.5	0.2	93.1	0.8	0.1	90.6	87.0	8.8	99.5	0.8	0.2	15.3	0.3	0.1	96.1
210	**500**	7.3	2.5	97.3	10.6	1.3	95.8	0.2	0.1	97.9	0.3	0.1	97.6	16.3	1.7	99.8	3.1	0.4	34.9	0.3	0.1	96.9
240	**500**	5.1	2.8	98.1	2.0	0.4	97.0	0.1		100	0.1		100	9.3	1.0	100	4.3	0.6	61.7	0.1	0.1	97.3
270	**500**	5.5	2.4	99.0	1.4	0.3	97.9										3.5	0.5	83.5	0.1		97.5
300	**500**	6.2	2.7	100	0.9	0.3	98.5										1.3	0.3	91.7	0.1	0.1	97.8
330	**500**				0.7	0.2	98.9										0.2	0.1	93.1	0.0	0.0	98.0
360	**500**				0.7	0.2	99.3										0.2		94.5	0.1		98.2
390	**500**				0.6	0.2	99.7										0.2		95.9	0.1		98.5
420	**500**				0.5	0.2	100										0.2		97.3	0.1		98.7
450	**500**																0.2		98.7	0.1		99.0
480	**500**																0.2		100	0.1		99.2
510	**500**																			0.1		99.5
540	**500**																			0.1		99.7
570	**500**																			0.1		100
600	**500**																					
630	**500**																					
660	**500**																					
690	**500**																					
720	**500**																					
750	**500**																					
780	**500**																					
Total		629.8	36.6		160.5	8.6		3.5	0.4		4.2	0.3		5542.7	312.1		16.1	0.9		33.6	2.6	

(Acc. %: Accumulation %)

Min	Temp. (°C)	Irradiated steel			Steel			Irradiated aluminum			Aluminum			Irradiated Boral (top)			Irradiated Boral (middle)			Irradiated Boral (bottom)		
		H-3 (Bq/g)	2sd	Acc. %	H-3 (Bq/g)	2sd	Acc. %	H-3 (Bq/g)	2sd	Acc. %	H-3 (Bq/g)	2sd	Acc. %	H-3 (Bq/g)	2sd	Acc. %	H-3 (Bq/g)	2sd	Acc. %	H-3 (Bq/g)	2sd	Acc. %
30	**50**	0.1		0.0	0.10	0.04	2.1	0.8	0.1	0.0	0.5		3.7	0.1	0.2	0.01	99.7	10.1	1.5	0.3		0.3
60	**150**	1.2	0.2	0.4	0.31	0.06	8.6	8.2	0.9	0.1	0.5		7.3	3.4	0.5	0.3	467.4	46.9	8.7	0.3	0.2	0.6
90	**200**	13.7	1.4	4.8	1.00	0.14	29.1	47.3	4.8	0.7	0.5		10.8	11.7	1.3	1.4	365.9	36.7	14.3	1.0	0.3	1.5
120	**297**	113.8	11.4	41.1	1.46	0.18	59.3	295.0	29.6	4.3	0.9	0.3	17.4	38.7	4.0	5.0	338.7	34.0	19.5	2.9	0.5	4.1
150	**342**	80.8	8.1	66.8	0.78	0.11	75.4	733.2	73.4	13.2	3.0	0.6	40.2	82.4	8.4	12.6	378.0	37.9	25.2	6.2	0.8	9.6
180	**497**	44.4	4.5	81.0	0.38	0.07	83.1	491.0	49.2	19.1	1.9	0.5	54.7	62.0	6.4	18.3	201.2	20.3	28.3	4.4	0.6	13.6
210	**500**	19.6	2.0	87.3	0.16	0.05	86.5	475.8	47.6	24.9	0.5	0.3	58.3	46.8	4.8	22.6	131.5	13.3	30.3	3.8	0.6	17.0
240	**500**	16.3	1.7	92.4	0.15	0.05	89.6	721.3	72.2	33.7	0.2	0.3	60.1	36.5	3.8	26.0	106.1	10.8	32.0	3.1	0.5	19.7
270	**500**	8.5	0.9	95.2	0.08	0.04	91.3	614.9	61.6	41.2	0.5		63.7	40.8	4.2	29.8	131.3	13.3	34.0	2.9	0.5	22.3
300	**500**	4.7	0.5	96.7	0.09	0.04	93.2	531.6	53.2	47.6	0.5		67.5	47.9	4.9	34.2	313.8	31.5	38.8	3.3	0.5	25.3
330	**500**	3.4	0.4	97.7	0.10	0.04	95.2	464.3	46.5	53.3	0.5		71.1	80.4	8.2	41.6	717.5	71.9	49.8	5.5	0.7	30.2
360	**500**	2.7	0.3	98.6	0.08	0.04	96.9	632.7	63.3	60.9	0.5		74.6	70.8	7.2	48.1	617.3	61.9	59.2	4.6	0.7	34.3
390	**500**	1.6	0.2	99.1	0.09	0.04	98.7	743.4	74.4	70.0	0.5		78.2	102.6	10.4	57.6	710.2	71.2	70.1	6.4	0.8	40.0
420	**500**	0.8	0.2	99.4	0.06	0.04	100.0	562.0	56.3	76.8	0.5		81.9	89.4	9.1	65.9	543.0	54.5	78.4	6.2	0.8	45.6
450	**500**	0.5	0.1	99.5				545.5	54.6	83.4	0.5		85.6	79.0	8.0	73.2	402.2	40.4	84.5	5.9	0.8	50.9
480	**500**	0.3	0.1	99.6				331.0	33.2	87.5	0.5		89.3	73.3	7.5	79.9	312.0	31.3	89.3	6.6	0.8	56.8
510	**500**	0.2	0.1	99.7				299.5	30.0	91.1	0.4		92.7	62.3	6.4	85.7	211.6	21.3	92.5	7.4	0.9	63.5
540	**500**	0.1	0.1	99.7				242.7	24.3	94.0	0.5		96.5	50.5	5.2	90.3	154.8	15.6	94.9	7.7	0.9	70.4
570	**500**	0.1	0.1	99.7				160.1	16.1	96.0	0.5		100.0	33.3	3.5	93.4	96.9	9.8	96.4	5.6	0.8	75.4
600	**500**	0.1		99.8				117.7	11.8	97.4				23.0	2.5	95.5	67.6	6.9	97.4	5.7	0.8	80.5
630	**500**	0.1	0.1	99.8				72.5	7.3	98.3				16.2	1.8	97.0	47.0	4.8	98.1	4.8	0.7	84.8
660	**500**	0.1		99.9				53.3	5.4	99.0				10.8	1.2	98.0	34.4	3.6	98.7	3.8	0.6	88.2
690	**500**	0.1		99.9				32.3	3.3	99.3				8.4	1.0	98.8	29.3	3.1	99.1	3.7	0.5	91.5
720	**500**	0.1	0.1	99.9				25.5	2.6	99.7				6.8	0.8	99.4	26.5	2.8	99.5	4.3	0.6	95.3
750	**500**	0.1		100.0				17.5	1.8	99.9				3.7	0.5	99.8	17.4	1.9	99.8	2.8	0.4	97.8
780	**500**	0.1		100.0				11.0	1.2	100.0				2.6	0.4	100	13.3	1.5	100	2.5	0.4	100
Total		313.4	15.1		4.9	0.3		8230.4	209.2		13.0	0.9		1083.4	27.1		6534.6	169.3		111.6	3.3	

(Acc. %: Accumulation %)

Min	Temp. (°C)	Stainless steel (top)			Stainless steel (side)			Stainless steel (mid)			Irradiated cadmium			Copper (top surface)			Copper (side surface)			Copper (middle)		
		H-3 (Bq/g)	2sd	Acc. %	H-3 (Bq/g)	2sd	Acc. %	H-3 (Bq/g)	2sd	Acc. %	H-3 (Bq/g)	2sd	Acc. %	H-3 (Bq/g)	2sd	Acc. %	H-3 (Bq/g)	2sd	Acc. %	H-3 (Bq/g)	2sd	Acc. %
30	**50**	0.4	0.2	0.1	0.1	0.1	0.0	0.1		0.0	0.183		3.7	0.2		0.2	0.2		0.5	0.1		13
60	**150**	1.0	0.2	0.2	0.9	0.2	0.1	0.1	0.1	0.1	0.193		7.7	0.7	0.2	0.9	0.2		1.0	0.1		26
90	**200**	9.7	1.1	1.4	11.2	1.2	1.2	1.2	0.2	0.4	0.19		11.6	8.0	0.9	8.2	0.4	0.2	1.9	0.1		40
120	**297**	18.1	1.9	3.8	32.1	3.3	4.3	2.2	0.3	1.0	0.281	0.13	17.3	32.7	3.4	38.2	2.2	0.4	7.0	0.0	0.0	40
150	**342**	56.6	5.8	11.1	103.5	10.5	14.4	9.4	1.0	3.7	0.453	0.129	26.5	33.0	3.4	68.4	5.5	0.7	19.7	0.0	0.0	41
180	**497**	89.4	9.1	22.6	148.1	14.9	28.8	27.0	2.8	11.3	0.398	0.133	34.6	18.8	2.0	85.7	11.4	1.3	45.8	0.0	0.0	45
210	**500**	111.1	11.2	36.9	160.6	16.2	44.4	46.8	4.8	24.5	0.165	0.124	38.0	6.5	0.8	91.6	12.1	1.3	73.5	0.1	0.0	51
240	**500**	86.7	8.8	48.0	113.1	11.4	55.4	37.0	3.8	35.0	0.15	0.128	41.0	2.8	0.4	94.2	4.9	0.6	84.8	0.1	0.0	58
270	**500**	87.9	8.9	59.4	108.1	11.0	65.9	36.8	3.8	45.4	0.129	0.129	43.7	1.6	0.3	95.7	2.3	0.4	90.1	0.1	0.0	63
300	**500**	74.9	7.6	69.0	90.6	9.2	74.7	32.6	3.3	54.6	0.198		47.7	1.3	0.3	96.9	1.8	0.3	94.3	0.1	0.0	73
330	**500**	70.6	7.2	78.1	82.9	8.4	82.7	42.4	4.3	66.6	0.198		51.8	0.9	0.2	97.7	0.6	0.2	95.7	0.1	0.0	78
360	**500**	55.9	5.7	85.3	61.6	6.3	88.7	39.3	4.0	77.7	0.188		55.6	0.6	0.2	98.2	0.6	0.2	97.2	0.1	0.0	85
390	**500**	39.3	4.1	90.4	40.7	4.2	92.7	29.6	3.0	86.1	0.185		59.4	0.5	0.2	98.7	0.3	0.2	97.8	0.1	0.0	90
420	**500**	24.6	2.6	93.5	25.1	2.6	95.1	16.4	1.7	90.7	0.188		63.2	0.5	0.2	99.1	0.2	0.1	98.3	0.0	0.0	94
450	**500**	20.0	2.1	96.1	20.2	2.2	97.1	14.0	1.5	94.6	0.202		67.3	0.3	0.2	99.4	0.2	0.1	98.8	0.0	0.0	97
480	**500**	12.6	1.4	97.7	12.8	1.4	98.3	9.6	1.0	97.4	0.197		71.4	0.3	0.2	99.6	0.2	0.1	99.2	0.0	0.0	98
510	**500**	8.8	1.0	98.9	8.6	1.0	99.2	4.6	0.5	98.7	0.09		73.2	0.2	0.1	99.8	0.2	0.1	99.6	0.0	0.0	99
540	**500**	5.8	0.7	99.6	5.0	0.6	99.7	3.1	0.4	99.5	0.2		77.3	0.2	0.1	100.0	0.2	0.1	100.0	0.0	0.0	100
570	**500**	3.1	0.4	100.0	3.5	0.5	100.0	1.6	0.2	100.0	0.204		81.4									
600	**500**										0.129		84.1									
630	**500**										0.063	0.085	85.4									
660	**500**										0.128		88.0									
690	**500**										0.122		90.5									
720	**500**										0.133		93.2									
750	**500**										0.125		95.7									
780	**500**										0.21	0.084	3.7									
Total		776.7	24.1		1028.9	33.0		353.9	11.0		4.9	0.3		109.2	5.4		43.6	2.2		0.9	0.0	

(Acc. %: Accumulation %)

Min	Temp. (°C)	lead			Graphite (DMTR)			Graphite (CONSORT)						
		H-3 (Bq/g)	2sd	Acc. %	H-3 (Bq/g)	2sd	Acc. %	H-3 (Bq/g)	2sd	Acc. %				
30	**50**	0.132	0.153	1.4	0.5	0.2	0.0	0.1	0.1	0.0				
60	**150**	0.121	0.154	2.7	6.2	0.7	0.0	0.2	0.1	0.0				
90	**200**	0.242		5.3	24.3	2.6	0.0	1.2	0.2	0.0				
120	**297**	0.178	0.16	7.1	63.3	6.5	0.1	3.5	0.4	0.1				
150	**342**	0.355	0.18	10.9	138.6	14.0	0.3	10.0	1.0	0.2				
180	**497**	0.756	0.212	18.9	284.5	28.6	0.7	28.0	2.9	0.5				
210	**500**	0.674	0.217	26.1	316.6	31.8	1.2	78.8	7.9	1.5				
240	**500**	0.6	0.21	32.4	394.2	39.6	1.7	403.2	40.4	6.7				
270	**500**	0.788	0.212	40.8	720.3	72.2	2.7	1165.0	116.6	21.5				
300	**500**	0.938	0.225	50.8	3192.2	319.3	7.1	1591.7	159.2	41.7				
330	**500**	0.521	0.191	56.3	4138.9	414.1	12.8	1123.9	112.5	56.0				
360	**500**	0.546	0.191	62.1	8320.6	832.4	24.3	1161.7	116.2	70.8				
390	**500**	0.141	0.155	63.6	8851.2	885.3	36.5	780.9	78.1	80.8				
420	**500**	0.306	0.163	66.8	8822.6	882.6	48.7	586.1	58.7	88.2				
450	**500**	0.246		69.4	8742.5	874.3	60.8	367.8	36.8	92.9				
480	**500**	0.254		72.1	6852.1	685.5	70.3	202.7	20.3	95.5				
510	**500**	0.241		74.7	5325.8	532.8	77.6	131.8	13.2	97.1				
540	**500**	0.238		77.2	4467.0	446.7	83.8	67.9	6.8	98.0				
570	**500**	0.245		79.8	3799.8	380.1	89.1	49.3	5.0	98.6				
600	**500**	0.69	0.214	87.1	2627.0	262.9	92.7	35.4	3.6	99.1				
630	**500**	0.251		89.8	1518.7	152.0	94.8	24.7	2.5	99.4				
660	**500**	0.146	0.165	91.3	1453.0	145.4	96.8	16.1	1.7	99.6				
690	**500**	0.255		94.0	904.6	90.6	98.0	11.0	1.2	99.7				
720	**500**	0.159	0.152	95.7	650.2	65.1	98.9	8.2	0.9	99.8				
750	**500**	0.141	0.159	97.2	473.8	47.5	99.6	7.0	0.8	99.9				
780	**500**	0.261		100.0	289.4	29.1	100	4.8	0.5	100				
Total		9.4	0.8		72378	2128		7861	280					

(Acc. %: Accumulation %)

Appendix.9 ^{3}H contamination in container from structural concrete

^{3}H in the air of the container (Kilner jar)										
Room temperature										
Time (min)	**Pre furnace bubbler**					**Post furnace bubbler**				
	^{3}H (Bq/ml)	2sd	Total mass (g) of aliquots sample (0.1 M HNO_3)	$^{3}H_{total}$ (Bq)	2sd	^{3}H (Bq/ml)	2sd	Total mass (g) of aliquots sample (0.1 $MHNO_3$)	$^{3}H_{total}$ (Bq)	2sd
10	0.417	0.045	19.65	8.2	0.9	0.010	0.004	19.26	0.19	0.08
20	0.794	0.083	19.84	15.8	1.6	0.011	0.004	19.29	0.21	0.08
30	1.011	0.104	20.94	21.2	2.2	0.018	0.005	20.21	0.36	0.10
Freezer										
10	0.043	0.007	19.59	0.8	0.1	0.010	0.004	19.44	0.19	0.08
20	0.067	0.010	19.07	1.3	0.2	0.009	0.004	20.17	0.18	0.08
30	0.079	0.011	20.93	1.7	0.2	0.013	0.004	20.88	0.27	0.09
Sample ID	**Room temperature**					**Freezer**				
	^{3}H (Bq/ml)	2sd	Total volume (ml)	$^{3}H_{total}$ (Bq)	2sd	^{3}H (Bq/ml)	2sd	Total volume (ml)	$^{3}H_{total}$ (Bq)	2sd
Jar	0.1	0.01	10	0.7	0.1	0.010	0.004	10	0.1	0.04
Polythene bag (inside wash)	0.5	0.1	10	5.2	0.55	0.979	0.101	10	9.79	1.01
Polythene bag (outside wash)	0.01	0.004	10	0.1	0.04	0.005	0.003	10	0.05	0.03
Outside of open vial	<0.005	-	10	<0.05	-	<0.005	-	10	<0.05	-
Outside of open vial	<0.005	-	10	<0.05	-	<0.005	-	10	<0.05	-
RO water in open vial	38	4	10	377	38	0.040	0.007	10	0.4	0.1
RO water in closed vial	0.02	0.005	10	0.2	0.05	< 0.003	-	10	<0.029	-
Cardboard	27	3	5.402	146	15	3	0.4	5.275	18	2
^{3}H remained in concrete	499	50	1	499	50	1046	105	1	1046	105

Appendix.10 ^{3}H contamination in container from bioshield concrete

^{3}H in the air of the container (Kilner jar)										
Room temperature										
Time (min)	**Pre furnace bubbler**					**Post furnace bubbler**				
	^{3}H (Bq/ml)	2sd	Total mass (g) of aliquots sample (0.1 M HNO_3)	$^{3}H_{total}$ (Bq)	2sd	^{3}H (Bq/ml)	2sd	Total mass (g) of aliquots sample (0.1 $MHNO_3$)	$^{3}H_{total}$ (Bq)	2sd
10	0.150	0.019	19.420	2.9	0.4	0.005	0.005	19.23	0.10	0.09
20	0.383	0.042	19.310	7.4	0.8	0.006	0.005	19.57	0.12	0.09
30	0.403	0.044	19.190	7.7	0.8	0.011	0.005	19.56	0.22	0.10
Freezer										
10	0.024	0.007	19.120	0.5	0.1	0.006	0.005	19.27	0.12	0.09
20	0.035	0.008	19.600	0.7	0.2	0.006	0.005	20.55	0.12	0.10
30	0.059	0.010	20.310	1.2	0.2	0.005	0.005	19.75	0.10	0.09
Sample ID	**Room temperature**					**Freezer**				
	^{3}H (Bq/ml)	2sd	Total volume (ml)	$^{3}H_{total}$ (Bq)	2sd	^{3}H (Bq/ml)	2sd	Total volume (ml)	$^{3}H_{total}$ (Bq)	2sd
Jar	0.02	0.01	10	0.2	0.06	<0.004	-	10	<0.043	-
Polythene bag (inside wash)	0.8	0.1	10	8.0	0.84	0.576	0.061	10	5.76	0.61
Polythene bag (outside wash)	<0.004	-	10	0.04	-	<0.004	-	10	<0.041	-
Outside of open vial	<0.004	-	10	<0.042	-	<0.004	-	10	<0.042	-
Outside of open vial	<0.005	-	10	<0.047	-	<0.004	-	10	<0.044	-
RO water in open vial	28	3	10	282.4	28.31	0.013	0.006	10	0.13	0.06
RO water in closed vial	0.02	0.006	10	0.2	0.1	<0.004	-	10	<0.043	-
Cardboard	8.058	0.820	4.2	34	3	1.327	0.148	3.9	5	1
^{3}H remained in concrete	6210	205	0.99	6148	203	6433	201	0.99	6369	199

Appendix.11 ^{3}H contamination by RO water from active structural and bioshield concrete

With structural concrete													
RO water in an open vial													
Time (day)	Total volume of water (ml)	Room temperature				Fridge				Freezer			
		^{3}H (Bq/g)	2sd	^{3}Htotal (Bq)	% contaminated	^{3}H (Bq/g)	2sd	^{3}Htotal (Bq)	% contaminated	^{3}H (Bq/g)	2sd	^{3}Htotal (Bq)	% contaminated
D1	10	12	1	120	0.3	4	0.4	40	0.1	0.4	0.04	3.9	0.01
D5	10	136	14	1359	3.7	50	5	504	1.4	5.2	0.5	51.5	0.14
D10	10	391	39	3914	10.7	144	14	1435	3.9	0.5	0.1	4.7	0.01
D15	10	714	71	7138	19.6	243	24	2434	6.7	0.4	0.0	4.3	0.01
D20	10	998	100	9980	27.4	448	45	4476	12.3	0.6	0.1	6.5	0.02
D30	10	1560	157	15600	42.8	641	64	6413	17.6	0.3	0.04	3.5	0.01
RO water in a closed vial													
D1	10	<0.008	-	0.08	0.0002	0.008		0.08	0.0002	<0.008	-	0.08	0.0002
D5	10	0.047	0.009	0.47	0.001	0.009	0.005	0.09	0.0002	<0.007	-	0.07	0.0002
D10	10	0.162	0.019	1.62	0.004	0.049	0.008	0.49	0.0013	<0.005	-	0.05	0.0001
D15	10	0.346	0.037	3.46	0.009	0.068	0.01	0.68	0.0019	<0.005	-	0.05	0.0001
D20	10	0.481	0.051	4.81	0.013	0.139	0.017	1.39	0.0038	0.003	0.003	0.03	0.0001
D30	10	0.826	0.086	8.26	0.023	0.226	0.026	2.26	0.0062	<0.005	-	0.05	0.0001
Details of used concrete													
^{3}H concentration		8950Bq/g											
Used mass		4.093				4.147				4.115			
$^{3}H_{total}$		24558				24882				24690			

With bioshiels concrete													
RO water in an open vial													
Time (day)	Total volume of water (ml)	Room temperature				Fridge				Freezer			
		^{3}H (Bq/g)	2sd	^{3}Htotal (Bq)	% contaminated	^{3}H (Bq/g)	2sd	^{3}Htotal (Bq)	% contaminated	^{3}H (Bq/g)	2sd	^{3}Htotal (Bq)	% contaminated
D1	10	1	0.2	15	0.2	0.5	0.1	5	0.1	0.02	0.01	0.2	0.004
D5	10	9	1	95	1.6	3	0.3	29	0.5	0.07	0.01	0.7	0.01
D10	10	18	2	184	3.1	6	1	64	1.1	0.07	0.01	0.7	0.01
D15	10	29	3	288	4.8	11	1	114	1.9	0.15	0.02	1.5	0.03
D20	10	35	3	346	5.7	17	2	168	2.8	0.27	0.03	2.7	0.04
D30	10	40	4	396	6.6	25	3	255	4.2	0.47	0.05	4.7	0.08
RO water in a closed vial													
D1	10	0.07	0.01	0.7	0.01	<0.005		0.05	0.00	<0.005	-	0.05	0.001
D5	10	0.08	0.01	0.8	0.01	0.114	0.014	1.14	0.02	<0.005	-	0.05	0.001
D10	10	0.04	0.01	0.4	0.01	0.033	0.006	0.33	0.01	<0.005	-	0.05	0.001
D15	10	0.01	0.00	0.1	0.002	0.004	0.003	0.04	0.001	<0.004	-	0.04	0.001
D20	10	0.02	0.01	0.2	0.003	0.004	0.003	0.04	0.001	<0.005	-	0.05	0.001
D30	10	0.35	0.04	3.5	0.06	0.010	0.004	0.10	0.002	0.028	0.005	0.28	0.005
Details of used concrete													
^{3}H concentration	6045.49Bq/g												
Used mass	ca 1g												
$^{3}H_{total}$	6045.49 Bq												

Appendix.12 ^{3}H contamination by various materials from different kinds of active materials

Sample and packing state	Room temp					Fridge					Freezer				
	^{3}H (Bq/g)	2sd	Total mass (g)	$^{3}H_{total}$ (Bq)	% contaminated	^{3}H (Bq/g)	2sd	Total mass (g)	$^{3}H_{total}$ (Bq)	% contaminated	^{3}H (Bq/g)	2sd	Total mass (g)	$^{3}H_{total}$ (Bq)	% contaminated
Desiccant															
Silica gel (SG) in open	61	6	5	306	0.18	835	84	5	4175	2.3	3.1	0.4	5	16	0.01
Silica gel in polythene bag	37	4	5	184	0.11	67	7	5	333	0.2	0.2	0.1	5.000	1.1	0.001
Silica gel in a double bag	9	1	5	46	0.03	29	3	5	146	0.1	0.2	0.1	5	1.0	0.001
Cellulose paper in open	39	4	0.148	6	0.003	356	36	0.147	52	0.03	21	2.5	0.146	3	0.002
water (open)	54	5	10	543	0.3	339	34	10	3392	1.9	0.15	0.02	10	2	0.001
water (closed)	0.07	0.01	10	0.7	0.0004	0.13	0.02	10	1.3	0.00	0.01		10	0.1	0.00004
Metal															
Silica gel in open	11	1.2	5	57	21.8	4.3	0.5	5	21.6	6.1	0.3	0.1	5	1.6	0.5
Silica gel in polythene bag	7	0.7	5	33	12.6	0.5	0.1	5	2.6	0.7	0.1	0.1	5	0.6	0.2
Silica gel in a double bag	2	0.3	5	11	4.1	0.2	0.1	5	1.0	0.3	0.19		5	1.0	0.3
Cellulose paper in open	4	0.8	0.144	1	0.2	13.4	1.8	0.152	2.0	0.6	1.0	0.6	0.145	0.1	0.04
water (open)	16	2	10	155	59.0	1.5	0.2	10	15	4.1	0.03	0.007	10	0.3	0.1
water (closed)	0.03	0.01	10	0.3	0.1	0.01		10	0.1	0.02	0.007		10	0.1	0.02
Concrete															
Silica gel in open	647	65	5	3234	8.8	680	68	5	3402	9.2	4.7	0.5	5	23.3	0.1
Silica gel in polythene bag	348	35	5	1738	4.7	33	3	5	165	0.4	0.3	0.1	5	1.3	0.004
Silica gel in a double bag	216	22	5	1081	3.0	19	2	5	93	0.3	0.2		5	1.0	0.003
Cellulose paper in open	26	3	0.149	4	0.0	232	24	0.150	35	0.1	50	5	0.136	6.8	0.02
water (open)	1250	125	10	12496	34.1	262	26	10	2620	7.1	0.4	0.048	10	4.3	0.01
water (closed)	1.5	0.2	10	15	0.04	0.6	0.1	10	6.1	0.02	0.01		10	0.1	0.0002
Emitter details															
Desiccant	0.552g, 171120Bq					0.586g, 181660 Bq					0.509g, 157790 Bq				
Metal	2.394g, 263.34 Bq					3.242g, 356.62 Bq					2.903g, 319.33 Bq				
Concrete	4.093g, 36632.35 Bq					4.147g, 37115.65 Bq					4.115g, 36829.25 Bq				

Appendix.13 ^{3}H contamination depend on materials being contaminated

Absorber	Room temperature					Fridge					Freezer				
	^{3}H (Bq/g)	2sd	Used mass (g)	$^{3}H_{total}$ (Bq)	% contaminated	^{3}H (Bq/g)	2sd	Used mass (g)	$^{3}H_{total}$ (Bq)	% contaminated	^{3}H (Bq/g)	2sd	Used mass (g)	$^{3}H_{total}$ (Bq)	% contaminated
Zeolite	483	48	5.161	2493	8.9	709	71	5.235	3713	13.3	118	12	5.072	600	2.1
CaSO4	551	55	5.112	2815	10.1	659	66	5.188	3418	12.3	105	11	5.087	533	1.9
Silica gel	583	58	5.098	2972	10.7	441	44	5.15	2273	8.1	85	9	5.047	430	1.5
Concrete	1337	134	0.662	885	3.2	168	17	0.597	100	0.4	18	2	0.546	10	0.04
Plastic	3	0.4	1.415	5	0.02	3	0.3	1.855	6	0.02	0.5	0.1	1.232	1	0.002
Metal	0.1	0.02	4.942	0.3	0.001	0.1	0.02	4.965	0.4	0.001	0.04	0.02	4.617	0.2	0.001